

FRONTISPIECE

Small pebbles and granules
saltating up the foreshore
in the leading edge of the
swash.



SWASH ZONE PROCESSES: AN EXAMINATION OF
WATER MOTION AND THE RELATIONS BETWEEN
WATER MOTION AND FORESHORE RESPONSE ON
SOME MIXED SAND AND SHINGLE BEACHES,
KAIKOURA, NEW ZEALAND

A thesis presented for the Degree
of Ph.D. in Geography in the
University of Canterbury,
Christchurch, New Zealand.

by

R.M. Kirk.

1970

B.
18.55
(59)

TABLE OF CONTENTS

| | <u>Page</u> |
|--|-------------|
| Frontispiece | v |
| Table of Contents | ix |
| List of Figures | xxiii |
| List of Tables | xxxv |
| List of Plates | xxxix |
| ABSTRACT | xxxxi |
| INTRODUCTION | 1 |
| Scope of the Investigation | 8 |
| Significant Processes and Responses in the Swash Zone | 8 |
| Scales of Time, Distance and Area | 10 |
| Nature of the Study Area | 13 |
| Wave Characteristics | 14 |
| Beach Profiles Selected for Experiments | 16 |
| Tidal Influences | 18 |
| PREVIOUS WORK | 20 |
| Shoaling Waves | 20 |
| Energy Dissipation in Shoaling Waves | 22 |
| The "Null Point" Hypothesis | 23 |
| Wave Steepness and Beach Cut and Fill | 25 |
| The Wave Drift Profile | 27 |
| Summary of Shoaling Wave Characteristics | 29 |

| | <u>Page</u> |
|--|-------------|
| Breakers | 31 |
| Energy Dissipation in Breaking Waves | 33 |
| Types of Breaking Wave | 35 |
| Asymmetries of Water Motion | 39 |
| Circulation of Water and Sediment through the Breaker | 41 |
| Swash Phase Relations | 44 |
| Summary of Breaker Conditions | 47 |
| The Swash Zone | 50 |
| Water Motion in the Swash Zone | 51 |
| Measurements of Swash and Backwash Velocity | 54 |
| Theory of Swash/Backwash Flow | 56 |
| Sediment Sorting in the Swash Zone | 63 |
| Morphological Changes in the Swash Zone | 68 |
| FLOW DYNAMICS | 74 |
| Characteristics of Fluid Flow | 75 |
| The Transition from Laminar to Turbulent Flow | 77 |
| Bed Roughness and its Effects on Fluid Turbulence | 78 |
| Gravity Waves | 83 |
| Regimes of Flow | 88 |
| The Transport of Sediment by Fluid Flow Settling Velocity | 91 |

| | <u>Page</u> |
|--|-------------|
| Theory of Sediment Entrainment | 93 |
| Initiation of Grain Motion | 96 |
| Saltation | 99 |
| Cessation of Motion | 100 |
| Rate of Bed Load Transportation | 102 |
| Suspended Load Transportation | 106 |
| Rate of Transport of Suspended Material | 112 |
| Total Transport in a Stream | 114 |
| Total Transport in a Wave Regime | 115 |
| Effects of Mixed Size Distributions on Transport Rate | 119 |
| Effects of Particle Shape on Transport and Deposition | 123 |
| Effects of Grain Roundness on Sediment Transport | 127 |
| Bed Morphology Resulting from Sediment Transport | 128 |
| Summary of Swash Zone Dynamics | 132 |
| INSTRUMENTS AND TECHNIQUES | 136 |
| Principles of Measurement | 136 |
| Instrumentation | 138 |
| A. Sensing Heads | 139 |
| 1. The Dynamometer | 139 |
| Calibration of the Dynamometer | 140 |
| Flow Parameters Sensed by the Dynamometer | 143 |
| 2. The Depth Guage | 145 |

| | <u>Page</u> |
|---|-------------|
| B. The Shore Unit | 146 |
| The Sediment Sampler | 150 |
| Bed Level Surveys | 151 |
| Laboratory Analysis of Sediments | 152 |
| GENERAL DYNAMICS OF THE SWASH ZONE | 157 |
| Runup Height | 157 |
| Flow Phase Relations in the Swash Zone | 159 |
| Distributions of Velocity in the Swash and Backwash | 162 |
| Velocity Profiles Across the Shore | 165 |
| Flow Reversals near the Breaker | 168 |
| Relative Energy Distributions Across the Swash Zone | 169 |
| Variations in Flow Energy with Breaker Height and Period | 171 |
| Summary of Phase Effects on Flow Energy and Velocity | 173 |
| ASYMMETRIES OF FLOW | 174 |
| Flow Discharge in the Swash and Backwash | 175 |
| Water Circulation through the Swash Zone | 175 |
| Asymmetries of Flow at the Bed | 179 |
| The Transport of Sediment in Asymmetric Flows | 184 |
| Longinov's Method | 186 |

| | <u>Page</u> |
|---|-------------|
| TURBULENCE IN THE SWASH ZONE | 194 |
| Velocity Fluctuations at a Point | 195 |
| Distributions of Velocity and Pressure in Swash and Backwash Flows | 198 |
| Relative Intensity of Turbulence | 201 |
| A. Distribution Across the Shore | 201 |
| B. Vertical Distribution of Turbulence | 203 |
| Turbulence Factor | 204 |
| The Scale of Turbulence | 206 |
| Variations in Flow Regime | 210 |
| Bed Roughness | 210 |
| Standing Waves and Hydraulic Jumps | 213 |
| Case 1 | 216 |
| Case 2 | 217 |
| Effects of Varying Breaker Heights on Backwash Scour | 218 |
| FLOW TURBULENCE, FLOW ENERGY APPLICATION AND FORESHORE EROSION | 220 |
| Discussion of Flow Processes | 221 |
| Relations Between Flow Volumes, Flow Regimes and Elevation Change | 225 |
| Net Deposition | 226 |
| Erosion and Deposition | 226 |
| Erosion of the Profile | 229 |

| | |
|--|-----|
| BED SEDIMENTS | 233 |
| Mean Size and Sorting of Swash Zone Sediments | 235 |
| Statistical Aspects of Grain Size Distributions | 239 |
| Characteristic Grain Size-Frequency Distributions | 242 |
| Size-Frequency Distributions at Different Points Across the Shore | 244 |
| MODE AND RATE OF TRANSPORT OF BED SEDIMENTS | 248 |
| Vertical Distributions of Transported Sediment | 249 |
| Mode of Sediment Transportation | 255 |
| Rates of Sediment Transport Across the Profile | 260 |
| Relations Between Transport Rate and Measured Flow Properties | 266 |
| Particle Dynamics | 269 |
| Depth of Disturbance | 273 |
| SEDIMENT SORTING IN THE SWASH ZONE | 276 |
| Sorting for Size | 276 |
| Effects of Transport Rate on Bed Distributions | 283 |
| Flow Phase State and Sediment Sorting | 289 |
| Shape Sorting in the Swash Zone | 292 |
| Sorting of Sediments by the Groundwater Sheet | 299 |

| | |
|---|-----|
| TIDAL VARIATIONS IN SWASH ZONE PROCESSES | 307 |
| Variations in Flow Energy through the Tide | 308 |
| The Tidal Cycle of Changes in Morphological and Sediment Characteristics | 311 |
| CONCLUSIONS | 321 |
| SUMMARY OF PRINCIPAL RESULTS | 333 |
| SUGGESTIONS FOR FURTHER RESEARCH | 337 |
| ACKNOWLEDGEMENTS | 341 |
| REFERENCES | 343 |
| GLOSSARY OF TERMS | 367 |
| LIST OF SYMBOLS | 372 |

LIST OF FIGURES

| <u>Figure No.</u> | | <u>Following Page</u> |
|-----------------------|--|---------------------------|
| 1. | Location of the study area | 13 |
| 2. | Beach profiles selected for study | 16 |
| 3A. | Shoaling wave characteristics | 20 |
| 3B. | The swash and breaker zones | 20 |
| 4. | Displacement of mean and maximum water levels during breaking and runup | 34 |
| 5. | Relations between wave steepness, beach slope and breaker type | 35 |
| 6. | Surface profiles for three types of breaker | 36 |
| 7. | Asymmetries of wave motion in the nearshore zone | 39 |
| 8A. | Water circulation in the breaker zone | 42 |
| 8B. | Two idealised types of circulation system | 42 |
| 9. | Phase properties of breakers and swash | 45 |
| 10. | A comparison of Solitary waves and swash | 56 |
| 11A. | Theoretical critical swash lengths | 61 |
| 11B. | Theoretical critical swash velocities | 61 |
| 12A. | Theoretical sediment sorting under low energy conditions | 65 |
| 12B. | Theoretical sediment sorting under high energy conditions | 65 |
| 13. | Zones of profile erosion and deposition under equilibrium conditions | 69 |

| <u>Figure No.</u> | | <u>Following Page</u> |
|-----------------------|---|---------------------------|
| 14. | Tidal Cycle of changes in an equilibrium beach | 70 |
| 15A. | Turbulent exchange in a hydraulic jump wave | 85 |
| 15B. | Surface profile of a standing wave system | 85 |
| 16. | Regimes of flow in a broad, open channel | 88 |
| 17. | Relation of grain diameter to settling velocity, threshold velocity and roughness velocity | 94 |
| 18. | Competent velocity of sediment motion | 99 |
| 19A. | Relation of concentration ratio of suspended sediment to the threshold velocity | 110 |
| 19B. | Relations between flow velocity, grain size and state of sediment motion | 110 |
| 20. | Forms of bed load transportatinn in relation to current speed and grain size | 128 |
| 21A. | Principal units of the instrument system | 137 |
| 21B. | Operating positions of the units in the swash zone | 137 |
| 22. | The Dynamometer | 138 |
| 23. | Calibration curves for the Dynamometer | 142 |
| 24. | Electronic circuitry of the instrument system (<u>In pocket</u>) | |
| 25. | The sediment sampler | 150 |
| 26A. | The relation between runup height and breaker height | 158 |
| 26B. | Mean swash length as a function of breaker height | 158 |

| <u>Figure No.</u> | | <u>Following Page</u> |
|-----------------------|--|---------------------------|
| 27A. | The relation between phase ratio and swash length | 159 |
| 27B. | Variations in breaker height and swash length | 159 |
| 28. | Typical Dynamometer velocity traces | 162 |
| 29A. | Distributions of swash and backwash velocity | 165 |
| 29B. | Shore-normal profiles of swash and backwash velocity | 165 |
| 30. | Flow reversals at lower foreshore stations | 168 |
| 31A. | Distribution of mean swash energy across the shore | 170 |
| 31B. | Distribution of mean backwash energy | 170 |
| 31C. | Distribution of net mean relative energy level | 170 |
| 32. | Frequency distributions of swash and backwash energy at different breaker heights | 171 |
| 33A. | The "Water Budget" of the swash zone | 176 |
| 33B. | Discharge profiles for swash and backwash | 176 |
| 34. | Net swash zone discharges | 178 |
| 35. | Asymmetries of swash/backwash flow for three breaker conditions | 181 |
| 36. | Relation between asymmetry of flow times and net mean relative energy level | 182 |
| 37A. | Critical erosion velocities in relation to velocity traces | 187 |
| 37B-E. | Longinov proportional net pressure diagrams | 187 |

| <u>Figure No.</u> | | <u>Following Page</u> |
|-----------------------|---|---------------------------|
| 38. | Cumulative probability distributions of swash and backwash velocity fluctuations | 199 |
| 39. | Cumulative probability distributions of swash and backwash pressure fluctuations | 199 |
| 40A. | Relative intensity of turbulence at different points across the shore | 201 |
| 40B. | Relative intensity of turbulence at different positions above the bed | 201 |
| 41A. | Turbulent eddy sizes at different positions across the shore | 208 |
| 41B. | Sizes of turbulent eddies at different elevations above the bed | 208 |
| 42. | Particle sizes and flow speeds of swash zone sediments in relation to flow type | 211 |
| 43. | Flow regimes in the swash zone | 215 |
| 44A. | Backwash flow depth and velocity profiles | 216 |
| 44B. | Backwash Froude number plots | 216 |
| 45. | Backwash Froude number profiles for varying breaker heights | 218 |
| 46. | Changes in foreshore elevation as a function of net mean relative energy level | 224 |
| 47A. | Relations between foreshore change and flow processes for surge and low phase flow | 226 |
| 47B. | Flow-foreshore relations for transition phase conditions | 226 |

| <u>Figure No.</u> | | <u>Following Page</u> |
|-----------------------|--|---------------------------|
| 47C. | Flow-foreshore relations for high phase flow states | 226 |
| 48. | Bed sediment size-frequency distributions | 242 |
| 49. | Size-frequency distributions from different points across the shore | 244 |
| 50. | Size-frequency distributions from different points across the shore | 246 |
| 51. | Size-frequency distributions of suspended sediments | 250 |
| 52. | Vertical concentration gradients of transported sediments | 251 |
| 53. | Dominant mode of transport of swash zone sediments | 256 |
| 54. | Four profiles of net dynamic sediment transport rate and foreshore elevation change | 263 |
| 55A. | The relation between dynamic bed load transport rate and rate of bed elevation change | 266 |
| 55B. | Relation between flow power expended at the Dynamometer and dynamic rate of sediment transport | 266 |
| 55C. | The relation between mean maximum current speed and dynamic rate of sediment transport | 266 |
| 56. | Depths of bed disturbance in the swash zone | 273 |

| <u>Figure No.</u> | | <u>Following Page</u> |
|-----------------------|--|---------------------------|
| 57. | Vertical distributions of mean nominal diameter in the swash and backwash | 277 |
| 58. | Net transport rates of bed load component size fractions across the shore | 278 |
| 59. | Effects of differential transport rates on local bed sediment distributions | 283 |
| 60. | Tidal fluctuations in mean energy envelope curves | 308 |
| 61. | Characteristic tidal cycle of transitional conditions on coarse gravels | 312 |

LIST OF TABLES

| <u>Table No.</u> | | <u>Following Page</u> |
|------------------|---|-----------------------|
| 1A | Swash zone process and response factors studied | 8 |
| 1B | Conceptual model of swash zone process/response relationships | 9 |
| 2. | Published measurements of swash/backwash velocities | 54 |
| 3. | Limits of flow regimes | 87 |
| 4. | Sizes and velocity ranges of dynamometer plates | 141 |
| 5. | Summary of data records obtained with the dynamometer | 149 |
| 6. | Swash/backwash discharges and levels of groundwater storage | 177 |
| 7. | Mean and maximum pressures recorded in the swash zone | 180 |
| 8. | Example of proportional net pressure calculations | 186 |
| 9. | Turbulence levels associated with velocity fluctuations | 200 |
| 10. | Turbulence factors of pressure fluctuations | 205 |
| 11. | Approximate Reynolds Numbers and Drag Coefficients of bed sediment grains in the swash zone | 270 |

| <u>Table No.</u> | | <u>Following Page</u> |
|----------------------|---|---------------------------|
| 12. | Percent pebble shapes in samples trapped in the swash and backwash | 295 |
| 13. | Shape sorting coefficients for samples trapped in the swash and backwash | 296 |
| 14. | Mean field permeabilities for the upper part of the swash zone | 302 |
| 15. | Velocity levels attained by effluent groundwater runoff | 304 |

LIST OF PLATES

| <u>Plate No.</u> | | <u>Following Page</u> |
|----------------------|---|---------------------------|
| 1. | Steep, well sorted shingle profile, Station B, South Bay | 17 |
| 2. | Flatter, mixed sand/shingle profile, Station D, South Bay | 17 |
| 3. | The Dynamometer and the mounting used to obtain records near the bed | 139 |
| 4. | The Dynamometer and one of the mountings used for obtaining vertical velocity profiles | 139 |
| 5. | The Shore Unit showing the recorder and amplifier/control panels | 147 |
| 6. | Low phase swash conditions | 227 |
| 7. | Transition phase flow conditions | 227 |
| 8. | High phase flow under storm conditions | 230 |
| 9. | Saltation of sediment grains in the upper, forward portion of swash flow | 258 |
| 10. | Rhomboidal ripple marks on mixed sand/shingle at Station C. | 305 |
| 11. | Well developed rill marks on the central and lower foreshore at Station D. | 305 |

ABSTRACT

While much work in coastal geomorphology has been concerned with the analysis and description of morphological and sedimentological changes occurring on the sub-aerial beach face, relatively little effort has been applied to the detailed investigation of the processes responsible for the production and modification of these features.

Only scattered, fragmentary observations of such fundamental properties as swash velocity, backwash velocity, flow depths and durations exist in the literature and these data have been poorly co-ordinated with other information relating to input wave parameters, grain size, slope and profile dimensions which is necessary to a complete understanding of the forces governing swash zone morphology.

In an effort to bridge this gap an instrument system has been designed and constructed for the measurement of flow speeds, pressures, asymmetries, depths, levels of groundwater storage and outflow, and of flow durations. In association with the observations of these and other process factors several responses to the flow regime were also sampled. These included alterations to grain size parameters of bed sediments, transport rates of solids in the swash and backwash, vertical distributions of sediment in both swash and backwash, and changes in bed elevation.

An electromechanical force-plate dynamometer was employed

for the measurement of flow speed and duration and a small parallel-wire gauge sensed depth fluctuations in swash and backwash flows. The output from both of these units was recorded on a strip chart for later analysis.

A total of twentyone data sets were derived in this way from four profiles located on mixed sand/shingle beaches at Kaikoura, east coast, New Zealand. Two profile stations have steep, well sorted shingle foreshores while the other two are flatter and are composed of mixed sand and shingle. A wide range of breaker heights, periods and types is received at all four stations. More than 3,000 individual measurements of swash/backwash flow conditions were obtained from these four stations under varying wave, tide and foreshore conditions.

Analysis of this and associated data relating to sediment transport indicates that the flow/sediment system of the swash zone on the study beaches is bounded approximately by current speeds of 100 to 250 cm/sec. and by grain diameters of 1.0 to 50.0 mm. Because of the high energy nature of the system and the large range of grain sizes available for transport, the conditions for initiation of motion are rapidly and frequently exceeded and particles are transported at high rates. Sorting processes are thus dependent upon the net rates of transport of individual size fractions in the flows rather than on critical selection of individual sizes from the bed. The latter situation applies only to very large particles and these are quantitatively infrequent on the study beaches.

The concentration profiles of entrained sediments in the water column vary with differences in turbulent structure so that mean current speed is a poor estimator of flow sediment load. Between 50 and 95% of the sediment load in both the swash and backwash occurs in the lower one tenth of the water column so that transport is dominantly in the bedload phase. This feature is especially pronounced in the backwash. Bedload sediment motion in the swash zone occurs mainly in the form of sheet flow, though antidunes may be formed in the backwash and saltation is locally important near the swash limit.

Energy levels in both the swash and backwash rise with increasing wave height and period, the backwash becoming dominant at higher energy levels. The chief determinant of the flow structures and morphological results of given flow regimes is the phase ratio of swash period to breaker period. For low values of the ratio there is little interference between incoming and outgoing flows, up to one third of the swash volume may be stored in the beach, the flow regime is dominantly tranquil, and the foreshore accretes. Circulation of sediments through the breakers is intermittent and would appear to occur mainly in rip currents.

For values of the ratio near unity (transitional conditions) a scour zone is developed by the backwash owing to alterations in flow structure during downslope passage of the water and some erosion occurs, thus offsetting swash deposition to some

extent. At high values of the ratio interference between incoming and outgoing flows is continual. The backwash scour zone is very wide and seaward circulation of sediments through the breaker is continuously developed. Flow turbulence and asymmetries are at maximum levels and suspended-load transport accounts for a quantitatively significant proportion of total load transport. The foreshore erodes intensively.

Characteristic sediment sorting processes are associated with these flow regimes. Tranquil, low energy conditions result in truncation and mixing of the finer fractions. Polymodal or bimodal size-frequency distributions may be produced by deposition at the swash limit. For higher energy flow regimes transport of whole bed size ranges occurs, though individual component fractions may move at differing net rates and in net opposite directions. Where wide ranges of sizes occur on the bed bimodal distributions are produced by backwash scour owing to selection and preferential erosion of a mid-range fraction.

Owing to the retarding effect of groundwater storage all of these processes have a strong tidal aspect with maximum swash and backwash energy levels occurring some time after high water during the ebb tide phase. High rates of groundwater return to the backwash may result in significant fluidisation of bed sediments. Residual groundwater flow in the form of thin surface sheets results in the formation of rills and rhomboidal ripple marks.

INTRODUCTION

In recent years the search for a more satisfactory explanation of the processes controlling beach erosion and deposition has resulted in the application of more sophisticated instrument systems, sediment tracing techniques, and analytic techniques to problems of coastal research. However, most of this endeavour has been concentrated upon the zone seaward of the breakers where the movements of water and sediment are at least partially amenable to treatment by the notions of classical wave mechanics.

On the other hand, however, the study of shore-face erosion and deposition in the zone of breaking waves and runup has proceeded little beyond the earliest qualitative descriptions of the types of water motion occurring. Investigators have succeeded only in defining the factors that cause variations in breaker type and in linking these in a general manner to types of foreshore response. In contrast to the difficulties of breaker study, changes in foreshore elevation have been repeatedly surveyed in great detail by numerous workers.

Concerning this situation Kemp (1958, p. 45) has noted that the terms "destructive" and "constructive" waves have been common in the literature for well over a hundred years

and that investigators are still forced to classify waves at the shore in relation to their effects on it rather than in terms of their innate flow properties.

While breakers have not proved susceptible to detailed theoretical analysis, the surge phenomena of swash and backwash resulting from breaking have been comparatively little studied. The latter are of special importance on a steep shingle beach where there is little tidal translation of the breakers. Therefore, much of the erosion and deposition occurring on such beaches is occasioned by swash and backwash.

Thus, the primary aims of this investigation are to describe the nature of the water movements in the swash zone and to assess the relations between them and sediment transport. Added importance is given to the study of such problems since Zenkovich (1967, p. 262) notes that wide beaches are the best protection for any coast against erosion and that the creation and maintenance of wide beaches is one of the main objects of coastal defences.

As many authors have noted investigations of coastal problems were given a considerable impetus during World War II and since that time work has proliferated on a number of fronts. These appear to have crystallised around two principal themes; the first of these being what will be termed an analytic approach, and the second being a deductive approach.

The analytic approach has been essentially theoretical in nature with workers concentrating on the application of

classical wave mechanics to problems of coastal erosion and sedimentation. Waves and the transformations induced in them by varying bottom conditions have been examined across the whole shoaling range from deep water to breaking. Work has been mainly concerned with describing the nature of water motion under particular shoaling ranges, and with relating these movements to changes in beach volume. Munk (1949) for example, is concerned entirely with the applicability of solitary wave theory to water motion near the breaker zone.

Probably the most popular technique applied under this approach has been dimensional analysis of the particular phenomena under study, combined with experimental correlation of selected groups of dimensionless parameters under controlled conditions in wave tanks. The relations between wave steepness and beach erosion and deposition have been extensively studied in this manner (Waters, 1939; Bagnold, 1940; 1947; Watts, 1954; Ippen and Eagleson, 1955; Hayami, 1958; Kemp, 1958; and others). Most of these deal with the area seaward of the breakers. However, those which are concerned with the area landward of the breakers are almost exclusively devoted to the problems of predicting runup and overtopping due to long waves such as those generated by tsunamis (Grantham, 1953; Savage, 1959; Saville, 1962; Muraki, 1966; and Van Dorn, 1966).

On the other hand, the deductive approach has been dominated by field investigations having a statistical rather

than a theoretical bias. Most work here has been concerned with the zone landward of the breakers. Foreshore sediments and changes in bed elevation have been sampled and correlated generally with gross changes in the energy level of incident waves (Dolan and Ferm, 1966; King, 1951; Zeigler, Hayes and Tuttle, 1959; Schiffman, 1965; Sonu and Russell, 1966; and others). Harrison, Pore and Tuck (1965) were able to develop predictor equations linking beach processes and responses for a limited range of foreshore types and Krumbein (1947; 1959) has extensively examined the use of statistical techniques in the "sorting out" of geologic variables in the littoral environment.

This approach has also witnessed the development and extensive use of fluorescent tracers (e.g. Ingle, 1966; Yasso, 1965), and of radioactive indicators (e.g. Davidsson, 1958; Kidson, Carr and Smith, 1958; Kidson and Carr, 1959); in studying a wide range of problems involving sediment on or seaward of beaches. As well, a number of other studies have dealt with the bed forms found on the sub-aerial beach (e.g. Demarest, 1947; Evans, 1951; and Emery and Gale, 1951).

However, all of these studies suffer a common difficulty in that detailed information on the processes causing foreshore change, ripple formation or tracer dispersion is usually lacking. At best crude information on flow velocity has been obtained by timing floats or dye patches, and frequently process factors thought to be applicable in field studies are

described by analogy with laboratory studies or with hydraulic theory.

Further, Ingle (1966) pointed to what is, at best, only a partial correlation between field and laboratory investigations. This is largely because:-

"qualitative and quantitative field investigations of (sediment) movement have been carried out almost entirely in the hydrodynamically complex area shoreward of the breaker zone. Conversely most model studies of sediment motion have been conducted under conditions simulating those in the area seaward of the breaker zone, which is a comparatively simple hydrodynamic environment" (Ingle, 1966, p.101).

Of the analytic investigations Van Dorn (1966, pp. 21-23) has said:-

"there is no continuous self-consistent mathematical description of the behaviour of a periodic wave system of finite height, originating in deep water, propagating normal to the shore over an arbitrary bottom profile and terminating in uprush and/or reflection from the shoreline. Instead there exists a large number of piece-wise solutions, each of which treats a certain class of waves over a limited range of transformation, until the asymptotic domain of its boundary conditions is exceeded, at which point one must jump to another solution until the shore is finally reached. An investigator who wants to know what happens at the beach, beginning in deep water must then jump several mathematical hurdles in passing from the beginning to the end state, attempting during this process to maintain continuity in wave amplitude and slope, while conserving some property such as displaced volume, energy or momentum. Unfortunately, one has no assurance that these properties are conserved - and, in general, they are not. Energy, for example, is lost continuously all along the route; some is reflected, some is lost in bottom friction, and a great deal is lost in turbulence if the wave breaks".

To this we should add the problems of understanding the relations between wave motion of any given type and the

sediment entrainment processes.

Because of these transformations in shoaling waves Dolan and Ferm (1966, p. 210) argued that, "waves per se have little direct effect on the sub-aerial beach except in the form of swash and backrush" and for similar reasons Van Dorn regarded his expressions for the runup characteristics of long waves as "recipes", rather than as solutions of the problem.

It is therefore clear that, at the present time, a more complete description of the forces governing beach erosion and deposition would be greatly aided by detailed field studies of the breaker and swash zones. It is in these areas where the application of wave energy is most intense and where theory is least satisfactory.

It has been shown that these environments are hydrodynamic-ally complex. This is because water movements in the onshore and offshore directions are highly asymmetrical with respect to time and space and because the impulse pressures comprise both a hydrostatic component due to depth of water, and a dynamic component due to the accelerations and decelerations of the water masses. Also, it has been demonstrated that there is a gap in knowledge between studies of beach face response to wave action (the deductive approach) and the studies of variation in offshore waves and bottom morphology (the analytic approach). This problem area of the beach environment is occupied by the breaker and swash zones.

This investigation is concerned with only one of these areas, the swash zone, and since the flow phenomena are so complex, "experiments conducted in wave tanks with fixed beach slopes are considered to be of limited value in the understanding of wave action in the beach zone" (Kemp, 1958, Vol.2, p.3). Therefore, with regard to the present state of knowledge, it is suggested that investigation of the swash zone might be best served by a detailed field investigation of the variations in water motion and sediment transport in order to more closely integrate field and laboratory studies of the beach environment.

The study is presented in two major portions. The first is concerned with assessing the contributions of previous studies to the description of morphologically significant foreshore processes. It also deals with the methodology of beach foreshore studies and attempts to delineate those areas where future research is most needed. Since there is little explicit theoretical basis to much of the work in the literature a review of the appropriate notions of water and sediment motion (derived largely from fluvial hydraulics), has been included.

The second section of the report is concerned with the application and testing of the views developed in the first portion using a large body of data gathered from the swash zone of natural mixed sand/shingle beaches.

Scope of the Investigation

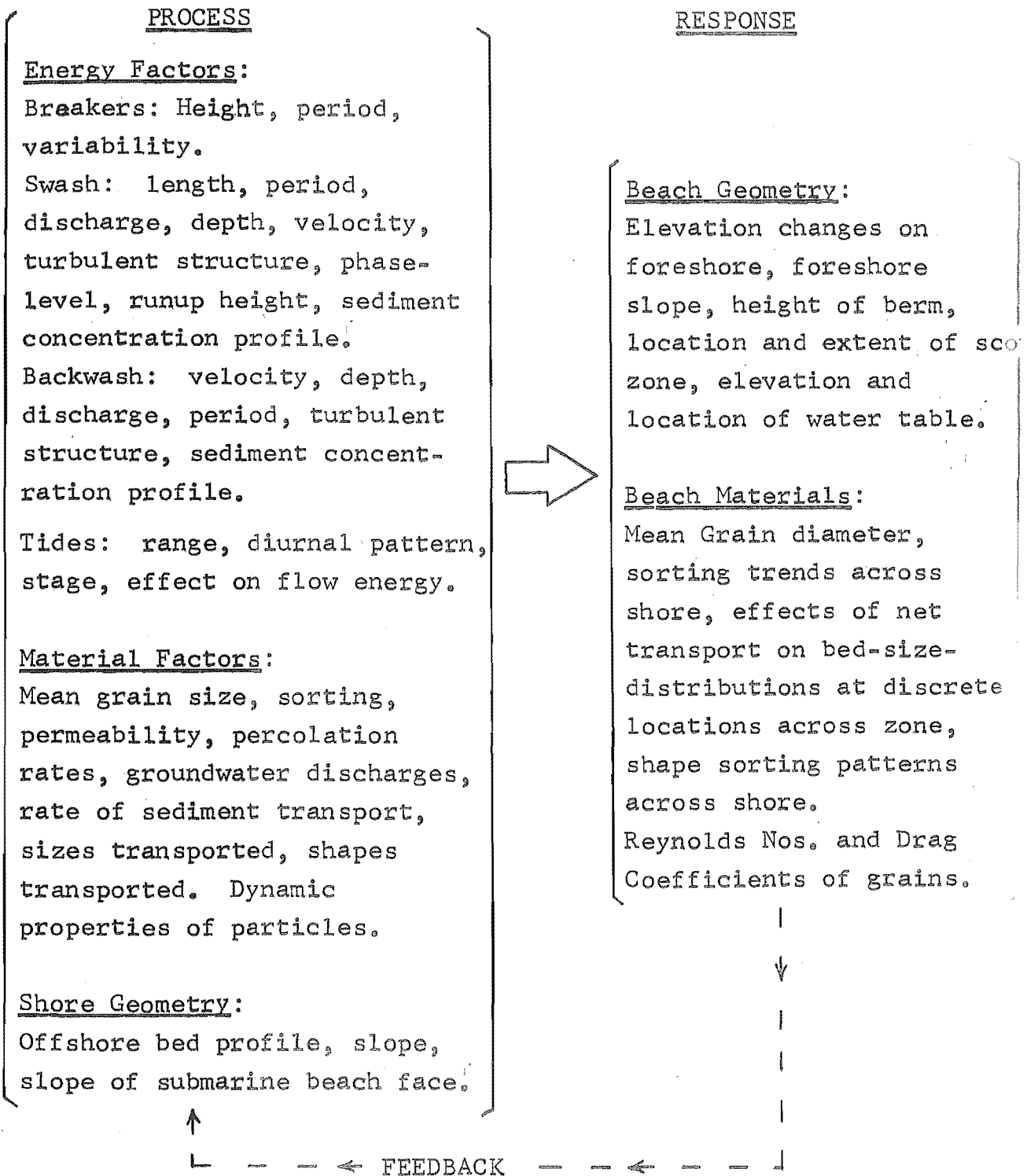
Since there have been few previous studies of the detailed nature of swash zone processes, the first requirements of the present investigation were the selection, design and development of instruments and techniques that would be capable of sampling water and sediment movements in the swash and back-wash.

Swash zone flow phenomena are of short duration and vary continually in depth and velocity. Also, Krumbein and Slack (1956) have noted that it is a zone characterised by wide variations in grain size and sorting. Therefore a statistical or sampling approach to the problem of gathering data on the various process and response factors has been adopted in this investigation.

Significant Processes and Responses in the Swash Zone. Since the swash zone is a hydrodynamically complex environment in which a relatively large number of variables interact to influence shore morphology, there is considerable utility in the adoption of a conceptual framework which expresses the functional organisation of all of the important factors. The general format of the "Process-Response" model of Krumbein (1963) has been adapted for this purpose. Such an approach is extremely useful since it enables the arrangement of a large number of process and response factors into what are thought to be significant groupings, any combination

TABLE 1A

Swash Zone Process and Response Factors
Examined in this Investigation



of which may be selected for detailed study. Thus, "in part, the search for an optimum model (of beach processes and responses) requires a search for the underlying principles of data interlock and feedback so that these can ultimately be expressed in functional relationships" (Krumbein, 1963).

Table 1A lists all of the major variables studied during this investigation under the general headings of "Process" and "Response". Independent process factors can be seen to include input wave characteristics and the tidal forces. The ultimate response factors dependent upon the action of the process forces include alterations to foreshore elevation, slope and particle characteristics. The complexity of the system is indicated by the fact that many of the variables listed in the table may be regarded as either processes or responses.

Thus, to some extent, the characteristics of beach materials and foreshore geometry obtaining at any given time will influence subsequent events until such time as full adjustment between processes and responses is achieved. For example, the foreshore slope "inherited" from past periods of swash/backwash action will determine to some degree, the distribution of swash and backwash energy at any given subsequent point in time. Foreshore slope, an ultimate response factor, may thus "feed back" as a short term process influencing future slopes.

Principal variables studied in this investigation which

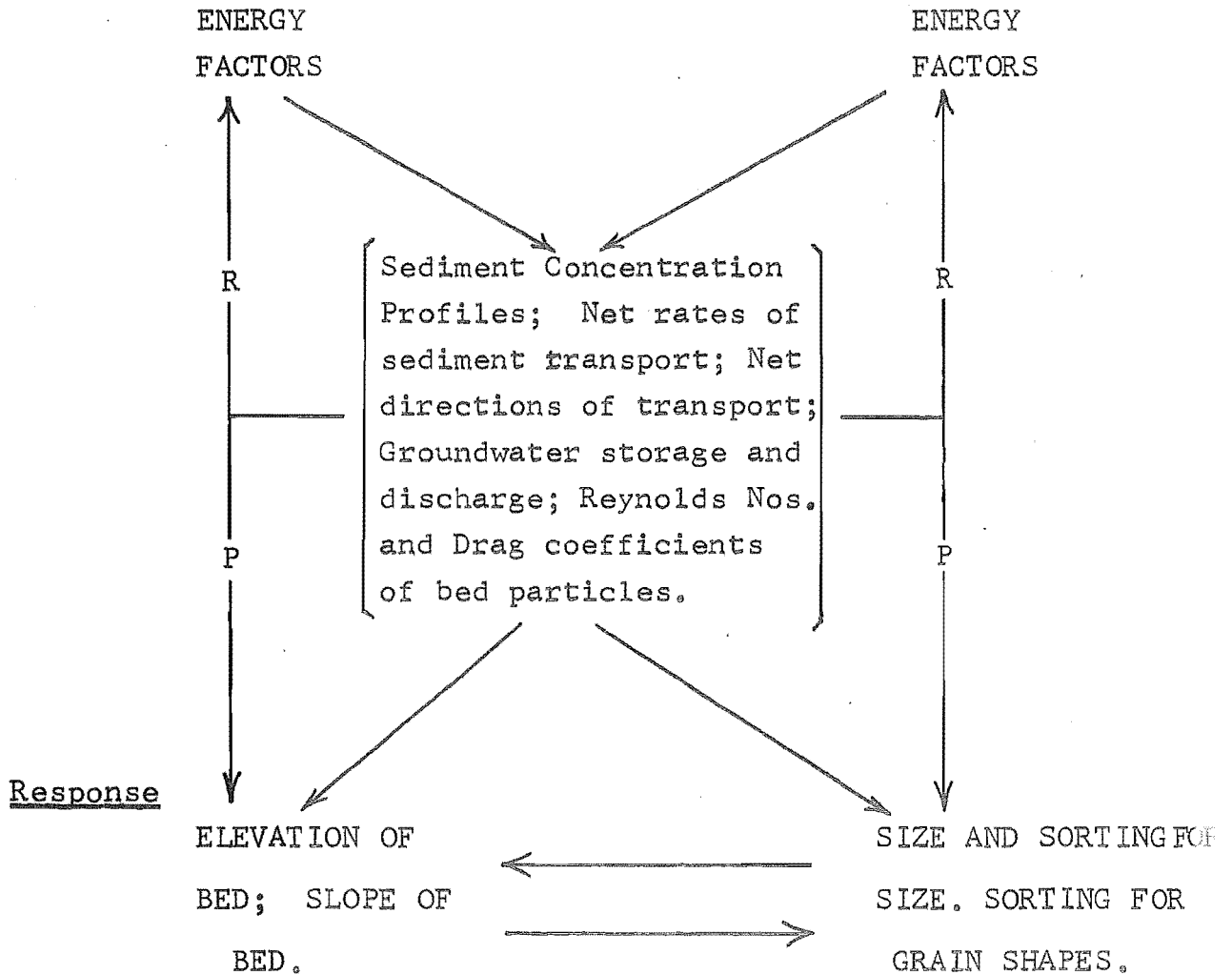
TABLE 1B

Conceptual Model of Processes and Responses
Affecting Swash Zone Morphology and Bed
Material Characteristics

MORPHOLOGY

MATERIALS

Process



R = Response

P = Process

may be viewed as both processes and responses are shown in Table 1B. Sediment concentration profiles in both swash and backwash for example, are thus responses to flow speed and structure (energy factors) but they may also be viewed as primary processes controlling foreshore morphology and beach material characteristics.

These variables possessing intermediate degrees of dependency and which are capable of dual functions are thus potentially of great value in the study of shore morphology and it will become apparent that many new insights into the action of coastal processes derive from their detailed examination.

Scales of Time, Distance and Area. Complexity of the swash zone environment derives not only from the relations and interactions among variables but also from the very variable scales of time and distance over which the actions and reactions outlined above occur.

Schwartz (1968) investigated the literature on beach changes in order to assess the mean times required to regain an equilibrium profile following alterations in process factors that ranged in magnitude from variations in waves through tidal fluctuations to major changes of mean sea level. He assigned the term "micro-scale" to responses occurring in the swash zone over single tidal cycles and concluded that bed level fluctuations averaged 12 cm. The mean time required to restore equilibrium of the profile after disturbances

of this magnitude was of the order of 30 minutes.

Two further features characterising the swash zone may be drawn from this. First, it is clear that changes occur rapidly in the swash zone; and secondly that the various process and response factors operate at a number of widely differing time scales. For example, study of water and sediment motion in both the swash and the backwash requires observations over a period of seconds whereas a time scale of minutes or even hours is more appropriate to the analysis of the bed changes resulting from these processes.

For these reasons the present study has been confined to the sampling of water and sediment flow conditions on a time-mean rather than an instantaneous basis. Velocity fluctuations at given places on the shore have been recorded as means over short periods of from two to five minutes. Sediment transport past these points has been treated in a similar fashion, while changes in bed elevation were measured at hourly intervals through the tidal cycle.

On the other hand, the analysis of the data gathered in the above manner falls into two parts. The first of these is concerned with establishing the nature and intensity of sediment motion in the swash and backwash respectively, while the second deals with the overall erosive effects of a given swash/backwash flow regime. Hence, both the swash and the backwash may be thought of as flowing masses of water each

capable of moving bed materials, and each having characteristic velocities, periods and structures. On the other hand, the net erosive effect over a period of hours may be regarded as a function of the relative efficiencies and rates of transport in the offshore and onshore directions.

With regard to the first aspect it will be shown that water motion in the swash consists of the mass translation of water onshore in the form of a surge and that the corresponding backwash occurs in the form of a mass flow of water accelerating under the influence of gravity. Therefore, the individual flows can be considered to possess at least some of the properties of river flow in a broad, open channel. In such a situation the wetted perimeter of the channel is closely approximated by the flow depth. Thus, the present study is confined to changes in two dimensions across the shore.

Variations in processes and responses across the shore are examined in profile only. Effects due to lateral circulation of water or longshore drift of sediments are not specifically considered in this study. A further consequence of this approach is that the investigation of flow structures and sediment transport draws heavily on the notions of fluvial hydraulics. Swash and backwash in these respects are treated as distinct but closely related flow phenomena.

Finally, the assessment of the net erosive effects of a given set of wave/foreshore conditions has been approached

by considering the relative water volumes entering and leaving the swash zone at a given time, together with the time periods occupied by each type of flow. It will next be shown that this has been done for four fundamentally different sets of foreshore conditions and a wide range of incident wave conditions. It is this latter (or "budget"), step of the analysis which may be hoped to provide the link with previous studies concerned with the correlation of input wave characteristics and changes in foreshore elevation.

Nature of the Study Area

The areas selected for field study of the above problems are the mixed sand and shingle beaches located to the north and south of Kaikoura Peninsula on the east coast of South Island, New Zealand. The locations of this section of the coast and of the sites of the experiments are shown in Figure 1. As can be seen from the diagram the coastline is aligned NE/SW and faces to the south-east. This is typical of many beaches along the east coast of the South Island. The two major mixed sand/shingle beaches shown in Figure 1 are separated by the Tertiary limestone and mudstone series of the Kaikoura Peninsula. The dominant mineralogy of the study beaches is greywacke.

The northern beach is some ten miles long while its southern counterpart stretches only half of this distance. The central location and seaward projection of the peninsula

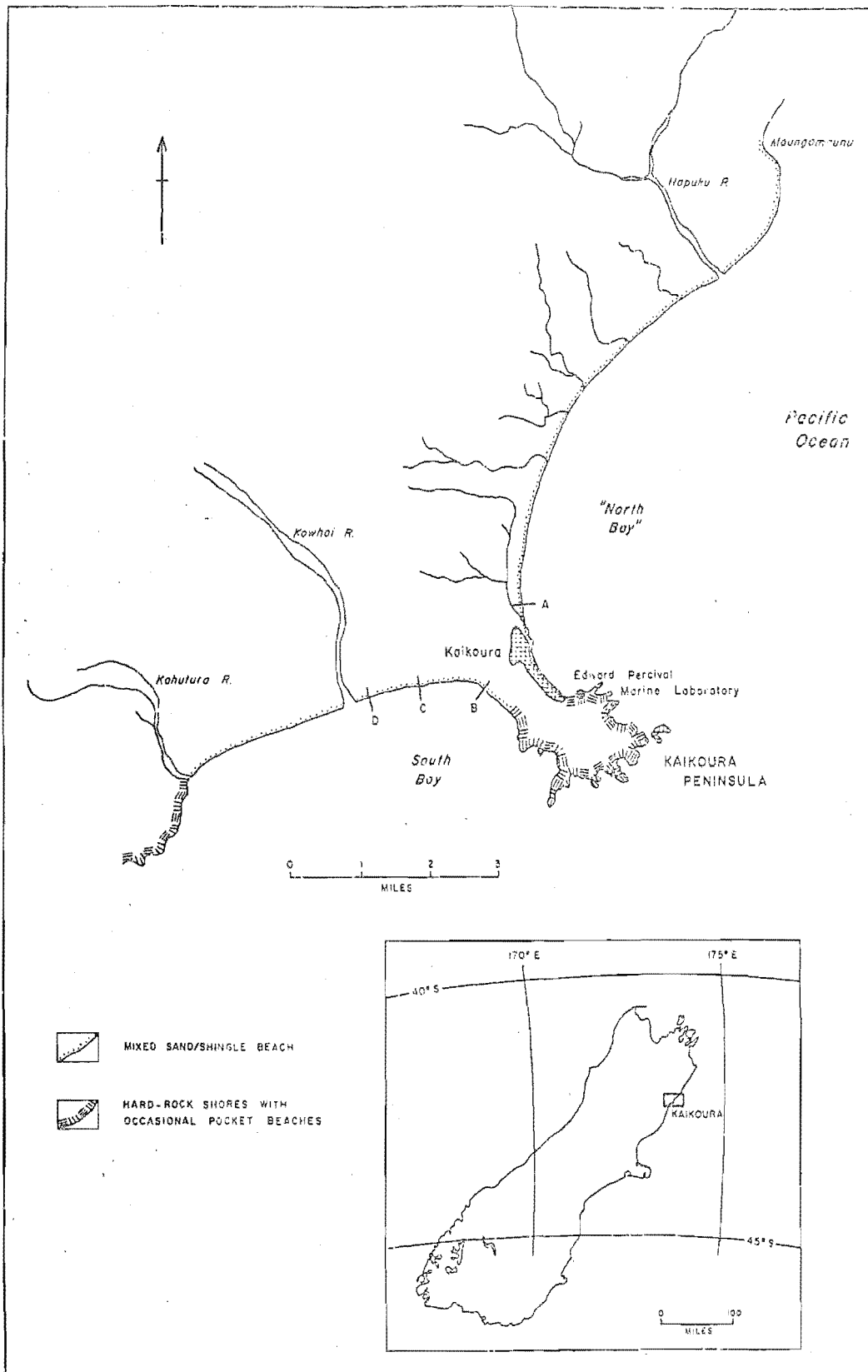


FIGURE 1. Location of the study area.

have important effects on wave refraction in the area, which result in significant longshore variations in wave height and energy for most wave approach directions.

The continental shelf off Kaikoura is narrow so that ocean swell is little modified by shoaling during its passage toward the shore. Also, the beaches drop steeply into deep water seaward of the breaker zone so that shoaling transformations occur predominantly over very short distances. The resulting breakers are usually of the plunging type so that the surf zone is never wide. Exceptions to this pattern are found in areas where the degree of wave refraction is sufficient to reduce wave energy to a low level. This is especially true of the areas where the beaches abutt the Kaikoura Peninsula. In addition, during storms from the south when both wave height and length are large, waves "feel bottom" some distance offshore. The crests then spill considerably before finally plunging onto the beach face. Similar effects are produced when these waves are accompanied by strong following winds.

Wave Characteristics. McLean (1969, pers. comm.) has studied the relations between short and long term variations in beach morphology and sediments along the two beaches. This work included the gathering and analysis of data on aspects of the local "wave climate". It is clear from this that the shores of the study area are of the east coast

swell type of Davies (1964). As well they are high energy shores in terms of the classification of Tanner (1960), since mean annual wave height is in excess of 50 cm. Wave heights average 1-2m. at the shore and storm waves are typically 3-5m. high (McLean and Kirk, 1969, p. 143). Such waves result in highly turbulent swash and backwash at the shore.

It is apparent from Figure 1 that fetches in directions lying north, east and south of the beaches are unlimited. Therefore it is likely that both waves emanating from storm centres far out in the Pacific and more locally generated waves are received.

Analysis of 330 daily observations from the Edward Percival Marine Laboratory in Kaikoura as well as of several sets of observations made on given days north and south along the beaches indicate two features of importance regarding the waves breaking on the beaches. First, there is only slight variation in the distributions of wave height with either seasonal progression or approach direction. High waves may be received from all directions at any time of the year, but there is some tendency for higher waves to occur in spring, winter and autumn. On the other hand, there is a significant variation in wave period. This is strongly correlated with approach direction. Thus, waves from the southerly quarter are associated with periods in the range 10-11 seconds while those from the north-east have characteristic periods in

the range 7-8 seconds.

Secondly, within this setting there are significant longshore variations in wave height. Breaker height tends to increase away to the north and south of the peninsula but for either a given north-east or southerly wave train there is a corresponding lee effect to the south or north of the peninsula respectively.

Thus, the beaches were considered ideal for the type of experiment conducted in this investigation since a wide range of breaker and swash conditions was available at any one time along the shore. Also, the incidence of storm waves did not necessarily hinder field work. This was because frequently a suitable alternative site could be adopted on the lee side of the peninsula. Finally, it will be shown that this lee effect also made it possible to study swash and backwash resulting from a range of breaker types.

Beach Profiles Selected for Experiments. Figure 1 indicates the stations selected as experimental sites and the characteristics of these are shown in Figure 2. Selection was based on the need to cover a representative range of foreshore types and water motions. It can be seen from Figure 2 that four stations were chosen. Of these three are to the south of the peninsula and one lies to the north. Figure 2A indicates that the profiles increase in width from north to south.

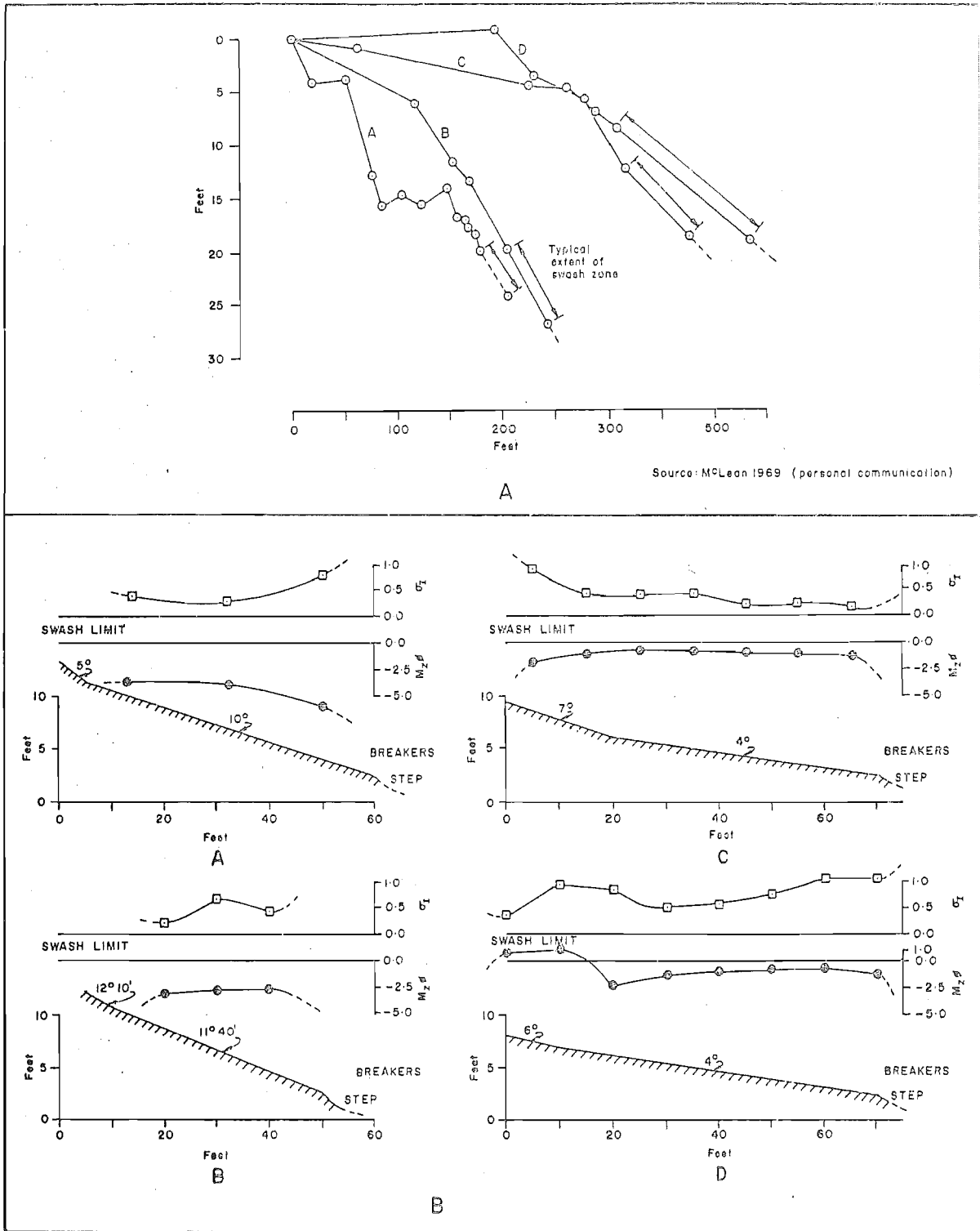


FIGURE 2. Beach profiles selected for study.

Station A is the steepest of all the profiles. It is comprised of a steep bank of coarse gravel ($Mz\phi$ averages -3.5ϕ). The materials are well sorted and secondary berms are frequently present (Fig. 2A). This station is exposed to short period north-easterly swell and storm waves. Breakers are usually of the plunging type and the swash zone is narrow (50-60 feet). Figure 2B shows that mean grain size increases toward the breaker while sorting decreases.

Station B on the other hand, lies in a comparatively sheltered zone. Figure 2B and Plate 1 indicate that it also has steep slopes, but that the swash zone is even narrower. Grain size is finer than at station A but the beach deposit consists similarly of pebbles and granules. Sand is not present on either profile. Grain size and sorting trends parallel those at station A.

Perhaps the most distinctive features of station B are related to the nature of wave breaking and swash motion. Here there is strong refraction and little recognisable breaking except under storm conditions. Rather the wave surges up the foreshore. The motion of the swash and backwash may be likened to that of a pendulum with almost equal, steadily recurring flow times.

Station C lies further southwest and hence is more exposed to wave action. Here and at station D the breakers are almost always of the plunging type. Also, Figure 2B



PLATE 1. Steep shingle profile, station B, South Bay. Swash Zone is narrow and water motion tends to be of the surging type.



PLATE 2. A much flatter, mixed sand-shingle profile, station D. Here the swash zone is wider and there is marked asymmetry of flow times and pressures.

indicates that these stations are notable for the presence of coarse sand in the beach deposit. Both may be classified as having mixed sand and shingle foreshores. At station C there is only a small amount of sand present and the coarse fraction is concentrated on the small pebble and granule sizes. Sorting trends exhibit a decrease seaward toward the breaker similar to those of the stations previously described. On the other hand, at station D the upper part of the swash zone is frequently characterised by the presence of a sand lense (see Fig. 2B; Plate 2). Consequently, there are wide variations in sorting across the foreshore.

At the latter two stations the swash-zone is consistently wider and breaker action more intense than at stations A and B. During storms from the southerly quarter the active swash zone at stations C and D may be well over 100 feet wide.

In summary, it may be stated that the four stations chosen represent a cross-section of the types of beach morphology and sedimentary deposits found in the area. In addition it is clear that these four locations receive a characteristic range of breaker and swash types.

Tidal Influences. Tides in the Kaikoura area are semi-diurnal, with high water occurring twice a day at intervals averaging 12.3 hours (N.Z. Tide Tables, 1969). The basic time scale of the field experiments was thus approximately 12 hours, the tidal cycle. The tidal streams change direction four times daily.

Flood tide sets to the north while the ebb flows south along the coast.

The tidal range at Lyttelton is 6.3 feet on springs and 5.4 feet at neaps. Observations during field experiments confirmed that the tidal range on the study beaches is of a similar order. It has already been mentioned that the beaches are characterised by steep slopes and plunging surf so that there is very little tidal translation of the breaker zone.

The main effects of the tide consist in increasing the intensity of breaker action at high water. It will be demonstrated that this results in longer, faster swashes. The combination of spring high water and southerly storm waves has been shown to result in especially intensive erosion of mixed sand shingle beaches of the coast of the Canterbury Bight (Kirk, 1967). Finally, the tidal rise and fall of mean water level at the shore affects the position of the beach water table and therefore the extent of the zone of saturation. A wet foreshore has been shown to be a factor promoting beach erosion (Grant, 1948; Emery and Foster, 1948; Duncan, 1964).

PREVIOUS WORK

It has been stated above that most previous studies have been concerned with the area seaward of the breakers. Since breakers constitute the primary inputs of water to the swash zone and since the surf line constitutes the seaward boundary of the flow features studied during this investigation, it is appropriate to consider first the nature of shoaling and breaking waves. This will be followed by a review of work relating specifically to the swash zone.

Shoaling Waves

As ocean waves run onshore from deep to shallow water the effects of friction between the wave form and the sloping bed become apparent. The wave profile for swell in deep water approximates a regular sinusoidal form. As shallow water is entered the wave velocity and length decrease, the wave steepens and height increases until the wave train consists of peaked crests separated by relatively flat troughs. Near the breaker the process is accelerated so that the breaking wave may attain a height several times greater than the deep water height (Shepard, 1963, p. 66).

Typical breaker and shoaling wave characteristics are shown in Figure 3 and have been adapted from Iversen (1952, Fig. 1, p. 10), and Harrison et. al. (1968, Fig. 4, p. 11).

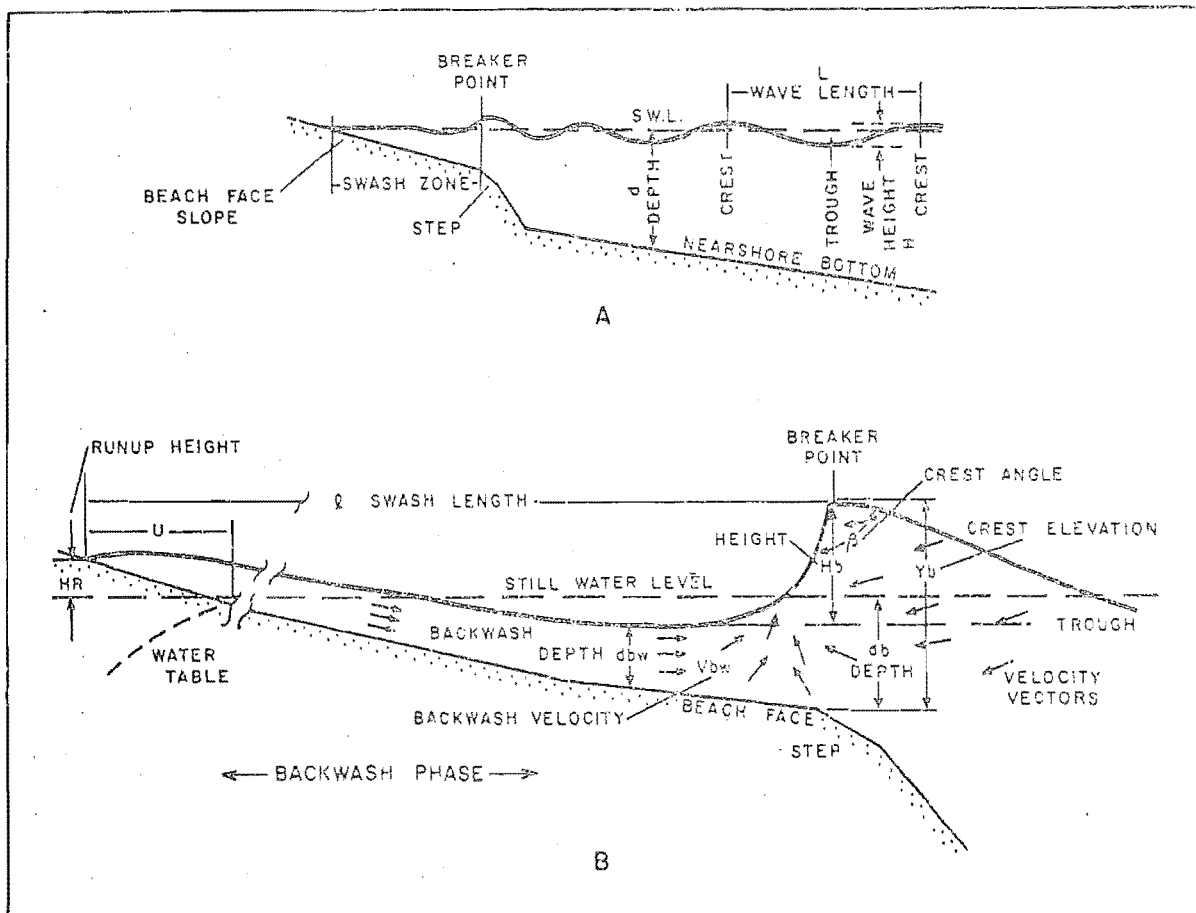


FIGURE 3A. Shoaling wave characteristics.

3B. The swash and breaker zones showing flow lines and significant dimensions. Swash zone flow is shown for the backwash phase.

Definitions of these and other terms and symbols used throughout the text may be found in the glossary.

Kemp (1958, p. 38) has noted that there is a limiting value of steepness attainable by waves in process of generation ($H_o/L_o = 0.14$). This limiting value is an important factor governing the distribution of wave energy across the spectrum from short to long periods. Short waves have a limiting deep water steepness ($H_o/L_o = 0.076$), after which they lose energy as fast as they gain it. This same limiting value will therefore affect waves as they move into shallow water with a consequent tendency toward superelevation of the wave crest as length and velocity are reduced by friction. Van Dorn (1966, p. 39) suggests that the effects of this transformation are not pronounced until very close (often within one wave length), of the depth at which breaking occurs. The break point is immediately preceded by a very rapid increase in the wave height and by marked asymmetry of the wave crest profile.

Bretschneider (1962) demonstrated a further important effect of shoaling transformation. He showed that shoaling had a filtering effect on wave period. It was found that the predominant period shifts toward shorter periods as the water depth decreases. "The implication is ... that the significant periods observed in shallow water over the continental shelf are shorter than those which would be observed beyond the

continental slope. In very shallow water (where) shoaling becomes important, a secondary peak occurs at higher periods".

Energy Dissipation in Shoaling Waves. Energy dissipation due to friction and percolation into a permeable nearshore slope were investigated by Putnam and Johnson (1949) and by Putnam (1949) respectively. It was concluded that the reduction in wave energy caused by bottom friction is negligible for steep slopes until the wave is in water shallower than one half wave length. Height changes due to bed friction are negligible in the first 60% of the distance landward of $d/L_0 = 0.5$. The effect is only appreciable over the final 20% of this distance. Thus, in general the rate of energy dissipation in shoaling is small, but it is cumulative so that on steep-to shores such as the shingle beaches of the Kaikoura coast waves may be expected to arrive at the shore retaining most of their deep wave energy. The effect of percolation into the bed was found to be much lower than that of friction unless the bed is very permeable and very flat. Sverdrup and Munk (1946) evaluated all the data available and stated that for all slopes in the range $1/20$ to $1/300$ the frictional loss of energy does not exceed 10% of the original wave energy and is much smaller on average.

On the other hand, Inman and Bowen (1963) demonstrated from an evaluation of the relation between wave power

(i.e.: rate of application of energy), and sediment transport in this zone that about 10% of the total power expended by waves is used in transporting sediment.

The "Null-Point" Hypothesis. As has been stated previously, many studies of sediment motion and beach erosion have been performed for this zone. Most of these rest on the assumption that the increasing asymmetry of wave forms and orbital velocities can be described by successively higher approximations to sinusoidal deep water wave theory. Munk (1949) has shown good agreement between solitary wave theory (which may be regarded as a limiting case of oscillatory wave motion), and measurements of wave parameters on sandy oceanic coasts. Also, it was demonstrated that the theory explained many features of wave breaking. In deep water the significant parameters are thus wave length and wave steepness (H_o/L_o). In shallow water the wave conditions are nearly independent of wave length (and therefore wave period). The important parameters in the zone immediately seaward of the breakers are water depth (which governs velocity); and the ratio of wave height to water depth (which will be shown to control breaking).

As shoaling transformations produce increases in the degree of asymmetry of orbital velocities and flow times individual water particles no longer describe closed orbits. Motion at the bed becomes parallel to it and a mass movement

of water toward the shore is initiated. The fact that forward motion of the water beneath the shoaling wave crest is more rapid than seaward motion under the trough was early recognised as a potential mechanism of sediment sorting. Thus, a given grain size under given wave conditions is thought to have a "null-point" on the submarine slope where onshore and offshore forces on the particles are at balance. The null points of successively smaller grains lie at increasing distances from the shore. The concept was first stated by Cornaglia in 1898 and is evaluated by Munch-Petersen in Svendsen (1950). Subsequently, a number of model studies were carried out by Eagleson, Glenne and Dracup (1963), and others. Miller and Zeigler (1958; 1964) attempted theoretical and field analysis of the null-point hypothesis. Longinov (in Zenkovich, 1967, pp. 44-118) has conducted extensive field investigations of wave pressure distributions in the shoaling zone. It was concluded that in general the hypothesis was valid, but that the theory is imperfect since it fails to distinguish between suspended and bed load movement. The movement of gravel, for example, is predominantly as bed-load under nearly all wave conditions while sand passes into suspension load with increasing wave intensity. Once suspension of sediment becomes significant the vertical structure of the water column becomes important. Secondary currents may move sediment in directions contrary to those

determined by the net wave forces at the bed as will be shown.

Wave Steepness and Beach Cut and Fill. Also, as has been mentioned, many studies have dealt with the relation between deep water wave parameters (most notably wave steepness), and beach cut and fill. Both the reason for this and the link with the null-point studies of sediment sorting lie in the fact that steepness is a direct measure of the onshore and offshore velocities under the wave crests and troughs respectively. Under swell conditions (low steepness), these velocities are net onshore at the bed. Under storm conditions (high steepness) the velocity differential is much lower and velocities are at a maximum. At $H_o/L_o = 0.03$ the velocity differential is zero. Studies of the relation between steepness and beach cut and fill include those by Waters (1939), Johnson (1949), Rector (1954), Watts (1954) and Scott (1954). Repeated observations demonstrated that an erosional "bar" profile is produced by steepnesses greater than 0.025 - 0.03 and that steepnesses less than 0.025 - 0.03 promoted beach fill and a "step" profile. These conditions correspond in a general fashion to storm and swell conditions on natural beaches.

However, the derived correlations between steepness and beach state varied greatly with beach slope and mean grain size (Iwagaki and Noda, 1963), so that "critical steepness" varies widely over a range of beach conditions. Further,

steepness values reported in field studies are usually much below the theoretical laboratory range of 0.025 - 0.03 (e.g. Kirk, 1967, p. 32; Kemp, 1960). The reasons for these discrepancies relate, as in the case of null-point theory, to the lack of detailed knowledge concerning water motion in and near the sediment layer, and to the complex inter-relations between the state of the beach face and the incident waves.

Iwagaki and Noda (1963) demonstrated that at low values of the ratio H_o/d_{50} (where d_{50} is a measure of mean grain size), sediment transport occurs mainly as bed load and at high values of H_o/d_{50} as suspended load. It has already been noted that suspended load is subject to redistribution by secondary currents.

Wells (1967, p. 497) stated that, "part of the failure of (the above) efforts to obtain a valid theory for sand movement by waves may be due to the insufficiency of the wave theory used". Nowhere had the interaction between incident waves of varying frequencies been considered. It was found to be necessary to employ the skewness of the probability distribution of the horizontal water velocity for second order gravity waves just above the bottom boundary layer in order to arrive at a precise definition for a (sediment) neutral line (null-point) which could lead to a prediction of beach conditions under wave action alone.

The neutral line corresponds to the position of zero skewness and the direction of net particle motion is determined by the sign of the skewness. The force of gravity (slope) was assumed to be negligible in relation to wave forces. In the null point hypothesis gravity is seen as a force acting on grains in the offshore (downslope) direction.

It was concluded that the neutral line always lies seaward of $d/L_0 = 0.090$ i.e. a position quite close to the breakers. Onshore movement decreased with decreasing wave length and the neutral line moved seaward with increasing wave length and period. Also, the neutral line moved seaward with increasing bandwidth (equivalent to variation in the period of incident waves at a given time; e.g. plus and minus 10% of predominant period).

The Wave Drift Profile. Because of increasing asymmetry of water particle motion in the onshore direction fluid particles move a net distance onshore with each wave. As a result of this, and also because waves breaking along the shore become waves of translation, a certain amount of water is piled up against the beach. A hydraulic head is therefore established and since over a long period the net water level at the shore remains constant (apart from tides), this water must return seawards. A "drift profile" comprised of an onshore mass translation component and a seaward return flow component

results. Zenkovich (1967, p. 23) notes that little is known about the detailed structure of this profile for particular conditions in spite of the effects it has on sediments lifted off the bed by wave motion. Munk (1949) gives a series of drift profiles for different relative depths (H/d) in which the onshore flow section is underlain by a seaward flow along the bed. Conversely, Wiegell (1965, p. 324) summarises laboratory measurements and concludes the reverse; that is, onshore transport at the bed and seaward return at the surface. However, in all cases the velocity of drift increased right up to the breakers.

On the other hand, Shepard and Inman (1950) examined drift currents on sandy beaches and found a tendency for all water outside the breaker to move seaward in one area and shoreward in another. The return flow occurred at discrete locations along the shore in the form of high velocity filaments known as rip-currents. The latter are short lived and changeable in position. Between rips there may occur longshore currents which carry masses of fluid to the main body of the outgoing currents.

In addition it is known that winds near the shore can have pronounced effects on the nature and intensity of mass transport. An onshore wind tends to promote pile up at the shore and to hasten wave breaking so that return flow near the bed may be accelerated. Beach erosion results.

Conversely, offshore winds tend to delay breaking and to lessen mass transport onshore near the surface. King (1953) examined these processes in both the field and laboratory and showed that onshore winds increase the destructive effects of steep waves. The significance of the little studied drift profile thus has two aspects of especial importance to a study of swash zone processes. The first of these is related to the distribution of suspended sediment and the second concerns the interchange of water and sediment through the breaker zone. This latter aspect will be examined in the discussion of breakers.

It is now clear that the mechanics of wave and sediment motion in the nearshore zone are generally well understood. Model studies, theoretical analyses and field experiments have given the grossly simplified relationships to work with. It will be demonstrated that the same cannot be said of either the breaker or the swash zone.

Summary of Shoaling Wave Characteristics. It has been shown that waves in shallow water shorten in length and lose velocity toward the breaker while crests become elevated and steeper and troughs flatten. Toward the shore there is an increasing asymmetry of the flow times and velocities associated with given crests and troughs (the skewness of the velocity distributions increases). This leads under varying conditions to size-sorting and cut and fill of the beach deposit, though

many details of these processes remain obscure. There is little energy dissipation in this stage either by friction or by percolation into the bed. Near the breaker the development of asymmetry accelerates dramatically and the distribution of flow in the water column is complicated by the presence of seaward flowing return water. The latter may be located at a variable number of positions both vertically through the water column and horizontally along the shore. As well rips are variable with respect to time, altering by the minute and with the winds and tides. All of these processes of wave transformation are drastically altered by the process of breaking.

A large body of literature relating to the study of wave processes in the nearshore and offshore zones has been briefly summarised above since it does not directly affect the present study. However, the outline given enables certain conclusions to be drawn concerning the study beaches of the present investigation. It is unlikely that on steep beaches having relatively deep water close inshore significant modification of the energy levels of incoming waves takes place in the shoaling zone preceding breaking. On the Kaikoura beaches the only major potential source of offshore energy modification is therefore wave refraction. Thus, on the study beaches the descriptions of beach cut and fill and sediment sorting are to be found in analysis of swash and

breaker zone processes where large amounts of energy are dissipated very rapidly over very short distances (usually under half of one wave length).

Breakers

There are two aspects of breakers of particular significance in the present study. The first of these is concerned with the factors promoting breakers of various types. This conditions the nature of the swash and the intensity of the backwash. The second relates to the circulation of water and/or sediment through the breaker to the nearshore zone. Material entrained by the backwash must either be deposited at the base of the breaker or carried alongshore to a rip current if there is no interchange across the breaker zone under a given surf regime.

The properties of breakers are difficult to treat theoretically since the break point is a mathematical singularity and the process of breaking is non-conservative of energy. Also, in breaking the water motion is known from model studies to possess significant vertical accelerations. These can no longer be accommodated as in the theories of unbroken waves.

There is therefore no generally accepted criterion for the onset of breaking except that most authorities agree that breaking will occur whenever the wave orbital velocity at the crest exceeds the local phase velocity (Van Dorn, 1966, p. 39). As the waves shorten and steepen and lose speed toward the

shore the crests become increasingly unstable so that when wave steepness exceeds a limiting value breaking ensues. In Stokes theory this value is expressed in terms of maximum crest angle. If the angle is less than 120° then orbital velocity exceeds phase velocity. An alternative criterion is that the wave breaks if asymmetry of the crest develops to the point where the front face exceeds the perpendicular. The wave then collapses forward.

Beach slope exerts a strong influence on the nature of breaking and there are two external phenomena which will hasten development of the above conditions. The first, an onshore wind, has already been mentioned. Such a wind accelerates the upper parts of the crests to a level beyond the wave phase velocity. The second is the presence of an opposing current. Waves in deep water will break if the velocity of the opposing flow attains a value equal to one quarter of the wave phase velocity (Yi-Yuan Yu, 1952). Similar effects may occur in rip current zones and at the base of the breaker where backwash water is at maximum velocity.

Defant (1960, p. 126) notes that there are three exceptions to these criteria. Abrupt slope changes will promote breaking at considerable depths. Very steep storm waves break deeper than predicted and very flat waves break shoaler than predicted. Munk (1949, p. 389) demonstrates

that waves on uniform slopes may be expected to break in water 1.28 times deeper than the wave height ($H/d = 0.78$). Iversen (1952) has shown that the horizontal velocities of water motion are greatest under the crest of a wave about to break and that vertical velocities are greatest just shoreward of this point (See Fig. 3B and Fig. 8A).

Energy Dissipation in Breaking Waves. It is thus clear that wave breaking gives rise to intense turbulence and rapid dissipation of energy. Wave energy possessed in deep water is dissipated along the route to the shore by friction losses, plus turbulent losses in the breaker, plus friction in the swash, plus the potential energy associated with an inshore rise of water level, plus friction in the backwash; and, plus reflected energy (Kemp, 1958, p. 44). Healy (1953) considers turbulent losses as the most important for beaches and deduces that the energy absorbed by a given beach is proportional to the slope, being 40% for a 30° slope, 80% for a 10° slope and 95% for a 5° slope. Thus, on the steep study beaches most of the wave energy arriving at the shore is absorbed in breaking and in swash and backwash. Little energy is reflected seaward. Also, hydrodynamically rough foreshores (gravels) further reduce the level of energy reflection. Therefore until the wave breaks, practically the same amount of energy is transferred to an ever decreasing

volume of fluid as the depth decreases. This is brought about by an increase in wave height (Zenkovich, 1967, p. 34), though the energy loss involved in breaking rapidly reduces height.

The latter features are exhibited in Figure 4 which shows the fluctuations in wave height and mean water level associated with some laboratory breakers (Bowen, Inman and Simmons, 1968, p. 2573). These experiments demonstrated the existence of a "set-down" seaward of the break point and of a steady rise in mean water level ("set-up") on the landward side. Set-down outside the breaker can be seen to be small and is due to reflection of energy from the concrete beach slope. On the other hand, Figure 4 indicates that the set-up on the landward side of the breaker is at least as large as wave amplitude. Theory and experiment are in good agreement save for the immediate vicinity of the break point where wave height is larger than predicted. It can be readily seen that the wave profile is no longer sinusoidal as in deep water.

As noted previously, the velocity distributions in this zone are very complex. In agreement with Wells' (1967) hypothesis concerning the skewed nature of the velocity distributions Koontz and Inman (1967) have shown that much of the energy possessed by waves in this zone is contained by second and higher order harmonics of the motion so that

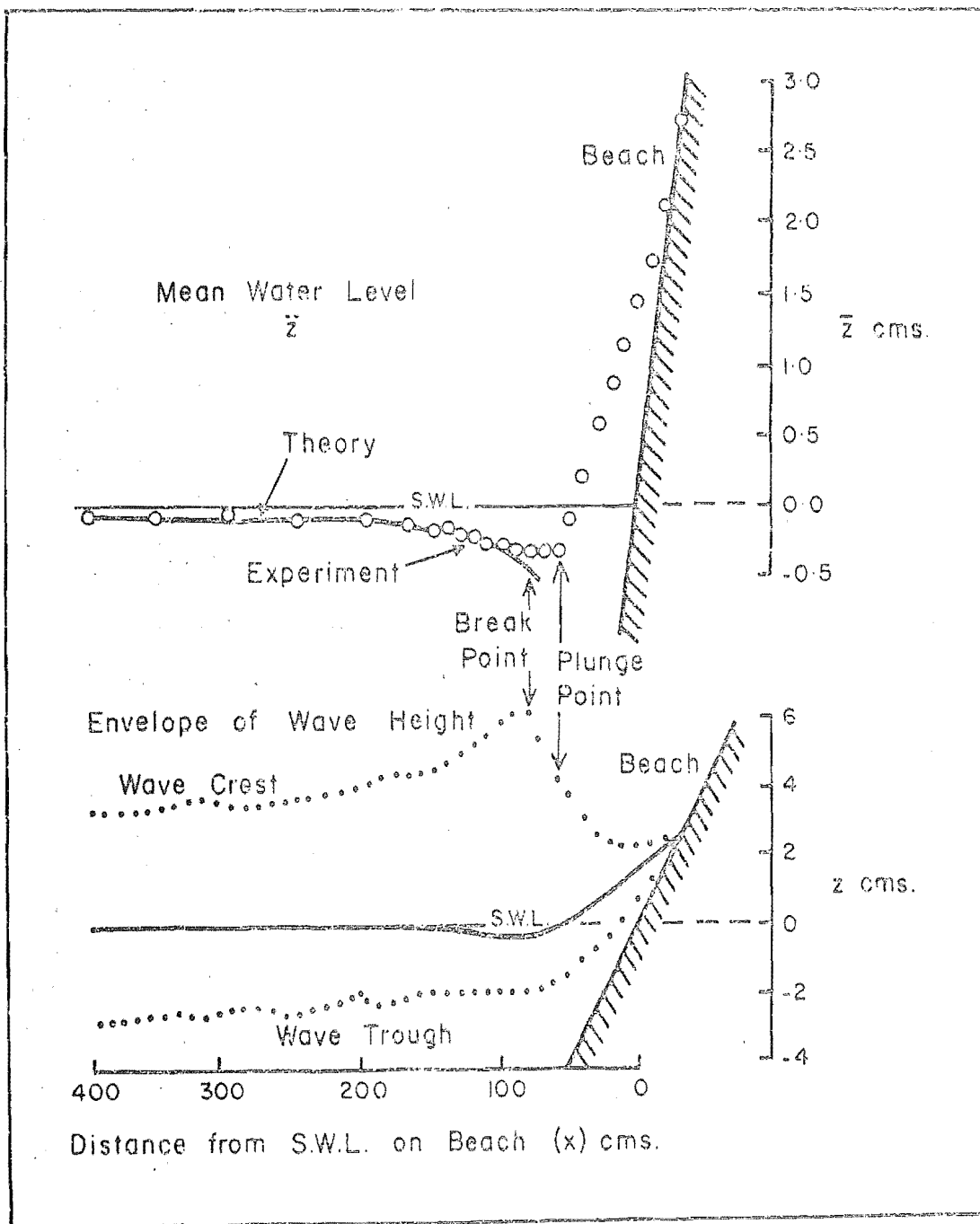


FIGURE 4. Displacement of mean and maximum water levels during breaking and runup in a laboratory experiment. $T = 1.14$ sec., $H_s = 6.45$ cm., $H_D = 8.55$ cm., slope = 1:12.
 Source: Bowen, Inman & Simmons (1968, Fig. 2, p. 2573).

linear theory is no longer adequate. This accounts for the frequently observed discrepancies between theory and experiment.

Types of Breaking Wave. Breaking waves are characterised by a wide variety of forms which are broadly dependent upon beach slope and wave steepness. (See Fig. 5). The diagram indicates that steep slopes and/or low steepnesses tend to induce plunging or surging rather than spilling breakers. Characteristic water profiles associated with these three breaker types are shown in Figure 6. It can be seen that in spilling breakers the crest does not collapse but rather there is a continuous but minor discharge from the crest and the wave gradually subsides toward the beach. Conversely, in plunging breakers the crest steepens and hollows until the forward face overhangs the trough. The wave then collapses onto the beach (Fig. 6B). Considerable vertical accelerations both upward and downward are involved in this type of breaker. This is the predominant type of breaker on the study beaches. Surging, on the other hand, is confined to very steep slopes and to very low wave steepnesses and is notable for the absence of a well defined plunge point. Figure 6C indicates that the water near the bed at the wave front moves ahead of the crest in bore-like fashion and that the water level declines slowly behind the surge.

Suquet (1950 - in Kemp, 1958, p. 39) examined breaking characteristics on slopes ranging from $1/5.7$ to $1/25$ and

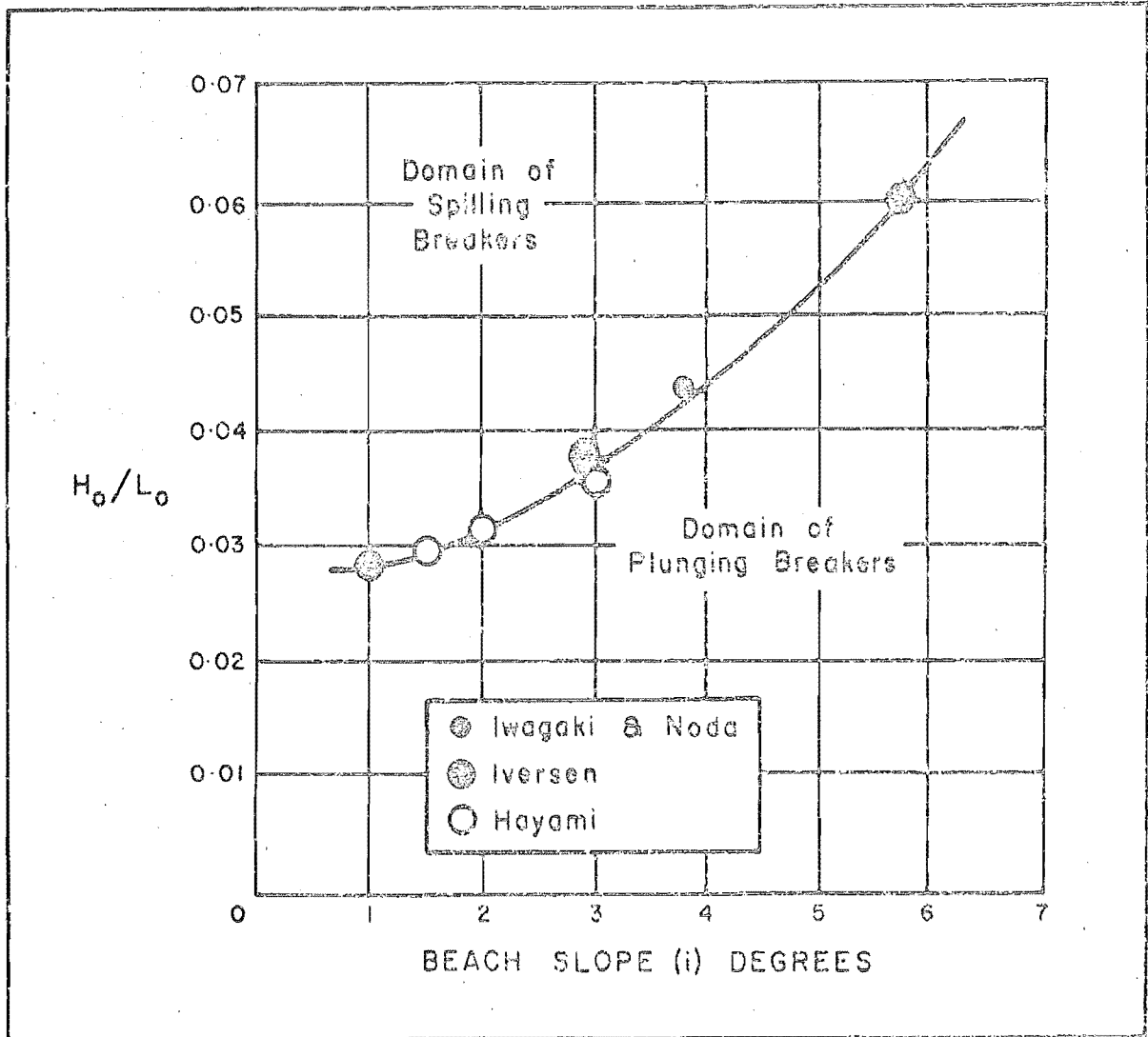
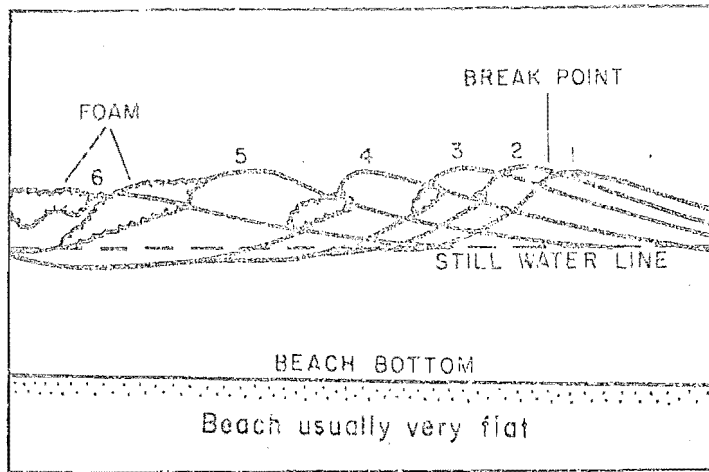


FIGURE 5. Relations between wave steepness (H_0/L_0), beach slope (i), and breaker type. Source: Iwagaki and Noda (1962, Fig. 12, p. 207).

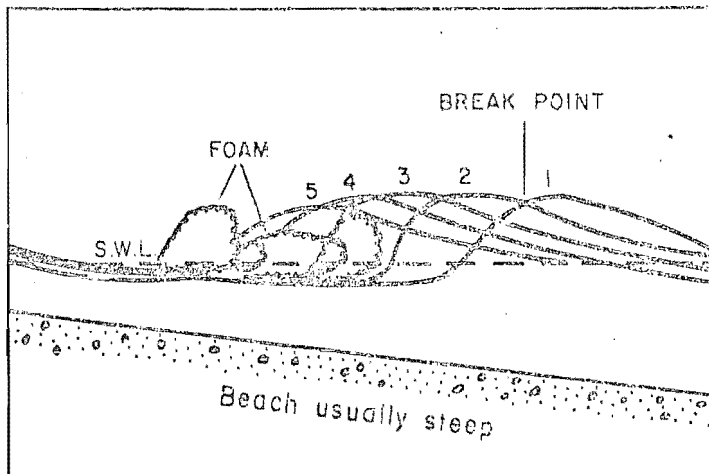
found that for the steepest beaches and $H_o/L_o = 0.03$ a curling plunger resulted. The subsequent runup on the beach was in the form of a "jet de rive" or surge of high velocity and a strong return, meeting the next wave at the plunge point. On the 1/25 slope breaking was in the form of a roller which spread out as a thin sheet as it moved up the beach. The return was equally feeble. It is thus clear that beach slope can greatly affect breaker and swash type for a given incident wave. Plunging breakers initiate a strong swash after the flow-field has been re-formed following the plunge. The equally strong backwash that results has further effects on the next breaker since it opposes the wave flow field and enhances the next plunge. A roller on a flatter slope, on the other hand, results in weak swash and backwash flows and in ponding of water at the base of the breaker. This may result in deposition at this site.

In relation to the critical steepness theory of beach cut and fill outlined above Hayami (1958) and Iwagaki and Noda (1963) have noted a correlation with breaker type. Beach erosion tends to be associated with spilling breakers (see Fig. 5) since H_o/L_o is greater than 0.025 to 0.03; while plunging breakers tend to promote beach fill. This will be shown to be largely untrue of the shingle beach where considerable amounts of erosion have been measured under plunging wave regimes alone. In such cases the

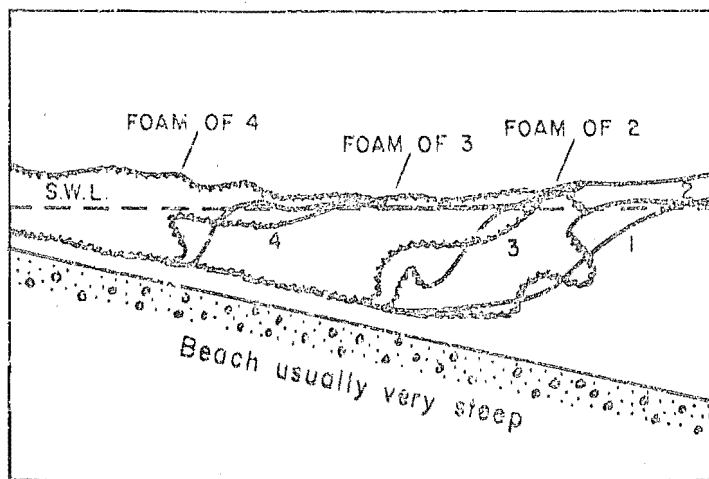
FIGURE 6. The surface profiles show the wave form before, during and after breaking. Numbers opposite profile lines indicate relative times of occurrences.
Source: Wiegel (1965, Fig. 7:30, p. 174).



A. Spilling Breakers



B. Plunging Breakers



C. Surging Breakers

FIGURE 6. Three types of breaker.

distinction between plunging and rolling noted above may have more applicability. However, the energy levels and frequencies of occurrence of the various steepnesses shown in Figure 6 range widely so that it will be necessary to investigate the inherent variability of input wave regimes in order to clarify this point.

Mason (1952) carried out similar studies to Suquet and concluded that plunging and spilling represented the extremes of a continuous range of breaker types. Galvin (1968) investigated this further and established a more detailed classification of breaker types. Most relevant to the present study was the creation of a "collapsing" breaker category intermediate between plungers and surges on steep slopes. Here breaking occurs over the lower half of the wave and only a small air pocket is enclosed (Galvin, 1968, Table 3, p. 3654).

Iversen (1952 A; 1952 B) confirmed previous results and extended the range of observations. His work dealt more explicitly with the role of backwash in breaking and may be summarised as follows: (Kemp, 1958, p. 40):

- (1) Breakers on slopes of 1/10 are 40% higher than on 1/50 for the same wave.
- (2) Similar waves all break in the same depth of water.
- (3) The 1/10 slope produced greater backwash velocity with a smaller depth of flow than for flatter slopes.

- (4) For flat slopes (1/20 to 1/50) backwash velocity is almost independent of H_o/L_o and is equal to 0.15 to 0.20 of wave velocity at breaking.
- (5) For a steep slope backwash velocity increases as H_o/L_o increases.

A promising approach to the problems of breaker study is that of Le Mehauté (1962) who demonstrated that on steep slopes there is a maximum amount of energy that a solitary wave can transmit toward the shoreline over a given depth. This maximum is reached at $H/d = 0.78$, the breaking depth. If the amount of energy passing through a given vertical section is larger than the maximum value, a spilling or "non-saturated" breaker will dissipate the difference. Runup is negligible. Conversely, there is a limiting amount of energy that can be dissipated by spilling along a given length of bed. Hence when the slope steepens the regulating effect of spillage either attains its limit, or has insufficient time to act, and the wave plunges. Such a breaker is fully "saturated" and significant runup results. Intermediate breaker types result from varying degrees of energy saturation. Munk (1949) employed similar reasoning in calculating that the discharge (q) from the breaker per foot of crest per unit time is given by:

$$q = \frac{4}{\sqrt{3} \gamma^3} \cdot \frac{H_b^2}{T} \dots\dots\dots 1$$

where: λ is relative breaking depth, $H/d = 0.78$;
 H_b is breaker height in feet; and T is wave period in seconds.
Thus discharge varies as the square of breaker height so that
the 40% height enhancement noted by Iversen (1952A; 1952B)
can be expected to result in high discharges into the swash
zone of steep shingle beaches.

Asymmetries of Water Motion. The development of the wave
asymmetries leading to the above breaker characteristics has
been investigated in the field by Longinov (1958 - in Zenkovich,
1967, pp. 40-53). Asymmetries for waves on a "deep water"
coast off a shingle beach are shown in Figure 7. The values
were obtained with pressure recorders similar in function to
that employed in this study. It can be seen from the diagram
that all of the pressure and time asymmetries diverge notably
from unity as relative wave heights increase. Values above
unity on the graph indicate shoreward movement while values
below unity relate to net seaward movements.

Though absolute pressure (A_p^m) on the bed increases
steadily toward the breaker the asymmetry of the pressures
in the onshore and offshore directions (A_p) tends to attain
a maximum value. As noted by Van Dorn (1966) these effects
become apparent at a distance of half to one third wavelength
from the breaker. It is clear from the diagram that there is
a net pressure gradient onshore but the coefficient of the

FIGURE 7. Asymmetries are expressed as functions of relative depth (H/d). Derived from Longinov (1958 - in Zenkovich, 1967, Fig. 11, p. 50). Values are for a "deepwater coast". i.e. pebble beach with a flat nearshore bed at 2 m. depth.

A_{pt} = asymmetry of pressures times asymmetry of times.

A_t = asymmetry of flow times.

A_p^m = pressure increment per metre of wave path.

A_p = asymmetry of pressures.

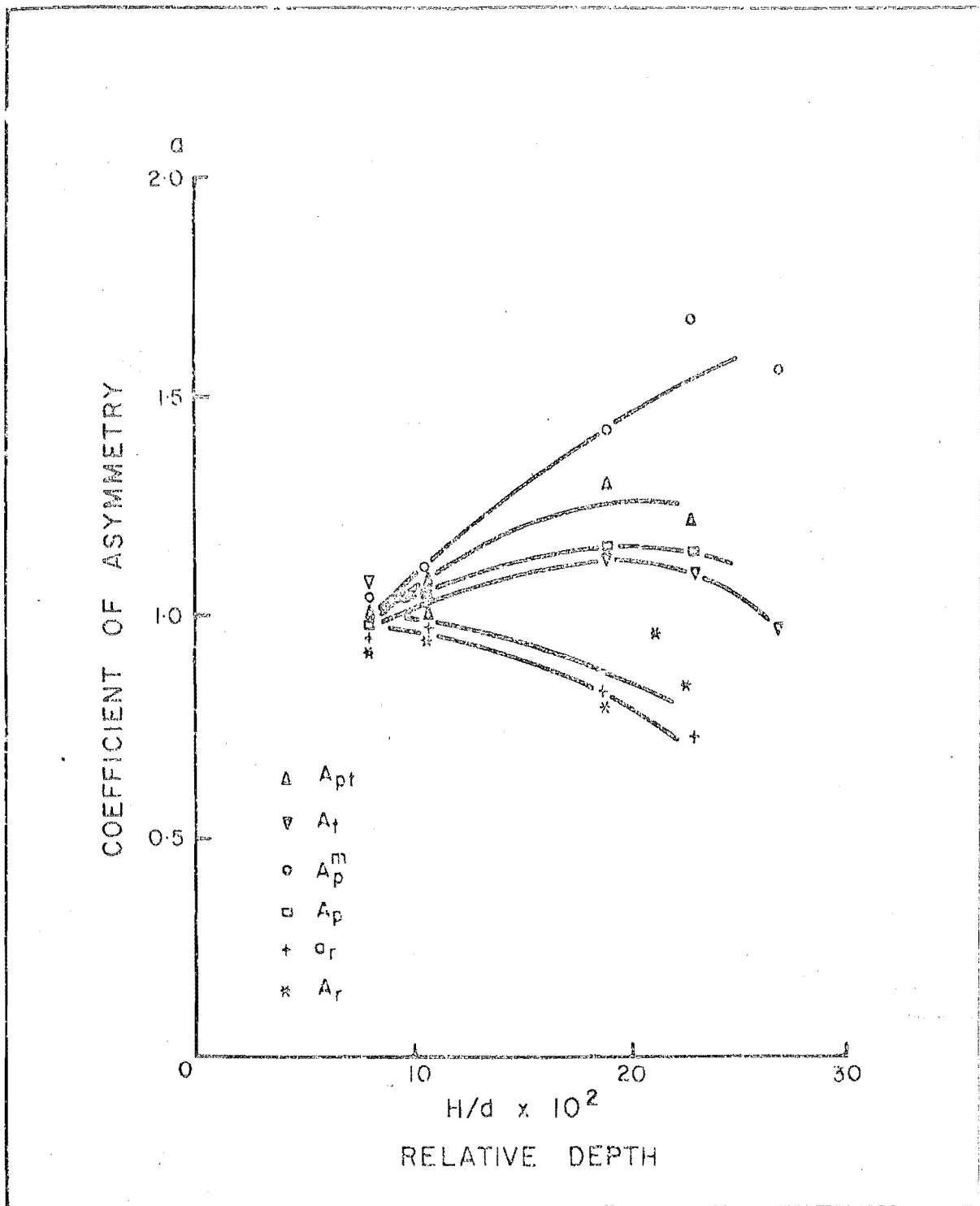


FIGURE 7. Asymmetries of wave motion near the bed in the nearshore zone.

asymmetry of the durations of these pressures (A_t) rises onshore and then declines again indicating the effect of seaward flowing return water piled up at the beach. "This is one of the basic differences between the (field observations) and Cornaglia's (hypothesis) which assumed that an increase in the rate of movement of the water was always associated with a reduction in the duration at a given stage" (Zenkovich, 1967, p. 51).

As well as longitudinal pressures in the direction of wave motion breaking waves also generate shock pressures. The effects of the latter have been studied in relation to forces on cliffs and wharf-piles but they are also capable of significant morphological effects on open beaches. The overall shock pressures exerted by waves breaking on a beach foreshore are greatest for plunging breakers and least for spilling breakers (Carstens, 1968, p. 46). The occurrence of such pressures depends crucially on wave phase (Bagnold, 1938), while their magnitude depends upon water mass, velocity and air content.

On a steep shore the importance of these pressures lies in the fact that plunging breakers may cause significant lifting of coarse sediments from the bed as a result of impact forces. The writer has observed large pebbles flung clear of the breaker on numerous occasions. Carstens (1968, p. 49) demonstrates that a water cushion is very effective in reducing shock pressure. Thus, the importance of a dry beach

(without backwash at the moment of impact), is that the forces exerted by plunging breakers are higher, as is the possibility of significant suspension of sediment. Therefore impact forces by collapsing breakers landing on a slow-moving sheet of backwash water or by plunging breakers which are out of phase with the backwash, should be much lower than at times when flow is cleared before the arrival of the next breaker. This aspect of breaker action is very important because it governs both sediment entrainment at the inception of the swash and the disposal of sediment entrained by the backwash. Consequently, it is a subject which will be analysed in greater detail at a later stage.

For the present however, it raises the vexing question of the nature of the interchange between the beach face and the nearshore bottom through the breaker line.

Circulation of Water and Sediment Through the Breaker. It has previously been shown that the area immediately landward of the breaker zone on a shingle beach is characterised by a high degree of turbulence and bed disturbance. The movement of material in this zone may be oscillatory or translatory or both so that the ultimate resting place of materials continually or intermittently disturbed in this area will depend on the net movement of the water. The nature of the drift profile for particular conditions has been shown to be difficult to assess. Consequently, only the broadest outline

of interchange through the breaker may be garnered from the few observations made in model studies.

The discussion of drift profiles suggested that for low wave steepnesses interchange across the breaker was either in the form of a composite drift profile having a seaward return component at some variable depth, or in the form of discrete rip currents fed by lateral water movements landward of the breaker. Figure 8A indicates this situation. Bagnold (1940) observed this type of condition at low wave steepnesses in a model and concluded that there were distinctly separate circulation cells landward and seaward of the breaker. Sediment was unable to pass through the breaker to the near-shore bottom.

On the other hand, at high steepness values another condition notable for merging of the circulation cells was observed. Hamada (1951) obtained similar results (see Fig. 8B, 1 and 2) and termed the low steepness, discrete circulation case "flow system". This occurred under plunging breakers and the exchange rate of fluid was low. For spilling breakers (high H_o/L_o) on the other hand, a "wave system" was set up. Here there was a large head of water against the shore and consequently a significant amount of energy was reflected from the breaker zone. A second plunge vortex was established and sediments entrained by the backwash were carried seaward through the breaker. It is interesting to note that Figures 8A and 8B, the one derived from field study and the other

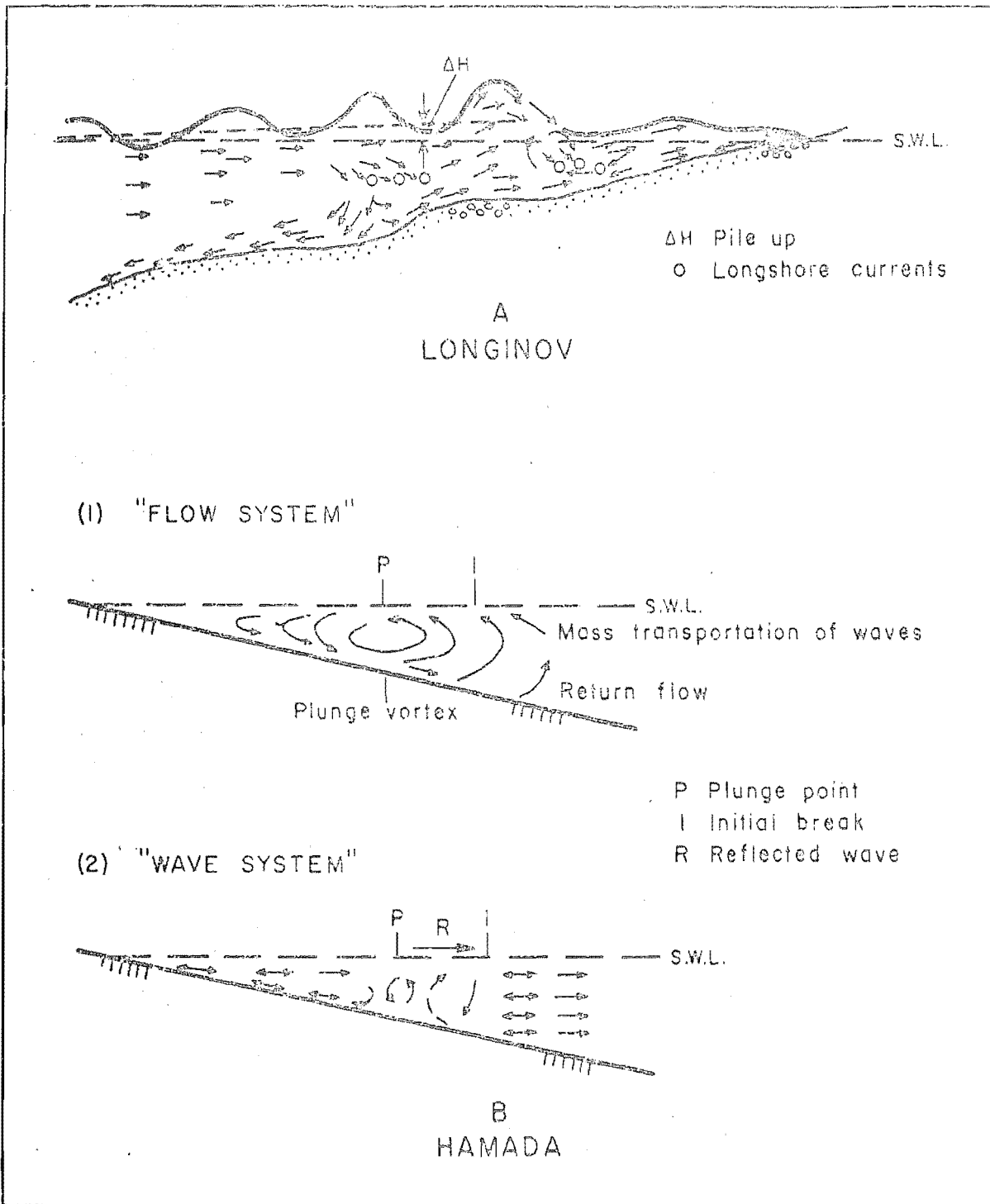


FIGURE 8A. Circulation in the breaker zone. Adapted from Longinov (1954).

8B. Two idealised types of circulation system after Hayami (1958).

from the wave tank, show certain overall similarities. In both onshore flow occurs at the surface while offshore flow is confined to the bed. Also, in both the probable sites of longshore currents are located immediately landward and seaward of the breaker.

King (1959, pp. 125-127) observed similar trends in a model study of beach erosion and deposition. Seaward of the break point almost all sediment movement was onshore. This volume increased with increasing wave height and period. However, there was an abrupt change in motion at the breaker. Landward of the breaker line the direction of movement was much more complex, depending upon relative volumes, speeds and flow times of the swash and backwash. Swash acted with a high velocity but for a longer time so that, given constant percolation into the beach, for greater wave steepness the water volumes ascending and descending the shore increased. King argued that once the backwash reached the critical velocity required for transport of the beach sediment then net seaward flow of sediment resulted since the backwash operated for a longer period than the swash. Reasoning of this type cannot be applied to natural foreshores since water motion in both directions is at all times considerably above the level of critical erosion velocities for all save the largest particles. Also, it has been mentioned that erosion does occur at low values of wave steepness. In fact the many studies of natural

beaches that have observed profile erosion, deposition and erosional/depositional combinations have nearly all been performed under conditions of low steepness when field work is least hampered. The central problem of this study is to detail the processes responsible for these changes observed in natural beaches so that while descriptions furnished by models such as King's may accommodate the gross changes between erosive and depositional phases; parameters such as deep water wave steepness would appear to be inadequate for the description of water motion after breaking and therefore to be of limited value in directly explaining foreshore behaviour.

Swash Phase Relations. A more promising approach lies through a consideration of wave phase relations as stated above.

Johnson and Eagleson (1966 - in Ippen, 1966, p. 412) have noted that the amount of fluid exchange across the breaker zone depends upon the relative timing of the wave breaking and the arrival at the breaker station of the backrush from the previous wave. When the two are coincident little exchange takes place, since the breaker is formed primarily from surf zone fluid. When the two are widely separated there is complete exchange. The authors note that this situation is complicated on a natural foreshore where lateral circulation is possible.

Kemp (1958; 1960; 1963) has formalised this type of notion by considering the ratio of wave period to swash period ("phase difference"). He demonstrated experimentally

and in the field that the relationship between the phase of a wave at the plunge and at the swash limit was an index of stability or instability of the profile. Figure 9 indicates the essential characteristics of this concept. The strong influence of significant breaker height on swash length (and hence on swash period) at three stations along a natural shingle beach can be seen in Figure 9A. It is interesting to note that the differences between stations tend to be eliminated at greater breaker heights. For the observations shown above 40% of the swash lengths lay between instantaneous mean water level and the swash limit (Kemp, 1963, p. 134).

Figure 9B indicates that the decay rate of swash velocity is also correlated strongly with swash length and thus with breaker height. It is therefore clear that "phase difference" must increase with breaker height. These observations in the field confirmed what had earlier been established in the laboratory, as is shown in Figure 9C. This diagram shows that initially the phase difference or swash period remains constant at a value of $0.3T$, even though swash length increases.

As the swash length is further increased a critical point is reached after which phase difference increases with increasing wave height. The zone of constant phase difference is termed the "surge zone" and water motion resembles that of a simple pendulum. An increase in breaker height results in increased swash velocity but the time of the surge remains

FIGURE 9. Data in A and B were derived from field study at three stations on a shingle beach. C is from laboratory investigations of phase relations. $H_{b1/3}$ represents significant breaker height.

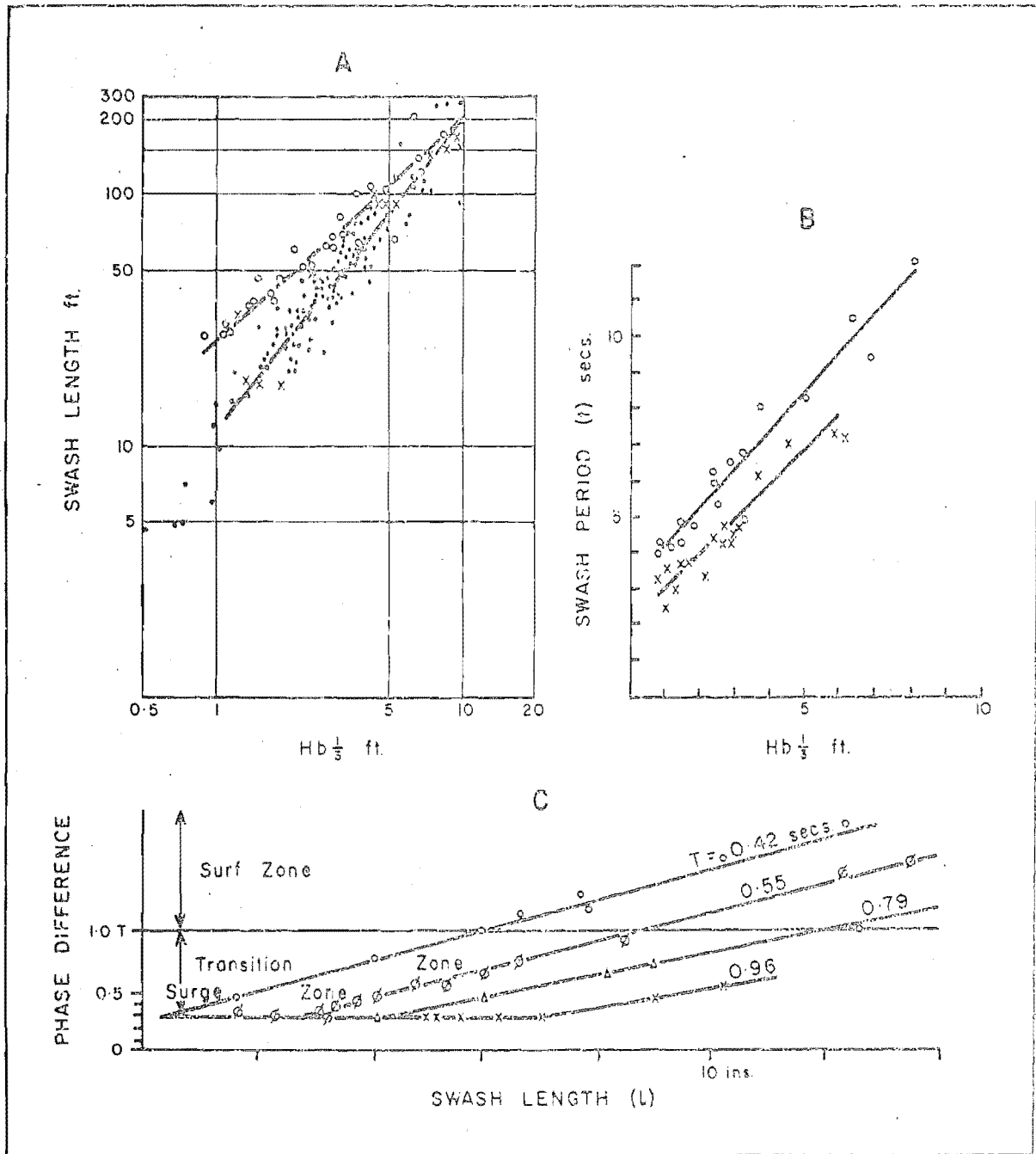


FIGURE 9. Phase properties for breaking waves and swash. After Kemp (1963) (A and B) and Kemp (1960) (C).

and in the field that the relationship between the phase of a wave at the plunge and at the swash limit was an index of stability or instability of the profile. Figure 9 indicates the essential characteristics of this concept. The strong influence of significant breaker height on swash length (and hence on swash period) at three stations along a natural shingle beach can be seen in Figure 9A. It is interesting to note that the differences between stations tend to be eliminated at greater breaker heights. For the observations shown above 40% of the swash lengths lay between instantaneous mean water level and the swash limit (Kemp, 1963, p. 134).

Figure 9B indicates that the decay rate of swash velocity is also correlated strongly with swash length and thus with breaker height. It is therefore clear that "phase difference" must increase with breaker height. These observations in the field confirmed what had earlier been established in the laboratory, as is shown in Figure 9C. This diagram shows that initially the phase difference or swash period remains constant at a value of $0.3T$, even though swash length increases.

As the swash length is further increased a critical point is reached after which phase difference increases with increasing wave height. The zone of constant phase difference is termed the "surge zone" and water motion resembles that of a simple pendulum. An increase in breaker height results in increased swash velocity but the time of the surge remains

constant. Under these conditions there is negligible interchange between the water shoreward and seaward of the breaker and nor is there any tendency for lateral circulation to develop.

With further increase in wave height the critical limit for surge conditions is exceeded. The beach crest begins to retreat and the time taken for swash to reach the crest increases so that the time available for backwash is consequently reduced. As a result the backwash does not terminate before the next breaker plunges. This is termed the "transition zone" of flow and is characterised by unstable flow and lateral circulation (Kemp, 1960, p. 269). Beach cusps are developed under these conditions and there is some interchange of nearshore and swash zone water across the breaker.

As the phase difference increases further, the partly oscillatory nature of the swash and backwash gradually gives way to continuous flow into and out of the breaker zone. Continuous flow is developed when the phase difference is unity (swash period equals wave period) and flow for phase differences greater than wave period is termed "surf zone". The change from transition zone to surf zone also denotes the change from a step-type depositional profile to a bar-type erosional form (Kemp, 1960, p. 270).

From the above it is clear that phase difference is a dominant factor in determining the characteristic shape of

a beach profile. It is a parameter which holds in both the model and on natural beaches and which is not subject to the same scale limitations of dynamic similarity that affect critical wave steepness theory. In relation to the study beaches of this investigation it will be shown that stations on the open beach are dominantly in the transition zone condition. Inherent variability in natural wave trains means that on a given occasion waves and swash are constantly passing from an in-phase to an out-of-phase state and reverting again, the morphological condition of the beach foreshore depending on the time-mean condition. It may also be concluded that on these beaches there is some intermittent exchange of fluid, and perhaps sediment, across the breaker to the nearshore submarine face of the beach deposit. At times when there is no exchange sediment dumped at the base of the breaker by the backwash and recycled by the swash may be regarded as being in quasi-oscillatory equilibrium even though the grain sizes present may be small relative to the respective velocity regimes. Station C (Fig. 1) is dominantly in surf-zone phase conditions and little exchange may be expected save for during storms.

Summary of Breaker Conditions. Breakers have proven difficult to study so that most investigations have described them in relation to their erosive effects on the shore. One exception to this is the energy saturation concept of Le Méhauté (1962).

Breaker type has been shown to be strongly influenced by wave steepness and beach slope but the effects of these two variables are difficult to assess for particular field conditions. Plunging breakers occur on steep slopes at low wave steepnesses and thus form the most common type occurring on the study beaches.

Most of the wave energy arriving on steep shingle shores is dissipated in breaking and in swash/backwash. Asymmetries of the wave form, pressure and velocity distributions are well developed at breaking. There is a net pressure gradient onshore but flow times are more evenly balanced owing to the action of seaward flowing return water.

The nature of the mass transport drift profile is complex and imperfectly understood. Seaward return may occur at varying positions in the water column and is not uniform along the shore since rip currents may drain all the return water in a particular location. Suspended sediments may be carried seaward through the breakers in either of these situations but most experiments indicate that there is insignificant exchange of sediment across the breaker zone unless wave steepness is large.

Plunging breakers initiate a strong swash and an equally vigorous backwash. Collapsing breakers, on the other hand, occur on flatter slopes and result in a deeper, slower swash and a feeble backwash. Shock pressures due to the vertical

impact of water projected from a plunging breaker are greatly lessened if the foreshore is cushioned by a sheet of backwash water. This may affect the degree of sediment entrainment by a wave at the impact point since velocities near the bed would be lower than if the bed was exposed to wave action.

While the critical wave steepness governing foreshore cut and fill, and therefore breaker type, varies greatly with beach slope, grain size and wind direction for both models and field conditions, it has been shown that discharge into the swash zone varies as the square of wave height, but only as the first power of wave length (period). Thus, contrary to the situation in deep water the relation between wave height and wave length in shallow water is very complex.

Consistent with the effect of wave height on swash discharge Kemp (1958; 1960; 1963) has demonstrated that breaker height exerts a strong control on both swash length and duration. Therefore swash velocity is closely related to breaker height so that the relation between wave period and swash period becomes an important parameter governing morphological activity in the swash and breaker zones.

From this Kemp demonstrated that at low-phase conditions in both the field and the laboratory a step-type depositional profile developed. At high-phase conditions beach profiles eroded. Only under high-phase wave action was there continuous

exchange of fluid and sediment through the breaker zone.

Since the phase difference concept offers a better level of dynamical similarity between model and prototype and in view of the fact that it is an easier parameter to measure in the field than the more conventional wave steepness, it will be adopted throughout the remainder of this report. The term "low phase" will be applied to conditions of long period and/or low wave height while the term "high phase" will refer to waves characterised by short period and/or large wave height. This is because these terms afford a more precise description of energy conditions on the shingle beach foreshore than the terms "storm" (high steepness) and "swell" (low steepness). The latter terms, at least in the context of New Zealand coasts, correspond more to the distinction between relatively frequent swell waves arriving from far distant generation areas and much less frequent storm waves consisting of a mixture of swell and more locally generated, wind-modified waves; than to the day by day variations in the modified ocean swell trains breaking on the shingle beaches of the Kaikoura coast.

The Swash Zone

Taken together as a functioning system of reversing flows, a given swash/backwash regime may behave in a quasi-oscillatory or in a translatory fashion depending on phase relations, as

has been shown. It is with regard to this aspect in its broadest senses that most field and laboratory studies of the swash zone have been oriented. Gross changes in the swash/backwash regime have been related to sediment sorting, beach cut and fill, and to the occurrence of various bed forms such as ripples, dunes and cusps.

The first section of the following review will deal with these studies. Secondly, since the swash zone is inherently highly turbulent and since turbulence is fundamental to sediment motion, it will be necessary to review the appropriate theory of fluid motion before proceeding to a detailed study of sediment transport in the swash zone. This theory is derived mainly from the literature of the study of fluvial hydraulics.

Water Motion in the Swash Zone. Palmer (1934) early noted the erosional character of high-phase wave conditions on shingle beaches. This was attributed to the greater role of the backwash as opposed to that of the swash. Conversely, beach accretion was argued to be due to a low phase type of condition where swash flow predominated and pebbles were moved up the beach to become stranded at the upper limit of the tidal rise. The "difference between the two actions was determined by the rapidity in succession of the waves upon the shore" (Palmer, 1934, p. 571).

Cornish (1898) and Lewis (1931) adopted similar

explanations for the "downcombing" of shingle beaches by high phase waves. The swashes were observed to ride over one another thus producing a relatively more powerful offshore flow in the backwash. Hence, if beach permeability remains constant, as wave height rises a progressively smaller proportion of the swash volume is lost through percolation into the beach face. Thus backwash volume and velocity increase with rising wave height. It was suggested that the beach was combed down to some flatter slope at which swash/backwash velocities would be more nearly equal.

Cornish (1898) also recognised that simultaneous movements of fine and coarse particles could occur in different directions on the shore face. While coarse materials could only be moved onshore in the swash, fines were mobile in both the swash and the backwash. Since the fines were thrown into suspension it was argued that they might be carried seaward by return currents.

Evans (1939) reasoned further that the rate of motion of foreshore sediments would be greatest near the median line of the swash zone. This was because material in the upper part of the zone moved slowly owing to the low frequency of swash lengths reaching the area, while the material below the median might move offshore (fines winnowed out), or saltate around a mean position (coarse lag), or possess only a low rate of net transport. Fine materials entrained lower down

the foreshore would be deposited as lag sediments at the swash limit because of infiltration of swash water.

A significant feature of these early studies was the recognition of the fact that large storm waves were not entirely destructive of shingle beaches as is the case with sand shores. While large amounts of sediment could be moved seaward much was also thrown high by the swash. This results in the building of steep shingle berms which are often many times higher than normal high tide level (King, 1959, p. 281).

Bascom (1951) in a study of trends in sediment size in the swash zone observed that the largest grains were always found in the zone of maximum turbulence under the breaker. Mean size may decrease landward of this point (e.g. Evans, 1939), or may be more variable (e.g. Krumbein and Slack, 1956).

It can be seen from the above that the earliest observations of the swash zone established the broad factors influencing beach cut and fill as well as identifying the major sorting processes. Thus, variations in wave size influence not only the amount of material of a given size that is transported, but also condition the directions in which the members of a range of grain sizes will move simultaneously. The latter aspects have formed central themes of much subsequent study.

While the movement of swash is conditioned by breaking wave characteristics, backwash is the result of gravitational

forces. Swash velocity therefore depends upon wave height and breaker type whereas backwash velocity is a function of slope angle and rate of groundwater emission from the beach face. The kinetic energy of the swash is converted to potential energy as the bore climbs the slope and then reconverted to kinetic energy in the backwash. Thus the backwash dissipates energy not given up in friction and percolation during swash flow.

Swash begins in the confused zone where the wave flow field reforms after breaking. Pyskin (in Zenkovich, 1967, p. 259) showed that water moves in a continuous mass up the foreshore until at 75-80% of the distance it divides laterally into separate tongues. Flow is highly turbulent.

Backwash, on the other hand, begins quietly and gains energy rapidly as the flow accelerates down the slope under the influence of gravity. It may also achieve considerable levels of turbulence before the flow decelerates at the base of the oncoming breaker.

Measurements of Swash and Backwash Velocity. While these characteristics have long been known there have been few attempts to measure swash/backwash velocities in the field. Table 2 gives published data from all types of beaches together with several parameters relating to beach cut and fill and to sediment sorting studies. It is clear from the table that the few data gathered are of a fragmentary nature.

TABLE 2

Some Published Determinations of Swash and/or Backwash Velocities
Together with Occurrence of Necessary Ancillary Data and Mode of Measurement

| Source | Method | Slope | Wave Height (Ft.) | Wave Period (secs.) | Mean Grain Size m.m. | Beach Cut/Fill | Swash v. (ft/sec) | Backwash v (ft/sec) | Beach Type |
|-----------------------|--------------------------------|----------|---------------------------------|---------------------|-----------------------|----------------|-------------------------|---------------------|--------------------------------------|
| Zenkovich 1967 p.259 | inferred from field ob | 0.1 | - | - | up to 1.0 cu. meter + | - | 33ft/sec | - | Shingle |
| Belov 1938 in Z.1967 | Not Spec. | - | - | - | 0.5 meter rolling | - | 26ft/sec | - | Limen Bay Crimea. |
| Miller & Zeigler 1958 | repeated timed floats | 0.1 | - | - | 1.0 mm. | - | - | 5.34 | Sand |
| " | computed | 0.1 | 3.2' | - | 1.5 mm. | - | - | 5.34 | Sand |
| " | computed | 0.14 | 1.5' | - | 1.5 mm. | - | - | 6.13 | Sand |
| Demarest (1947) | Not Spec. | 0.1-0.23 | - | - | - | - | - | 4.0 | Sand and pebbles |
| Dolan and Fern (1966) | Timed swash fronts past stakes | - | Low 1-2' Med 2-4' High 4' | - | 0.84 2.0 4.0 | - | 4.0 * 6.0 * 5.5 * | - | Sand at mod., high flow energy. |
| Ingle 1966 | timed floats | - | 3.0 3.5 4.4 | 13.0 9.0 12.0 | 0.168 0.146 - | - | 4.1 7.1 6.7 | 1.8 3.1 2.7 | Fluorescent tracing of fine med.sand |

Note: Data is for all types of beach deposit. + Velocity max. inferred from sizes moving.

* Median values.

Rarely have both swash and backwash data been obtained and frequently no information is available concerning wave height and/or period. Similarly, measurements have been derived using crude averaging techniques at a variety of positions on the shore. The results are thus non-comparable and so are of little value in theoretical analysis.

Dolan and Ferm (1966) have published the most thorough observations to date. These were derived by timing the travel of swash fronts past evenly spaced stakes set in the foreshore. A disadvantage of the method will be shown to lie in the fact that the swash front is atypical of the flow body behind it. In spite of this and the lack of backwash measurements the authors were able to demonstrate high inverse correlations between swash velocity and slope, and swash velocity and beach slope. In agreement with Kemp (1958) a high positive correlation between breaker height and beach slope was obtained. All correlations declined in strength with increasing wave energy. This was because at lower energies, "a measurement of swash velocity reflects the speed of a mass of water in actual and continuous contact with the beach surface during the entire uprush/backwash cycle". At high phase conditions, "waves commonly arrive so quickly that one swash may actually move shoreward over another, and all tend to be underridden by the backwash. Under such

circumstances the mass of water ... may have less direct contact with the beach face" (Dolan and Ferm, 1966, pp. 211-212).

Theory of Swash/Backwash Flow. By contrast, laboratory investigations have contributed more detailed knowledge on the structures and velocities of swash/backwash flows. In swash the water motion consists of a wholly translatory mass movement toward the shore, apart from the confused area in the immediate neighbourhood of the breaker where some residual rotatory motion may occur. Swash flows may thus be described according to the theory of gravity waves. The velocity of such a wave depends primarily upon wave height and depth of water and is given by:

$$C = \sqrt{g(H + d)} \quad \dots\dots\dots 2.$$

where: C is the wave celerity, g represents the acceleration due to gravity, H is wave height and d is water depth.

Iversen (1952A) used this relation to describe both swash and backwash velocities in studying the forms of breaking waves. Figure 10 shows general agreement between solitary wave theory and a measured swash velocity profile for small laboratory waves (Kemp, 1958, Fig. 106). As can be seen from the diagram the only area of marked difference between the computed and observed velocities occurs in the area of flow reformation at the base of the breaker. However,

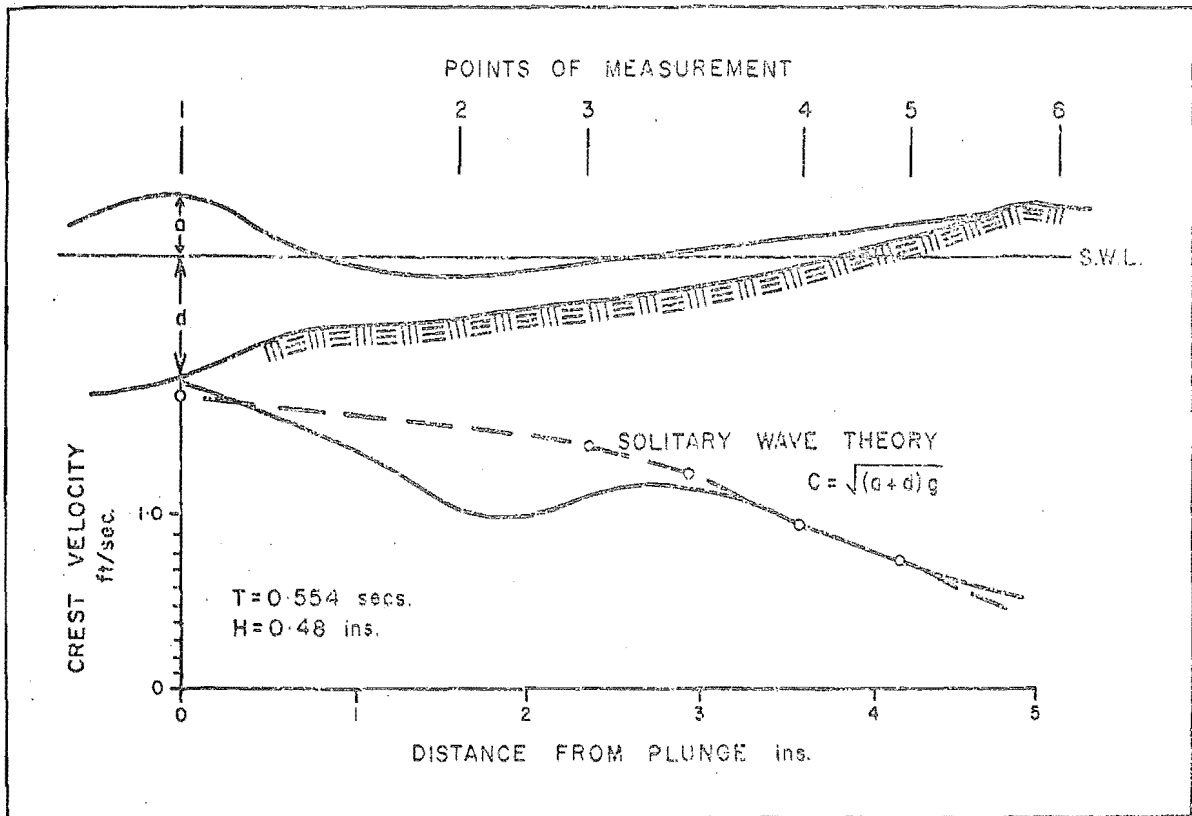


FIGURE 10. A laboratory velocity profile for swash derived from a solitary wave (solid line). The zone of flow reformation (decreased velocity) is apparent in the first two inches of the flow length. Elsewhere agreement with theory (dotted line) is adequate.
Source: Kemp (1958, Fig. 106).

regular swash flow is quickly established.

Characteristic properties of gravity waves according to Zenkovich (1967, p. 36) are that horizontal displacements occur in a single direction and range from zero at the bed to a maximum at the surface. The wave form is characterised by an isolated crest or bore which has no corresponding trough (see Fig. 10). Stephenson (in Zenkovich, 1967, p. 36) has calculated that the force of a wave of translation may be as much as six times that of an oscillatory wave of the same height. Swash flows, like breakers, are thus highly turbulent and give rise to considerable bed disturbance.

The backwash also takes the form of a gravity wave and it has already been shown that the relative timing of backwash and breaker is an important control of foreshore morphological activity. However, the writer is not aware of any published analyses of the details of backwash flow structures.

Kemp (1960, p. 270) noted that, "the conditions of dynamical similarity (between model and prototype) are most likely to be found in the turbulent profile forming zone between the break point and the limit of the swash". On the basis of the sensitivity of the phase difference parameter and on the applicability of gravity wave theory to swash zone flows (as is shown in Figure 10), Kemp developed a more explicit formulation for swash flow structures. An important aspect of any relationship of this type is that

it must reconcile two generally acknowledged discrepancies between models and natural beaches; namely:

- (a) The frequently observed higher critical wave steepnesses in models.
- (b) The occurrence of steeper equilibrium foreshore slopes in models.

The dominant parameters chosen to represent beach profile formation were thus: breaker height and swash length (representing wave parameters); grain size and particle fall velocity (representing sediment parameters); and beach slope (representing foreshore geometry).

For beach materials of a given specific gravity, Kemp obtained the following relationship between the beach profile dimensions and wave characteristics:

$$l = K \cdot H_b \left(\frac{H_b}{D} \right)^n \dots\dots\dots 3.$$

where l is swash length, H_b is breaker height and D is mean grain size. Swash length and breaker height are expressed in feet and grain size (D) in millimeters. The relationship applies only to swash in the transition and surf regions of phase difference. For surge conditions the expression takes the form:

$$l \propto (H_b)^n$$

The power (n) has a numerical value of the order of 0.5 and Kemp (1960, p. 272) obtained a scatter of values between

0.45 and 0.65 for laboratory experiments. The value of K was found to be 24.

Having obtained a working empirical relation for swash length the next steps in the analysis were concerned with expressions for swash velocity and for specifying equilibrium conditions (i.e. profile state at phase difference equal to unity).

Since the phase difference involves the time, t , for the wave to travel from the break point to the swash limit and since the envelope of swash height decreases almost linearly with distance, x , from the break point (see Fig. 10); then the wave height, H , above the still water level at any point a distance, x , from the breakers is given by:

$$H_x = h_b \left(1 - \frac{x}{\ell} \right) \dots\dots\dots 4.$$

where: h_b is height above s.w.l. at breaking. It has been demonstrated above that the velocity of a gravity wave is given by:

$$C = \sqrt{g (H + d)}$$

and since both depth of breaking (d_b) and h_b are proportional to the breaker height (H_b) (since $H_b/d_b = 0.78$), then:

$$C \propto \sqrt{g \cdot H_b}$$

and $C = \sqrt{k \cdot g \cdot H_b} \dots\dots\dots 5.$

Thus by introducing equation 4 Kemp obtained:

$$C_x = \sqrt{k \cdot g \cdot H_b \left(1 - \frac{x}{l}\right)} \dots\dots\dots 6.$$

as an expression for swash velocity, C, at any point, x, between the breakers and the swash limit. From the above Kemp was able to examine the nature of the phase difference relation.

Hence the time taken for the wave to travel an elemental distance, dx, is, dt, so that at velocity C_x:

$$dt = dx/C_x$$

from which the time, tx, for the swash to reach position x is given by:

$$tx = \int_0^x dx/C_x$$

Thus by substitution for C_x and integration the total time required for swash to travel from the break point to the limit is

$$t = \left(\frac{-2l}{k \cdot g \cdot H_b}\right)^{\frac{1}{2}} \left[\left(1 - \frac{x}{l}\right)^{\frac{1}{2}} \right]_0^l \dots\dots\dots 7.$$

since full swash is achieved at x = l the expression reduces to:

$$t = \left(\frac{2l}{k \cdot g \cdot H_b}\right)^{\frac{1}{2}} \dots\dots\dots 8.$$

As has been previously indicated the change from step to bar type profiles occurs when swash period (t) equals wave period (T) so that the ratio t/T equals unity. At this stage

for a given wave period the critical condition is given by:

$$T = \left(\frac{2l}{k \cdot g \cdot H_b} \right)^{\frac{1}{2}} \dots\dots\dots 9.$$

Several sets of measurements of wave period, swash period, swash length and breaker height were collected at the outset of this investigation in order to examine equation 9. Substitution of the data into the equation resulted in a mean value for k equal to 1.281. The expression was then solved for swash length so that the critical curves of swash length shown in Figure 11A could be calculated.

The diagram shows critical swash lengths for varying wave periods and breaker heights. It can be seen that critical length increases rapidly with increasing wave period. Thus for a given wave period variations in breaker height can result in swashes longer or shorter than the critical length. Similarly Figure 11B indicates the instantaneous swash velocities at given locations on the shore. The latter curves are drawn for the critical lengths of Figure 11A, and show almost linear decreases in velocity over much of the shore. However, in all cases there is a rapid fall off near the swash limit.

From the above an important process operating on natural beaches, but not included in Kemp's analysis may be noted. All natural wave trains are inherently variable so that swashes which are longer than the critical for a given wave

FIGURE 11A. Critical swash lengths for a range of wave periods and breaker heights.

FIGURE 11B. Computed swash velocities for a range of breaker heights and swash lengths. Data is derived from field measurements at station D.

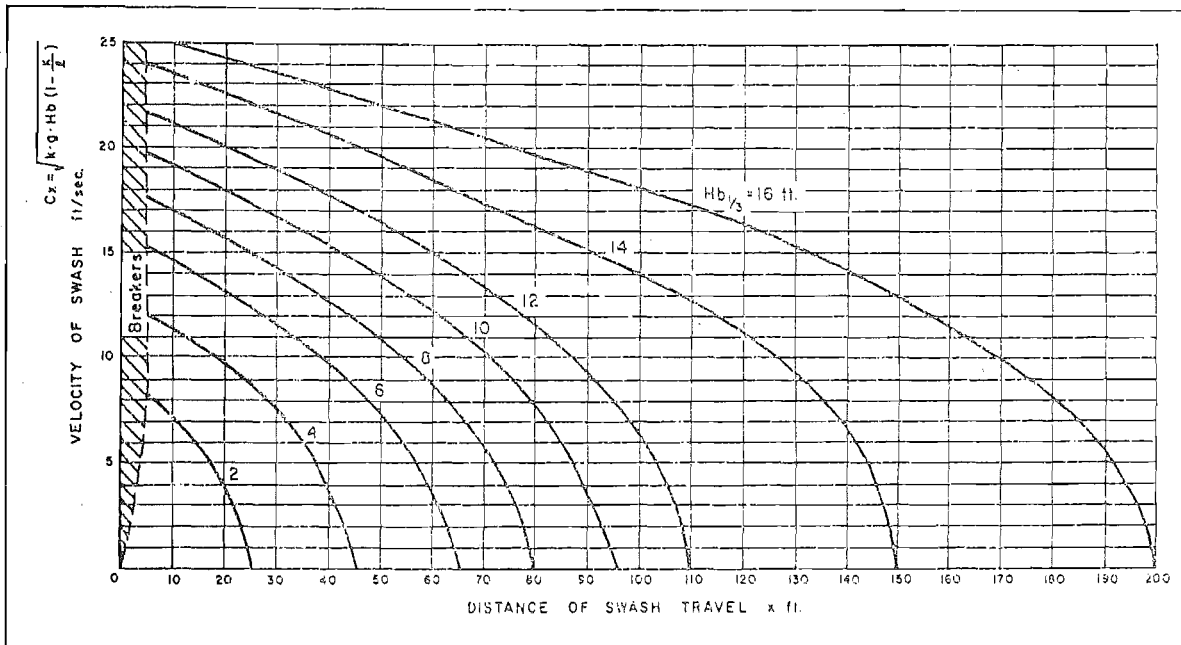
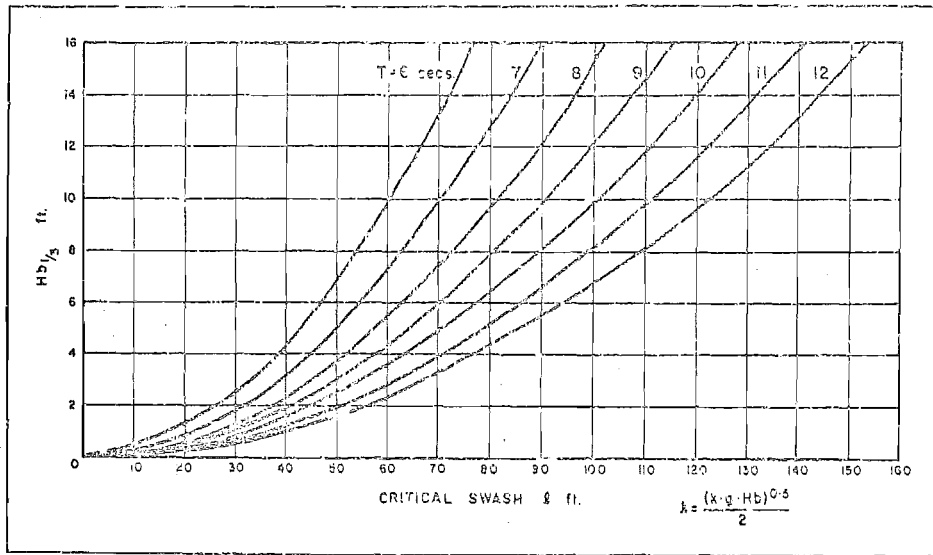


FIGURE 11. Equilibrium characteristics of swash flow after Kemp (1960).

period will effectively constitute surf phase events. These may promote scour of the foreshore. Conversely, many swashes resulting from a particular wave train will be shorter and slower than critical requirements. These may be in a transitional or surge phase state and deposition may result. This situation has aspects of the commonly recurring statistical problem of analysis of variance. From the standpoint of theory workers have been concerned with the differences in behaviour between sets of wave conditions.¹¹ Conversely, the field worker attempting to explain changes in the beach deposit at any one time must be concerned with the variations within a given wave train. Conditions characterised by high levels of variability in swash length, period and velocity may result in short term erosional effects in the swash zone which are very similar to those produced by large storms.

As far as natural shores are concerned, it is suggested that Kemp's critical phase analysis applied to variability of breaker height in a given incident wave train may constitute a valuable index of the locations and intensities of bed disturbances occurring in the swash zone. Wholly sub-critical swash regimes may be expected to produce different morphological effects from partially critical and wholly super-critical conditions at any given energy level. Evidence derived from analysis of swash/breaker flow conditions will later be presented in support of this view.

It is clear from the above that few prior field measurements of flow in the swash zone have been made. Early studies demonstrated some general erosive properties of changes in swash/backwash flow regime but apart from the detailed dimensional and experimental examination by Kemp (1958; 1960) little progress has been made toward developing a general theory of beach face modification by swash/backwash action. It will next be demonstrated that much the same is true of the study of sediment sorting in the swash zone.

Sediment Sorting in the Swash Zone. Sorting of sediments in the swash zone depends upon at least three major factors, (Folk, 1965, p. 4): (1) size range of sediments supplied; (2) type of deposition; and, (3) current characteristics. Of particular importance in the swash zone of the study beaches are the first and third factors since velocities are high in both the onshore and offshore directions.

Many investigators have noted that beach sediments tend to be amongst the best sorted of any natural deposits. Folk (1965, p. 4) suggests that this is due to the "bean spreading" action of waves on sediment grains as opposed to the dumping of particles under river and other types of flow.

The wide range of grain sizes found on the study beaches (see Fig. 2) makes for complex foreshore morphology and dynamics because sand is displaced in suspension, whereas rolling

sliding and saltation are more characteristic of the motion of shingle. More specifically, it was demonstrated above that the ratio of wave height to mean grain size exerts strong controls on critical wave steepness, critical swash length and on breaker type for a given section of beach. The resulting wide range of the ratio H/D on mixed sand-shingle beaches means that they are more complex than either pure sand or pure shingle foreshores.

Inman (1949) in a general study of the mechanics of sediment sorting by wave action postulated that for moderate wave energy, coarse sediments move onshore owing to the rapid surge under the wave crest while the fines move seaward as suspended load in rip currents or bed drift. It was argued that there is always a sand size for which the net transport is zero and that this will be the predominant foreshore sediment. In consequence it will be locally well sorted. Owing to a unique relationship of settling velocity, roughness velocity and threshold velocity, the median diameter likely to be the most highly sorted in water was shown to be 0.18 mm.

Eagleson, Glenne and Dracup (1963) investigated hydrodynamic theories linking sediment sorting processes with the equilibrium characteristics of sand beaches in the offshore zone. The sorting process was examined experimentally by observing the effects of wave action on

known size distributions at several stations across a model beach. Two criteria of sediment motion were considered. The first, incipient motion diameter (D_i) is that size which can just be moved by the fluid forces at a given location while the second, established (oscillatory) motion diameter (D_e) is that size for which net motion is zero at a particular part of the shore.

The effects of large and small waves on a unit sediment distribution were postulated in the manner indicated by Figure 12. The diagram shows that for low wave conditions (Fig. 12A) D_i is smaller than D_e and removal of the fines results. The distribution is thus still unimodal but is truncated at the fine end.

Tanner (1966) observed inflexions of this type in natural beach sand size distributions derived from low energy shores. He termed the truncated region a "surf break", which for his data was located at approximately 1.5ϕ . It was suggested that on higher energy shores the break passes into larger grain sizes, possibly into the pebble fraction.

On the other hand, Figure 12B suggests that two breaks are formed under high energy conditions. The first of these can be seen to be located at the point of truncation of the fines while the second occurs at the established motion diameter. Particles intermediate in size between these two critical diameters are fully mobile hence a bi-modal distribution

FIGURE 12. Theoretical sorting for incipient size larger (A) and smaller (B) than equilibrium motion diameter at a given location. Adapted from Eagleson, Glenne and Dracup (1961, Figs. 19; 20).

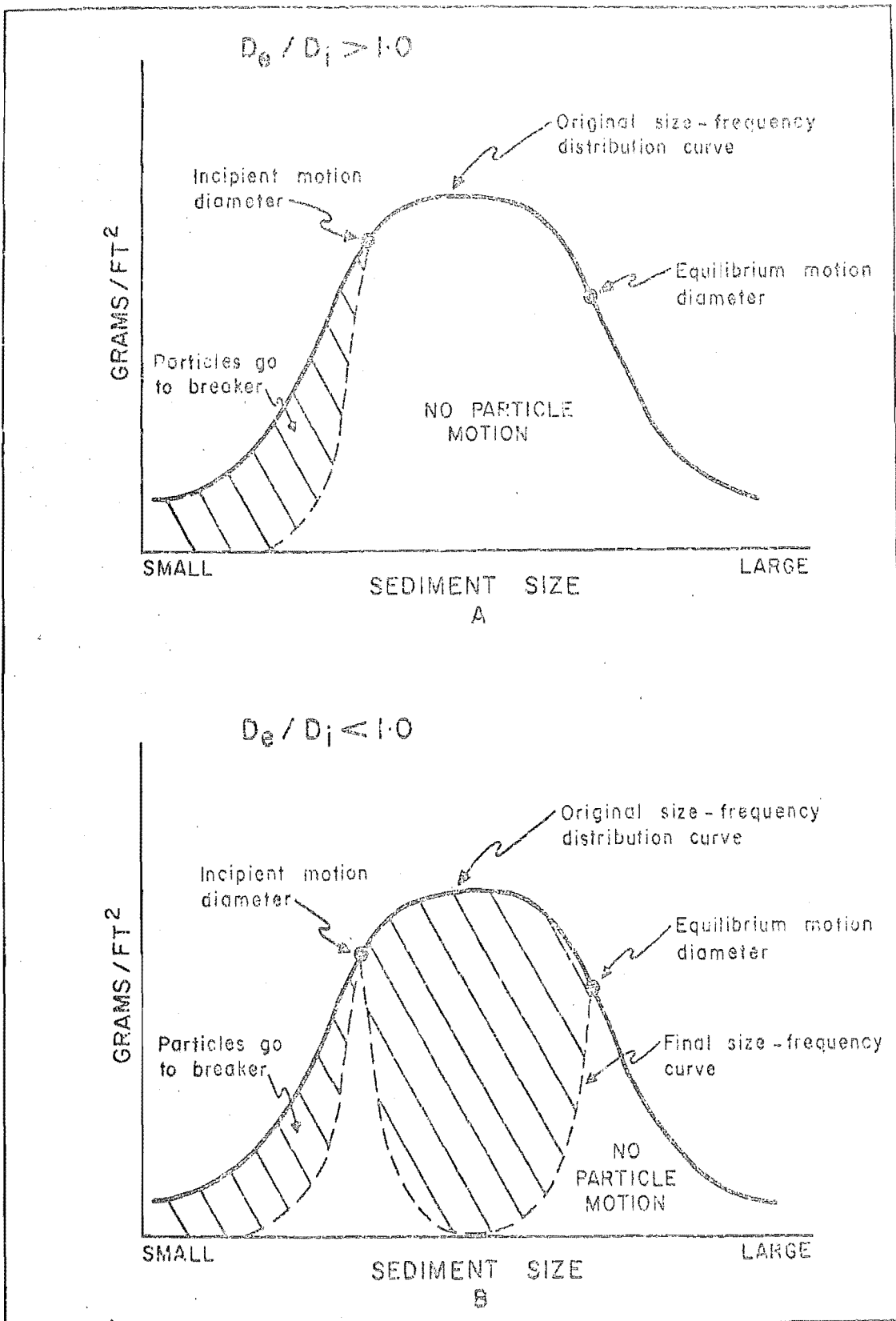


FIGURE 12. Theoretical sediment sorting processes.

having peaks in the sand and pebble fractions results. In support of this many investigations have reported bimodal distributions of sediment size from the highly turbulent breaker zone (e.g. Bascom, 1951; Miller and Zeigler, 1958). Furthermore, it is a higher energy condition such as that indicated in Figure 12B which is most likely to obtain in the swash zone of the study beaches since energy levels are perennially high.

However, it should be noted that because swash and backwash energies vary widely across the shore both of the situations shown in Figure 12 may exist simultaneously at different parts of the shore. Thus, a complex situation exists in which bed sediments are constantly winnowed and enriched to form grain size distributions made up of a number of separate elements deposited under different conditions.

Tanner (1958; 1964) has examined the statistical properties of the zig-zag shaped distributions made up in this way and suggests that the dominant processes of formation are simple mixing and filtering of the various grain size elements. A feature of all eight experiments conducted by Eagleson, Glennie and Dracup (1963) was the stranding of fine materials at the swash limit while coarse particles lagged under the breaker. Ingle (1966) reported a similar tendency for fluorescent sand particles to become stranded at the swash limit of natural sand beaches.

A comparison between theories and experiment on sorting was attempted by Miller and Zeigler (1958) for sand beaches. The analysis was performed separately for the offshore, breaker and swash zones. Two hypotheses of swash zone sorting were proposed, one with no seaward particle motion under gravity and one with both seaward and landward motion. The latter produced the best agreement with natural beach sorting patterns. Also, an attempt was made to predict the sorting action of the backwash by considering the effects of local flow depth, velocity and beach slope on the initiation of grain motion. An "edge velocity" just sufficient to move particles of the mean size on the foreshore was calculated using appropriate flow depth and slope data. This was then related to the mean maximum velocity of the backwash at different points across the shore. The resulting locations of initiation of motion of different grain sizes were then expressed in terms of distances from the beginning of the backwash. The method is approximate since it rests on a velocity profile the form of which is largely assumed. Accordingly agreement with the observed distribution of grain sizes across the shore was only fair.

Thus, sediment sorting in the swash zone has been little studied from the standpoint of governing processes. However, it should be noted that the phenomena are complex in that they result from continual mixing and winnowing of particles by

varying swash/backwash flow regimes.

Coarse particles tend to be located under or near the breaker while fines may be transported toward the swash limit or offshore. Bimodal distributions of sediment size may occur near the breaker where fines are abstracted as suspended load and where the larger grains may be in a state of oscillating equilibrium. Landward of this point a variety of distributions resulting from the mixing of differing ranges of sizes under active transport is more characteristic. While an increase in wave energy may produce an increase in mean grain size on the foreshore, the extent to which any of the above effects will be apparent at a given time and place is a function of the available range of sizes at that location. This effect should be at a maximum on the mixed sand-shingle beach. The morphological effects resulting from continual reworking of the beach deposit will now be considered.

Morphological Changes in the Swash Zone. As indicated previously, the study of foreshore morphological changes has long been a principal concern of coastal geomorphologists. Accordingly, the types of foreshore response produced by differing wave conditions are generally well known. Since these alterations to foreshore geometry represent ultimate responses to variations in swash/backwash process factors the present investigation is concerned with their explanation in terms of innate swash and backwash flow properties, rather

than in terms of differences between input wave conditions. The following description of foreshore morphological changes may therefore be regarded as an assemblage of observational data toward which much of the subsequent analysis and explanation of the process data will be directed.

Beach foreshores vary considerably in their relative mobility so that changes in elevation and location of stations occur on a number of different time and magnitude scales. Accordingly, a profile which neither progrades nor retreats over a period of time may be regarded as being at equilibrium for experimental purposes. However, it must be recognised that this state of net stability over a period of perhaps months is made up of a series of individual erosive and depositional events. This means that the long term mean profile will be contained within a "sweep zone" the upper limit of which is formed by the combined maximum accretion levels while the lower level is marked by the combined maximum erosive events. At any given time the profile may be eroding, building or both. In the offshore zone these events are controlled dominantly by wave action, but for the foreshore and break-point step areas Dolan and Ferm (1967, p. 14) have shown that tidal action must be considered in addition to waves.

Strahler (1964) examined the characteristic tidal cycle of changes occurring on a beach which was at equilibrium

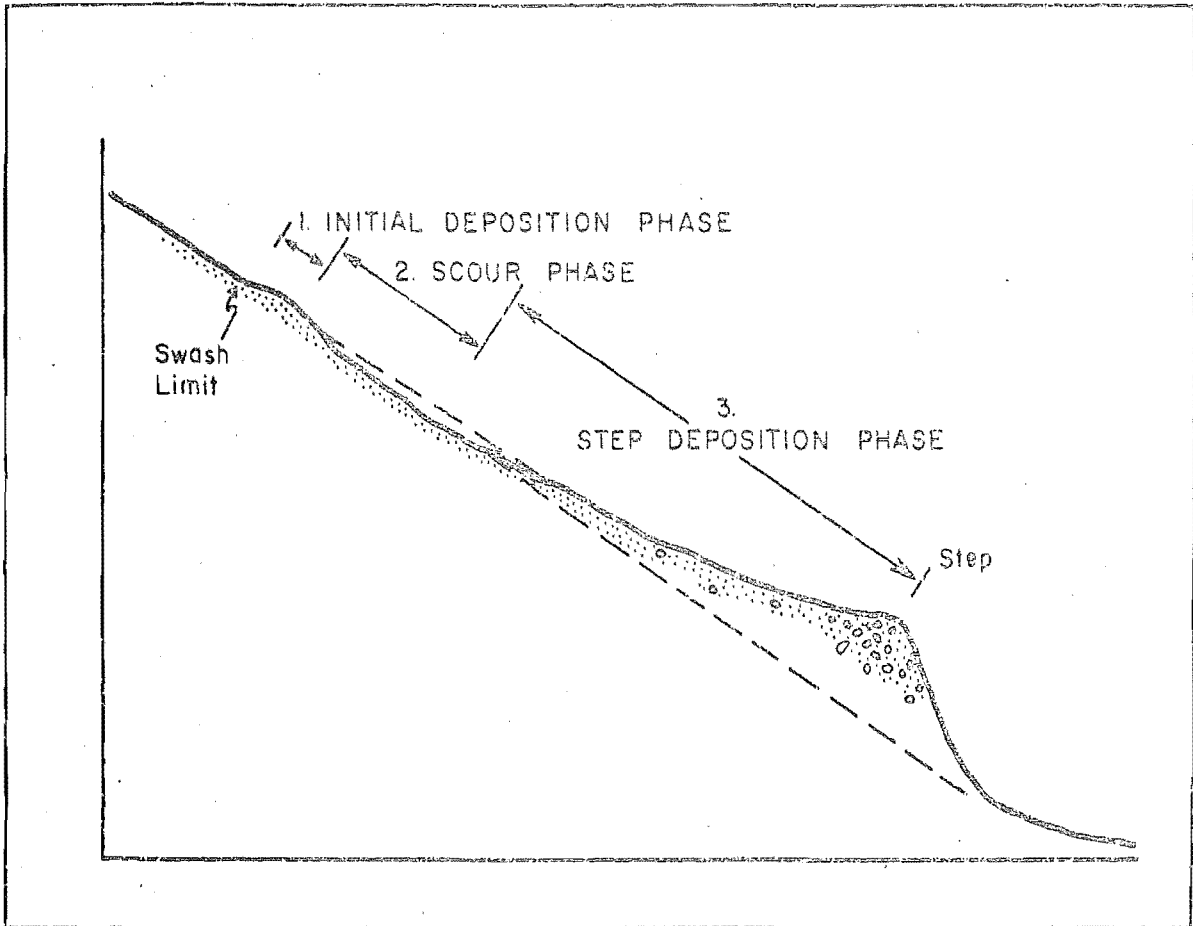


FIGURE 13. Locations of zones and erosion and deposition in the swash zone during an equilibrium cycle of tidal advance and retreat. Adapted from Strahler (1964, Fig. 10).

according to the definition above. Thus, the profile exhibited constant slope and position upon which rhythmic minor variations in morphology were observed to correspond with tidal progression and recession of the swash zone. Figure 13 demonstrates the nature of these changes.

A prominent gravel step was formed by deposition near the breaker. This gave way landward to a zone of scour which was succeeded in turn by a small area of deposition at the swash limit. Wave energy level was low during the observations and little is known about the processes responsible for the observed features.

Figure 14 indicates that on the rising tide the swash initiates deposition of medium sand near the upper limit. As the water level rises this is succeeded by the scour phase. Later still in the tide scour is followed by the deposition of a wedge of sand and gravel at progressively higher elevations. The seaward termination of this wedge occurs in the form of a gravel step beneath the breaker.

"Step-phase" deposition continues through the hours around high tide with mean sediment diameter increasing and sorting decreasing at all stations on the foreshore. It can be seen from Figure 14 that the magnitudes of erosion and deposition are at a maximum immediately landward of the breaker.

This sequence of events can be seen to be reversed almost

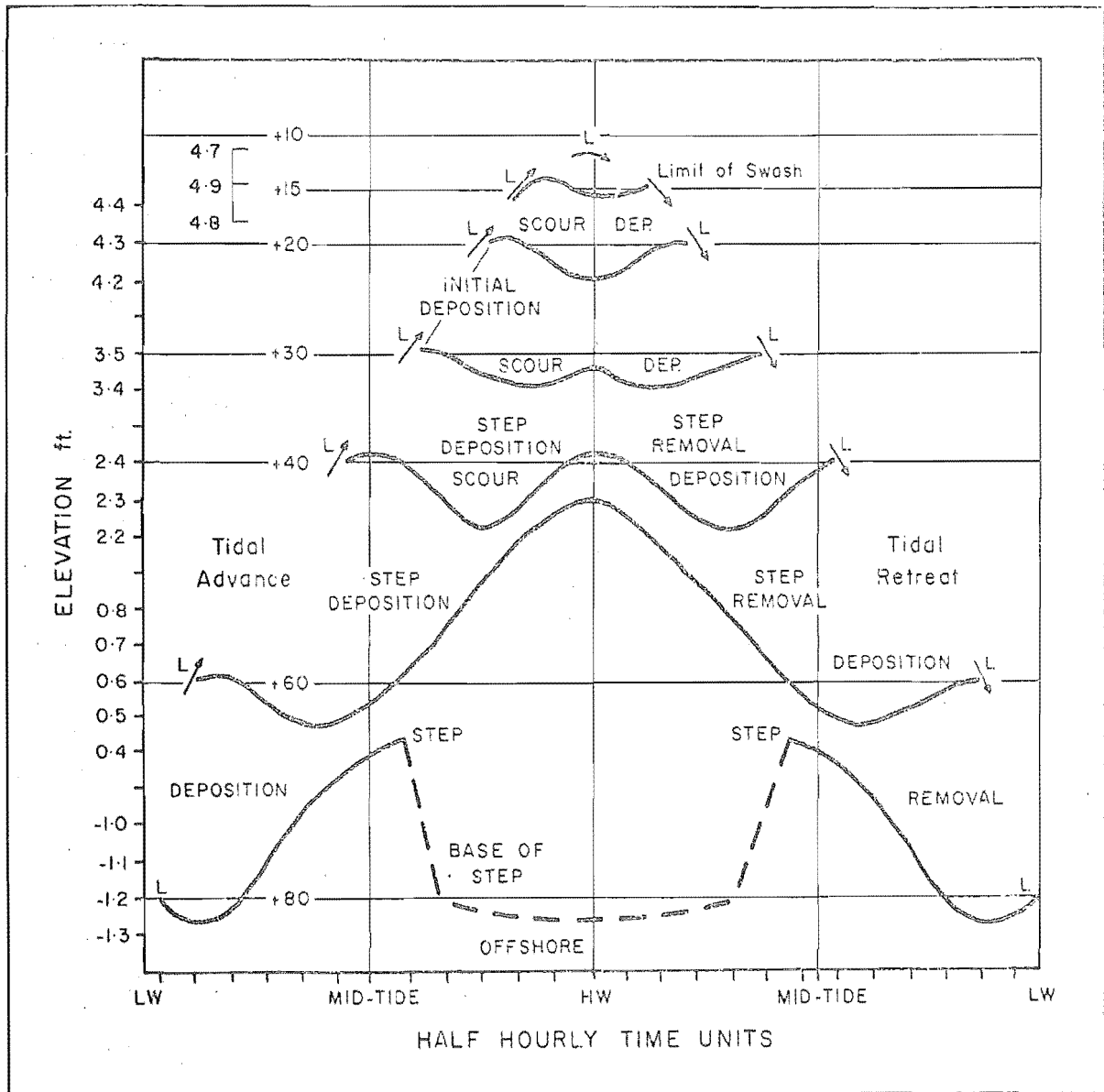


FIGURE 14. Tidal cycle of changes in an equilibrium beach. After Strahler (1964, Fig. 9).

exactly on the falling tide. Thus, on an equilibrium profile the beach is restored to its original conditions of slope, size and elevation. Strahler noted that under low wave conditions about 0.2 feet of sand was removed and redeposited in the mid-swash zone.

For other than equilibrium conditions King (1959, p. 280) records that a shingle foreshore at Chesil Beach, Dorset was cut back over 5 feet in 3 hours by short, steep waves. On the following day some 2-3 feet of vertical cut was observed over a period of only one hour.

It may therefore be stated that the foreshores of the study beaches are continually disturbed by swash/backwash, the magnitude of the disturbance depending upon wave energy and on the degree of adjustment achieved by the foreshore to the previous wave conditions. As has been mentioned previously Schwartz (1968) concluded that the mean amplitude of low energy swash zone changes was of the order of 10 cm. while the mean time required to achieve balance at this scale of disturbance was of the order of 30 minutes.

Sedimentation cycles of foreshore cut and fill occurring at tidal frequencies have also been observed by Otvos (1965) and King (1951). These authors noted that the depths to which sand was disturbed by waves varied with breaker height and grain size. Higher waves and larger particle sizes are associated with greater depths of disturbance. Experiments

similar to those of Otvos and King, though with differing results, were carried out on a shingle beach foreshore by Kirk (1966).

Columns of painted stones were buried in the foreshore and later excavated in order to record depth of disturbance. On a pebble slope of 4° ($Mz\phi = -3.08$) depth of disturbance for a breaker height of 4 feet ranged from 0.75 - 4.0. The disturbance was greatest on the lower foreshore and diminished toward the swash limit. Also, the disturbance was maximised at high water.

Results were obtained both for cases of net foreshore erosion and for net deposition and the disturbance values were found to be of comparable orders. Thus, the beach face is constantly disturbed irrespective of changes in absolute beach elevation. The magnitudes of the above disturbances lay between values obtained by King for fine sand and those by Otvos for medium to coarse sand. This result is probably due to the differing responses of sand and pebbles to wave action as previously demonstrated.

Emery and Foster (1948) and Grant (1948) have shown that the position of the beach water table can significantly affect beach face disturbance. Due to storage effects in the beach deposit fluctuations in the level of the water table may lag behind tidal changes in swash/backwash water levels by up to three hours. A dry beach with a low water

table was shown by Grant to promote deposition since swash water losses by percolation are at a maximum. On the other hand, if the water table is high, as for example during the late phases of the ebb tide, beach scour results from the addition of groundwater to the backwash. These effects may be expected to be minimal on freely permeable shingle foreshores.

Other bed features occurring in the swash zone include swash marks (Emery and Gale, 1951) and rills and ripples (Demarest, 1947). Careful observations by Demarest showed that rhomb-shaped ripple marks and rills were formed by the residual water sheet on steep foreshores following backwash. Since the formation of these features depends upon current speed and dynamic structure of the water column, discussion of them will be deferred until the examination of flow structures.

FLOW DYNAMICS

It is increasingly true that studies of processes involving the action of running water must draw on results from a wide variety of fields. Sundborg (1956, p. 133) notes that contemporary studies of fluvial processes must be based on the results of other studies in theoretical hydrodynamics, practical soil mechanics and on other avenues of research. The state of flow on a beach, as on a river bed or surface affected by wind action, determines the active forces whilst the structure and form of the bed determine the reaction to these forces.

Sundborg further notes that because of this modern investigations of the processes controlling erosion, transportation and deposition of sediments have generally adopted as an initial hypothesis, some conception of fluid flow, based either on theory or experiment. Most morphologically important processes relating to fluvial flow have been treated in this way (Mathes, 1947, Kalinske, 1945; 1947 - in Sundborg, 1956, p. 133; Inman, 1949; Bagnold, 1942; 1968). Inasmuch as it is flowing water, resulting from broken sea waves, that causes sediment motion on a shingle beach foreshore, this approach will be adopted in the present investigation. However, only those aspects of flow dynamics essential to an

understanding of the morphological activities of flows in the swash zone will be considered. A comprehensive review of flow dynamics may be found in Rouse (1938). The subsequent presentation draws extensively on the published reviews of theory and experiment by Sundborg (1956), Inman (1949); 1963) and Bagnold (1942; 1968) and by Inman and Bagnold (1966).

Characteristics of Fluid Flow

Fluid flow may be assigned to one of two types, either laminar or turbulent depending on the way in which the fluid particles move. Laminar (or stream-like) flow is characterised by the condition that layers of fluid slip over contiguous layers without the occurrence of mixing between the layers (save for small scale molecular mixing). The stream lines remain separate from one another and the flow may be variable or constant with respect to space and time.

Since all real fluids possess a certain viscosity there is an internal friction that resists flow. When a layer of fluid slides over another the friction between them gives rise to a shearing stress, according to Newton's fundamental relation:

$$\tau = \mu \frac{du}{dz} \quad \dots\dots\dots 10.$$

where: τ is the tangential force per unit area, μ is the

coefficient of molecular viscosity; and du/dz is the velocity gradient perpendicular to the direction of motion (and is thus in the same direction as τ).

Laminar flow seldom pertains to the swash zone, except near the swash limit on very fine beds. This is because if the velocity gradient becomes higher, or if the bed becomes rougher laminar flow gives way to an eddying motion accompanied by intense lateral mixing. Grant (1948) indicates that a film of water 1cm. deep on a sand foreshore cannot flow faster than 3 cm. per second without turbulent flow occurring.

This eddying flow is termed turbulent flow. It is always variable with respect to time and space and may be regarded as comprising a complex secondary movement superimposed upon the primary translatory flow. It is customary to describe a turbulent flow by the average velocity \bar{U} , but Inman (1949, p. 53) notes that the velocity at any instant is the vector sum of the average velocity and a random (secondary) fluctuation due to turbulence such that:

$$U = \bar{U} + u \quad \dots\dots\dots 11.$$

For turbulent flow the equation comparable to eqn. 10 is:

$$\tau = A_z \frac{d\bar{u}}{dz} \quad \dots\dots\dots 12.$$

Where A_z is the eddy viscosity which accounts for the space exchange of momentum due to random fluctuation in

turbulent flow. Both μ and A_z have the dimensions $ML^{-1}T^{-1}$ (Inman, 1949, p. 53). Inman notes that A_z is many orders of magnitude larger than the molecular viscosity μ , and that Sverdrup et al. (1942, p. 91) have shown A_z to range from 1 - 1,000 c.g.s. units for ocean currents. Further, while μ is independent of the state of motion A_z is variable with flow state. Thus, turbulence is an extremely complicated phenomenon and one which is by no means completely understood. However, a consideration of even its most general properties is of value in any study of sediment entrainment.

The Transition From Laminar to Turbulent Flow. In turbulent flow inertial forces dominate over the frictional forces which govern laminar flow. The transition between these two states is most usually characterised by Reynolds' criterion (Sundborg, 1956, p. 135), which expresses the proportions of inertial and frictional forces governing a given flow:

$$R = \frac{u \cdot l}{\nu} \quad \dots\dots\dots 13.$$

where u is a characteristic velocity such as the mean for a particular cross-section, l is a characteristic length such as the depth of flow, and ν is the kinematic viscosity. $\nu = \frac{\mu}{\rho_f}$ (and where ρ_f is the fluid density). When R is small frictional forces predominate and flow is therefore laminar. At higher values of R inertial forces increase until at some critical velocity turbulence is developed. The value of R at

which flow ceases to be laminar varies within certain limits depending upon external conditions. The most important of these is the roughness of the boundary surface since in natural channels this surface is comprised of sediment grains which may be transported by turbulent flow.

Bed Roughness and its Effects on Fluid Turbulence

Inman (1949, p. 53) demonstrates that A_z in equation 12 can be defined as:

$$A_z = \rho_f \ell^2 \left| \frac{d\bar{u}}{dz} \right| \dots\dots\dots 14.$$

where ℓ is the "mixing length"; ρ_f is the fluid density and $\frac{d\bar{u}}{dz}$ is the absolute magnitude of the shear. Over a rough surface ℓ must have a definite value, since turbulence extends to the very bottom, and for a fluid of indifferent stability may be written as:

$$\ell = k_o (Z + Z_o)$$

Where k_o is von Karman's constant and is approximately 0.4 z is measured positive upwards and z_o is the roughness length related to the height of the roughness elements (sediment grain diameter in this case). Combining equations 12 and 14 gives the von Karman - Prandtl expression for boundary currents over a rough surface:

$$\bar{U} = \frac{u^*}{k_o} \log. \frac{z + z_o}{z_o} \dots\dots\dots 15.$$

Where the factor u_* is equal to $\sqrt{\tau/\rho_f}$ and is called the Friction Velocity. u_* has the dimensions of a velocity and is proportional to the average velocity \bar{U} . A coefficient γ is defined by $u_* = \gamma \bar{U}$; and it can be seen from equation 15 that γ is a function of the height at which \bar{U} is measured above the bed and of the bed roughness (i.e. z affects the height at which \bar{U} is determined and z_0 relates to the roughness elements). Munk (1947) has reviewed the literature on the determination of the value of γ and it appears that it has a constant value over a rough surface but that it decreases at a certain critical wind speed below which the bed becomes smooth (Inman, 1949, p. 54).

Equation 15 is not applicable to flow over a smooth surface. This is given by:

$$\bar{U} = 5.5 u_* + \frac{u_*}{k_0} \log. \frac{u_* z}{\nu} \dots\dots\dots 16.$$

The stress occurring in turbulent flow may be written in Reynold's form as:

$$\tau = -\rho \overline{u' w'}$$

where u' and w' are the instantaneous velocity fluctuations in the x and z directions respectively .

Further, if it is assumed that a correlation exists between u' and w' then the friction velocity is proportional to the mean of the absolute velocity fluctuations. Also, if it is assumed that the turbulence is isotropic, the

friction velocity is equal to the mean of the absolute value of the velocity fluctuations:

$$u_* = \sqrt{\tau/\rho_s} = |\bar{u}'| = |\bar{w}'|$$

Inman (1949, p. 54) states that von Karman's law for flow over a smooth surface gives the thickness of the laminar sub-layer at the bed as:

$$\delta = \frac{\lambda \cdot \nu}{u_*} \dots\dots\dots 17.$$

where: λ is a constant.

Inman argues from 17 that if the bed is to be considered rough the roughness elements must project above the laminar layer and that, in turn, this assumption suggests that some constant value of the ratio of bottom grain diameter, d , to the thickness of the laminar sub-layer may be a criterion distinguishing between rough and smooth beds.

Sutherland (1967) in a study of sediment entrainment by turbulent flows has examined the motion near the bed. Experiments in flumes led to the formation of the hypothesis that grain motion is initiated by turbulent eddies which disrupt the viscous (laminar) sub-layer and impinge directly on the grain surface. Thus if the value of δ from equation 17 is substituted, the ratio d/δ may be written in the dimensionless form of a Reynolds number:

$$\frac{u_* d}{\nu} = \text{constant}$$

Inman (1949, pp. 54-55) adds that the work of Nikuradse (1933), Fage (1933) and White (1940) places the boundary between smooth and rough surfaces at a critical value of u_*d/ν such that:

$$\frac{u_*d}{\nu} \quad > \quad 3.5 \quad > \quad \frac{u_*d}{\nu}$$

Rough Surface Smooth Surface

Therefore a critical friction velocity $u_{*r} = 3.5 \nu/d$ can be defined at which the bed changes from hydraulically smooth to hydraulically rough (roughness velocity). Hence a smooth surface may give rise to a higher value of critical Reynolds number than a rough one in the same position. Also, Sundborg (1956, p. 135) makes it clear that a small disturbance may render a previously stable flow unstable, with no attendant change in the value of R.

It is clear that a transitional range of R exists within which the flow may be either turbulent or laminar. Sundborg notes instances of turbulence occurring at R_{crit} more than ten times smaller than in other experiments where the flow was laminar. However, there is a generally accepted figure of R c. 500 below which flow remains laminar whatever disturbances occur.

It is important to note that the Reynolds criterion is not always the best for characterising the transition from laminar to turbulent flow, particularly for flows with

depths of only a few millimeters. Here a type of apparently turbulent flow has been observed for R considerably below 500 (Sundborg, 1956, p. 136).

This may be of considerable importance on the shingle beach foreshore where downslope transportation of sand and even of small pebbles has been observed in the groundwater sheet and in groundwater rills which appear in the interval between seaward return of water in the backwash and the succeeding swash. These flows have a maximum depth of 1-2 cm (Demarest, 1947).

It appears that the flow velocity corresponding to the lower limit of turbulent motion can be alternatively stated in an expression known as Horton's criterion (Sundborg, 1956, p. 136):

$$V_{\text{crit}} = 0.021 \frac{v}{n^2 D^{\frac{1}{2}}}$$

where n is a roughness coefficient and D is the depth of water. Thus, R_{crit} becomes proportional to depth of water and inversely proportional to the square of the roughness coefficient. Obviously if the flow depth is small and the bed is very rough as on a shingle beach foreshore, R_{crit} is very low indeed.

An alternative explanation offered by Sundborg is that gravity waves are easily developed on a rough, steeply sloping bed. This, "may result in a local state of turbulence even

though the undisturbed flow is well below the critical Reynolds number". Robertson and Rouse (1941 - in Sundborg, 1956, p. 136), and Hjulstrom (1935) have demonstrated that turbulent mixing results from these gravity waves. The latter explanation is supported by the wave forms readily observed on the water surfaces of both groundwater sheets and rill-wash flows down the foreshore, but much closer examination is warranted.

Gravity Waves

A further characteristic of the state of flow is the ratio of flow velocity to the velocity of propagation of small gravity waves. The significance of this particular criterion is highlighted by the fact that both swash and backwash flows have already been shown to be of the gravity type. Whereas R indicates the effect of viscosity this ratio relates to the effects of gravitational acceleration on the flow. The velocity of propagation of gravity waves is given by:

$$C = \sqrt{g \cdot h} \quad \dots\dots\dots 18.$$

where g is the gravitational constant and h is the depth of water. If the flow velocity $U = C$ a wave disturbance is unable to travel upstream. This has effects on the slope of the water surface and hence, on the local energy grade-line.

The ratio $U/\sqrt{g.h}$ is known as the Froude number and like R is dimensionless. When $F < 1$ the flow is said to be tranquil (or streaming), and when $F > 1$, as shooting (or rapid). In tranquil flow disturbances are transmitted upstream and obstacles cause a rise in water level upstream of them. However, in shooting flow the motion upstream of an obstacle is not affected. Irregularities near the shore of a water course with shooting flow give rise to small stationary oblique waves, while stationary cross waves are set up behind obstacles in tranquil water (Sundborg, 1956, p. 137).

Where the flow alters from tranquil to shooting the water level falls evenly (as in the late stages of a swash), but when there is a transition from shooting to tranquil flow, (as at the slack water at the base of the breaker, or where the oncoming breaker causes a sudden reduction in U in the backwash); the change may be very abrupt. This may give a turbulent surface wave, known as a hydraulic jump. In such a wave some of the kinetic energy of the shooting flow is converted to turbulent energy and locally intensive sorting of the bed may result.

In the range $1 > F < 2$ the transition may not involve a definite jump (Rouse, 1938, pp. 384-385), but rather give rise to a series of standing waves. This is most likely to occur if the flow depth is only slightly more than the critical. Gravity waves have a least velocity of 23.2 cm/sec, but this applies only to water deeper than 0.5 cm since

FIGURE 15. Turbulent exchange and surface profiles of surges. C = direction of current velocity. Y_1 = depth of undisturbed flow. Y_2 = depth of disturbed flow following passage of surge. Adapted from Rouse (1938, Figs. 220; 221).

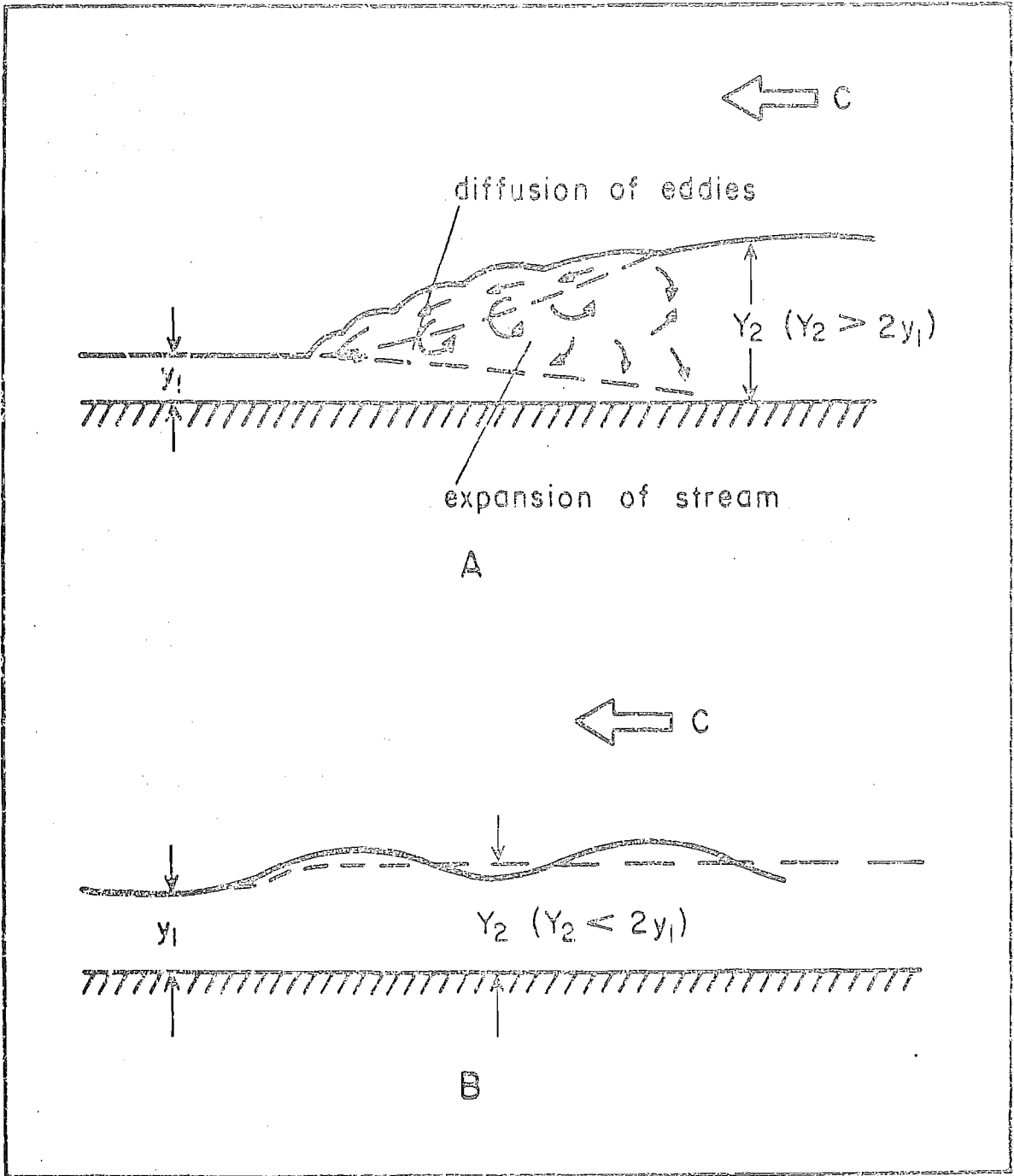


FIGURE 15A. A hydraulic jump wave.
 15B. A standing wave system.

below this value surface tension affects the wave celerity (Robertson and Rouse, 1941 - in Sundborg, 1956, p. 137).

Therefore it is unsafe to apply Froude's criterion to water less than 0.5 cm. deep and it may prove unsatisfactory below depths of 1.0 cm and transitional velocities of 30.0 cm/sec. since there is probably a transition range between tranquil and shooting flow at these depths.

In discussing further details of the properties of gravity shock waves (Rouse, 1938, pp. 383-396) observed that a different rate of energy loss is established by the passage of a surge. This is because both depth of flow and mean velocity are altered. Figure 15 shows the two characteristic profiles of such waves. It can be seen from Figure 15A that in the case of a hydraulic jump wave the maximum energy loss takes place at the wave front where there is generally violent eddy motion.

"To an observer looking down upon a passing surge, the front of the disturbance seems to be covered by a surface roller in a high state of agitation ..., a distorted vortex with a horizontal axis, which to all outward appearances remains distinct from the fluid passing underneath. Nevertheless careful observation ... will establish beyond question the intimate relation of this roller to the fluid passing beneath (see Fig. 15A). Small masses of rotating fluid are constantly being fed from the underside of the roller into the passing flow" (Rouse, 1938, pp. 383-384).

At the same time that the eddies spread downward across the flow the resultant mixing process accomplishes the

necessary upward expansion of the mean flow. The eddy motion therefore extends from the top to the bottom of the flow section and the intense level of turbulent agitation of the fluid is not reduced to a normal value for a considerable distance upstream from the front of the surge.

Figure 15 also shows that a jump wave will occur only if the depth of the disturbance is more than twice as great as the depth of the undisturbed flow ($y_2 > 2y_1$, and $F > 2$). As has been shown above for Froude numbers between one and two a standing wave regime is established (see Fig. 15B). A surge originally having the form indicated by the broken line on the diagram forms an undular profile because the wave front tends to advance more rapidly than the section just behind it, leaving a depression in the surface. The latter is followed by the development of further crests and depressions, and so on, the amplitude of the depressions gradually decreasing with distance from the wave front.

The depth of a standing surge such as that shown in Fig. 15B is thus a function of the original flow depth. Bakhmeteff and Matzke (1936 - in Rouse, 1938, p. 389) found that a value of the Froude number equal to 1.73 marked the boundary between the undular and the jump wave conditions. The maximum attainable height of a jump wave corresponded to a Froude number of 2.77.

Though the above characteristics were determined for a flat bed Rouse (1938, p. 390) points out that not until

the bed slope exceeds 0.1 are there appreciable changes in the wave form, but if the slope is excessive the presence of a surface roller will not necessarily indicate deceleration of the flow beneath since the high velocity stream may plunge deep and continue for some distance in the shooting state.

Also, it is clear that a change in flow section must necessarily disturb water motion. Thus, for example, a jump may form at an abrupt change in channel slope. Here a surge develops and travels upstream until a state of equilibrium rate of energy loss is achieved in an area where flow varies less rapidly.

From the above it may be concluded that surges of both the jump and undular types can be expected in the swash zone, especially in the backwash where the transition from shooting to tranquil flow occurs high on the shore as the flow gains depth and velocity. The phase relations governing the relative volumes of water entering and leaving the zone will strongly influence the incidence, severity and location of these extremely turbulent, localised releases of energy. Also, secondary surges may occur in the swash where it is underridden by the backwash during high phase conditions.

It is important to stress that while both swash and backwash in the tranquil (non-jump) state of flow may transport considerable quantities of sediment, the incidence of jump waves in the zones of transitional flow must be

TABLE 3

LIMITS OF FLOW REGIMES

| <u>Laminar</u> | | <u>Turbulent</u> | |
|----------------|----------|------------------|----------|
| R < 500 | - 2,000 | R > 500 | - 2,000 |
| Tranquil | Shooting | Tranquil | Shooting |
| (F < 1) | (F > 1) | (F < 1) | (F > 1) |

Source: Sundborg (1956, Table 1, p. 137)

regarded as a powerful additional erosive force in the backwash. This effect will be greatest in areal extent and intensity of action during high phase conditions.

Regimes of Flow

Combining Reynolds criterion with Froude number gives a total of four possible regimes of flow as outlined in Table 3 and Figure 16. These have been reproduced from Sundborg (1956, Table 1, p. 137 and Figure 1, p. 138). In laminar, tranquil flow (at $F < 0.5$) over a rough surface there is often an intermittent uneven motion (intermittent or "slug" flow) with pulsation or undulation that causes turbulence (Robertson and Rouse, 1941 - in Sundborg, 1956, p. 138). Figure 16 shows the four types of flow and includes the regime of slug flow. It is important to note the effect that temperature has on the limits between the various regimes. This is because temperature is a primary control of density and hence of viscosity. It can be seen from the diagram that laminar flow, as mentioned earlier, can only occur for slow flows or for very small depths. Thus, in natural water courses and on beaches the flow may be said to be predominantly turbulent.

The only exception to this general rule is in close proximity to the bottom where the variable velocity components in the immediate neighbourhood of sediment grains are small

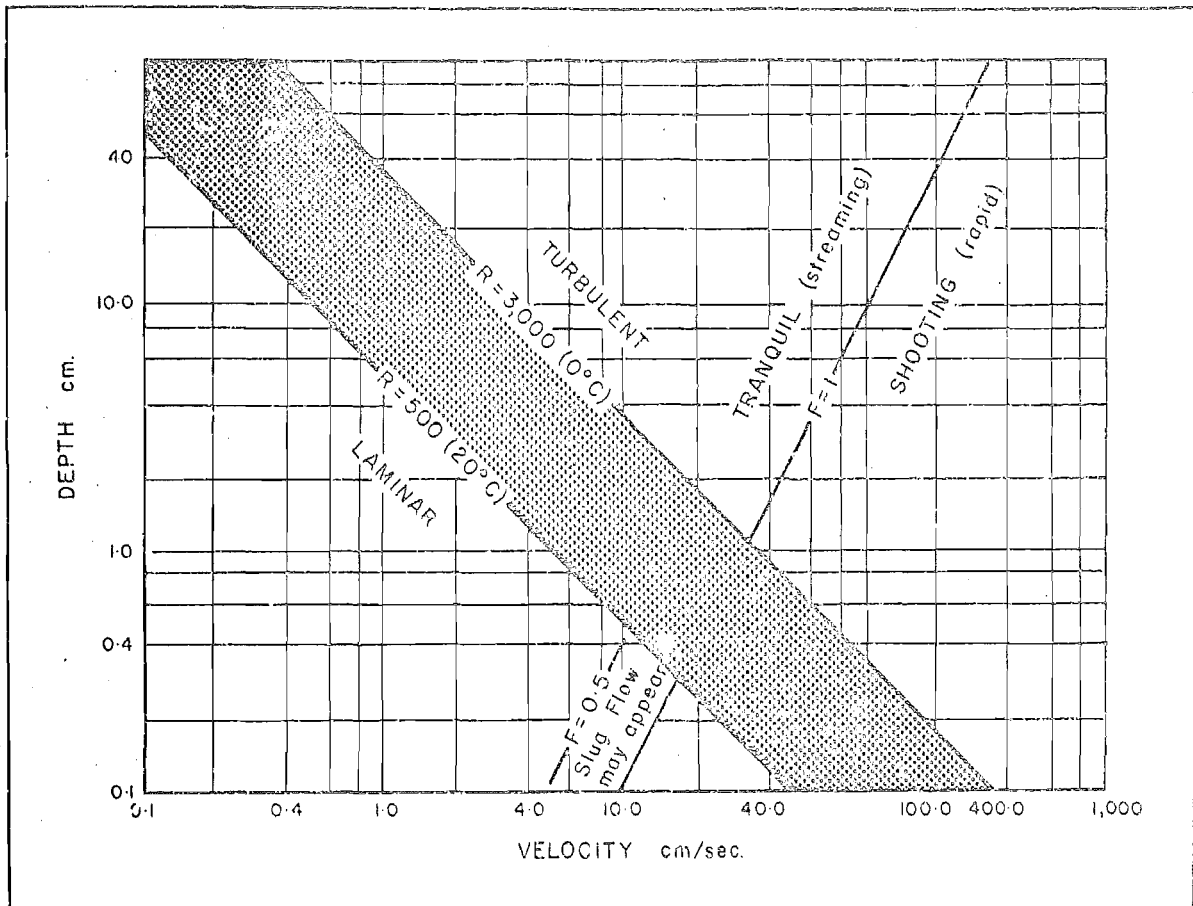


FIGURE 16. Regimes of flow in a broad, open channel. Note the influence of water temperature on the limit between laminar and turbulent flow.
 Source: Sundborg (1956, Fig. 1, p. 138).

and hence a laminar sub-layer may exist i.e. in this zone viscous forces may predominate over inertial forces. This, as has been shown, depends upon the roughness of the bed which imparts to the flow in a laminar boundary layer, a secondary disturbance which may develop until its effects extend practically throughout the entire water column (in which case the flow becomes turbulent); or may die out (in which case the flow in the boundary layer remains laminar).

In conclusion it can be seen that a full range of flow types has been described in relation to present notions of hydraulic theory. It is now possible to describe the dynamic characteristics of swash and backwash flows on a shingle beach foreshore, and to evaluate their significance with regard to sediment entrainment processes. A great deal of very detailed work has been concerned with the manner in which turbulent flows initiate sediment motion but this will not be treated fully here, since it is not a central concern of this investigation. Rather, a series of broad principles consistent with the characteristics of flow outlined above will be presented. In this way the relations between types of sediment transport and variations in turbulent flow may be examined in sufficient detail to clarify later treatment of swash zone data derived from this investigation.

The Transport of Sediment by Fluid Flow

The theory of sediment transport is developed largely from the laws of general physics and embodies the theory of fluid flow outlined above. The theory of sediment entrainment has mainly centered around attempts to define the conditions responsible for initiation of grain motion (Hjulstrom, 1935; 1939; Rubey, 1938; and others) and many experiments in laboratory flumes have been conducted. Owing to the complexities of natural water courses few results from natural streams are available. Similarly, as has been demonstrated few evaluations of theory have been carried out for ocean wave environments (Einstein, 1948; Manohar, 1955; Caldwell, 1956; Putnam, Munk and Traylor, 1949 and Inman 1963), and most of these have been in connection with the prediction of the amounts of material moved by longshore (wave-induced) currents. No theoretical study known to the author relates to the swash zone, though the operative forces may be expected to be similar to those of other environments.

The following discussion will first consider the requirements for and nature of initial grain motion. This will be followed by an examination of the characteristics of sediment flow in high concentrations. Characteristics of natural sediments will be considered also. Finally, the bed forms resulting from transportation will be discussed.

Settling Velocity. Bagnold (1968, p. 46) notes that since sediments are heavier than water they are pulled downward by gravity, transport consisting of the shearing movement of the solids, together with the fluid, over a bed of solids. "It follows from these two facts that the excess weight of the transported solids, whatever may be the degree of their dispersion within the fluid, must be supported by an equal and upward force ... and that this supporting force derives from the process of shearing" (Bagnold, 1968 p. 46).

Newton proposed that a particle falling in a fluid will accelerate under the force of gravity until the "frictional drag" of the fluid approaches the value of the impelling force (Inman, 1949, p. 55). After this a constant velocity c , the settling velocity is attained. The frictional drag law of Newton rests on the assumption that the drag force F_D is proportional to the square of the velocity:

$$F_D = C_D B \rho \frac{V^2}{2} \dots\dots\dots 19.$$

where C_D is a dimensionless coefficient called the drag coefficient; B is the projected area of the particle in the direction of motion (equal to $\pi d^2/4$ for spheres); and V is the relative velocity between the particle and the fluid.

Inman (1949, p. 55) shows that Newton's assumption of the constancy of the drag coefficient is not found to hold. Rather C_D is a function of Reynolds number.

For a small particle settling in a fluid gravity acts

downward and a buoyant force (given by Archimedes principle) acts upward. The difference between these two forces is known as the impelling force and for spherical particles is given as $\frac{1}{6} \pi g \rho' d^3$; where g is the acceleration due to gravity and ρ' is the difference in density between the particle and the fluid.

By equating the impelling force to the drag force the settling velocity is found to be:

$$C = \sqrt{\frac{4}{3} \frac{g}{C_D} \frac{\rho' d}{\rho}} \dots\dots\dots 20.$$

C_D is equal to $24R$ for the region of viscous settling (diameters smaller than 0.18mm). Substitution of this value in 20 gives Stokes Law for the settling velocities of small particles:

$$C = \frac{1}{18} \frac{g}{\nu} \rho' d^2$$

This formulation is not applicable to diameters larger than 0.18 mm because in this case, turbulence is developed by the passage of the grain through the fluid. Rubey (1933) has developed a more general relation which agrees with observed values for settling velocity over a wider range of grain sizes than covered by Stokes Law. This function is plotted against particle size in Figure 17. As has been mentioned, Inman (1949, p. 55) notes that a spherical quartz grain of 0.18 mm. diameter has a settling velocity in water of approximately 2cm/sec. which corresponds to a Reynolds number for the grain

which is equal to the critical value of the bottom roughness criterion, $u_* d/\nu = 3.5$. The latter function is also plotted in Figure 17.

Theory of Sediment Entrainment

A stream of water must attain a certain minimum velocity before particles lying on the bed may be moved. Depending on the speed of fluid flow the sediment motion may be of one of three types. At low speeds the particles will roll or creep along the bed but at high speeds they will be transported in a suspended state. For intermediate speeds particles may saltate or move in leaps owing to eddies in the fluid and abrupt changes in velocity (Zenkovich, 1967, p. 94).

The first type of motion is a bed-load phenomenon and the velocity of grain motion is less than that of the current. For rolling particles Zenkovich (1967, p. 94), shows that according to Airy's Law the linear dimensions of a grain are proportional to the square of the current velocity:

$$\frac{c^2}{gd} = K \left(\frac{\rho_s}{\rho_f} - 1 \right) \dots\dots\dots 21.$$

where d is the diameter of the particle; c is the current speed; ρ_s and ρ_f are the densities of the grain and fluid respectively; and k is a coefficient dependent on particle shape. For materials of constant specific gravity the right hand side of the expression may be taken as constant.

If the velocity of flow increases the rate of particle motion (V) is approximately the difference between the current speed and the speed at which the grain begins to move: $V = C - V_0$. Zenkovich further notes that under some marine conditions the path traversed by a grain during a given stage of grain motion will not necessarily be wholly by rolling. If the particle becomes suspended for any time then for this portion of its path it will move at the same speed as the fluid.

The fluid speed necessary to suspend a given grain may be of the order of five times that necessary to initiate rolling (Zenkovich, 1967, p. 95). Also, it is important to note that the speed required to initiate motion (threshold velocity), is always slightly greater than that required to maintain motion of the grain. The ratio of these speeds varies between 1.3 and 1.5.

Penck (1894 - in Zenkovich, 1967, p. 95), studied grain movement along slopes, both upslope and downslope. For a horizontal bed he obtained:

$$C = a \sqrt{r \cdot \tan p} \quad \dots\dots\dots 22.$$

where C is the rate of fluid flow in meters/sec.; r is the radius of the particle in meters; a is a shape coefficient (assumed by Penck to be 6.32); and p is the angle of rest of the particle.

For sloping beds the effect of the weight of the

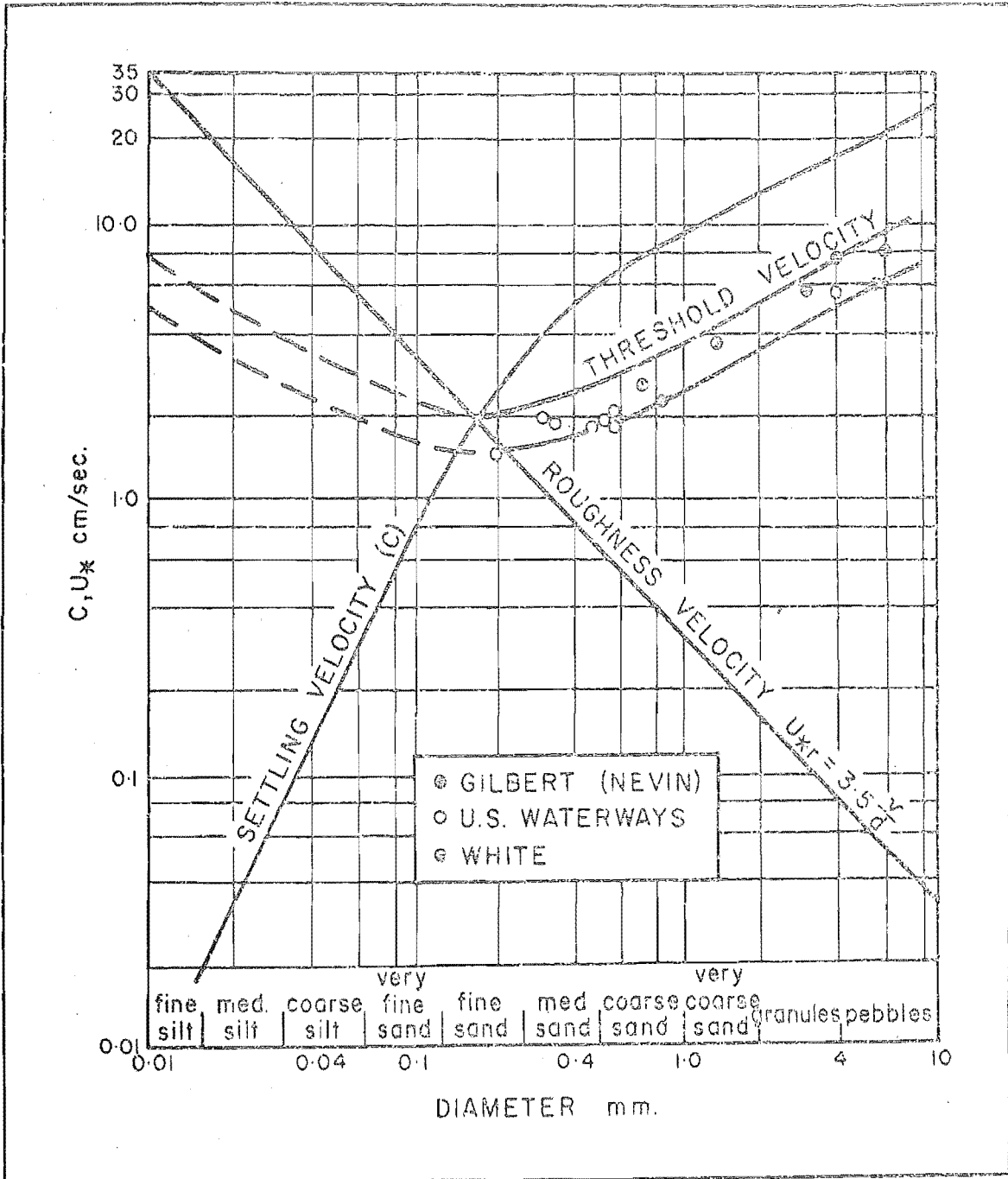


FIGURE 17. Relation of grain diameter to settling velocity, threshold velocity and roughness velocity.
 Source: Inman (1949, Fig. 2, p. 56).

particle requires a greater speed of fluid flow to cause grain motion upslope and a lesser speed for motion downslope.

Thus:

$$C = 6.32 \sqrt{\frac{r \sin (p+\phi)}{\cos p}} \dots\dots\dots 23.$$

where ϕ is the angle of inclination of the slope with respect to the horizontal. ϕ is negative for inclination with the current and is positive for inclination against the current. If ϕ is greater than p the grains will roll down the slope until the angle of repose is adopted.

In swash and backwash flow and under oscillatory wave motion water is projected both up and down the slope so that the net sorting effect on grains will depend upon the ratio of the speeds necessary to move grains up and down given slopes.

Zenkovich (1967, p. 95) demonstrates from equation 23 that for slopes up to 5° the ratio of these speeds is near unity, but that for steeper slopes the difference is appreciable. For example, on a 10° slope the ratio has a value of 1.43. This would imply considerable asymmetry of the flows. This will be shown to be of fundamental importance in understanding the erosive nature of swash and backwash flows on the shingle beach.

Though the above has served to demonstrate some important factors in sediment movement by water it is not possible to employ the approach in calculating movement and transportation

of sediment along the sea bed. This is because the expressions do not contain quantitative measures relating wave accelerations to the resulting types of sediment motion. Nor do they specify the effects of water motion in the immediate vicinity of the sediment grains. These factors are considered in later work by Bagnold (1942; 1968), Inman (1949; 1963) and others.

Initiation of Grain Motion. It has already been shown that movement of particles will not occur until a critical drag force, which is some function of grain size, is exceeded. The work of Shields (1936), White (1940) and Bagnold (1942) has shown that the critical drag force, f_c , on a spherical particle may be written as:

$$f_c = \alpha g \rho' d^3 \tan \phi \quad \dots\dots\dots 24.$$

The coefficient α depends upon the type of flow, and ϕ is the angle of internal friction of the grains, which is approximately equal to the angle of repose of the grains (Inman, 1949, p. 56). Miller and Byrne (1966) have studied the angle of repose for single grains on a fixed, rough bed. For sand grains (0.088 - 0.70 mm. diameter), they found that the angle of repose increases with decreasing size and with decreasing sorting. Departures from grain sphericity and increased angularity were associated with increasing angle of repose. Average mass angle of repose for well rounded

sand was $32.2 - 33.5^\circ$ and $34.0 - 39.0^\circ$ for angular sand. Angles of repose for single grains were much higher than this so that care is warranted in the application of single values for mass angle of repose in expressions such as 24 above.

If a sand is of uniform diameter, d , the number of grains exposed to the fluid drag is p/d^2 where p is the packing coefficient (defined as d^2 times the number of exposed grains per unit area). The critical drag force per unit area is thus $f_c p/d^2$ or:

$$\tau_c = p \alpha g \rho' d \tan \phi \quad \dots\dots\dots 25.$$

The factor α can be shown to be a function of the roughness criterion and experiments show it to have a value 0.25 for values of $u_* d/\nu$ greater than 3.5 (White, 1940 - in Inman, 1949, p. 57); i.e. for turbulent flow.

The critical drag force can now be expressed in terms of a critical frictional velocity, u_{*c} :

$$u_{*c} = \sqrt{\tau_c / \rho'} \quad \dots\dots\dots 26.$$

The critical value of u_* at which sediment motion begins owing to the drag force of the fluid is known as the "threshold velocity" (Bagnold, 1942, p. 86).

The above has dealt with a critical drag force or its equivalent velocity which may be computed from an average velocity profile using equation 15 but Inman (1949, p. 57)

states that it is important to note that even if momentarily the value of u_{*c} is exceeded, movement will result. Thus, the important parameter is the instantaneous velocity, U , comprising the average velocity, \bar{U} , plus the velocity related to random fluctuation, U' (see equation 11). Kalinske (1943 - in Inman, 1949, p. 57) shows that the instantaneous drag force may be many times larger than that computed from the average velocity.

A broad curve including some of the experimental values of threshold velocity are shown by the parallel solid lines in Figure 17. Inman (1949, p. 57) states that these values were calculated from experimental critical drag forces obtained by White (1940), the U.S. Waterways Experiment Station, and from Nevin's (1946) analysis of data obtained by G.K. Gilbert.

It is clear from Figure 17 that the threshold velocity gradually decreases with decreasing grain diameter until a size of approximately 0.18 mm. is reached. It will be remembered that at this size u_*d/ν becomes less than 3.5 and the bed becomes effectively smooth, so that individual grains cease to shed small eddies. The drag instead of being carried by a few grains is more evenly distributed over the whole bed. Hence, the velocity required to initiate sediment motion increases for grain sizes less than 0.18 mm. Hjulstrom (1939, p. 12) has shown that this is

generally true for wind flows as well as for running water.

Menard (1950) notes that both the critical drag force of Rubey (1938) and the critical friction velocity of Inman (1949) are related to forces acting at the bed. They are not mean velocities, though they can be related to this, as has been shown. Hjulstrom (1939, pp. 10-12) has demonstrated the relationship between mean velocity ("competent velocity") and grain size. This is shown in Figure 18. It can be seen that the curve is of the same form as that for threshold velocity but the limits between motion and cessation of movement are more diffuse, reflecting the use of average velocity as the independent variable. The importance of this curve will be demonstrated when consideration is given to the bed forms resulting from sediment movement.

Saltation. Once motion of the grains has been initiated some particles may be lifted off the bed. A particle returning to the bed under the influence of gravity may "bounce" or strike another particle, causing it to leave the bed. The initial rise of particles from the bed may be partly explained by an upward force due to the presence of a steep velocity gradient near the bed (Jeffreys, 1929 - in Inman, 1949, p. 57). Kalinske (1943) believes that saltation is not important in water although Gilbert (1914), Bagnold (1942), and others have observed it. Kalinske concluded that the flow of water at

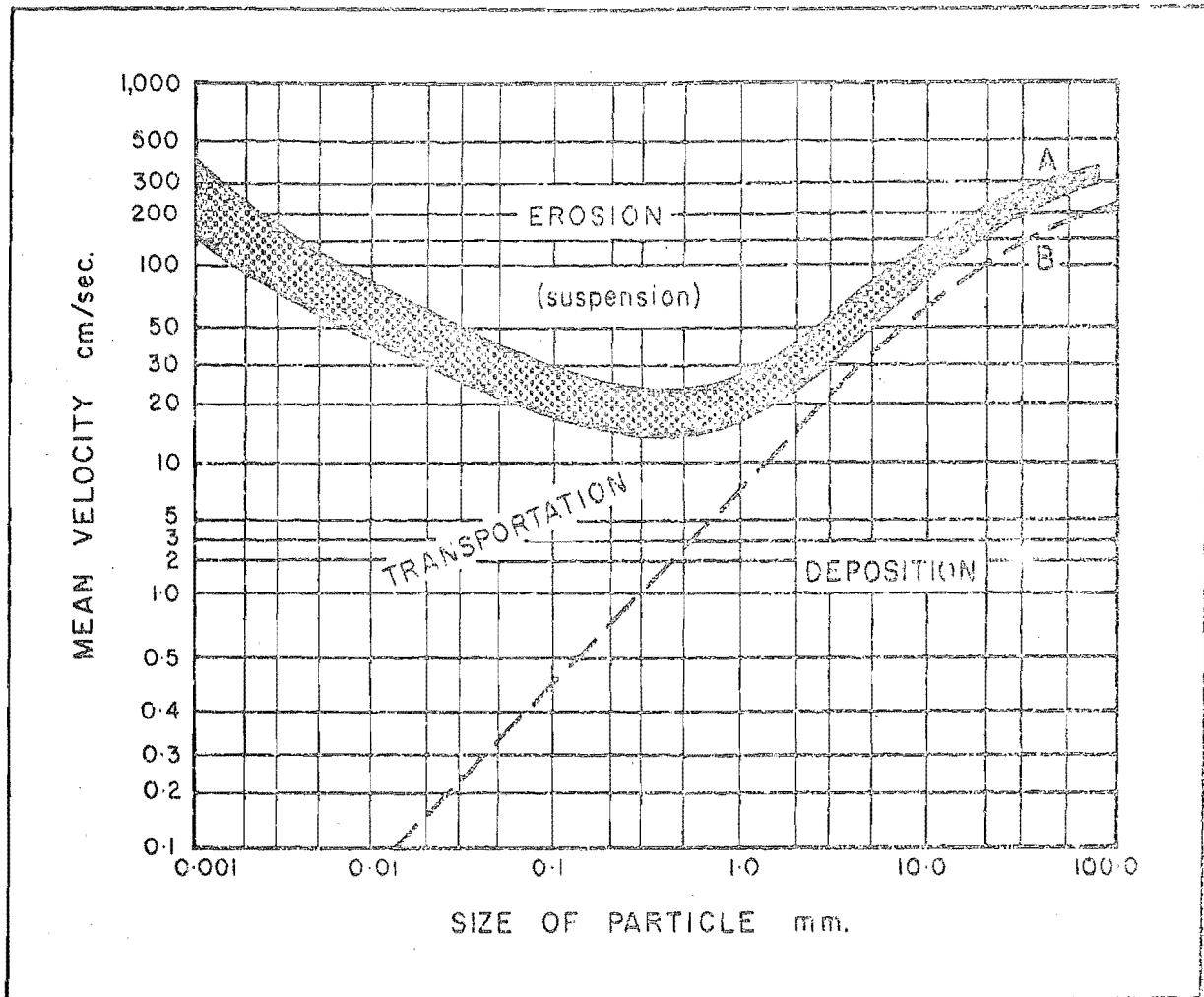


FIGURE 18. Competent velocity of bed-load sediment motion (A) and lowest transportation velocity (B). After the work of Schaffernak (1922).
 Source: Hjulstrom (1939, Fig. 1, p.10).

velocities sufficient to produce appreciable suspension would be turbulent, so that movement of grains would occur in suspension. Menard (1950, p. 158) notes that "for the same shear, the resistance (to motion) depends on the density of the medium. Hence the rebound of a grain in water should be about 1/800 of that in air".

Menard (p. 158) argues further that the distinction is a matter of definition: "The observed high concentration of suspended sediment near the bed may be thought to result from saltating grains which leap only a certain distance from the bed, or it may be considered as due to the vertical gradient in the concentration of suspended material which is expressed by the eddy viscosity, A_z ." See equation 14.

It would therefore appear that saltation of fine grains in water is minimal. However, for pebble sized particles in shallow water such as swash or backwash flow where pebbles may be projected clear of the water column, it must be considered as an active process affecting bed erosion and deposition.

Cessation of motion. Figures 17 and 18 both indicate lower velocity limits for the movement of given grain sizes. Menard (1950, p. 151) indicates that for sands (0.059 - 0.71 mm.) the velocity for cessation of motion was about 0.66 that of the competent velocity. A similar result is reported by Menard

for Schaffernak's (1922) work with grains larger than 5.0 mm. Hjulstrom (1939 p. 12) notes that for gravel the ratio between eroding velocity and lowest transportation velocity is about 1.4 to 1. Therefore the erosion velocity can be decreased for gravel about 30% before deposition begins. This is in agreement with Menard. Hjulstrom concludes that for given velocities and for particles ranging between 2 and 30 mm. in diameter, the particles that can be transported are about double the diameter of those that can be eroded. This is of great importance in studies of grain-size and sorting variations across the swash zone where current velocity varies greatly over a small distance. Sediments deposited at a given position in the zone have been eroded elsewhere under velocity conditions widely different from those at the point of deposition. For the same reason it does not follow that a given size moving in the water column at a given station, under measured velocity conditions, will be concurrently eroded from the bed at that station.

It is therefore necessary to consider the flow of grains in high concentrations, since given the velocities sufficient to move any given size and because these will be rapidly exceeded in the swash zone, the net effect on the bed morphology will depend upon the rate at which grains are removed or supplied to a particular area of the bottom.

Rate of Bed Load Transportation. Bagnold (1968; and pers. comm.) demonstrates that if fluid flow is regarded as a transporting machine then the energy conservation law may be written in the form: -

Rate of Transporting Work Done = Power Supply X Efficiency.
Power may be basically defined as the product of a force and the velocity with which it acts (i.e. Rate of doing work).

When no sediment is transported the whole of the power is dissipated in internal fluid turbulence, ultimately into heat. The efficiency of transport in this case is obviously zero. However, Bagnold notes that when sediment is transported, the flow can do work in moving it against friction, as has been demonstrated above. But the whole of this power cannot be converted into work because a dynamic fluid push necessarily involves a relative velocity or slip between the fluid and the grains being pushed. (As in the case of a sediment grain falling freely through water). There is always a loss, represented by the efficiency factor, e . As the flow stage is increased, e , rises from zero at the threshold of motion to some limiting value less than unity.

Further, the previous discussion has already separated total sediment flow into movement by two dominant mechanisms based upon the type of grain motion associated with each. Unfortunately, there is no practical method of separating the contributions of bed load and suspended load, to the total

load. The most usual practice is to regard all sediment trapped above some reference level (e.g. Sundborg, 1956, p. 215 took this level as 6cm. above bed level); as being suspended load, while everything below that level is treated as bed load. The obvious difficulty with this arises out of the above discussion of the role of saltation and the fact that the sediment concentration gradient is continuous from the bed upward. In saltation grain motion has aspects of both bed load and suspended load transport, and the significance of saltation in regard to the shingle beach foreshore has already been mentioned. It is important to remember for the purposes of the ensuing discussion that the separation of bed load from suspended load applies to the theory only.

In bed load transport the excess sediment weight is borne by the solid forces exerted at intermittent contact with the bed. Bagnold (1968, p. 45) gives the total transport rate as:

$$J = J_b + J_s$$

or:

$$j = j_b + j_s \text{ per unit width of flow}$$

where $j = mU$; the dry mass of sediment times current velocity. The most usual measure however, is not the dry mass of sediment but the excess weight in the fluid:

$$I = \frac{\rho_s - \rho_f}{\rho_s} g J = I_b + I_s \dots\dots\dots 27.$$

For bed load transport the solid forces bearing the grain weight are characterised by $\tan \phi$, the coefficient of friction. This is the ratio of the limiting frictional shear force to the perpendicular contact force ($\tau_c / \frac{\rho_s - \rho_f}{\rho_s} g$), and as has been shown this is approximately equal to the angle of repose for the grains.

The rate of work done in pushing the grains along the bed can therefore be written:

$$I_b \tan \phi$$

Equating this to input power efficiency Bagnold (1968, p. 47) obtains:

$$I_b = \frac{\Omega}{\tan \phi} e_b$$

or:

$$i_b = \frac{\omega}{\tan \phi} e_b \text{ per unit width of flow} \dots\dots\dots 28.$$

where ω is the total power available and e_b is the efficiency coefficient for bed load transport. For flow down a slope (standing at angle β), the expression becomes:

$$i_b = \frac{\omega}{\tan \phi - \tan \beta} e_b \dots\dots\dots 29.$$

This is because less power is required to move materials downslope than along a flat bed. This situation corresponds to bed load movement of grains in the backwash. For the swash, grains must be lifted upslope and so correspondingly

more power is required. Therefore the appropriate relation is:

$$i_b = \frac{\omega}{\tan \phi + \tan \beta} e_b \dots\dots\dots 30.$$

Inman (1963, p. 146) states that this relationship should also hold for oscillatory waves moving over the sea bed. "As the water shoals onshore the wave induced transport of sediment would decrease upslope By analogy, the term $\tan \beta$ would become positive rather than negative and the power available for transport would decrease" (onshore).

Bagnold (1963, p. 47) suggests that "theoretical reasoning from the concept of a moving flow boundary (indicates) that the efficiency e_b should reach a maximum constant value between 0.11 and 0.13 depending on the local Reynolds number for the slip velocity past the grains". Bagnold (p. 48) clarifies the above from a consideration of wind transport of grains.

"Wind-blown sand, as opposed to dust, is transported wholly as bed load, for the reason that the fines have already been carried away in suspension by winds of normal strength and dispersed over wide areas downwind, leaving the unsuspendable material behind. Wind-blown sand therefore provides a means of testing the theoretical efficiency value for bed load transport alone in the absence of concurrent suspension. Taking the effective wind velocity factor in the power expression as that measured at the height of the center of gravity of the sand cloud, the measured transport rates give efficiencies in close agreement with the theory."

Owing to the disturbance of the sand bed by the impacts of

the relatively very massive saltating grains, the bed behaves as a moving boundary at the threshold of movement, so the efficiency attains a constant value rapidly. This does not occur in water, and the efficiency does not reach its constant value until, at a higher flow stage, the bed is completely covered by a carpet of saltating grains. In water there is thus a transition range of flow stage within which the transport rate increases rapidly to an ultimate near-proportionality to the power available.

The part played by saltation in bed load transportation is clarified further by Bagnold (1968, p. 48):-

"Collisions occur as the solids are sheared over one another. Each collision, however viscous the fluid may be, must inevitably create equal and opposite components of momentum perpendicular to the planes of shear. Hence, successive collisions result in a dispersive stress between the solids in one layer and those of the next. This dispersive stress has been measured experimentally. It depends upon the rate of shear, the size, mass and concentration of the solids and the viscosity of the fluid. It is this stress which supports the bed load against gravity, as a dispersed cloud and maintains the dispersion in a state of statistical equilibrium. A tangential or shear stress must be applied to maintain the rate of shear. The ratio of these two stresses, tangential and perpendicular, constitutes the coefficient of solid friction $\tan \phi$. At high concentrations of solids both stresses become so large that the residual shear borne by the intergranular fluid can be ignored."

Suspended Load Transportation. In suspended load transport the grain weight is borne by the fluid and the grain travels at the same speed as the current. Schmidt (1925 - in Inman,

(1949, p. 58) assumed that the mass of sediment particles carried downward by gravitational settling must equal the amount carried upward by turbulent motion. This may be written in terms of z , distance above the bottom and the eddy viscosity, A_z as:

$$\log. \frac{S_z}{S_a} = -c \int_a^z \frac{dz}{A_z/\rho} \dots\dots\dots 31.$$

or: in terms of the velocities at these elevations and the frictional velocity u_* as:

$$\log. \frac{S_z}{S_a} = -c \int_a^z \frac{d\bar{u}}{u_*^2} \dots\dots\dots 32.$$

where S_z/S_a is the ratio of the concentration of sediment having a settling velocity, c , at height, z , to that at a constant height, a .

Thus, it can be seen that the theory of the vertical distribution of sediment in suspension is dependent upon the concentration gradient S_z/S_a . Inman (1949, p. 58) points out that under similar flow conditions, the ratio of the sediment concentrations is proportional to e^{-c} where e is the base of natural logarithms. Therefore fine material has a more uniform distribution with depth, and hence a smaller concentration gradient than coarse material such as that under investigation in the present study.

If the height, a , is considered to be infinitely close to the bottom, and the turbulence is sufficient to cause suspension, then the concentrations of the various grain sizes at height, a , are proportional to the amount of each grain size at the bed surface.

The significance of equation 32 was further elaborated by Inman (p. 58) by integrating it and employing equations 14 and 15 for the friction velocity and mean current speed for turbulent flow respectively:

$$\log_{10} \frac{Sz}{Sa} = - \frac{1}{k_0} \frac{c}{u_*} \log_{10} \frac{z + z_0}{a + z_0} \dots\dots 33.$$

in which z_0 again refers to the height of the roughness elements. Thus, z_0 is zero for flow over a smooth surface.

If it is assumed that the particles in suspension are spherical, of diameter, d , and of constant specific gravity then the settling velocity of the particles (equation 20) is a function of d only: $c = f(d)$. Setting $u_* = nc$ where n is any positive number Inman obtains:

$$\log_{10} \frac{Sz}{Sa} = \frac{1}{n k_0} \log_{10} \frac{z + z_0}{a + z_0} \dots\dots 34A.$$

Inman then argues that if fixed values for z and a in equation 33 are selected, any curve for which the ratio u_*/c is a constant is a curve along which the concentration ratio is also a constant. In a co-ordinate system u_* vs. d , it is argued, it is therefore possible to construct a family of

curves for constant values of the concentration ratio.

$$\text{Inman then selects: } \frac{z + z_0}{a + z_0} = \frac{z}{a} = 10$$

i.e. If the reference level is taken at 10cm above the bed, a, the equivalent roughness is consequently 1cm Sundborg (1956, p. 215) notes that a = 0.2cm is more appropriate to sand beds. A reference level of 10cm corresponds closely to the height at which the dynamometer used in this investigation determined mean maximum current speed.

Inman (1949, p. 59) obtained for $z = 10a$ the following expression:

$$\log_{10} \frac{S_z}{S_a} = - \frac{1}{n k_0} \dots\dots\dots 34B.$$

It is apparent from equation 34B that when $u_* = c$, $n = 1.0$ and:

$$\log_{10} \frac{S_z}{S_a} = -2.5 \quad (\text{for } z = 10a)$$

where k_0 in the above expressions is von Karman's constant; equal to 0.4.

The latter expression has been used by Inman (1949; 1963) and Sundborg (1956, pp. 213-219) as the limiting value of the logarithm of the concentration ratio for which suspension is significant.

"In effect, this means that if suspension is to exist to a significant degree, then u_* must be equal to, or greater than c , and under our arbitrary selection of elevations $z = 10a$, the logarithm of the concentration ratio must be equal to, or greater

than -2.5. This selection is in agreement with an analysis of experimental data by Lane and Kalinske (1939 and also Kalinske, 1941), which indicated that a value of unity for, n , the ratio of friction velocity u_* to settling velocity, c , is a criterion for the beginning of suspension. This criterion can also be justified on the basis that since u_* is equal to the mean of the absolute value of the vertical turbulent velocity fluctuations $|\bar{w}'|$, it should be expected that a significant degree of suspension can only exist if the settling velocity is less than $|\bar{w}'|$ " (Inman, 1949, p. 59).

A number of curves of constant concentration ratios are shown in Figure 19A. The limiting value of -2.5 for which suspension is significant is shown as a heavy line. The curve for which $u_* = c$ may also be interpreted as a plot of the settling velocity against particle diameter. It corresponds to the settling velocity curve of Figure 17.

Figure 19B shows an example of the way in which the suspension criterion, the threshold drag criterion and the criterion for the cessation of movement, may be combined in a u_* vs. d co-ordinate system for a particular case (derived from Sundborg, 1956, p. 218).

The calculations were based on the following expression which allows the use of the more readily measurable quantity u_{max} , rather than u_* :

$$\frac{Sz}{Sa} = \left[\frac{d-z}{z} \cdot \frac{a}{d-a} \right] \frac{6.25c \log. \frac{d}{z_0}}{U_{max.}} \dots 35.$$

where d is the flow depth, c is settling velocity and the other quantities are as previously defined. The material

FIGURE 19A. Relation of concentration ratio of suspended material to the threshold velocity. After Inman (1949, Fig. 3, p. 60).

FIGURE 19B. The relation between flow velocity, grain-size and state of sediment movement in uniform materials of density = 2.65 gr/cm^3 . The flow velocities are those 1.0 m. above the bed. Source: Sundborg (1956, Fig. 23, p. 218).

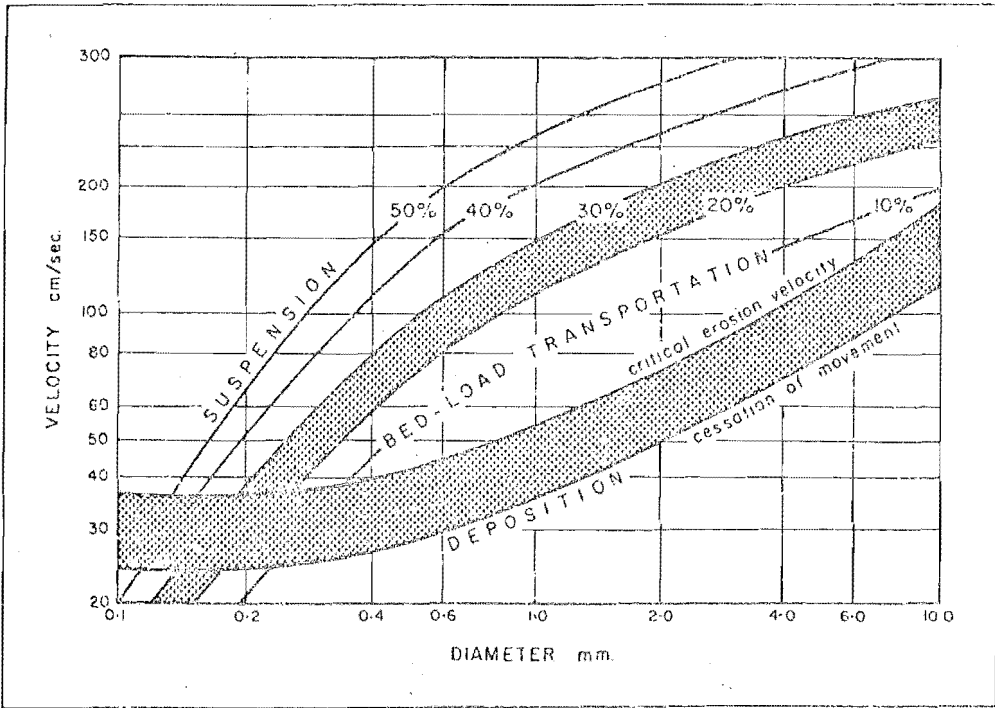
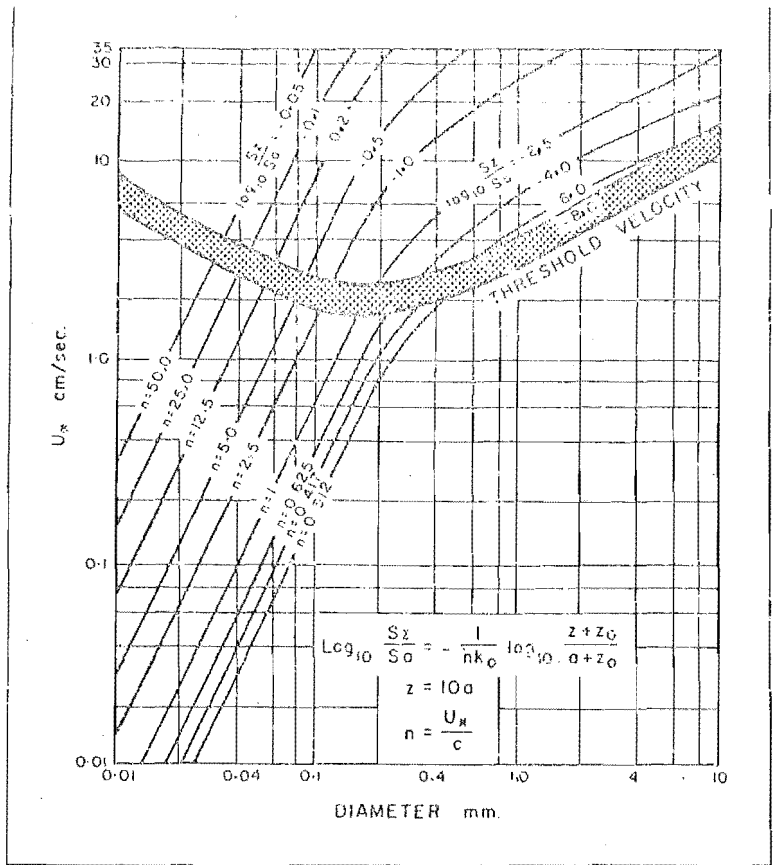


FIGURE 19A. Suspended sediment concentrations.
 19B. Mode of sediment transport.

considered is quartz ($\rho_s = 2.65 \text{ gr/cm}^3$), the flow depth is taken as 1.0 meter, and a is equal to 6.0cm. Thus, the equivalent roughness relates to sizes ranging from pebbles of 6.0cm. diameter to sand with ripples of this size. The relative concentration curves give the amounts of the various grain sizes at 10cm. above the bed which are respectively 10, 20, 30, 40, and 50% of the concentrations at the reference level, 6.0cm.

The curve corresponding to $u_x = c$ in Figure 19B is that for a 25% relative concentration. Sundborg (1956, p. 219) notes that the region of S_z/S_a between 20 and 30% has been dotted to indicate that this interval constitutes a diffuse boundary for the initiation of significant suspension. It can be seen that the diagram thus delimits different regions of sediment transport. It should be noted that because sediment concentrations vary from infinite at the bed to zero at some vertical elevation above the bed the theory is not applicable in close proximity to either the bed or the surface of the water.

Concerning Figure 19B Sundborg (p. 219) notes:

"For flow velocities less than the velocity for cessation of movement sediment can no longer be moved along the bottom. Deposition occurs instead. Within the dotted band between the velocity for cessation of movement and the critical erosion velocity there is transport of bed load but no real erosion. In the region between the two dotted bands there is transport of bed load and possibly erosion, but the amount of suspended material of the

grain sizes under consideration is small. Above and to the left of the upper dotted band the amount of suspended material increases. Farthest down to the left of the diagram there is a region where neither erosion nor transport of bed load can occur, but where transport and deposition of suspended material may be expected. The size of the finest material transportable as bed load may be obtained from the intersection of the two dotted bands. It will be seen that it is between 0.15 and 0.20mm It should be stressed that this limit is diffuse, and in no way excludes the possibility that coarser material may occur in suspension when the flow conditions are favourable."

Rate of Transport of Suspended Material. The equations for fluid flow carrying a dense suspended load can be formulated from reasoning analogous to that leading to the expressions for the rate of work done in transporting bed-load (Inman, 1963, p. 137).

If a dry mass of grains, m , is moved in suspension over a unit area of bed, then the dynamic transport rate, i_s of the grains as they are carried along by the stream at velocity U_s is:

$$i_s = \frac{\rho_s - \rho_f}{\rho_s} g m U_s \quad \text{per unit width ... 36.}$$

Since the immersed weight of the grains per unit area of the bed is:

$$\frac{\rho_s - \rho_f}{\rho_s} g m = \frac{i_s}{U_s}$$

the fluid must exert an equivalent normal dispersive stress

in order to maintain the grains in suspension, as has been demonstrated. If the grains have a settling velocity, c , relative to the fluid then the power expended by the stream in supporting the grains is the product of the normal stress and the settling velocity:

$$\begin{aligned} \text{Power expended in suspension} = Pc &= \frac{\rho_s - \rho_f}{\rho_s} \text{ g m c} \\ &= i_s \frac{c}{U_s} \dots\dots\dots 37A \end{aligned}$$

However, if the bed slopes at an angle β from the horizontal the power expended in maintaining suspension is reduced such that:

$$P = \frac{\rho_s - \rho_f}{\rho_s} \text{ g m c} \cos \beta$$

If this is applied to equation 37A the power expended in suspended load transport down a sloping bed at the dynamic transport rate i_s becomes:

$$i_s \left(\frac{c}{U_s} - \tan \beta \right) = \frac{\rho_s - \rho_f}{\rho_s} \text{ g m c} = e_s \omega \dots\dots\dots 37B$$

As in the case of bed load transport, if flow occurs up the slope then $\tan \beta$ in equation 37B becomes positive and the power expended increases correspondingly. The coefficient, e_s , is the efficiency of suspended load transport. Bagnold (1968, p. 53) indicates that it has a maximum constant value of approximately 0.01.

Inman (1963, p. 137) further notes that there is a similarity between the ratio c/U_s which affects the transport rate of suspended sediment and c/u_{*c} which determines the slope of the concentration gradient of suspended sediment. This is because U_s is proportional to u_{*c} and this in turn is proportional to the mean velocity \bar{U} , of the stream.

Total Transport in a Stream. The total transport is expressed as the sum of bed load and suspended load transport (equations 29 and 37B). Their sum gives the total dynamic transport rate, i , down a sloping bed as:

$$i = i_b + i_s = \left(\frac{e_b}{\tan \phi - \tan \beta} + \left(\frac{e_s}{c/U_s - \tan \beta} \right) \right) \omega \quad \dots\dots\dots 38.$$

or: $K \omega$

where K is a dimensionless expression equivalent to the section within brackets. K equates i to the total power available and may have values greater than one, especially for suspended load transport (Inman, 1963, p. 141). Its value will usually be several times larger than the sum of the efficiency coefficients ($e_b + e_s$). It has been shown that both e_b and e_s attain maximum constant values at some critical value of flow so that the total sediment transport rate becomes proportional to the total available power ω . Finally, it is important to remember that the above formulation stems

directly from the fact that total load is defined as the sum of bed and suspended load transport rates, but that these are not experimentally separable even under controlled laboratory conditions.

Total Transport in a Wave Regime. Inman and Bagnold (1966), have applied the above expressions to sediment transport across a littoral slope under wave accelerations. Inman and Bagnold state (p. 530) that the mean gradient of wave energy due to energy losses by bed friction and by surface turbulence within the surf zone, is always onshore. However, the energy gradient due to bed friction has been shown to be always in the direction of local flow relative to the bed. There are thus superimposed, local fluctuations onshore and offshore due to wave oscillations. The same may be argued to apply to the swash zone where wave oscillations are replaced by translational flows due to the breaking of waves and the associated return flows.

Inman and Bagnold show that the energy loss ΔE_1 over any unit area of the littoral slope, inclined at angle $\tan \beta$, due to bed friction and involving appreciable sediment displacement, may be assumed proportional to the mean force exerted by the water on the displaced sediment times the distance, x , that it is moved:

$$\Delta E_1 = a \frac{\rho_s - \rho_f}{\rho_s} g m_1 x_1 \cos \beta (\tan \phi + \tan \beta)$$

where m_1 is the mass of sediment displaced per unit area and, a , is a coefficient of proportionality.

It is argued further that owing to losses of various kinds, including percolation into the beach, the energy of the backwash will be less than ΔE_1 . Hence the corresponding frictional energy loss (ΔE_2) over the same area will be less:

$$\Delta E_2 = a \frac{\rho_s - \rho_f}{\rho_s} g m_2 x_2 \cos \beta (\tan \phi - \tan \beta) \dots\dots\dots 40.$$

If the profile is at equilibrium as much material is carried up the shore as down. Therefore:

$$m_2 x_2 = m_1 x_1$$

and:

$$\frac{\Delta E_1 - \Delta E_2}{\Delta E_1} = \frac{\delta E}{\Delta E_1} = \frac{2 \tan \beta}{\tan \phi + \tan \beta}$$

thence: $\tan \beta = \frac{\delta E \tan \phi}{\Delta E_1 + \Delta E_2}$

or writing: $\Delta E_2 = k \cdot \Delta E_1$

$$\tan \beta = \tan \phi \frac{1-k}{1+k} \dots\dots\dots 41.$$

This expression relates the net energy expended in sediment movement to the slope of the bed at that point. It is therefore clear that since the friction coefficient $\tan \phi$ is a constant for a given grain size, the slope of the shore, β , should be independent of the linear scale, but dependent

on the ratio of energy deficit: $\Delta E_1 - \Delta E_2 = \delta E$;
elsewhere to the loss ΔE_1 over the local area. If the
deficit is large so that k approaches its limiting value
of zero, $\tan \beta \rightarrow \tan \phi$ and the beach stands at the angle
of repose of the grains (Inman and Bagnold, 1966, p. 530).

Though the theory outlined above can be applied to the
offshore zone of oscillatory wave motion, certain difficulties
are apparent if it is applied to the swash zone. The theory,
as it stands, will explain in a qualitative way why a shingle
beach is steeper, in general, than one of sand. This is
because percolation losses into a shingle beach are large
so that ΔE_2 is small in relation to ΔE_1 and therefore the
energy deficit is large, and $\tan \beta$ increases. Also, the
theory will explain shoreline (profile) curvature. At the
seaward end of a profile where both swash and backwash are
powerful x_1 may be exceeded by x_2 since the backwash flows
parallel to the slope whilst the swash has considerable
vertical components of motion at this point. Thus in terms
of effective energy application, ΔE_2 may exceed ΔE_1 at this
point so that the energy deficit may become negative, resulting
in scour and local steepening of slopes. The result of this
process will be shown to be a slope which is convex upward on
the lower portion of the profile.

In the same way it can be shown that for the mid-shore
area the energy deficit approaches zero i.e. $\Delta E_2 = \Delta E_1$; so

that $\tan \beta$ becomes very small and the slopes approach the horizontal. For the upper foreshore only does the relation $\Delta E_1 > \Delta E_2$ hold. It will be shown that this is the only area where backwash energy is very small. In this area materials carried by the swash are deposited, resulting in a slope change between this section and the midshore which is concave upward. Thus, in the swash zone it may be said that the local fluctuations in energy direction and magnitude override the background decrease in energy gradient onshore. The type of flow at a particular location exerts a strong control on the way in which energy is applied to sediment motion, as has been demonstrated. Since the type of flow varies across the shore in both swash and backwash so too will the factors entering into the determination of ΔE_1 and ΔE_2 . Therefore foreshore slope is a more complex function of flow types than the theory will accommodate. Further, O'Brien and Morison (1952) have observed "fluidisation of the bed", resulting from vertical components of water motion in the surf zone. These may lift a large amount of sediment in addition to that which is entrained by the conventional drag mechanisms. The authors state that fluidisation may result in a mass movement of the upper part of the bed in a fashion fundamentally different from that of bedload motion.

Effects of Mixed Size Distributions on Transport Rate

The preceding discussion has treated only materials of uniform size and density. Even on a beach foreshore where sorting may be well developed a range of sizes is usually present on the bed. As has been demonstrated the primary effect of the bed material on the flow derives from the irregularity or roughness of the grain covered surface. Sundborg (1956, p. 186) points out that if the coarsest grains in a sediment are almost entirely exposed to the flow they will determine the roughness of the bed and the equivalent roughness will then be the same as the diameter of the largest grains. Under such conditions the magnitude of the boundary shear or tractive force will be greater than if medium sized grains had determined the roughness; assuming that the velocity at a given depth is the same in both cases. Bagnold (1968, p. 57) notes that probably 95% of the power expended in moving sediment is dissipated on the largest particles present. Conversely, the roughness of the bottom may be lowered (and similarly the tractive force), if finer particles fill the interstices between the larger grains.

"Addition of material to a previously homogeneous sediment can ... either raise or lower the roughness of the bed, depending on the relative proportions of the different fractions and the arrangement of the grains. Einstein (1950) found that in a not too heterogeneous mixture the grain size that determined the roughness of the bottom is 'that sieve size of which 65% of the mixture (by weight) is finer'". (Sundborg, 1956, pp. 186-187).

Further, if the equilibrium of individual grains is considered, it is clear that if coarser grains are freely exposed to flow they are without support from surrounding grains such as they possess in homogeneous sediments. They are thus more easily moved by a current. Conversely, if the coarse grains are embedded among fine grains they are unaffected by the flow until the fines are removed by the stream.

In the light of these considerations Sundborg (1956, pp. 187-188), has summarised the effects of entrainment and transport for mixed materials.

1. For very coarse material (down to 6-8mm), the flow is completely rough and the turbulence extends down into the spaces between the superficial particles. Even the smaller particles in the mixture are then subjected to the action of flowing water. The roughness of the bed and the turbulence is increased because of the shape resistance of pebbles or boulders and the eddies around the larger stones contribute to the entrainment and transport of finer material. Unless the flow velocity is very high the coarsest particles are moved only if the smaller particles that support them are moved. Their equilibrium is disturbed when the fines are removed and the stones roll or slide a short distance with the stream until they lodge fast again. An

"erosion pavement" of residual material is formed, and around the largest stones or boulders a characteristic pattern of erosion and deposition often develops.

Thus in coarse mixed material (larger than 6-8mm) the fine fractions are most easily entrained and transported.

2. For small grain sizes (smaller than 6-8mm and larger than 0.3mm) the main flow is still rough or transitional, but the turbulence does not extend fully into the spaces between grains. Consequently, the more shielded grains are not affected by the turbulent flow while the exposed grains are subjected to a relatively greater force. Fines will not therefore be entrained for the most part during initial stages of the erosion process. The concentration of the flow resistance to the most exposed grains is most marked for sizes of 0.8 - 1.0mm. At 0.3mm size the grains are all within the laminar sub-layer. In this latter case it is clear that the largest grains are most easily entrained during the initial stage of erosion, but this must also apply for grain sizes up to 0.18 - 1.0 mm. For grains between 0.8 - 1.0mm and 6 - 8mm the turbulence extends partly into the bed. Therefore the most easily dislodged particles in the initial stage of erosion are the smallest grains reached by the turbulence. These grains are often not the smallest nor the coarsest in a mixture but the medium

sized. The tendency for a medium size to be selected may be expected to be particularly prominent for grains in the 2-4mm interval. For fully developed transport the particles have a definite tendency to slide over a bed of finer particles. This is particularly true when the main flow is no longer fully rough i.e. for grain sizes under 2mm. This is in agreement with Hooke (1968) who examined sediment transport in a closed, recycling flume with a mixed bed consisting of sand (geometric mean = 0.22 mm) and granules (geometric mean = 2.35 mm). The mixture resulted in friction factors and sediment discharges lower than those obtained for finer, more uniform beds. The granules formed a carpet on the sand bed and lined ripple troughs, armouring them against turbulent eddies and reducing the amplitude of the bed forms.

Thus in mixed sediments between 0.8-1.0mm and 6-8mm the fraction most easily entrained is one of medium size, commonly 2-4mm. When transport is fully developed the coarser particles can slide over a bed of finer material. In mixed sediments between 0.3 and 0.8-1.0mm the coarsest fraction is most easily entrained. It may then slide over a bed of finer material.

3. For grain sizes less than 0.3mm the flow is smooth, and the process of entrainment depends largely on the

content of cohesive material in the mixture. The coarsest grains are most easily moved. After entrainment the material is transported for the most part in suspended form, with the exception of the coarse particles which move as bed load. Sundborg (1956, p. 188) concludes that:

"although according to the erosion curve (see Fig. 17), material with an equivalent grain size of 0.2-0.5mm is more easily eroded than any other equivalent grain size, it is not grains of size 0.2-0.5mm which are most easily set in motion in unsorted material where other fractions are also present. Instead it is grains of size 1-6mm that are least stable in a mixture. It is these latter grains that are most easily set in motion when bed load begins to be transported, and they are the last to come to rest when movement ceases. One can say that they constitute a fraction that is seldom allowed to rest by flowing water".

This is of great importance in consideration and analysis of grain size distributions and sorting processes in the swash zone of shingle beaches. However, there are yet other characteristics of grains that cause differences in transport behaviour from grains of uniform properties. Chief amongst these are particle shape and roundness.

Effects of Particle Shape on Transport and Deposition

It has long been known that beach pebbles are dominantly of the discoidal and flattened types. Kuenen (1964) has noted a preference for these types of pebble on beaches because

they offer greater resistance to movement than more spherical pebbles. Kirk (1967) has shown that greywacke derived pebbles on the mixed sand and gravel beach of the Canterbury Bight are comprised of over 95% bladed and disc - shaped grains and only 2.5% spheroidal particles. It will be shown that a similar situation exists on the study beaches of the present investigation.

It is clear that variations in particle shape will affect both the flow near the bed and the resistance of the particle to erosion. i.e. Shape influences the coefficient of drag and hence the critical tractive force for a given particle. This clearly will affect both the entrainment process and the settling characteristics of a given grain.

Romanovskiy (1966, p. 48) notes that Sokolov working with coarse sand (0.3 - 4.0mm) found that for particles of the same size class but different shapes, settling velocity could vary by a factor of more than 2. Romanovskiy (p. 54) demonstrates that the velocity of fall for particles up to 74mm. in diameter varies greatly with the thickness of the particle's mid-section. i.e. the area of maximum cross section. All particles fell with their maximum plane (the plane of the longest and intermediate axes), oriented perpendicular to the direction of motion. Romanovskiy provides tables and graphs for the evaluation of fall velocity for coarse grains of given shape, weight and diameter.

Krumbein (1942) studied fall velocity and critical traction force required to move particles of different shapes but constant specific gravity. Particles of higher sphericity, in general, had lower critical values than less spherical particles. In relation to settling velocity, the particles of highest sphericity settled most rapidly. Thus, the pebbles of lowest sphericity may be said to require higher initial forces to initiate motion and will be the last to settle for a given size range. The measure of sphericity used in Krumbein's study was that of Wadell (1934). This measure is defined as the ratio of the surface area of a sphere of the same volume as the particle to the actual surface area of the particle (Krumbein, 1942, p.621). Krumbein concluded that this measure did not completely explain the settling and flume behaviour of the range of pebbles studied.

Sneed and Folk (1958) introduced a new measure of shape that accounts for these variations in hydraulic behaviour. Wadell Sphericity does not include a measure for the in-equidimensionality of particles so that if "a rod measuring 100 x 10 x 10cm ... and ... a disc of 100 x 100 x 1cm ... were allowed to settle in water, the disc would settle much more slowly than the rod, despite the fact that they have precisely the same Wadell Sphericity". (Sneed and Folk, 1958, p. 118).

On the basis of the settling orientation of grains

(i.e. with the maximum plane perpendicular to the fall direction), Sneed and Folk introduced "maximum projection sphericity". This is based upon the ratio of the maximum projection area (plane of L and I axes) to the maximum projection area of a sphere of the same volume. This value, which includes departures from sphericity explicitly, is given by:

$$\Psi_p = \sqrt[3]{\frac{S^2}{L \cdot I}} \dots\dots\dots 42.$$

where S is the shortest axis. The axes are mutually perpendicular.

Folk (1965, p. 8) elaborates on this measure and refers to it as "effective settling sphericity". Thus, "if a pebble has a sphericity of 0.6 it means that a sphere of the same volume would have a maximum projection area only 0.6 as large as that of the pebble. Consequently the pebble would settle about 0.6 as fast as the sphere because of the increased surface area resisting downward motion". The flatter or more elongated a particle is relative to a sphere of the same volume, the slower it will settle in relation to that sphere. This feature is potentially of great importance in the study of pebble sorting on a shingle beach foreshore.

On the other hand, Sundborg (1956, p. 189) after

summarising evidence from flume studies of this problem indicates that the influence of particle shape on critical erosion velocity is insignificant in comparison with the influences of grain size and density. "Usually a slight increase of the erosion velocity may be expected for sharp edged and flat particles". Harrison and Alamo (1964) conducted an investigation of the dynamics of sand sized particles (0.2-0.7mm) at Virginia Beach, U.S.A. and concluded from an analysis of values for Reynolds number and the coefficient of drag that "their dynamic behaviour was not much different from that of perfect spheres" (Harrison and Alamo, 1964, p. 19). It is therefore probable that shape variations do not significantly modify the transport characteristics of sand sized grains. However, this may not be true of pebble and larger sizes.

Thus, in conclusion it can be said that for pebble sized materials the effect of shape on the initiation of transport is probably slight, but that shape variations can be expected to significantly modify settling behaviour and hence may be strongly reflected in the cross-shore depositional structures resulting from swash and backwash flow.

Effects of Grain Roundness on Sediment Transport

Measures of grain roundness relate to the degree of

rounding of particle edges and corners. The concept of roundness is thus independent of sphericity. Shields (1936) found that angular particles behave in a similar fashion to particles of low sphericity. i.e. they require a greater initial force to set them in motion than rounded grains, but once they are in motion they move at essentially the same rate as more rounded particles. Shields concluded that the initial effect is probably due to the fact that angular particles pack more tightly in the bed than rounded grains. The effects of variations in particle roundness on grain transport can therefore be regarded as minor in comparison with size, density and shape effects.

Bed Morphology Resulting From Sediment Transport

Menard (1950) examined the bed forms associated with various values of competent velocity. Data were derived from both laboratory flume studies and from natural channels. These are shown in diagrammatic form in Figure 20. It can be seen that the basal curve is the critical erosion velocity for grains of different sizes. Menard (1950, p. 150) notes that this is because bottom phenomena do not occur until the bed load is put into motion.

Current ripples appear when flow is tranquil and a bed which is rippled has a lower competent velocity than a smooth bottom. This is because the ripples increase the effective bed roughness. It is clear from Menard's work that

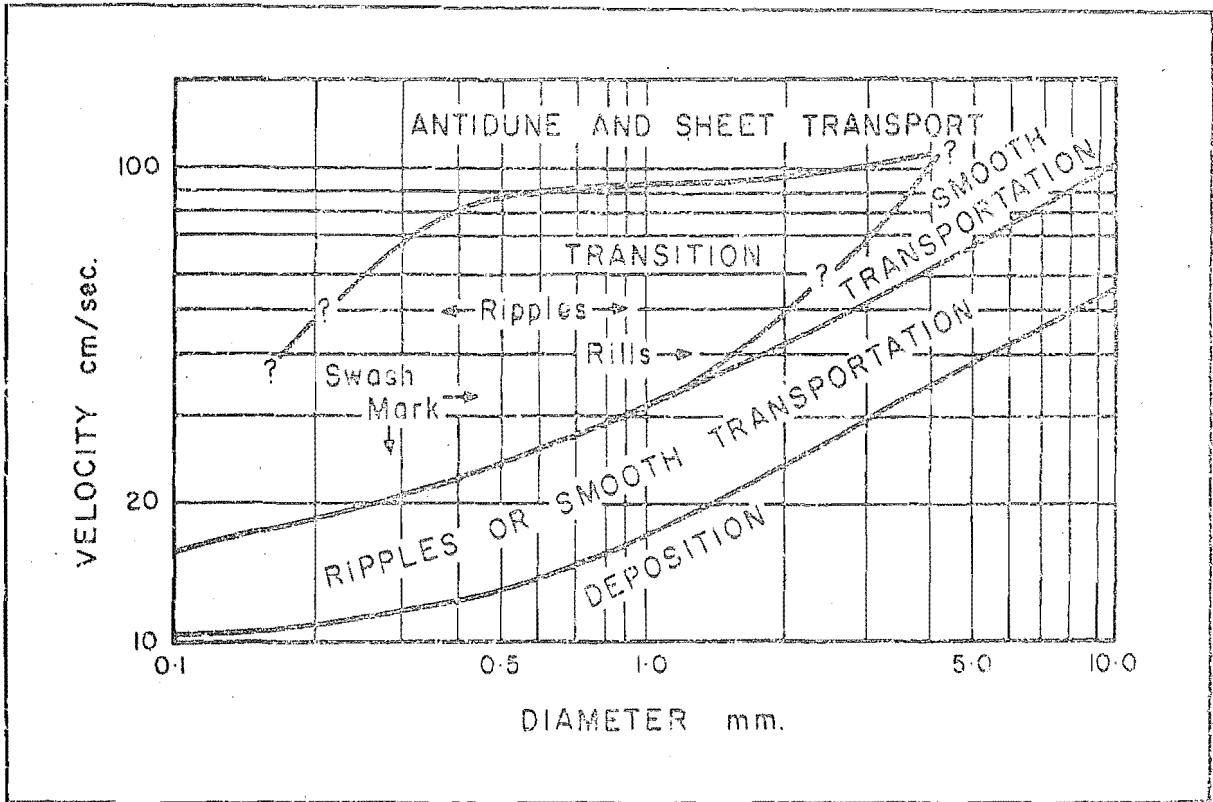


FIGURE 20. Generalised bed conditions in relation to grain size and mean current velocity. After Menard (1950, p. 154) with additions.

type of flow, as expressed by Froude number is as important in governing the bed morphology as the prevailing current velocity. This is because the critical velocity for motion depends upon flow depth in Froude's criterion. Menard (1950, p. 155) cautions that most data relating to ripple formation and destruction are quantitatively correct for shallow water only.

Ripples appear to form when the flow velocity is near the competent velocity of the bed particles and Menard (p. 158) notes that the mere existence of them suggests that erosion almost balances deposition, so that only a thin layer of the bed is in motion. Ripple formation appears to be confined to the sand sizes and may be characteristic of steep bed slopes. Menard (p. 155) suggests that beds comprised of grains larger than about 4mm. do not ripple in shallow water (see Fig. 20). For these grains movement may be "smooth" i.e. a thin layer of grains moves near the bed but no sinuosity of the profile is developed. Figure 20 also suggests why ripples are seldom found in well sorted coarse materials. It can be seen that the competent velocity and ripple destruction lines merge for larger grain sizes. This occurs because the flow type alters from tranquil to shooting in this region.

Evans (1949), Thompson (1937), Demarest (1947) and Emery and Gale (1951) have all recorded a variety of ripple

and ripple-like features occurring in the swash zone of sand beaches. Swash mark, small crescentic arcs of sediment at the limit of the swash, is produced by very slow, shallow flow. Demarest (1947) observed "rhomboidal ripples" that form in sand owing to the action of a thin sheet of water following the backwash of each wave. This sheet derives from discharging groundwater and effluent water from the infiltration of swash. The features were developed on slopes of 6-12°. Slopes lower than this did not provide enough acceleration of the flow sheet for formation to occur, and slopes higher than this caused destruction of the ripple, presumably because the flow type was altered. Bagnold (1968, p. 49) notes that rippling is confined to the lower efficiency levels of the processes governing the dynamic rate of transport of sediments.

If water motion is greater than a few cm/sec. more than competent velocity then ripples (fine materials) and smooth flow (coarser materials) give way to an antidune or sheet flow bed form. Antidunes are low, symmetrical, fast moving sand waves which migrate upstream. It will be remembered that a gravity wave can only move upstream if $F > 1$. Sheet flow of sediments also requires shooting flow (Langbein 1942). Menard (1950, p. 157) suggests that antidunes may result when stream slope is too steep to be in equilibrium with load and velocity. Therefore a scour phase (the antidune) may form

and move upstream. Nevin (1946) notes that antidunes occur on much steeper slopes than does the sheet flow mode of transportation, for comparable velocities in the flume data of Gilbert (1914). Figure 20 indicates that both antidunes and sheet flow may occur in coarse sediments.

In conclusion it may be said for coarse sediments such as those studied in the present investigation, that the movement of particles at low velocities (such as in the swash or backwash near the landward limit of water motion), will occur in a smooth phase. Ripples are unlikely to form except in mixed sand and shingle where the flow depth and velocity are small, and the slope is steep. This will be shown to occur in the groundwater sheet which follows backwash, after the manner described by Demarest (1947).

For turbulent shooting flows either antidunes or sheet flow will characterise the bed motion. Antidunes seem likely to form in the backwash where slopes may be steep and flow depth increases rapidly. For the most part sediment transportation should be in the sheet phase since adjustments of energy and load to bed slope are rapidly accomplished on a shingle beach foreshore.

A number of other bed forms occur on coarse beaches but these are related to the settling behaviour of irregularly shaped grains and so discussion of these structures will be left until data relating to the processes controlling sorting for particle shape are discussed.

Summary of Swash Zone Dynamics

The foregoing discussion has described many aspects of water motion and sediment entrainment in the swash zone. Of these probably the most important are the phase properties of swash flows since these govern the asymmetries of water motion, flow depths and velocities. As well as controlling the relative amounts of water entering and leaving the zone, these properties also govern the structures of individual flows. It has been demonstrated that for a given volume of flow, the type of turbulent structure can greatly affect the efficiency of sediment transport and therefore influence the type of morphology resulting.

It has been shown that the prediction of the behaviour of fluid flowing over non-cohesive sediment grains has occupied much previous work and proved very difficult. At present there is no general solution to the problem of the fluid-particle system. Particular problems must be studied by individual workers in varying degrees of isolation and according to a great many techniques. Many of the difficulties stem from the dependence of sediment transport on flow turbulence. This has prevented the development of a theory of sediment motion based on expressions which apply to a wide variety of flows.

After the initiation of particle motion, turbulence is

an important factor governing the interaction of the fluid and the bed. Thus, the bed profile is dependent upon the sediment particle movement which, in turn, depends strongly on the turbulent eddies set up by the profile shape.

Also, in view of the high energy nature of the study beaches the properties that govern the rate of sediment transport may be expected to be of greater geomorphological significance than those controlling the initiation of motion since the latter are probably exceeded quickly, almost instantaneously, in both swash and backwash. One difficulty inherent in considering the sediment transport rate across a given section of the flow is that the phenomenon depends not only on conditions at that section, but also upon the rate of transport further upstream. This presents relatively few problems in laboratory flumes where conditions of steady, uniform flow give rise to equally constant sediment flows at all points along the channel. For field experiments it is necessary to approximate the solids transport profile by sampling at a number of sections.

Also the above discussion of flow dynamics has clarified the reasoning leading to the choice of process and response variables shown in Table 1. First, a representative group of fluid flow properties must be measured. This group includes the pressures, times, depths, velocities and levels of turbulence of both swash and backwash flows. These variables affect

the distributions of flow structures across the shore.

Secondly, a group of response parameters must be measured in order to evaluate the manner in which entrained sediment is redistributed both vertically through the water column and laterally across the shore. This group can be expected not only to shed further light on the operative processes, but also determines the morphological expression of the processes on the shoreline. Important response parameters thus include the vertical and lateral distributions of sediment undergoing transport at any one time, the characteristics of the grain size ranges available for transport, and the variations in bed elevation resulting from sediment entrainment, transport and deposition.

As was indicated at the outset of this report, the first requirement of this investigation was an assemblage of instruments and field techniques appropriate to analysing the flows described above. The preceding review of previous studies has served on the one hand to demonstrate the general nature of swash/backwash flows and to relate these to work in other shore and nearshore environments. On the other hand, it has served to outline the problems involved in the study of morphologically significant processes in the swash zone as well as to specify in more detail those flow properties which are most likely to yield greater explanation of long-observed patterns of foreshore response to wave

action. The instrument system employed in this study was designed with many of these parametric requirements in view.

INSTRUMENTS AND TECHNIQUES

Principles of Measurement

Water movements in the swash zone have been shown to be essentially translational and because of percolation into the beach face, they are usually of small depth. Internally the zone can be separated into a lower permanently wetted section where percolating ground water and effluent swash water return to the surface, and a subaerial, intermittently wetted zone affected by wind action and the longer swashes of storms. Because of tidal and other variations in water level at the shoreline the demarcation lines between these zones vary continuously in position.

Owing to the turbulent nature of the flows, the presence of moving sediment in the water column presents an added obstacle to instrument operation. Schiffman (1965) found that these factors effectively prevented the use of such conventional devices for measuring fluid flow as pitot tubes and propeller driven current meters. However, in practice it is simpler to record flow by some Eulerian principle (mechanical or dynamical measurements of motion past a geographically fixed point), than by tracking the paths of

"parcels" of water with tracers or floats.

In the past floats have been timed over measured distances to obtain swash and backwash velocities (see Table 2).

Difficulties with this method include the fact that the result derived is an average value from an environment in which large variations in flow velocity occur within a few feet and from moment to moment. Norrman (1964, p. 82) notes that rigid volumes such as floats may behave in an anomalous fashion because of inertial effects in such a hydrodynamic situation.

Dolan and Ferm (1966) used a chart recorder and trip-pen to time the passage of swash fronts between rods spaced at known distances across the shore. The time distance between marks on the chart was thus directly proportional to swash deceleration. Though this represents a considerable improvement over the float method it suffers a similar disadvantage. Both methods describe surface flow only and provide no data on flow conditions at the bed. Further, it has already been shown that it is difficult to relate the passage of the swash front to the behaviour of the body of the flow which follows it (see Fig. 15A). Also, the method gives no data on the backwash.

It is therefore clear that the swash/backwash zone is a highly dynamic one difficult to work in, both physically and conceptually. Instruments for use in such an environment must be able to withstand the corrosive rigours of salt

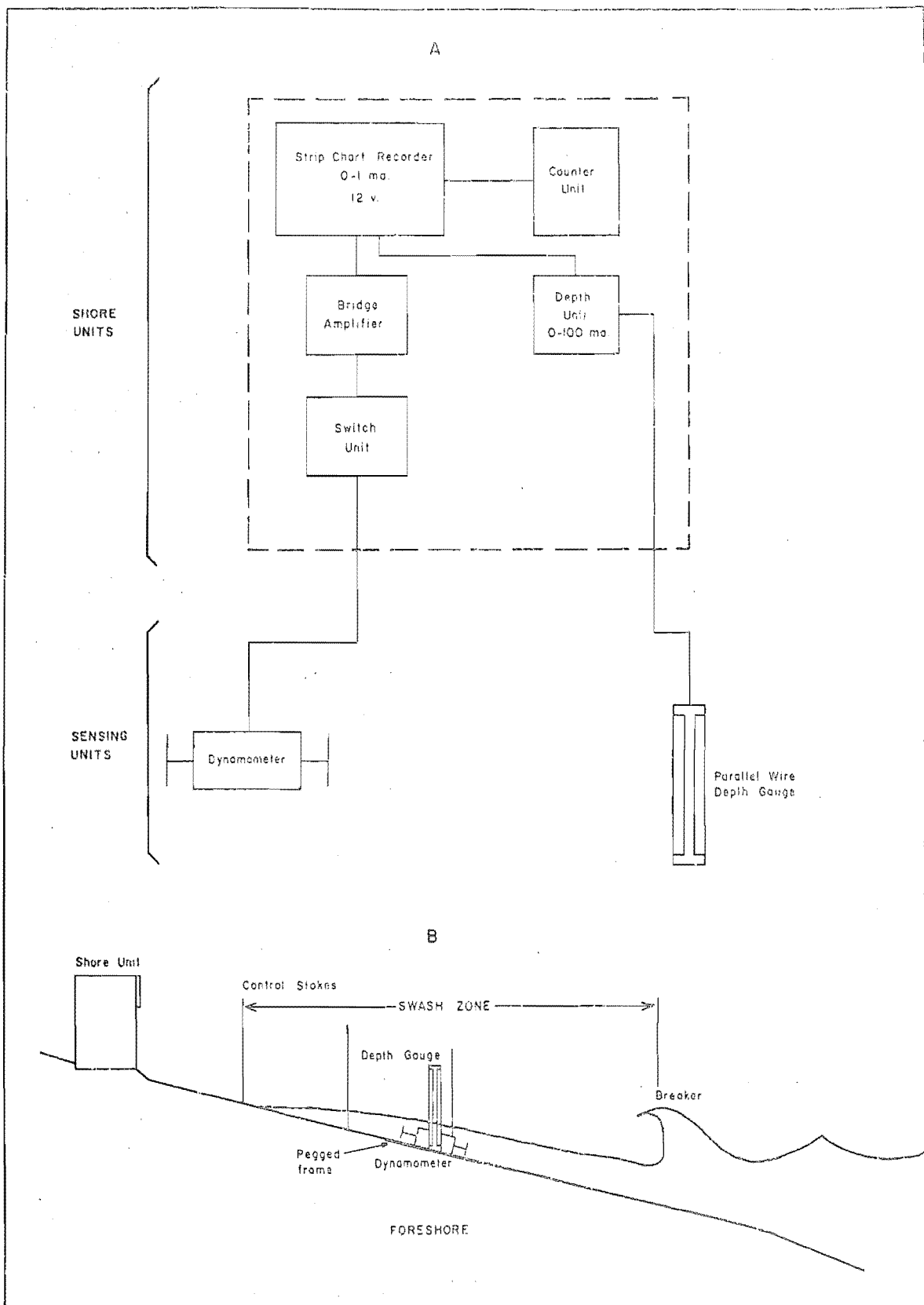


FIGURE 21A. Principal units of the instrument system.

21B. Operating positions of the units in the swash zone.

water, must respond quickly to rapid, sometimes severe fluctuations in head and velocity and yet withstand large applied forces. It has also been shown that measurements of the various process and response factors identified above must be made on a number of different time scales.

Because of the short duration of the flows (12-15 seconds at most), and the corresponding fluctuations in energy some form of recorded output was deemed essential. Also, an often overlooked criterion is an output form which permits ready abstraction of data and ease of analysis. Further, recording devices must be able to function in the presence of salt spray so that a sensitised chart paper is preferable to inked pens. Finally, where the instruments are to be used for short periods at a number of locations under varying conditions field portability is desirable. Factors of importance here include light weight, compact size, battery operation and low power drain.

Instrumentation

With the above requirements in mind the instrument system shown in Figure 21 was designed and constructed. Figure 21A is a schematic diagram of the system showing the component units and Figure 21B indicates typical operating positions of the sensing heads in the swash zone. As can be seen from the diagram the system comprises two chief units, the sensing heads and the shore unit. For this reason the sensing heads or data gathering units

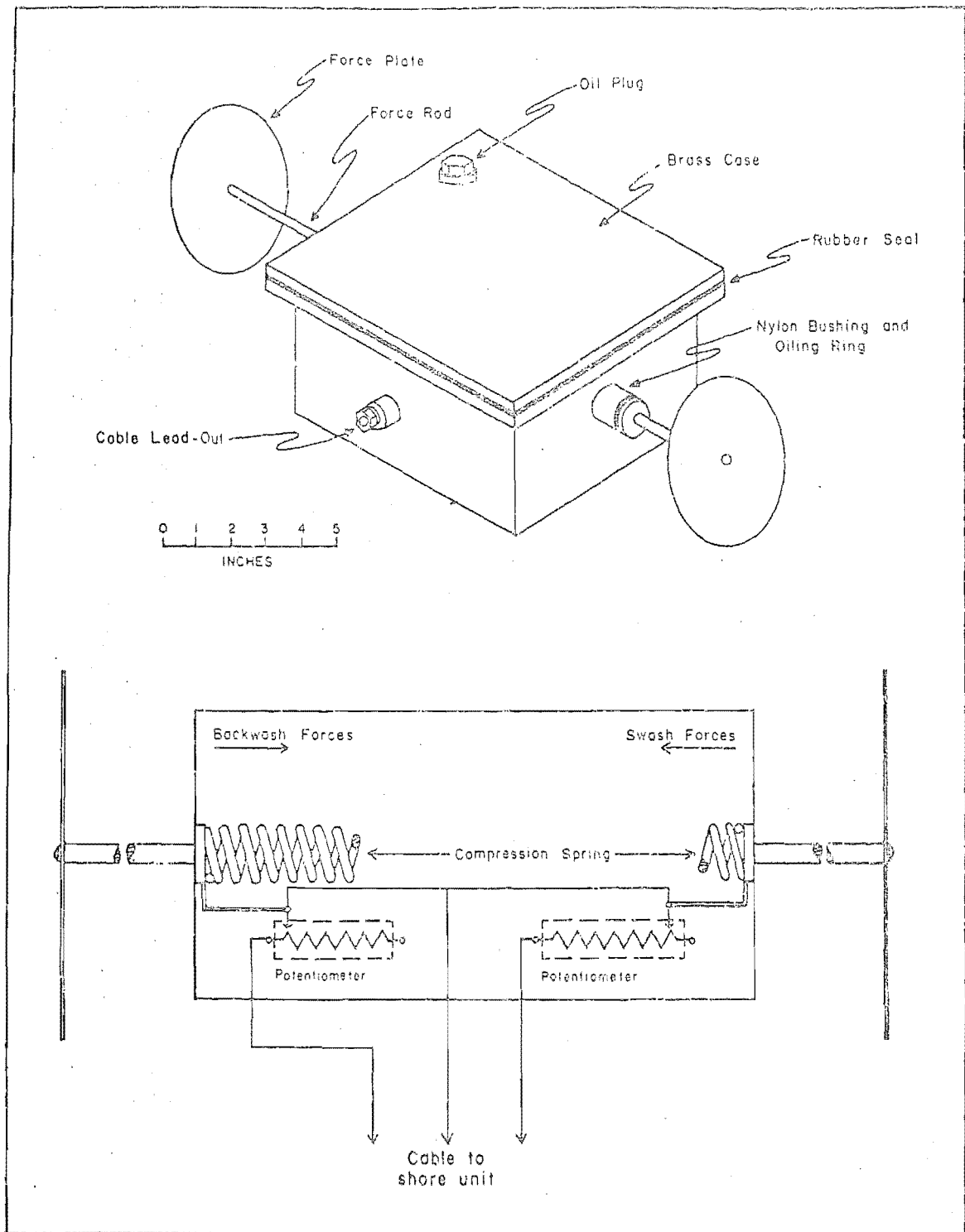


FIGURE 22. The Dynamometer.

will be described first and the shore unit (the data control and output section), will be treated secondly.

A. Sensing Heads

1. The Dynamometer. The instrument chosen in this investigation for the measurement of energy (velocity) is a variation of a general class of devices called dynamometers. These are similar in many respects to strain-gauges and are often used by engineers to measure forces on marine structures. Figure 22 shows the design and construction of the dynamometer. The present instrument is modelled closely after that employed by Schiffman (1965) in a study of swash-surf zone processes on sand beach foreshores.

"The dynamometer ... is of the electro-mechanical type. Two discs are used to measure, respectively, the force of water that has been given an acceleration shoreward by the breaking waves and the secondary movement of this water seaward under the influence of gravity. The forces acting on a disc are transmitted to a compression spring whose resulting displacement causes a corresponding change in a variable resistance. A pen recorder makes a permanent record of this change. Each rod acts independently on the spring and serves, in turn, as a backstop for the force exerted on the spring by the opposing rod. This gives the dynamometer a self-zeroing capability" (Schiffman 1965, p. 255).

The unit is housed in a watertight, oil-filled brass container and is linked to the shore unit and D-C power supply by 100 yards of three-core PVC cable. The instrument was either anchored to the bed on a Dexion and conduit frame (5' x 3') and pinned (see Plate 3); or mounted vertically

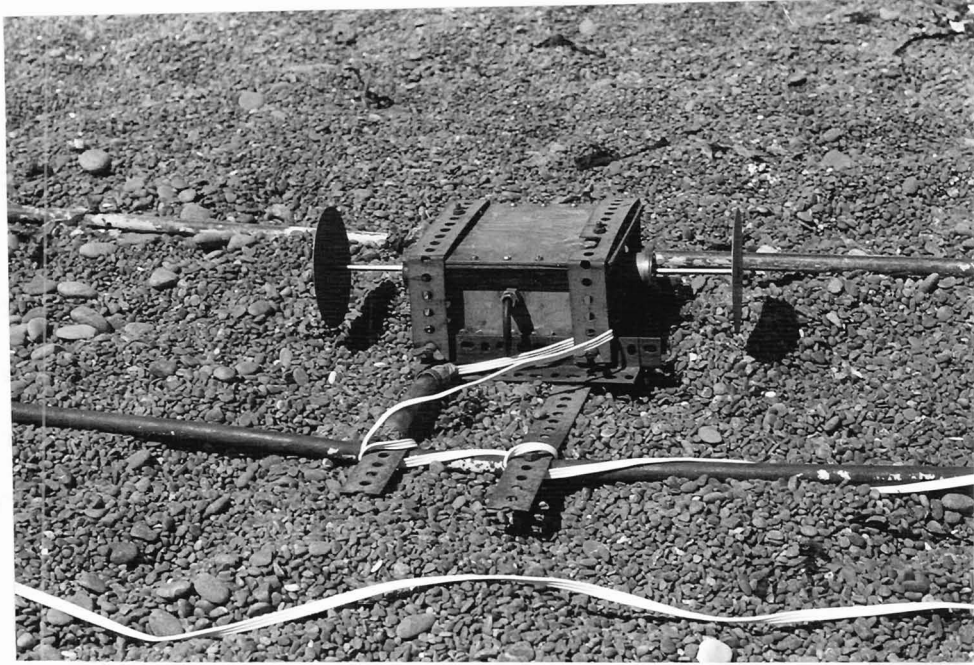


PLATE 3. The Dynamometer mounted on the conduit frame.



PLATE 4. Vertical mounting of the Dynamometer for obtaining vertical velocity profiles.

so that the plate centers could be lifted vertically to obtain vertical velocity profiles (see Plate 4). The horizontal conduit frame with the instrument weight upon it acts as a drogue, settling into the bed until the dynamometer case is flush with the surface. Pins are then driven in at either end of the frame.

Calibration of the Dynamometer. For ocean waves no standard exists; that is, calibration is not possible in the sense of comparing an instrument with a "standard" at least one order of magnitude more sensitive and having a known accuracy (Kinsman, 1965, p. 430). Thus, pressure or force sensing instruments such as the dynamometer produce records which contain elements of signal affected by hydrostatic and electro-mechanical filtering. Due to mechanical inertia very short period fluctuations are not recorded by such a system.

Consequently, the dynamometer was calibrated by two different methods. Firstly, a static calibration was performed and the velocity calculated from an equation for the force of water due to the drag on a plate normal to fluid flow. Following Schiffman (1965) it is assumed that force is proportional to the square of the velocity:

$$V = \sqrt{\frac{2 F_{\max.}}{C_D \cdot \rho_f A_p}} \quad \dots\dots\dots 43.$$

where: V is the velocity of the water flowing normal to the dynamometer disc; F is the drag force; ρ_g is the density of the fluid (taken as 1.03 Kg/m^3 at 0°C . and 1 ATM. pressure); C_D is the coefficient of drag, taken to be 1.12 (this value varying with Reynolds number); and, A_p is the area of the dynamometer plates. The value of $C_D = 1.12$ is applicable to flows of over 100 cm/sec. (Sutherland, 1969, pers. comm.). Also, in common with Schiffman three sizes of plate have been constructed to obtain a series of overlapping velocity ranges (see Table 4), though only the smallest was required on the study beaches.

The above calibration was deemed to be unsatisfactory if taken as the only criterion since the dynamometer as a whole may not exhibit the drag characteristics of a circular plate opposing the flow (Sutherland, 1968, pers. comm.). Bagnold (1969, pers. comm.) suggested that an appropriate calibration would be obtained by subjecting the instrument to solitary waves in a wave tank. It would then be possible to obtain velocity values from the theory of gravity waves (see equation 2). However, facilities for this were not available.

Instead the dynamometer was mounted on the bed of a 4 feet wide flume at the Civil Engineering Department, University of Canterbury and a calibration obtained for conditions of uniform, steady flow. The centers of the discs were

TABLE 4

Plate Sizes and Associated Velocity Ranges

| Plate Radius cm. | Plate Area cm. ² | Velocity Range cm/sec. |
|---------------------|--------------------------------|---------------------------|
| 6.5 | 132.7 | 26.2 to 303.0 |
| 8.5 | 225.9 | 18.06 to 207.0 |
| 10.5 | 346.4 | 16.36 to 188.0 |

located at a position equal to 0.4 of the available depth of flow. This ensured that the plates were in the region of the mean velocity core. Flow depth was determined with a point gauge mounted on a movable trolley and the flow velocity determined from the cross-sectional area of the flume and the input discharge rate ($V = Q/A$). The maximum velocity achieved in this way was approximately 110.0 cm/sec. and runs were performed with both rising and falling stages to assess hysteresis effects. Though the maximum velocity was not particularly high with respect to the capability of the instrument, it corresponds to the critical erosion velocity for particles of up to 10.0mm. diameter.

The results of these two calibration procedures are shown in Figure 23. The solid line denotes the static calibration while the triangles give values determined in the flume. It can be seen that the calibrations are by no means linear. Both discs have an initial region of slow response which reflect mechanical friction in the instrument. For the linear sections of the curves, the spring constants were found to be 1.2 Kg/cm and 1.13 Kg/cm for the swash and backwash plates respectively. Maximum deflection corresponds to a force of 2.75 Kg on the discs. The diagram also shows that there was general agreement between the two calibrations in the region of overlap. In general the flume tests produced higher pen deflections for equivalent velocities than the static calibration. The mean difference between

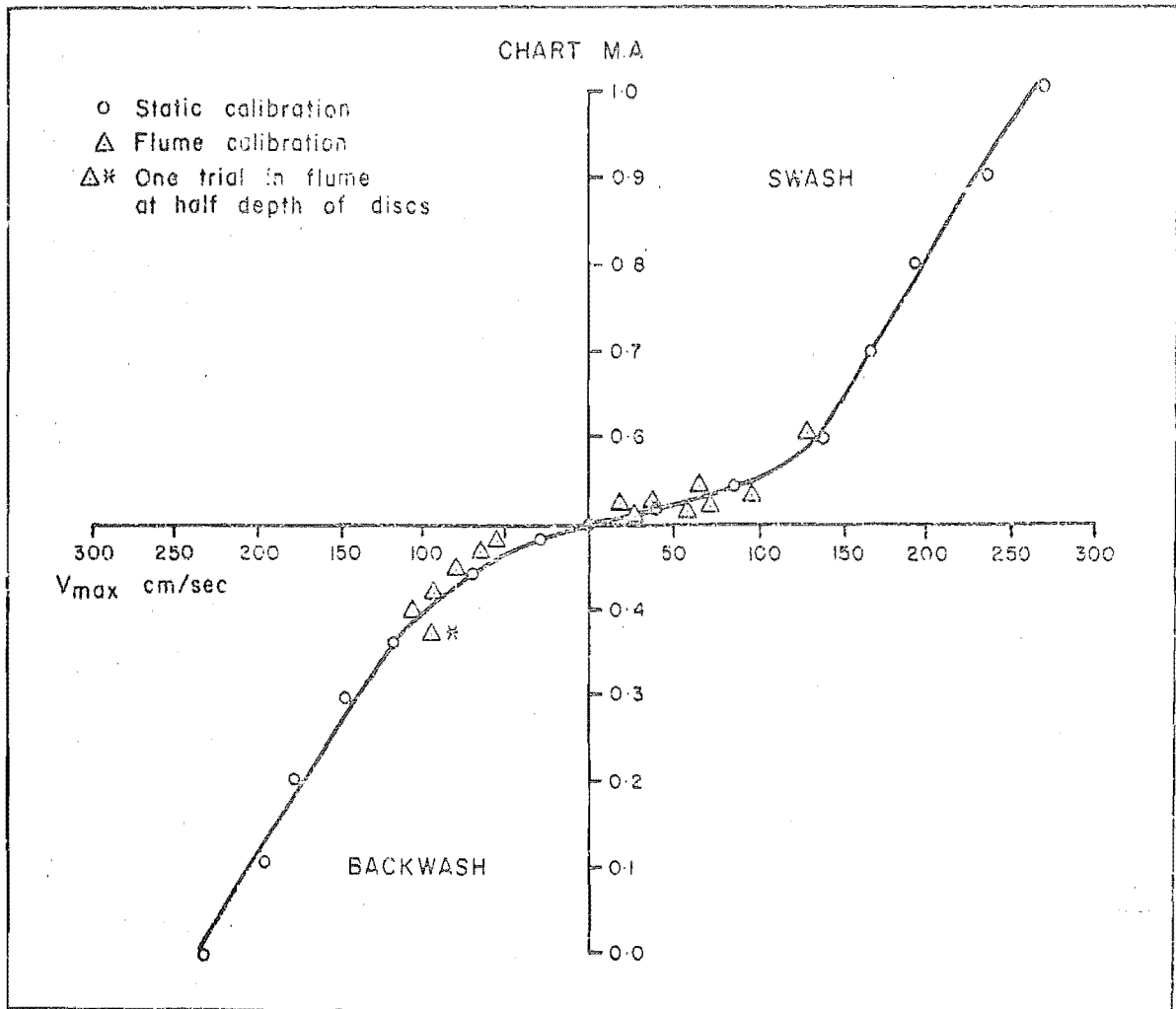


FIGURE 23. Calibration curves for the Dynamometer.

the two procedures was found to be 10.5% for the swash disc and 12.7% for the backwash disc. A maximum difference of 29.0% was found for a situation in which the dynamometer discs were only half covered by the flow. It would thus appear that the instrument may be used to obtain flow velocities to the nearest 10cm/second.

The height of the column of water measured at the bed depends upon the diameter of the dynamometer discs and is similar to Schiffman's instrument in being 15 to 20 cm at a distance of approximately 3 cm from the bed during field experiments.

Flow Parameters Sensed by the Dynamometer. The chart record obtained from the instrument contains a series of impulse force curves against time. A number of useful parameters may be derived from this. Hence, velocity values may be obtained directly, as can flow times. These are features of great value in the analysis of continuous records. Also, a measure of flow energy may be derived by measuring the areas under the curves such that:

$$\int_{t_1}^{t_2} F. dt \quad \sim \quad E \quad \dots\dots\dots 44.$$

The relative energy levels of the swash and backwash may be obtained by summing the areas under the respective sets of curves and dividing the totals by the interval of time over which each was operative. Measurement of the areas is easily

accomplished with a planimeter or by use of graph paper and a projection device to enlarge the curves. Schiffman (1965) notes that this arbitrary measure of energy reflects the number of readings in unit time together with the various parameters that influence the length of time that the individual forces act. Also, the data derived are conservative in the sense that the dynamometer has a lower response limit of considerable magnitude (e.g. 26 cm/sec. for the 6.5 cm. radius plates (see Table 4), so that flows with velocities below this limit will not be recorded.

If a velocity profile of the swash or backwash is taken from a series of points with the dynamometer it is possible to obtain flow discharge values from the following expression:

$$Q = \int_{x_1}^{x_2} V(x) \cdot dx \quad \dots\dots\dots 45.$$

Thus, the areas under the curves on a plot of velocity and position across the shore may be used to obtain a "water budget" of incoming and outgoing flows at any given station. It has already been shown that this is a very important aspect of swash zone processes. Finally, the product of the forces acting on the discs and the physical displacement of the discs is a measure of the power expended by the flow in doing work on the dynamometer. This concept is identical with that employed in the theory of sediment transport so

that there may be a close relation between power expended in sediment transport and that developed at the dynamometer for given flows.

More generally, much useful information can be obtained by an examination of the shapes of the impulse force curves, as demonstrated by Muraki (1966). Short, steep curves denote the action of fast moving bodies of water associated with high impulse forces while lower, more regular curves indicate lower pressures and slower but longer flows. Similarly, curves with multiple peaks indicate fragmentation of a water mass into "parcels" which are moving at different velocities and/or in different directions.

2. The Depth Guage.

Since the head of water (hydraulic gradient), at a particular location is of primary interest in connection with flow structures and percolation velocities, a small version of the conventional parallel-wire wave guage was constructed. The instrument consists of two heavy guage, low resistance copper wires mounted inside a $2\frac{1}{2}$ " inside diameter stilling tube. In operation, the water level rises and falls smoothly in the tube successively removing (rising level) or adding (falling level) resistance to the control circuit. The impulse thus generated is transmitted to a separate shore unit by a PVC cable and fed into a simple bridge balancing

circuit. This instrument is easily calibrated in a tank and was cheaply made. It requires little maintenance to ensure continued operation. However, because the galvanometer in the recording device has a proper period of 0.9 seconds and a critical damping of 200 ohms, a certain phase-lag will appear in the depth records. Hayami, Ishihara and Iwagaki (1953) state that the value of this lag is given by:

$$\text{Phase lag} = \tan^{-1} \frac{2hu}{u^2 - 1} \dots\dots\dots 46.$$

and; $u = \frac{T_p}{T_n}$

where: T_p is the period of the external force (taken as 2-3 seconds); T_n is the period of the galvanometer; and, h is the damping factor of the galvanometer (taken as 0.9).

Substitution of the appropriate values gives a mean phase lag for the depth recorder of 47° . All depth records must be adjusted accordingly.

B. The Shore Unit

The shore recording station used in association with the sensing units described is shown in Figure 21 and the electronics are set out in Figure 24. The latter diagram shows that the system comprises firstly, a 0-1 Ma (full-scale), 12 Volt D-C, Rustrak Model 188 strip chart recorder. This has

single channel capability only and a current measuring system was chosen in order to minimise line loss effects in the connecting cables. Secondly, a transistorised bridge amplifier constructed by the writer is used to control the input from the dynamometer. The latter unit was also designed for use in association with a conventional pressure/transducer wave gauge, By use of the damping control (S3 in Figure 24) it would be possible to record tide as well as wave levels.

A third unit of the installation is the controlled bridge circuit for the depth recorder. It can be seen from Figure 24 that the parallel wire gauge acts as a shunt across one limb of the bridge. The output of this unit can be alternatively switched to the chart but both control devices are provided with ancillary meters for visual observation of flow depth and velocity. Since the recorder is only a single channel unit a fourth component of the shore unit is an input switching system. The whole unit is completed by the three 6 Volt lantern batteries (dry-cell) necessary to power the system.

Plate 5 shows the physical arrangement of the various units. The whole assembly is mounted on a 20" x 14" x 10" Dexion frame and weighs about 15 pounds. It is completely field portable. The system together with the associated morphological and sediment sampling grids can be installed by a single operator in under an hour and is easily



PLATE 5. The shore unit. Chart recorder at top, data control and switch panels below. Battery pack at base. The tape case at lower left is 6" in diameter.

dismantled on conclusion of sampling.

The chart recorder employs sensitised paper so that salt spray and/or high humidity are no obstacles to operation. Recording is performed at the rate of 4"/minute because of the short durations of swash/backwash phenomena. In practice the system was used to sample swash/backwash parameters for perhaps 10 minutes in every hour of a tide cycle. Simultaneous measurements of morphological change and sediment movements were also made. An obvious disadvantage of the single channel system is that simultaneous recordings of several swash parameters could not be made.

However, an exception to this is provided by a time-pen unit added by the author. A trigger key on a long cable is used to trip a solenoid driving an extra pen on the recorder. This pen can be readily removed from the recorder when not in use and the cable length is sufficient to permit operation of the trigger by an observer in the water.

The application of this unit lies in time-frequency analysis of many swash/backwash phenomena. For example, it has been used to obtain time/deceleration curves for the swash after the manner of Dolan and Ferm (1966) by tripping the key each time the swash front passed a stake in a series spaced at 10' intervals across the shore. In this manner velocity profiles suitable for discharge analysis were derived. Further, the use of this technique in conjunction

with the dynamometer meant that point samples of bed velocity as measured by the dynamometer could be related to a known velocity distribution across the shore. Thus, it was possible to partially overcome the objections raised previously to the use of float and time/deceleration methods alone.

Additional uses of the time-pen include monitoring of wave, breaker or swash periods. Similarly, it is possible to determine whether swash flow is maintained for the maximum duration of the uprush or whether it reverses before the swash front has attained its upper limit on the shore. In this case the pen is tripped when a wave breaks and is released as the swash terminates. A cessation or reversal of flow is immediately apparent over the length of line trace by the pen.

Thus, an instrument system has been designed and constructed which, in the writer's opinion, combines a sufficient degree of versatility and sophistication with ease of operation and relatively low cost, to provide the basis for a detailed study of swash zone processes. Table 5 gives particulars of the records obtained with the instrument system. The data were derived from 21 separate field experiments at the four study profiles during the winter and summer of 1968-69. Breaker height ranged from 1.0 to 10.0 feet and included examples of the plunging, surging and collapsing types.

TABLE 5

Data Gathered with the Dynamometer 1968-69

| | | |
|---------------------------|---|-----------------------------|
| Chart run (4"/min.) | = | 630 feet. |
| Total Waves Recorded | = | 3,772 |
| Total Data Sets. (N) | = | 411 |
| Total Swash Sets Recorded | = | 208 |
| Total Backwash Recorded | = | 203 |
| Total Time of Flow | = | 3.8 hours |
| No. Swash Flows | = | 2,133 |
| No. Backwash Flows | = | 1,639 |
| Total time Swash Flow | = | 6,371 seconds = 1.77 hours |
| Total time Backwash Flow | = | 7,195 seconds = 1.999 hours |
| Mean Swash Flow period | = | 2.98 seconds. |
| Mean Backwash Flow period | = | 4.25 seconds. |
| Mean Swash velocity | = | 170.0 cm/sec. |
| Mean Backwash velocity | = | 140.0 cm/sec. |

Wave period ranged from 7.5 to 11.0 seconds. It is thought that this range of incident wave conditions together with the number of data samples gathered sufficiently represents the swash/backwash flow conditions at the study sites. Sediment sampling and morphological changes have received similar coverage.

The Sediment Sampler

Since the amounts of sediment moving in the water columns of the swash and backwash provide information concerning sediment transport rate and sorting processes, a sampler was constructed according to the design shown in Figure 25. The main criteria influencing this design were the necessity for minimum deformation of the flow and for a trap construction which, having intercepted the sediment particles, could not be evacuated by the turbulence of the reverse flow. It can be seen from Figure 25 that the trap has seven nozzles arranged vertically with 10cm. center spacings. The lowest trap is centered 3.5 cm from the bed. Each nozzle is 3.5 cm in diameter, thus presenting an area of 9.62 cm^2 to the flow. These trap structures consist of modified heavy-gauge plastic pipe junctions. It can be seen that a fine brass gauze has been fixed across the rear of each pipe fitting.

In operation, the flow enters the barrel of each trap and passes out the rear leaving behind the entrained sediment. The nozzles were arranged on the sampler so that the

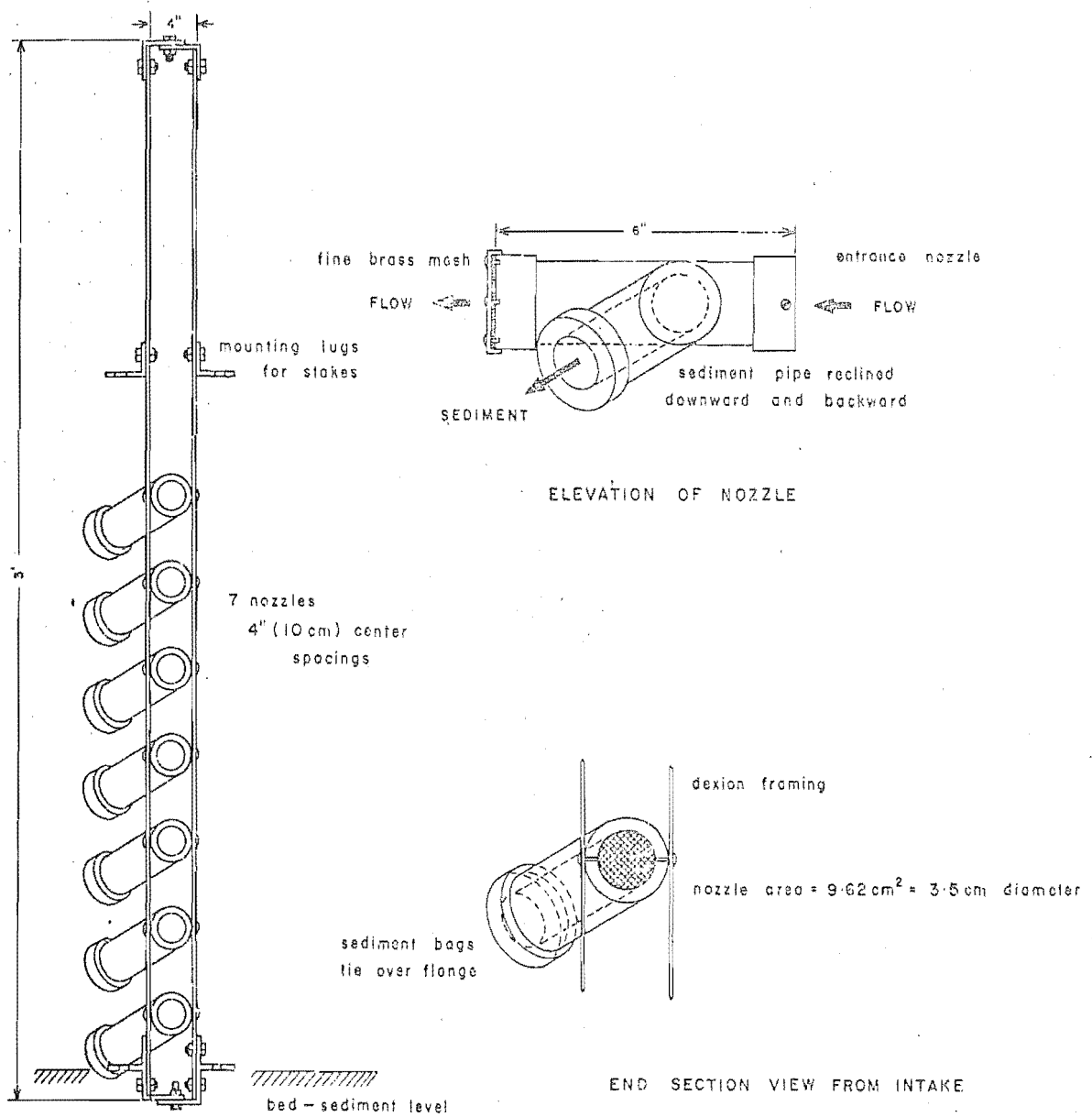


FIGURE 25. The Sediment sampler.

diagonally mounted junction tubes were directed downwards and rearwards. Thus, sediment entering the main barrel in the fluid is diverted down the inclined tube where it is caught by a cloth bag. Since these bags are permeable and since the sediment tubes are so long there is little chance that sediment reaching the bags can be lifted and removed from the traps by the vortex action of the reverse flow. While it is true that there has been no assessment of the efficiency of this trap arrangement it is felt that the instrument is superior to more conventional rigid trap structures where sediment particles fall into a cannister or bottle where considerable lifting forces may occur.

During the field experiments the sampler was run for periods of two to five minutes facing the swash following which the bags were changed and the instrument was then set to face the backwash. The retentive gauze in the rear of each trap was sufficiently fine to trap all but fine sand. The device was pinned to the foreshore with long steel stakes and no difficulty was experienced in handling. However, one possible improvement would be to reconstruct the unit using the same operational principles but incorporating a larger diameter trap barrel.

Bed Level Surveys

As mentioned previously, changes in bed elevation

were surveyed every hour through the tide cycle. This was facilitated by eight-gauge galvanized wire stakes inserted in the bed at 10' spacings from the swash limit to the breakers. The exposed length of each rod was measured to the nearest millimeter each hour using a steel tape mounted on a Duralumin rod. Beach slope was measured to the nearest degree with an Abney Level. Measurements of swash length and water table position were obtained with a one hundred foot linen tape.

Laboratory Analysis of Sediments

Two types of analysis were performed on the sediments gathered during field experiments. Firstly, analysis of sediments taken from the bed at each profile station was concerned with the determination of mean grain size, sorting, skewness and kurtosis of the grain size distributions. Secondly, samples obtained using the transported sediment sampler described were subjected to laboratory procedures suitable for the determination of mean nominal diameters. The latter parameter was adopted for the description of these sediments because laboratory data on sediment transport are usually given for spherical particles. The use of equivalent spherical diameter for the field data thus established a basis for comparison with flume studies.

A total of 183 bed samples and 122 samples from the

swash and backwash water columns were collected and analysed. For the bed samples, an aggregate dry weight of 100 to 200 grams was collected from the surface in accordance with standard practice. However, larger samples of mixed sand and shingle were collected because, "little is known of the reliabilities of samples for different ratios of particle size to sample size" (Krumbein, 1953). For this reason mixed sand-shingle samples were two to three Kilograms in weight.

Bed samples were washed to remove salt and oven-dried. Materials coarser than one eighth inch diameter were sieved by hand and the remainder was sieved for 15 minutes in an Endecott, "Endrock" sieve machine in the Physical Laboratory, Geography Department, University of Canterbury.

The weights of material retained on each sieve were converted to percentages of total sample weight and plotted cumulatively on log.-normal graph paper. Grain size was plotted on the abscissa and frequency on the ordinate. The sieves used conform to the British Standard Code of Practice No. 410 and are graduated according to the Wentworth scale of particle sizes. This was converted to the phi (ϕ) scale (Krumbein and Pettijohn, 1938, p. 84), to facilitate the computation of statistical parameters. Percentile values (ϕ) from the size-frequency distributions were transferred to IBM data cards and the Graphic Mean Diameter (M_z); Inclusive

Graphic Standard Deviation (σ_I); Skewness (Sk_G); and Kurtosis (K_G) coefficients (Folk, 1965), of each distribution were calculated on the University of Canterbury's 360/44 IBM computer. Subsequent analysis of grain size data was performed on the computer and on a desk calculator.

Grain aggregates caught by the sediment traps were also washed, dried and weighed before analysis. These samples were repeatedly separated using a sample splitter to obtain 25 grains for detailed examination. Though the sample size appears to be small student's t - tests failed to reveal any significant difference in the estimation of mean nominal diameter from sample sizes of 25 and 50 grains.

The shape of each particle was determined by measuring the three major axes of pebbles with vernier calipers. Measurements were accurate to within 0.1 mm. The longest axes were designated 'A', the intermediate 'B', and the shortest 'C' in accordance with Folk (1965). Effective Settling Sphericity (Ψ), flatness index (C/A) and other measures were calculated on the 360/44 computer for each of the particles. Also calculated were the values of mean effective settling sphericity and the standard deviations (σ_Ψ) of the distributions. The latter measure is employed as an index of shape sorting.

As mentioned previously, one of the most important parameters derived from these samples is mean nominal diameter.

Initially this was derived by the displacement method of Krumbein and Pettijohn (1938, p. 143). Individual particles were dropped into a 50 ml. Burette and the volume of fluid displaced read to the nearest 0.1 ml. Mean nominal diameter (Dn) was then derived for each particle according to:

$$D_n = \sqrt[3]{1.92 V} \dots\dots\dots 47.$$

where: V is the fluid volume displaced by a particle (in cc.). It was subsequently found that a reliable estimate of mean nominal diameter could be obtained from the axes of the individual particles according to:

$$D_n = \sqrt[3]{\frac{A \cdot B \cdot C}{\pi}} \times 1.908 \dots\dots\dots 48.$$

Tests (Student's t) failed to show a significant difference between the two methods. This is probably due to the generally good sorting of the trapped particles and to the general uniformity of particle shapes.

Thus, values of Dn were calculated for each particle at the same time as the shape parameters. Individual values were then extracted from the computer print-out and arranged in $\frac{1}{2}\phi$ frequency classes. Thence in a fashion identical with that used for the bed samples, percentile values were extracted and Folk parameters calculated with the grain-size programme described previously. In this way grain size parameters were obtained for the transported sediment

distributions that are readily referable to those of laboratory studies.

It can be seen from the above discussion that the data collected for this study relate to many of the parameters detailed earlier as being fundamental to a study of swash zone processes. It is now therefore possible to proceed to the analysis of this data.

GENERAL DYNAMICS OF THE SWASH ZONE

As a preliminary step toward establishing a general framework in which to set more detailed analysis of swash and backwash water motions, measurements of several overall properties of breakers and swash were made. The parameters treated in this manner include runup height, breaker height, swash length, wave period and swash period. Analysis of variations in these will be followed by a consideration of the distributions of flow velocity and energy both across the shore and for a range of input breaker conditions.

Runup Height

Runup height is defined as the height to which swash water rises above still water level on the shore face. Runup characteristics are completely different for waves that break than for those that do not (Van Dorn, 1966, p. 47), and the significance of the parameter lies in the fact that it controls the height to which littoral structures may be built.

Van Dorn (1966, p. 50) notes that there is no adequate theory for the runup of broken waves, but that there are many empirically derived expressions employing solitary wave

FIGURE 26A. Runup height as a function of breaker height. Height of breaker is that of each wave yielding significant runup within each sample. Open circles, $T = 11.0$ secs.; dots, $T = 10.0$ secs.; triangles, $T = 8.5$ secs.

FIGURE 26B. Mean swash length as a function of significant breaker height. Note therefore that this diagram refers to time-average conditions.

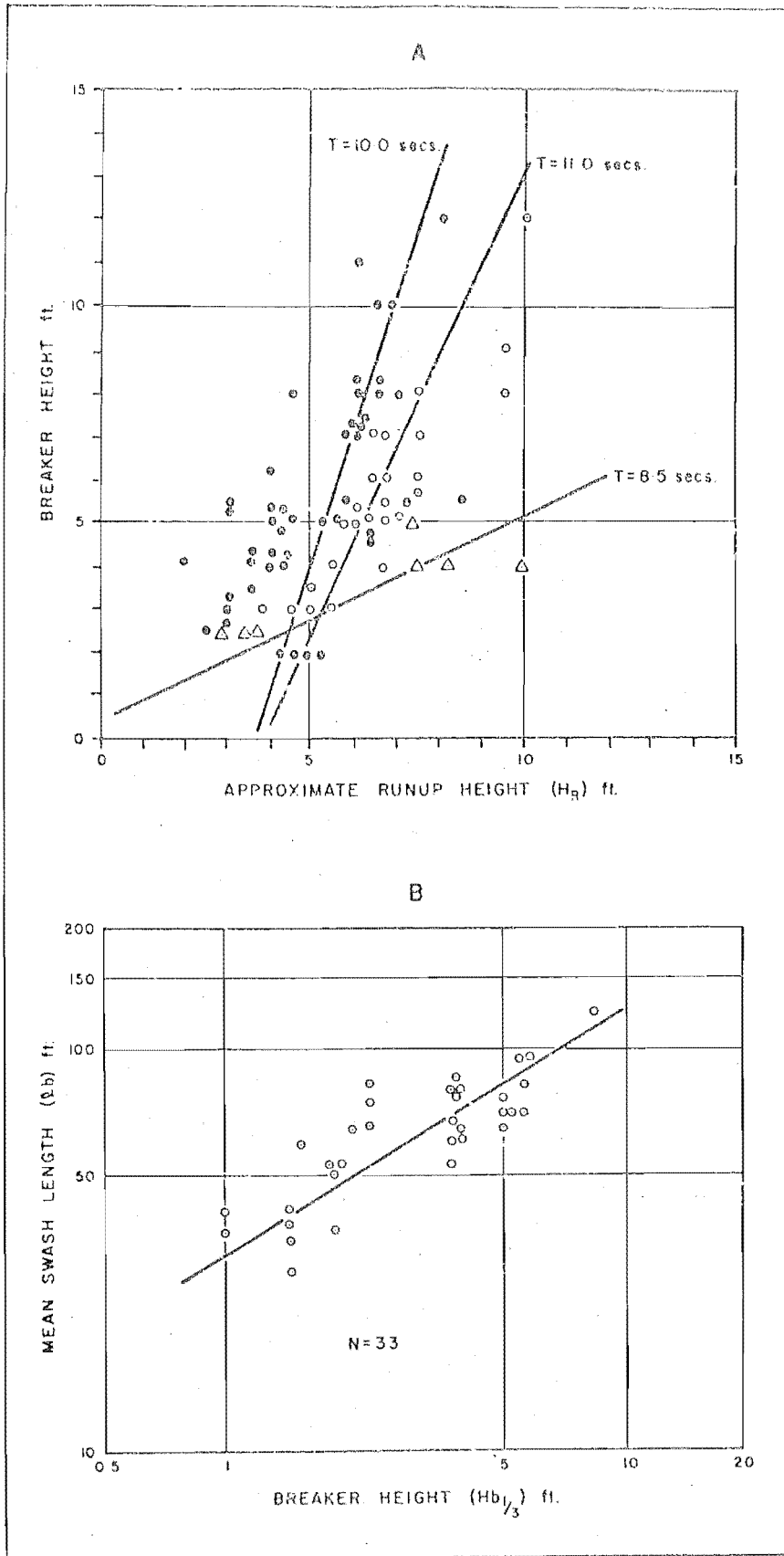


FIGURE 26. Breakers, runup height and swash length.

FIGURE 27A. Variations in swash phase
and length for two breaker
conditions.

FIGURE 27B-C. Observed variations in
breaker height and swash
length in relation to
"critical" height/length
requirements.

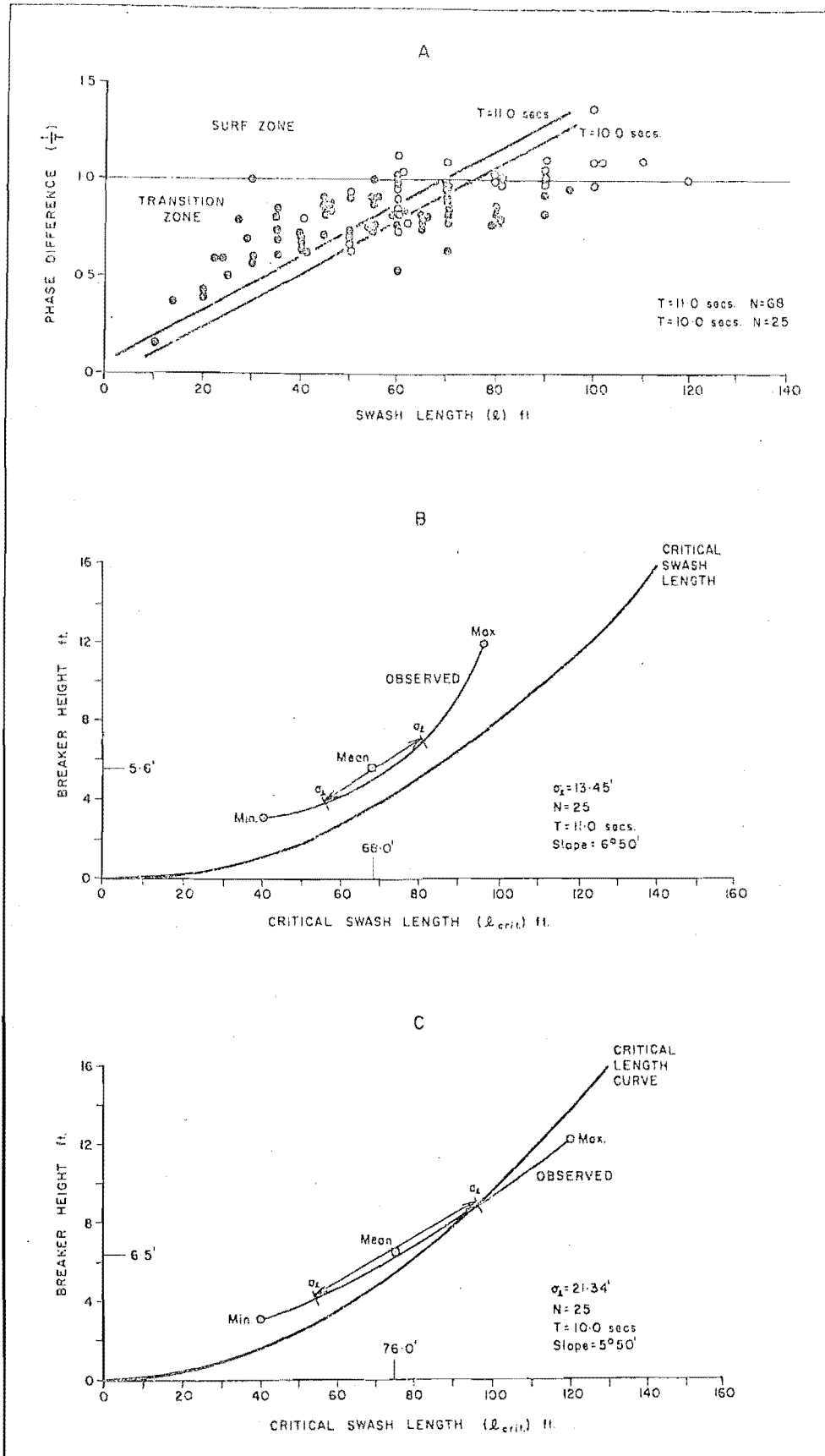


FIGURE 27. Variations in swash phase and length.

theory. These are usually of the form:

$$\frac{R}{d} = f_1 (S) \left(\frac{H}{d}\right)^{f_2} (S) \dots\dots\dots 49.$$

where: R is runup height, d is depth of water, S is beach slope, and H is wave height. Both the coefficients and the exponent are empirically determined. It is therefore clear that the largest values of runup occur for steep beach slopes. Savage (1959) obtained maximum runup values for laboratory experiments on high slopes and at low wave steepness.

Approximate runup values for three sets of field experiments are shown in Figure 26A. It can be seen from the diagram that the relationship between breaker height and runup height is approximately linear for each of the three wave periods sampled. Correlation coefficients ranged from 0.66 to 0.88. Also, the influence of foreshore slope on runup height can be noted. The short period, high runup character of the 8.5 second waves is largely due to the fact that the slope these values were obtained from (8°) was twice as steep as that for the 10.0 and 11.0 second waves (4°).

Since each set of data was derived during a single wave regime at a given station it is apparent that there was considerable variation in breaker height and subsequent runup at each station. Saville (1962), in an attempt to

define characteristic wave runup frequency distributions alludes to such variability of breaker height and period and states that in practice, runup relations are derived for the "significant" wave. i.e.: A wave having statistically described characteristics, typically the mean height of the highest one third of the waves. However, it will shortly be demonstrated that the morphological activity of the latter depends greatly upon phase relations among the whole input wave spectrum. Also, it is clear from Figure 26A that for given conditions swash/backwash structures may be expected to develop over a vertical range approximately equal to wave height during field experiments.

Flow Phase Relations in the Swash Zone

As an initial check on the applicability of the phase difference criterion to the swash zone flows of the study beaches a correlation between breaker height and swash length was obtained (Fig. 26B). The 33 observations cover all of the study sites and a good fit was obtained. It was therefore decided to further examine the phase relations of the flows with particular reference to the variation within wave trains, as stressed previously.

Figure 27A indicates the relations between phase difference and swash length for two field experiments at stations C and D. It can be seen that there are again

good correlations between the measured properties but the individual values are scattered widely with respect to Kemp's (1958) zonation into characteristic ranges of phase difference. Thus, in both data sets a few points fall in the surge range, most in the transition range, and a further few into the surf range of effect.

Also, it can be seen that if a given horizontal through the diagram is selected, then for a given wave period there is considerable variation in swash length. Thus, for constant phase difference equal to 0.7 and for the 11.0 second waves swash length varied from 30 feet to more than 70 feet. This example serves to highlight the importance of interference between oncoming waves and backwash so that waves in a given phase state with regard to swash and backwash may be considerably restricted in the lateral range over which they may produce morphological effects. A similar effect applies therefore to the distributions of runup height shown in Figure 26A. The highest one third of the breakers in each of the two cases shown fall into the range of surf zone conditions, and hence are associated to some extent with notions of shore-face erosion, circulation through the breaker etc.; while the body of the sample, occurring at intermediate breaker heights, is associated with transition zone flow conditions.

Thus, as was stated previously, it is of considerable

importance to examine the level of variability in given wave trains when assessing the level and type of morphological activity resulting. Such an analysis has been conducted for the two sets of data and the results are shown in Figures 27B and 27C. In each case the observed distributions of swash length have been referred to the appropriate critical swash length curve derived from the expressions of Kemp (1958, see equation 9), and employing the constants determined for the study sites. The observational data has been presented in terms of mean, maximum, minimum and variance of each wave train. Significant differences between the two conditions are immediately apparent. Firstly, the 11.0 second wave train resulted in a mean breaker height of 5.6 feet and a mean swash length of 68.0 feet; while the 10.0 second waves were associated with a mean breaker height of 6.5 feet and a mean swash length of 76.0 feet. Similarly, there are only small differences between the maximum and minimum values in the two cases. However, there are striking differences between the variances of the two data sets. The standard deviation of swash length for the 10.0 second waves is almost double that for the 11.0 second waves for similar beach slopes. The incidence of interference between breakers and backwashes was therefore considerably greater for the 10.0 second conditions. Because it has been shown that such interference results in a weakened swash action and a

correspondingly strengthened backwash action, it may be inferred that the erosive activity of the 10.0 second waves was considerably greater than that of the 11.0 second waves.

Further, it is clear from the diagrams that the observed distribution for the 10.0 second waves lies closer to the computed curve of critical swash length than does that for the 11.0 second waves. In fact the observed curve of Figure 27C lies across the critical curve whereas that of Figure 27B lies wholly in the transition range of sub-critical conditions. The level of variability of input wave conditions to the swash zone at any given time has thus been shown to be an important parameter governing the morphological activity of flows. Regardless of wave steepness and beach slope a high level of variation in input breaker conditions may be expected to result in increased erosive action of the backwash since the progress of the swash will be impeded. These effects can be further elucidated by study of the force/time traces recorded by the dynamometer.

Distributions of Velocity in the Swash and Backwash

Figure 28 shows a representative range of the types of chart trace obtained using the dynamometer. Swash flows are represented by those portions of the curves lying above the zero line while backwashes lie below the line.

Figure 28A indicates a typical record of a surging breaker ($H_b = 1.0$ foot). These waves were recorded on

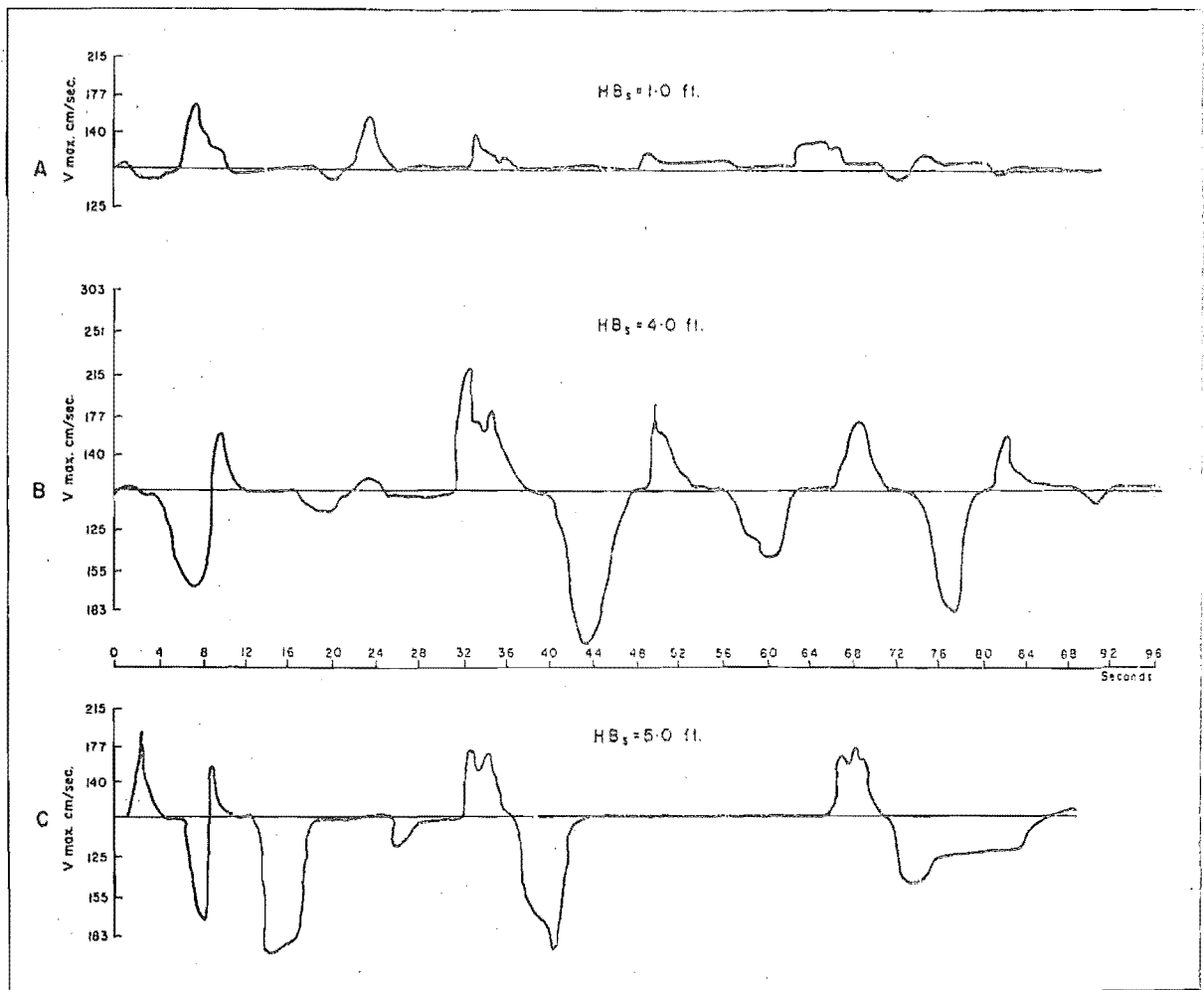


FIGURE 28. Typical Dynamometer velocity traces.

the steep (12°), well sorted shingle profile at station B, South Bay. It can be seen that the waves produced a swash of short length and very regular duration so that there was a pendulum-like motion of the water against the shore. Also, percolation losses resulted in thin backwash sheets so that few backwashes were recorded. Of particular interest is the pattern of flow. The trace exhibits several sharply defined, fast moving crests which were followed by a long, steady onshore flow averaging 3.23 seconds duration. Average backwash duration was 3.53 seconds.

A record of the swash/backwash resulting from "classical" plunging breakers ($H_b = 4.0$ feet) is shown in Figure 28B. The observation point in this case was at station C. The waves delivered long swashes (averaging 60-80 feet) up a planar slope (5°). Unlike the surges described above the plunging breaker record is notable for sudden reversals in flow direction and magnitude. Inflections in the crests of the swash curves indicate that there were considerable velocity variations within the flow. The unit volumes of water delivered to the shore appear to break into subunits or secondary eddies. Schiffman (1965) obtained similar records on sandy beaches. Also notable in Figure 28B is the non-linear nature of the backwash curves. Acceleration of the water mass begins gradually and then increases rapidly.

Figure 28C is also a record derived under plunging breaker conditions ($H_b = 5.0$ feet). These were storm waves which delivered very turbulent swash and much spray to the foreshore. The waves broke in a very much more confused fashion than those previously described. Much of the energy in them was dissipated in vertical water movements. Hence, the unevenness of the swash peaks is much more pronounced, but the mean velocity of the swash was only a little greater than that for the 4.0 feet waves. The vertical release of wave pressures in this manner is similar to the under-riding character of the backwash offered by Dolan and Ferm (1966) as an explanation for the decreasing degree of correlation between increasing swash velocity and increasing wave height.

On the other hand, relative to the swash, the backwash traces shown in Figure 28C have considerably larger amplitudes than those shown in Figure 28B. This increased backwash power results from the fact that water flung into the swash zone in whatever manner falls back to contribute volume to the backwash which then flows down the bed as one mass. It is thus possible to record backwash velocities that are considerably greater than those of the swashes that give rise to them. It will be noted that this effect is greatest for the largest breakers. The latter also tend to be more variable in form and height so that under such

conditions variation in swash length may be expected to be at a maximum and hence, interference between successive waves most frequent. A final aspect of importance concerning the amplitude and shapes of chart traces is that, in some respects, the sequence of curves from lowest to highest breakers is paralleled by observations from a series of stations across the swash zone. Thus, records from near the swash limit are similar to those of surging breaker conditions while those from stations near the base of the breaker contain secondary inflections and deep backwash spikes similar to those shown in Figure 28C.

Velocity Profiles Across the Shore. Characteristic across-shore distributions of velocity in both swash and backwash are shown in Figure 29. Figure 29A is a diagrammatic summary of all results derived from the four stations selected for study. Grand mean curves, upper and lower bounds and breaker positions have been indicated. In order to refer individual measurements derived from different observational periods to equivalent positions in the swash zone the measure of position employed in the diagrams (x/L_0) is the ratio of the distance x , of a given sample point from the swash limit, to the deepwater wave length ($L_0 = 5.12 T^2$). It is important to note that each data point on the diagrams represents a time-mean value for velocity and hence has

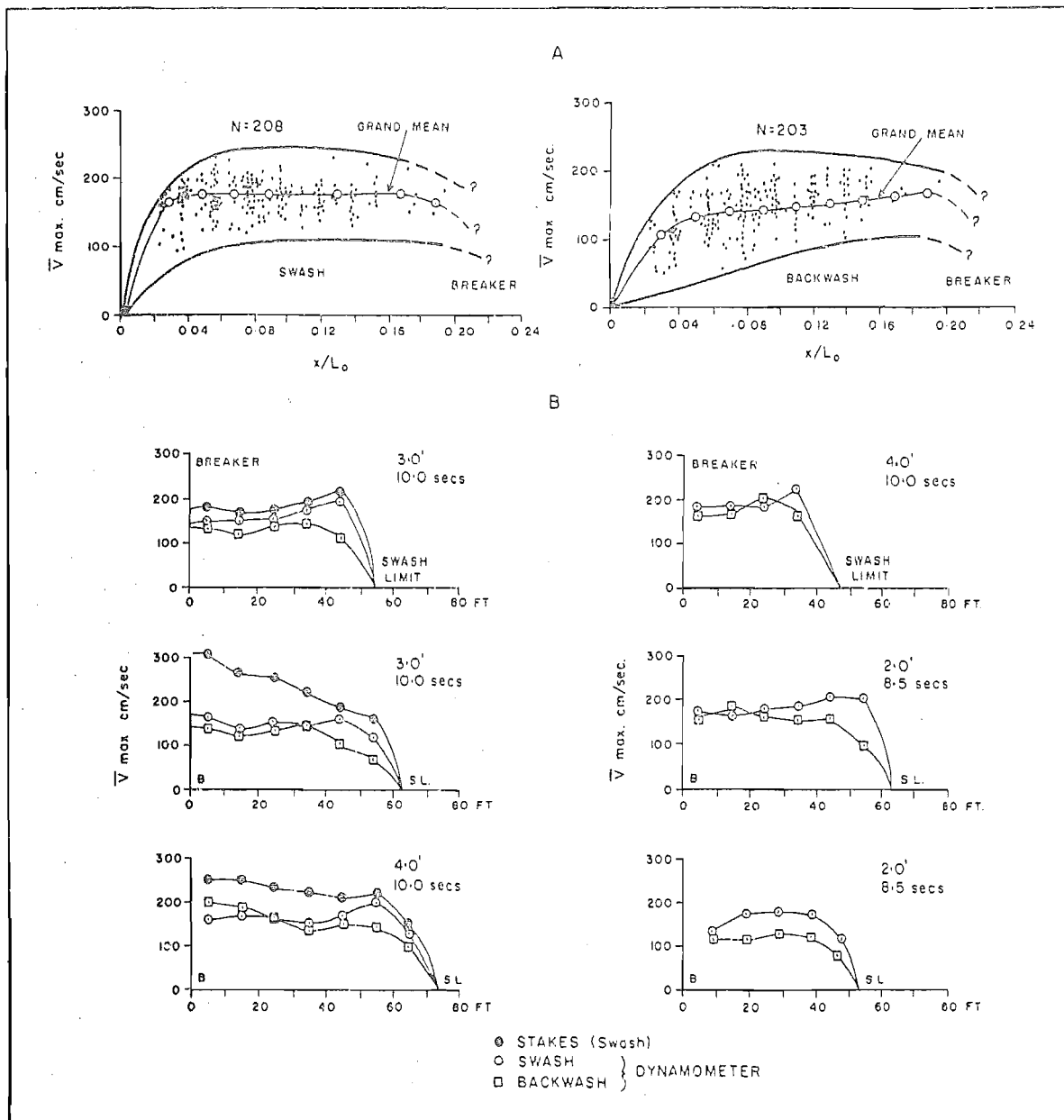


FIGURE 29A. Distributions of swash and backwash velocity.

B. Shore-normal profiles of swash and backwash velocity.

been derived from traces such as those shown in Figure 28.

Perhaps the most salient feature of Figure 29A is the wide range of velocity conditions sampled at all points across the shore. This is a reflection of the wide range of breaker heights, periods and foreshore slope conditions that were sampled. Variation in velocity is most marked near the upper limit of the swash zone where the foreshore is intermittently wetted.

The grand mean swash curve is notable for the almost linear velocity distribution across the lower and central sections of the shore. Rapid deceleration is only pronounced near the swash limit. The represents an important difference between the time-mean curve and an instantaneous curve of swash deceleration (see Fig. 11B) for the latter). By comparison, the deceleration of an individual swash by friction tends to follow an exponential curve. The backwash grand mean curve, on the other hand, begins less rapidly and accelerates more uniformly, achieving maximum velocities near the base of the breaker.

Several examples of individual velocity profiles are shown in Figure 29B. Also included are three examples of mean swash front velocity as determined by the stakes and trip-pen method of Dolan and Ferm (1966). It can be seen that the swash front profiles parallel the dynamometer

swash velocity profiles in a general fashion but that the swash front characteristically moves faster than the water near the bed in the following flow body. This supports Rouse's (1938) conclusion that the front of a surge is the zone of maximum turbulence.

The curves also indicate that for the upper part of the shore backwash velocity is considerably less than swash velocity. However, for the mid and lower foreshore areas backwash velocity equals or even exceeds swash velocity.

A further interesting feature of many of the swash curves is a region of high velocity located toward the upper limit of swash action. Thus, the time-mean velocity profile may decrease or remain linear over much of the shore but increase near the swash limit before rapidly declining to zero flow at the swash limit. This unexpected result can be explained in terms of the variability of breaker/swash conditions discussed above. While swashes of all lengths and intensities are recorded on the lower foreshore only the longer, more powerful flows are recorded at the upper stations. Thus, when considering the time-mean state of swash flow as opposed to the instantaneous decay of a single swash passing across the shore it is important to note that there is a high velocity zone capable of significant morphological effect located high on the profile of the shingle beach. Obviously this effect will be least for uniform breaker conditions and at a maximum

for breakers characterised by a wide range of heights.¹¹ Therefore, not only is the backwash scour effect maximised on the lower foreshore during variable breaker conditions, but also the depositional capabilities of the swash are enhanced at the upper limit of wave action.¹¹ This important conclusion will be further examined when considering the levels of discharge in the swash and backwash.¹¹

Flow Reversals Near the Breaker. In order to check the validity of Dolan and Ferm's (1966) statement concerning the underriding of swash by backwash at high phase conditions and to further examine the nature of swash trains possessing a high variance level several tests were made near the base of the breaker at each station using the dynamometer in association with the trip-pen as described during the discussion of the instrumentation.¹¹ As can be seen from Figure 30 the pen was tripped when a wave broke and was released when the swash terminated at the upper limit.¹¹ The diagram indicates the two possible flow states. First, flow at the dynamometer may cease at any time up to that of the full duration of the swash period.¹¹ Since the instrument has a lower velocity limit, recorded flow commonly ceased before the swash reached its upper limit on the shore.¹¹ Secondly, backwash may begin before the swash has terminated at the upper limit of wave action (see Fig. 30B). On several occasions during high phase

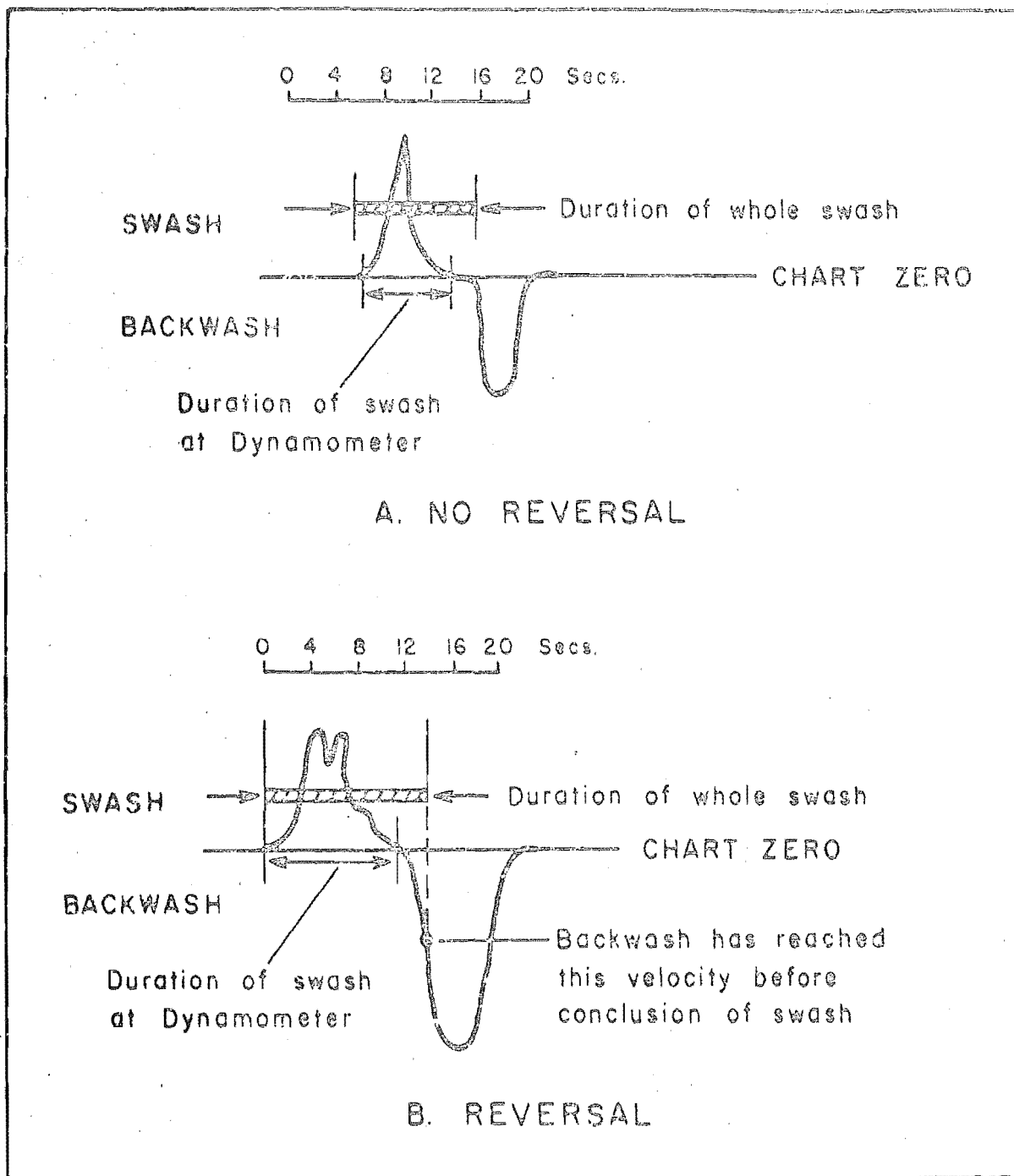


FIGURE 30. Flow reversals at lower foreshore stations.

wave conditions the latter was observed. On one such occasion a backwash velocity of 125.0 cm/sec. was attained before backwash began on the upper foreshore.

During high phase wave conditions which are characterised by extreme variability of swash length and breaker height, water piles up on the foreshore until it is able to break out against the oncoming swashes. Under such circumstances an almost steady offshore flow exists near the base of the breaker and each incoming breaker is sufficient only to halt this flow temporarily. The outflow results in a rapid drawdown of swash head in the immediate vicinity of the breaker. Swash velocities near the bed are low and water motion is confused. Flows of this type were never recorded during low phase wave conditions so that the above observations lend support to Kemp's (1958) conclusions regarding the nature of fluid exchange from the swash zone across the breaker zone. Further information concerning these flow characteristics may be derived from an examination of the relative energy levels at different stations across the shore.

Relative Energy Distributions across the Swash Zone

A measure of the relative energy levels at various parts of the swash zone has been derived by summing the areas under each individual set of swash and backwash curves and dividing each by the total times for which swash and backwash were

active (Schiffman, 1965). These measures have been taken as approximations to Bagnold's parameters ΔE_1 and ΔE_2 for the purposes of this investigation. In this way mean relative energy levels for both swash ($\overline{\Delta E_1}$), and backwash ($\overline{\Delta E_2}$) could be examined and a value of net mean energy level derived by simple subtraction ($\overline{\delta E} = \overline{\Delta E_1} - \overline{\Delta E_2}$). The measures represent the asymmetries of energy application at given stations and positive values refer to onshore energy balances while negative quantities refer to offshore net forces.

The results of this analysis are presented in Figure 31. Swash energy is at a maximum in the mid and upper foreshore regions and there is some indication of flow-field reformation immediately landward of the breaker. Backwash energy, by contrast, is more variable and attains higher absolute values more frequently than does the swash. In this case relative energy levels are highest in the mid and lower foreshore regions. Values of zero for ΔE_2 refer to cases where ΔE_1 was greater than zero but no backwash was recorded. The effect of increasing wave period is to widen the envelope of mean relative swash energy and to elevate the mean curve to higher energy levels. On the other hand, the principal effect of increasing height and variability of the breakers, is to elevate the mean relative backwash energy curve.

Figure 31C indicates the envelope of net mean relative energy level. It is readily apparent that offshore

FIGURE 31A. Distribution of mean swash energy across the shore. Dotted line is grand mean for all values.

FIGURE 31B. Distribution of mean backwash energy. Dotted line is grand mean curve.

FIGURE 31C. Distribution of net mean relative energy level across the shore. Dotted line is grand mean curve.

Note: Data are those for all breaker heights, periods and profile stations sampled during field experiments.

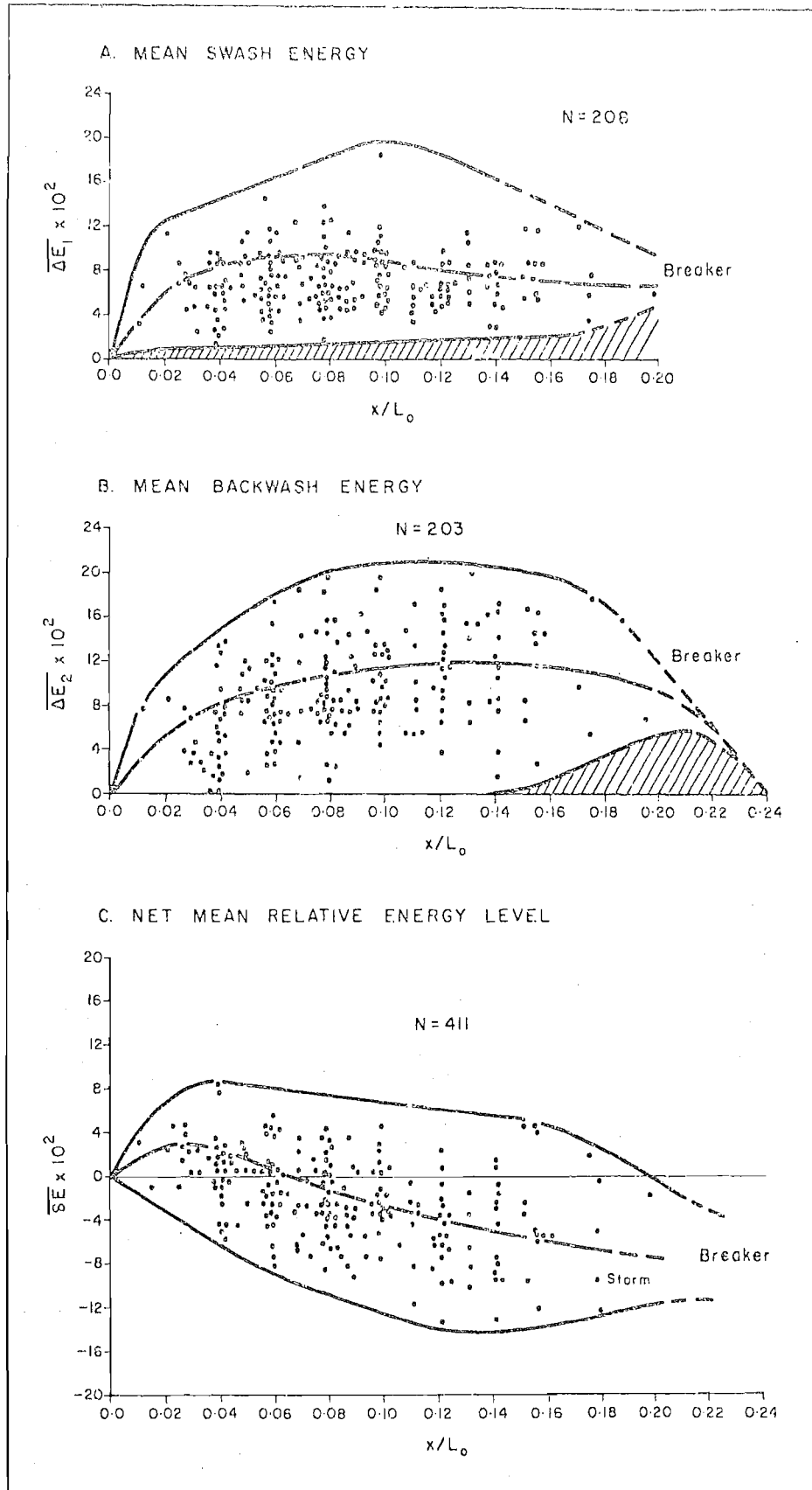


FIGURE 31. Flow energy envelope curves.

forces tend to predominate in the lower part of the swash zone while onshore energy balances are confined to the upper levels of swash action. It is in this latter area where percolation losses into the foreshore are most apparent. For any given swash/backwash regime there will be a point on the shore where the net energy balance is zero, neither onshore nor offshore forces predominating. The effect of increasing breaker height on this curve is to depress the mean trend so that negative energy levels obtain for much of the shore. Thus, while large forces are applied for short periods during swash flow these are often counteracted by lower forces acting for much longer periods of time in the backwash.

Variations in Flow Energy with Breaker Height and Period

On the assumption that the areas under the force/time curves represent an approximation to flow energy Figure 32 indicates the distributions of energy in the swash and backwash for a range of breaker heights of from 1.0 to 5.0 feet. All of the data are derived from stations low on the foreshore ($x/L_0 = 0.15$ to 0.18). It is apparent from the diagram that the data have been grouped by periods in one second intervals.

Characteristically there is an increase of mean energy level in both swash and backwash with increasing breaker height and energy is spread across a wider range of periods

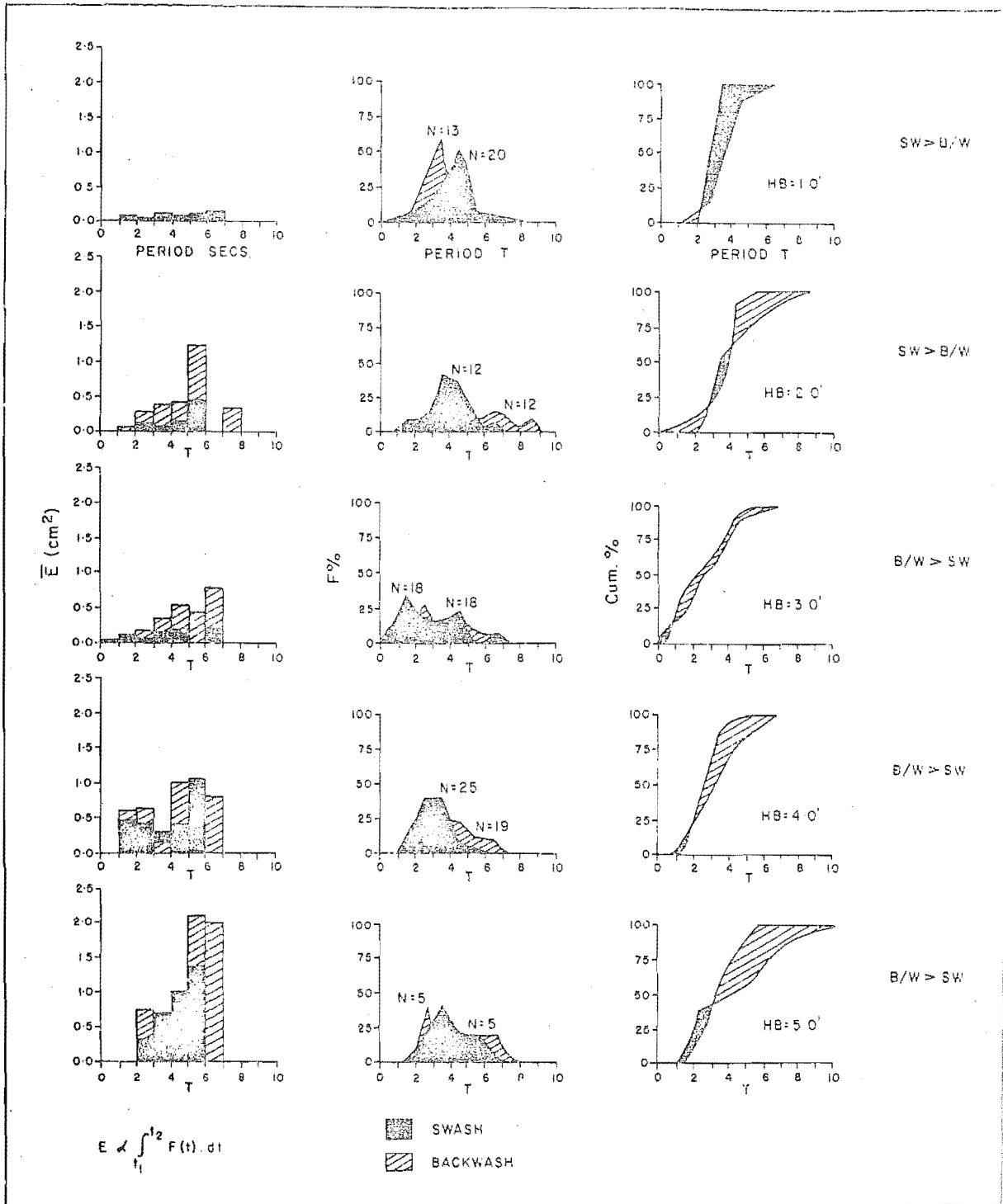


FIGURE 32. Frequency distributions of flow energy in swash/backwash flows for a range of breaker heights. Data grouped by period.

at higher breaker conditions.¹¹ Also apparent is the increase in backwash energy at longer periods with increasing breaker height.¹¹

The frequency of occurrence of different periods can be seen from Figure 32 to be polymodal for all save the smallest breaker heights.¹¹ The bi-modal character of the backwash frequency distributions at the larger breaker heights may be taken to indicate the piling up process occurring at high phase conditions as previously described.¹¹ Short period backwash flows thus represent interruptions caused by the arrival of subsequent swashes while the long period mode relates to intervals of sustained outflow from the swash zone.¹¹ In this sense the longer period mode is analagous to the nodes in the frequently observed surf-beat systems recorded on sand beach foreshores. Backwash flow times at all breaker heights tend to be less regular than swash flow periods.¹¹

Finally, the cumulative frequency graphs demonstrate that swash flow dominates only at the lowest breaker heights. For increasing breaker height at stations near the base of the breaker net onshore energy is confined to increasingly shorter flow durations.¹¹ This conclusion is in accordance with previous findings relating to variations in flow near the bed at high phase conditions in this area of the swash zone.¹¹

Summary of Phase Effects on Flow Energy and Velocity

In summary it has been shown that phase difference analysis can be meaningfully applied to the swash zone of the study beaches. A particularly important aspect of this is the examination of the level of variation in input breaker and resultant swash characteristics. A high level of variation affects both the characteristic flow durations of swash and backwash and the nature of the water column in the area immediately landward of the breaker.

Where swash length is widely variable backwash overrides the swash on the lower foreshore and almost continuous circulation through the breaker is developed. These processes may result in extensive scouring by the backwash regardless of wave period. Also extreme variability of swash length results in a net concentration of swash energy toward the upper limit of swash action.

Since the characteristic distributions of velocity and energy across the shore have been described it is now possible to proceed to a more detailed analysis of the asymmetries of pressure and velocity at given locations on the bed. It is these properties of flow that govern the entrainment, direction of net transport, and final resting place of bed sediment particles in the swash zone.

ASYMMETRIES OF FLOW

In the swash zone where wave motion is greatly distorted, the study and analysis of data relating to the asymmetries of flow pressures and durations is crucial to the examination of sediment motion since these properties condition first, the sizes of material lifted from the bed, and, secondly, the durations (distances) of travel of the sediment grains. Thus, the action of a very high applied pressure lasting for a short time may be expected to produce different sediment sorting characteristics than a low pressure acting for a longer period. In the first case, very large particles may be set in motion and significant suspension of finer sizes may occur, while in the second case, a more uniform range of finer sizes may be transported as bed load.

Since it has been previously shown that the swash zone of the study beaches is a high energy environment the situation is still more complex. In this case the asymmetry of the maximum pressures occurring (associated with the largest particles present) may be opposite in sign to that of the mean pressure (which will be linked with finer sediment size grades), so that simultaneous motion of grains may occur in different directions.

The magnitudes and signs of the asymmetries will depend upon the water column structures in the swash and backwash while the net sorting pattern produced over a period of hours will depend upon the sizes and speeds of the water masses giving rise to the flow structures. It is therefore intended to first examine the discharge or "water budget" aspects of swash zone circulation before proceeding to the analysis of flow asymmetries. Finally, the discussion will be concluded with a theoretical examination of the sorting processes produced by given patterns of flow asymmetry.

Flow Discharge in the Swash and Backwash

Flow discharges past given stations in both the swash and the backwash have been computed according to equation 45. The values presented therefore represent time-mean conditions as in the case of the velocity profiles they were derived from. The study of discharge relations in the swash zone has at least two important aspects. The first may be termed a circulation aspect and concerns the interchange and recirculation of water from the beach face across the breaker to the nearshore zone. Some aspects of this have already been described. The second aspect concerns the structures of individual water columns at various points on the bed of the swash zone.

Water Circulation through the Swash Zone. The water budget

of the swash zone is made up of inputs from the breakers and from the groundwater table and of outflows in the backwash and seaward return flows, as is shown in Figure 33A.

Groundwater flow is comprised of swash water derived by percolation and any residual groundwater outflow of terrestrial origin. Neither infiltration rate of swash nor seaward return flow of water was measured during field experiments so that a full examination of water budget is not possible.

However, the most salient aspects are presented in Figure 33B. The diagram shows discharge profiles for a range of input breaker conditions, and breaker discharge has been calculated from equation 1. As such it represents an instantaneous value rather than a time-mean condition. Groundwater discharges were obtained by measuring the percolation rate of water passing through the beach deposit using fluorescein dye. Dye was injected in the beach surface between swashes and the time and distance of travel to the point of emission on the beach face noted. A number of trials were carried out on each occasion in order to derive a reliable mean value for groundwater discharge. However, the method applies only to the interval after backwash when discharge is at a minimum and it can only be employed on the upper foreshore where the interval between flows is sufficient to allow undisturbed use of the technique.

Figure 33B and Table 6 show that there is a general

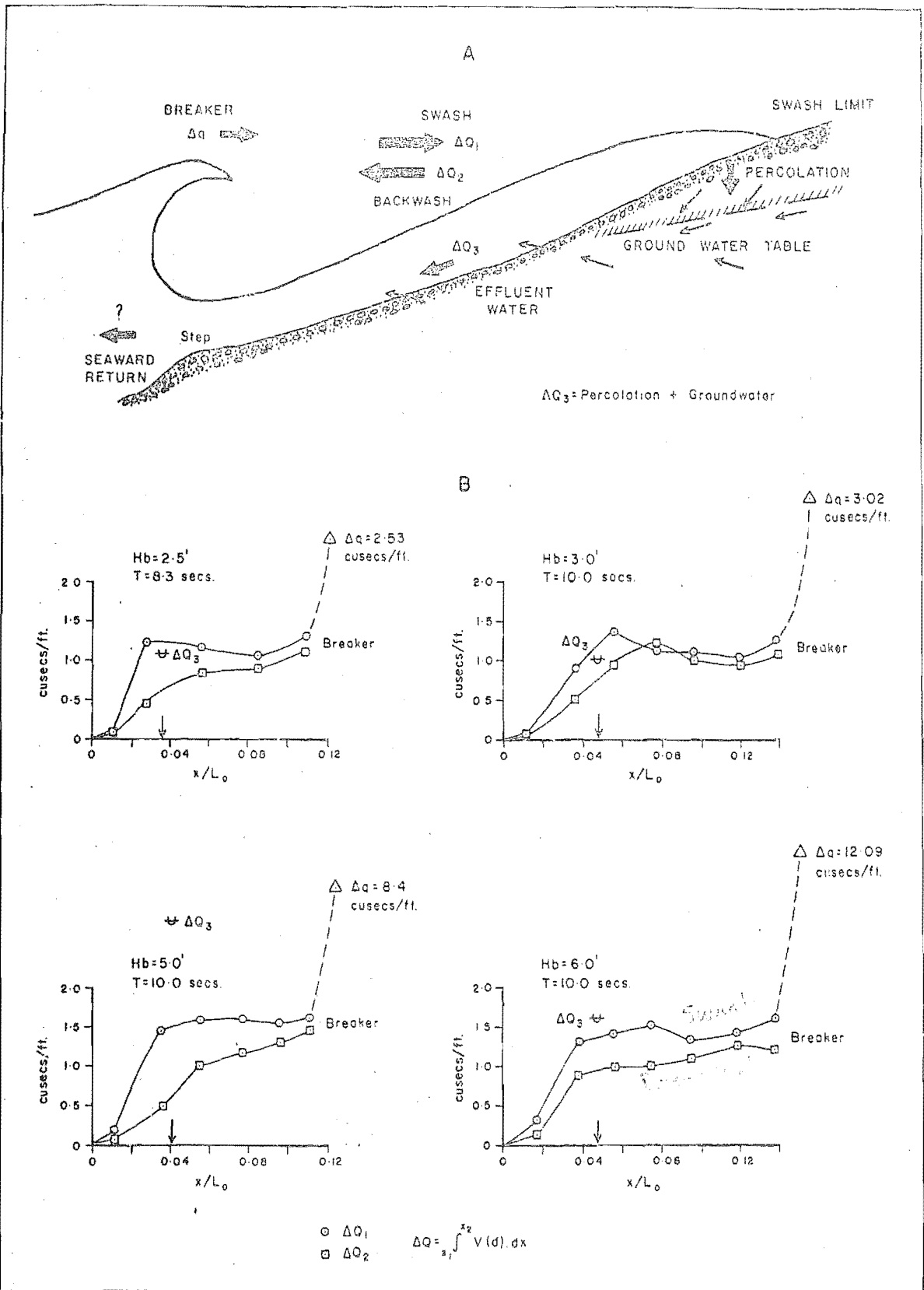


FIGURE 33A. The "Water Budget" of the swash zone.

33B. Typical discharge profiles for swash and backwash. Breaker discharge calculated according to equation 1.

increase in discharge level both in the swash and backwash with increasing breaker height and period. There is also a corresponding rise in the level of outflow from the beach water table. Table 6 also indicates that there is a general agreement between the dye technique and the velocity profile method concerning the volume of swash lost by percolation into the beach face. It can be seen that storage may affect up to one third of the swash volume at low breaker heights, but that there does not appear to be appreciable increase in the level of storage at large breaker heights. This result confirms Lewis' (1931) suggestion that the role of percolation of swash declines at large breaker heights.

From Figure 33B it can be seen that at some stations on the lower foreshore backwash discharge may exceed that of the swash. However, in most cases the level of percolation is sufficient to retard backwash discharge. It is also clear from the diagram that the swash discharge curves are similar in form to the velocity profiles presented previously in that they reflect constant discharge rates over much of the shore and either increase and/or drop away sharply near the swash limit. By contrast the backwash curves have two distinct regions; an upper, sharply rising limb which reflects downslope acceleration of the water and a rapid return to the surface of some infiltrated swash, and a lower almost constant limb of more slowly accelerating flow at

TABLE 6

Swash and Backwash Volumes

| <u>Breaker Height Ft.</u> | <u>Breaker Period Secs.</u> | <u>Flow</u> | <u>Volume cu. Ft/Ft</u> | <u>Difference cu. Ft/Ft</u> | <u>*Ground water Table</u> |
|-----------------------------------|-------------------------------------|--------------|---------------------------------|-------------------------------------|------------------------------------|
| 2.5 | 8.3 | ΔQ_1 | 3.38 | 0.79 | 1.24 |
| | | ΔQ_2 | 2.59 | | |
| 3.0 | 10.0 | ΔQ_1 | 6.81 | 1.05 | 1.08 |
| | | ΔQ_2 | 5.76 | | |
| 5.0 | 10.0 | ΔQ_1 | 6.25 | 2.36 | 2.9 |
| | | ΔQ_2 | 3.89 | | |
| 6.0 | 10.0 | ΔQ_1 | 8.15 | 1.46 | 1.18 |
| | | ΔQ_2 | 6.69 | | |

* Groundwater discharge measured by dye-injection method in upper section of swash zone.

near maximum backwash volume. It must be concluded that in cases where there is near equality of swash and backwash discharges on the lower foreshore that there is only a low volume of storage of swash water in the beach deposit. Consequently, on freely permeable sands and gravels where flows typically attain velocities in excess of 100 cm/sec. it is clear that infiltrated swash must be returned rapidly to the beach face. In turn this implies considerable escape velocities under the backwash flow sheet. This process may result in high level of bed "fluidisation" and thus greatly enhance the level of sediment entrainment. Maximum development of these lifting forces would occur on well sorted gravels since these deposits are the most permeable, and at locations where the water table sloped steeply seaward. The latter condition is most likely to occur during falling tide when the level of the groundwater table lags behind the retreat of mean water level on the shore.

In order to further clarify discharge conditions in the swash zone net discharge at various points across the shore has been plotted in Figure 34. The most striking feature of the diagram is the area of net swash discharge near the limit of the swash. Net water volume in this area may be up to twice as large as that occurring at any other part of the profile but the scatter of data points also indicates that this is the area of greatest variability of water mass

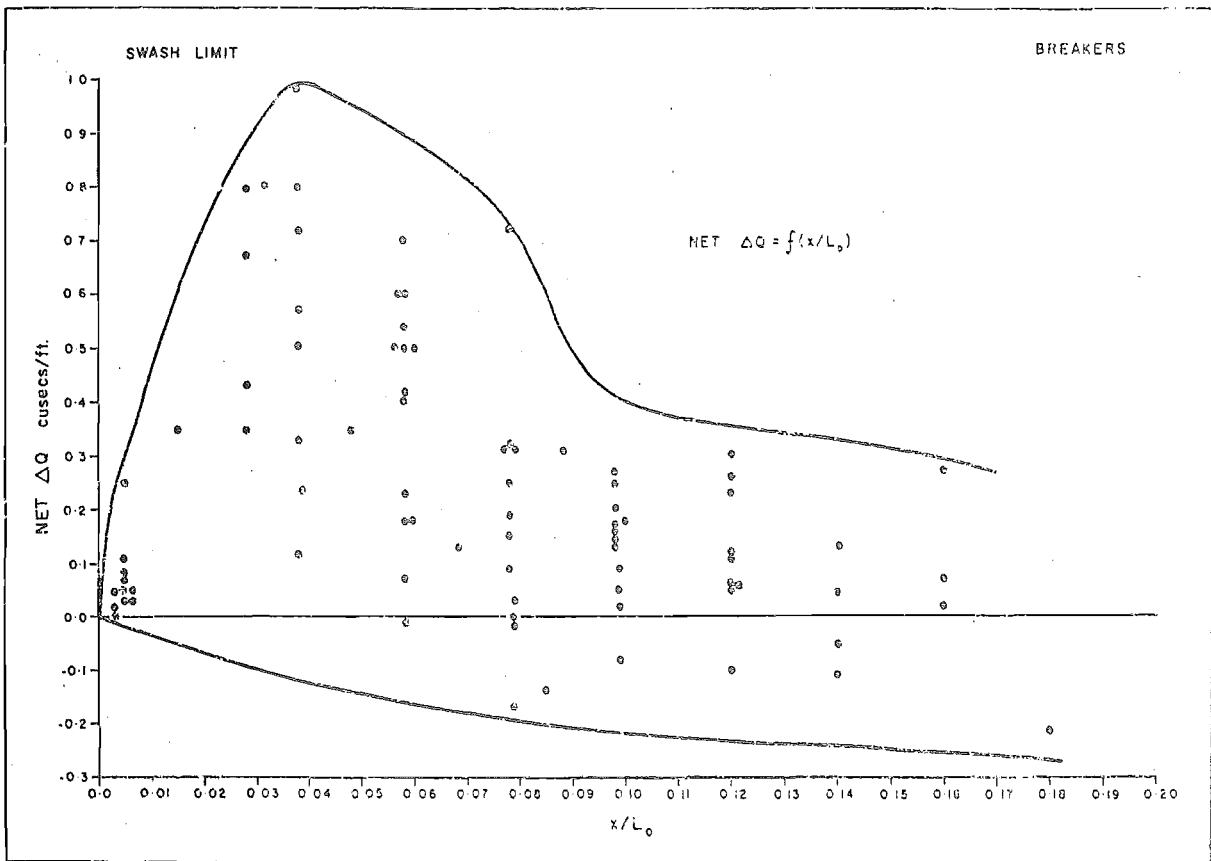


FIGURE 34. Net swash zone discharges.

size. Lower on the foreshore net discharges tend to be more uniform and may even be negative.

On the basis of the distributions of velocity and net discharge across the shore it is useful to separate the swash zone into two flow areas. First, there is an upper swash dominated area where velocities may exceed those at points lower on the shore and where discharge from the groundwater table is at a maximum. Secondly, there is a lower section where flow velocities and discharges are more nearly equal. In this latter zone the differences in sediment transporting capacity will relate more to differences in flow times and water column structure than to overall energy levels of flows.

Asymmetries of Flow at the Bed

The work of Longinov (in Zenkovich, 1967, pp. 40-53 and 129-135) gave a general outline of the asymmetry of water motion in the offshore zone of a Black Sea shingle beach (see Fig. 7), and established the dependence of flow asymmetries on relative water depth. Pressures were reported to increase right up to the breaker and the sign of the asymmetries altered from negative (seaward flow) to positive (landward flow). Similar flow properties have been computed from the dynamometer records thus enabling a partial comparison of flow properties both offshore and onshore of the breaker zone.

A representative group of mean and maximum pressures recorded in both the swash and backwash are listed in Table 7. It can be seen that mean horizontal bottom pressures (\bar{P}) in the swash varied from 11.0 to 22.0 gr/cm² for wave heights of from 2.0 to 5.0 feet and for periods ranging from 8.3 to 10.0 seconds. These values are approximately one order of magnitude greater than those recorded by Longinov in an off-shore environment. From this it may be tentatively concluded that absolute pressures on the beach profile increase landward as well as immediately seaward of the breaker zone. The highest mean pressures for the swash occurred at the base of the breaker while those of the backwash occurred some distance landward of this point. Maximum swash pressures followed the same areal trend as mean pressures and ranged from 18.7 to 36.5 gr/cm². Maximum pressures ranged from 8.2 to 31.0 gr/cm² in the backwash and their distribution across the shore reflects the process of gravitational acceleration in a steady rise toward the breaker. The observed decline in backwash pressures near the breaker probably reflects the deceleration resulting from oncoming swash water.

However, the directions of motions of sediment grains in these flows do not depend solely on the magnitudes of the various impulse forces but also upon the action times of the pressures.

"It is known that material is put into motion when the current attains the necessary initial velocity,

TABLE 7

Mean and Maximum Pressures Recorded
in the Swash Zone

| B R E A K E R | | | S W A S H | | Z O N E | |
|---------------|---------|---------|--------------------|--------------------|----------------------|--------------------|
| H_b | T | x/L_0 | <u>Swash</u> P | Pmax | <u>Backwash</u> P | Pmax |
| (ft.) | (secs.) | | gr/cm ² | gr/cm ² | gr/cm ² | gr/cm ² |
| 2.0 | 8.3 | 0.057 | 15.5 | 20.5 | - | - |
| " | " | 0.085 | 16.0 | 28.0 | 7.5 | 15.5 |
| " | " | 0.11 | 12.0 | 36.5 | 8.5 | 15.0 |
| 3.0 | 10.0 | 0.031 | 16.5 | 24.0 | 5.5 | 8.2 |
| " | " | 0.058 | 14.2 | 20.5 | 10.0 | 15.5 |
| " | " | 0.078 | 12.0 | 22.0 | 10.0 | 20.0 |
| " | " | 0.098 | 12.0 | 23.0 | 8.0 | 18.0 |
| " | " | 0.12 | 11.0 | 19.0 | 9.5 | 18.0 |
| 5.0 | 10.0 | 0.031 | 17.0 | 33.0 | 10.5 | 14.5 |
| " | " | 0.058 | 15.5 | 28.0 | 8.2 | 14.0 |
| " | " | 0.078 | 17.5 | 28.0 | 10.0 | 18.5 |
| " | " | 0.098 | 22.0 | 36.5 | 13.8 | 31.0 |

and ceases moving when the velocity declines to approximately the same level. Therefore particles of ever increasing size may be successively displaced in the oscillatory motion of bottom waters towards and away from the shore as the velocity increases, and they will come to rest in order of decreasing size as it decreases. This will be followed by the same motion in the opposite direction. The path of a particle of small size suspended in the water column will be approximately the same as the general transport of the water. In the displacement of particles of large dimensions an increasingly important part is played by the inequality of mean and maximum pressures ..." (Zenkovich, 1967, p. 130).

Though the statement applies to unbroken waves the same is true of the swash zone where onshore and offshore flows of varying velocity and duration succeed each other.

Graphs of several mean asymmetry ratios for three breaker conditions are plotted in Figure 35. The values are presented against relative location in the swash zone, quantities greater than unity indicating net shoreward movement and values below unity indicating net offshore motion in the water column. The coefficient of horizontal asymmetry of flow times (A_t) i.e. the ratio of recorded swash period to backwash period can be seen to vary from 1.24 to 0.76. Longinov obtained A_t values that ranged from 0.33 to 1.16 for unbroken waves seaward of the breakers. The wave trough thus could be up to three times as long as the crest in shallow water. By comparison swash zone flows at Kaikoura were found to be more nearly equal in duration. Of over 400 observations of A_t values less than unity were found to

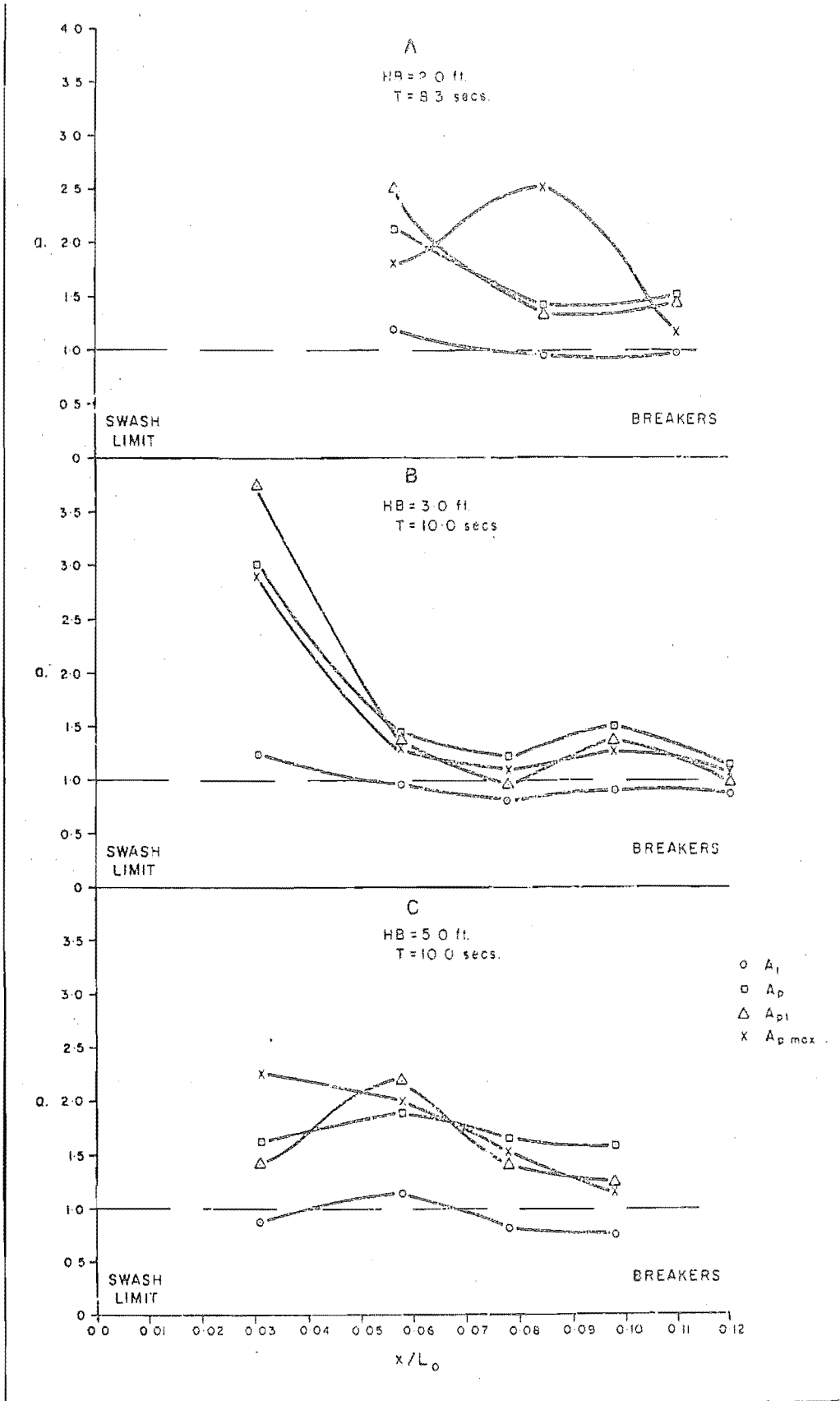


FIGURE 35. Asymmetries of swash-backwash flow for three breaker conditions.

occur on the lower foreshore while net onshore flow durations were confined to the upper foreshore. Figure 36 indicates that net offshore flow was associated generally with a net offshore energy balance and it has already been demonstrated that the latter condition is confined to the lower foreshore area. It can be seen from both diagrams that equal flow times ($A_t = 1.0$) characterise the central portion of the swash zone and that this condition tends to be associated with low net energy conditions. It is interesting to note that beach cusp formation was observed at such locations on two occasions during field experiments.

Reverting to Figure 35 it may be noted that the asymmetry coefficients of mean bottom pressure ranged between 1.2 and 3.0 (A_p) with the highest values occurring near the swash limit in all cases. The asymmetry of maximum pressures ($A_{p \text{ max.}}$) exhibited a similar range of from 1.05 to 2.93; the highest value again being obtained near the swash limit and the minimum value near the breaker. In all cases values greater than unity prevailed thus indicating an onshore pressure deficit in all observations. This finding is in agreement with Longinov's data from the offshore zone of the Black Sea beaches though swash zone pressures have been shown to operate at much higher absolute intensities. However, though there is an onshore pressure deficit and higher absolute pressure in the swash than in the backwash, the longer flow duration of the backwash (low A_t) may result in a net offshore energy

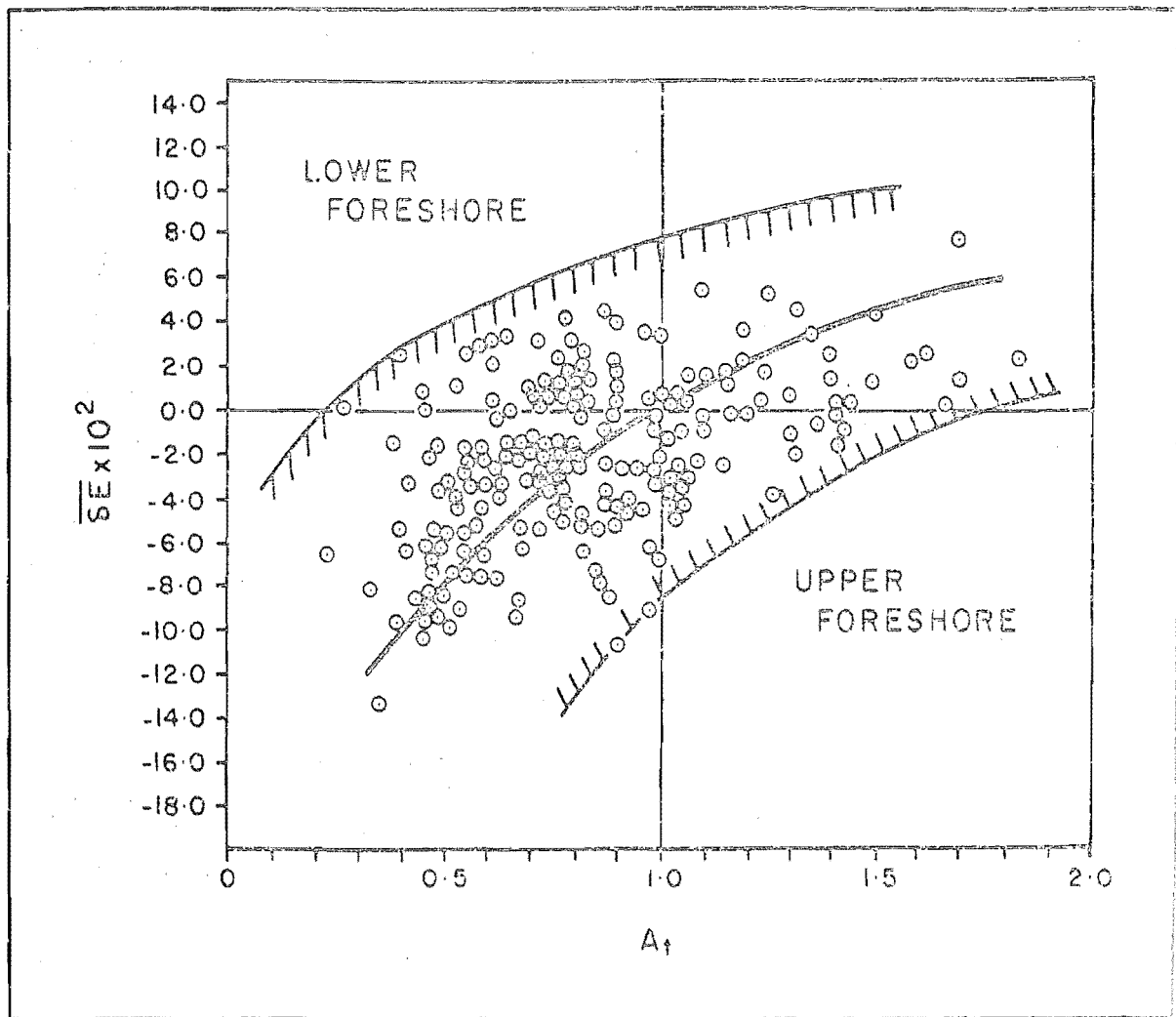


FIGURE 36. Relation between asymmetries of flow times and net mean relative energy level.

balance at lower foreshore stations. Thus, large sediment grains may receive a landward impulse from positions near the breaker while smaller grains are being eroded and transported seaward simultaneously.

A further term obtained by Longinov, the coefficient of the asymmetry of impulse pressure (A_{pt}) has been computed by multiplying the asymmetries of the mean pressures (A_p) by the asymmetries of their times of action (A_t). This coefficient is useful because it is indicative of the direction and rate of movement in the water column passing an observation point. Values of this parameter for the present study beaches can be seen to lie between 1.01 and 3.73, the maxima again falling in the upper part of the swash zone. The range of offshore values reported by Longinov for this measure (0.23 to 2.04) is much lower than for the swash zone.

It is therefore clear that absolute pressures tend to decline onshore as asymmetries diverge markedly from unity with progressive distance from the breaker. Also, the magnitudes of the pressures and the asymmetries increase with increasing breaker height. The only area of decline in asymmetries is near the base of the breaker where there is interference between incoming breakers and outgoing backwashes. Pressure coefficients are thus most notably affected.

In summary it may be said that absolute pressures on

the bed are greater in the swash zone than in the offshore zone. Accordingly the intensities of bed disturbance and sediment entrainment may be expected to be greater. Pressures are highest in the onshore direction near the breaker but net offshore energy flow may occur in this area due to the offsetting effect of longer backwash flow durations. On the other hand, toward the swash limit both absolute pressures and asymmetry coefficients indicate the dominance of swash flow under all conditions.

The Transport of Sediment in Asymmetric Flows

The above analysis has served to demonstrate the complex difficulties involved in predicting the directions and quantities of sediment transport in shore and nearshore environments. It is the purpose of this section to analyse one theoretical approach to this problem, that of Longinov (in Zenkovich, 1967, pp. 129-135), in order to further clarify the application of asymmetrical flows to the bed of the swash zone. Longinov's method involves the conversion of absolute bed pressures to fluid flow velocities and the relation of the latter to the requirements for initiation of motion of a range of grain sizes. Subsequent to this it is possible to derive an estimate of the net direction of particle motion by examination of the frequencies of occurrence of given pressure intervals in both onshore and

offshore flows.

As a working example, the critical velocity requirements for a range of grain sizes have been interpolated on a series of velocity curves from different stations across the shore (see Fig. 37A). The critical erosion velocities of the particle size ranges were derived from Zenkovich (1967, p. 96, Table 7). From this diagram it is clear that both swash and backwash flows have the potential to transport a wide range of sizes. Also, the capacity for transport increases toward the breaker. An additional feature of importance is that the period of slack water between swash and backwash decreases toward the breaker. Hence, the available settling time for sediment grains decreases in this direction.

Consequently, it would appear that sand and granules would be completely mobile as suspended load while cobbles and boulders, if present, would be rolled across the shore in both the onshore and offshore directions. Sand would probably be deposited at the swash limit. However, it is not possible to assess the net direction of transport of a given size grade from such an example since only a very limited amount of information concerning flow asymmetry is available. Longinov sought to overcome this difficulty by considering the distributions of net pressures in records lasting several minutes at each station.

Longinov's Method. As an initial step the total range of recorded pressures in a trace is divided into groups by absolute magnitude. Next the total time for which each selected pressure range was directed onshore or offshore is calculated and expressed as a percentage of the total duration of the trace. Then the percentage onshore and offshore flow durations of a given pressure interval are summed algebraically to obtain the net pressure deficit and multiplied by the mean pressure of the interval. This yields values of net proportional pressures that are expressed in relative magnitudes independent of the absolute duration of the trace. Finally, the summing of the proportional pressure values from the highest pressure groups to the lowest, with allowance for their sign, yields the proportional net pressure for each pressure group. It is argued that this quantity expresses both the direction and the intensity of sediment transport for the sizes corresponding to a given pressure group (Zenkovich, 1967, p. 130).

Table 8 gives an example of the calculations for a station located at the base of the breaker during 5.0' and 10.0 second wave conditions. From the table it can be seen that in order to convert the measurements of pressure fluctuations to terms defining the motion of various sizes, the quantities in the fifth column ($\bar{P} \Delta i$) are totalled from largest to

TABLE 8

Calculations Necessary For Constructing A
Distribution Graph of Proportional Net
Pressure For A Range of Grain Sizes

| P gr/cm ² | <u>i (half secs.)</u> | | <u>i (%)</u> | | Δi (%) | $\bar{P}\Delta i$ | $\int \xi$ |
|-------------------------|-----------------------|----|--------------|-------|-------------------|-------------------|------------|
| | + | - | + | - | | | |
| 0-5 | - | - | - | - | - | - | - |
| 5-10 | 24 | 48 | 10.1 | 20.2 | -10.1 | - 75.75 | + 45.0 |
| 10-15 | 11 | 56 | 4.6 | 23.5 | -18.9 | -330.75 | +120.75 |
| 15-20 | 20 | - | 8.4 | - | + 8.4 | +147.0 | +451.5 |
| 20-25 | 18 | 31 | 7.6 | 13.02 | - 5.42 | -121.9 | +304.5 |
| 25-30 | 15 | - | 6.3 | - | + 6.3 | +173.3 | +426.4 |
| 30-35 | 7 | - | 2.9 | - | + 2.94 | + 95.6 | +253.1 |
| 35-40 | 10 | - | 4.2 | - | + 4.2 | +157.5 | +157.5 |

100% 43.3% 56.7%

105 135

240 = 100%

smallest values taking the sign of each quantity into consideration. The reason for this operation is as follows. A grain that begins moving within a certain range of pressures (e.g. 17.5 to 27.5 gr/cm²) will continue to move at higher pressures. Within the time for which this group of pressures is active the grain will have a nominal impulse of -121.9; i.e. it will move seaward. During the action of pressures of 27.5 to 32.5 gr/cm² the particle will receive a new positive impulse (+173.3) towards the shore. It will also continue to move at pressures up to the maximum for the trace (37.5 to 42.5 gr/cm²) which Table 8 shows corresponds to additional positive impulses of +95.6 and +157.5. Adding these four values a net impulse (\sum) of +304.5 is obtained for particles of the given size. The computation is repeated in a similar fashion for grains of all other sizes. In order to examine the variation in transport capacity similar calculations may be made for a number of points across the shore.

Figures 37B through E show a series of proportional net pressure curves for different positions across the shore under a range of input breaker conditions. The groups of pressures have been plotted at an interval of 5 gr/cm² on the ordinate. Below this scale the sizes of the particles (mm.) that can be moved by the pressure classes have been indicated. The calculations in Table 8 are plotted as

FIGURE 37A. Critical erosion velocities of sediment grains in relation to typical chart velocity traces.

FIGURE 37B-E. Longinov proportional net pressure diagrams calculated for typical swash and backwash pressure traces. Station numbers increase from the swash limit toward the breaker.

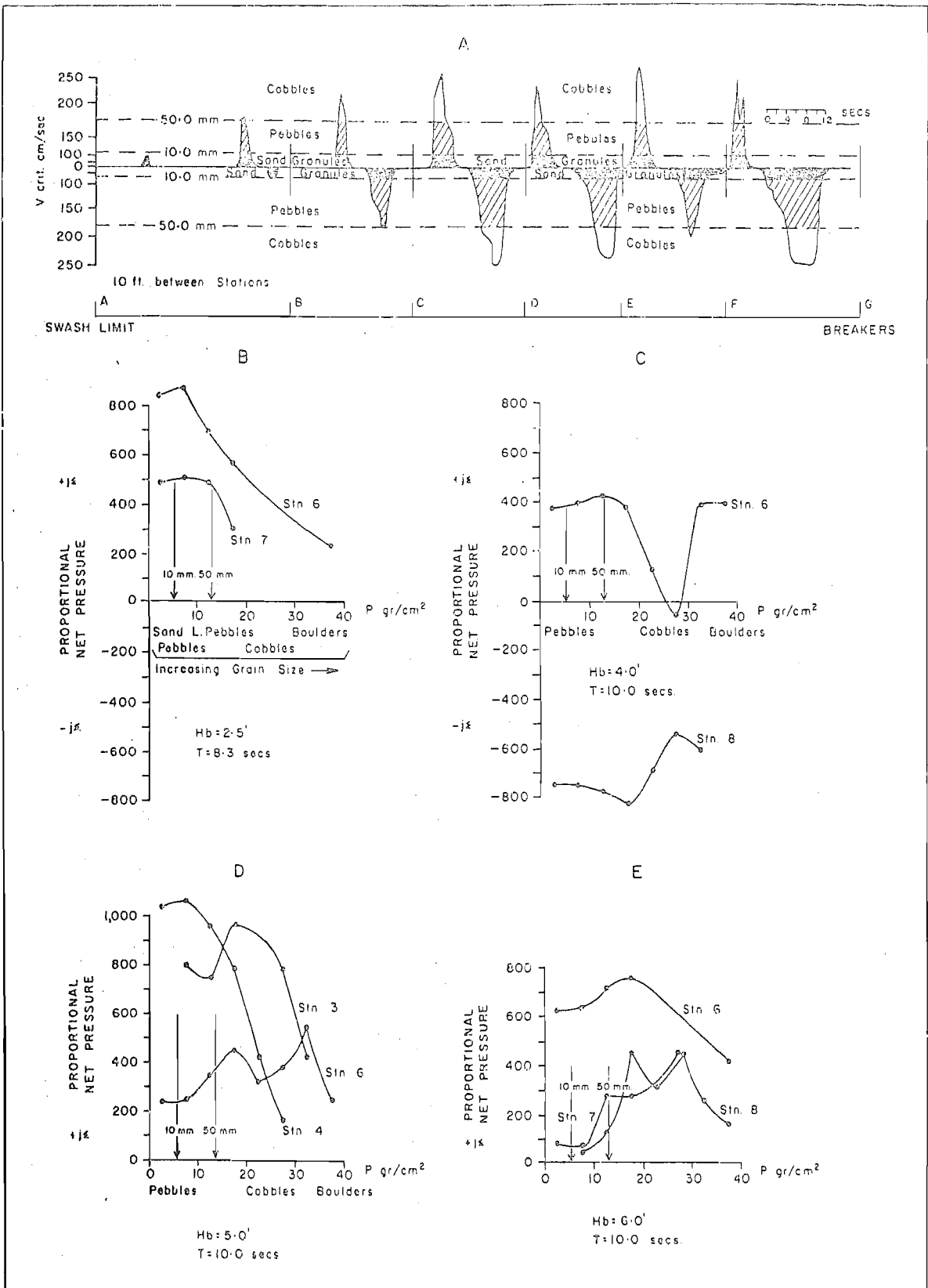


FIGURE 37. The potential for sediment transport in the swash and backwash.

"station 8" in Figure 37E.

Longinov divided the types of proportional net pressure curves observed in deep water into three major classes (A, B, C) depending upon whether the impulses were directed landward (type A - the curve lies above the ordinate); partially landward and partially seaward (type B - the curve lies across the ordinate); or wholly seaward (as in type C - the curve lying wholly below the ordinate in this case). Additional subdivisions of the major categories were made in order to specify the size range for which the maximum impulses were recorded. Hence, in subtype A₀ the pressures are all directed onshore and are at a maximum for the finest grain sizes (see Zenkovich, 1967, Figs. 40 and 41, p. 132).

It can be seen from Figure 37 that curves of the three major types have been obtained from the swash zone. However, there are important differences between the curves shown and those of Longinov.

First, as has been previously demonstrated, absolute pressures in the swash and backwash of this investigation are much higher than in the offshore zone of Longinov. Thus proportional net pressures calculated for the swash zone are generally more than 100 times those of the offshore zone. It can be seen from Figure 37B that even under low wave conditions there is sufficient transport potential to promote movement of all sizes up to cobbles and boulders. Transport is directed onshore and is at a maximum for the smaller grain

sizes. Though onshore transport is indicated for most wave conditions the mode of maximum disturbance passes to increasing grain sizes with increasing breaker height. Only one case of offshore flow of sediment is indicated (see Fig. 37C). These pressure records were derived during high phase wave conditions and indicate two maxima of onshore transport for station 6 located at the mid-shore position. The maxima relate to large pebbles and to boulders and are separated by a region of offshore motion of cobbles. By comparison sediment motion on the lower foreshore near the base of the breaker was entirely seaward, the maximum corresponding to the large pebble sizes. On the other hand, a tendency for a reversal of transport direction is indicated for the cobble sizes. The diagram thus indicates a potential transport situation in which pebbles are deposited on the upper foreshore, eroded from the lower foreshore and transported seaward through the breaker. Simultaneously it would appear that cobble sized stones would be in oscillating equilibrium across the foreshore. Boulders, if present, would receive impulses in the landward direction only. It should be noted that this transport situation is very similar to that proposed by Eagleson, Glenne and Dracup (1963) for high wave conditions (see Fig. 12B) when incipient motion diameter (D_i) is much larger than equilibrium motion diameter (D_e). The authors postulated that such conditions would result in bimodal distributions

of sediment size with spikes occurring at the equilibrium and incipient motion diameters. Pressure fields such as that of station 3, Figure 37D correspond to the opposite case where D_e is greater than D_i and truncation of a unit size distribution results.

A further feature of interest with regard to sorting patterns can be noted from Figures 37D and E. In both cases the proportional net pressure curves for the breaker stations (stations 6 and 8 respectively) are markedly bimodal. It has been shown that this area is the zone of maximum flow pressure so that at any one time it is this area of the bed which may be expected to be characterised by $D_i > D_e$. Also, Bascom (1951) and others have reported bimodal sediment distributions from this area of both sand and shingle beaches.

The analysis has served to demonstrate the general usefulness of Longinov's method as a theoretical tool in the study of shoreline processes. The diagrams indicate readily the directions of net transfer of sediments under shore and nearshore asymmetric flow conditions. In addition the data, which have been derived from natural beaches under a wide range of input wave conditions, serve to verify some of the notions of sediment sorting and transport developed in a more general fashion in laboratory studies.

However, the usefulness of the tool as a practical device for the prediction of natural beach behaviour is limited to a narrow range of wave and sediment conditions.

Thus, if the range of sediment sizes present on the foreshore during the flow fields shown in Figure 37 had been nearly equivalent to the range of pressures recorded then the diagrams would faithfully reflect the directions and rates of sediment transport. However, in all of the cases shown only small pebbles, granules and sand were present. Under such circumstances the finer fractions would be in suspension and sheet flow of bed sediments might be expected. The important quantity thus becomes the rate of transport of a given size fraction since the prevailing energy levels are far in excess of those required for the initiation of grain motion. As was demonstrated previously the most important controls of the rate of sediment transport are the power level of the flow and the efficiency of its application (see equation 38).

Where flow conditions are near the incipient motion velocity the efficiency of transport and the power expended on the sediment grains are minimal and the whole fluid/sediment system may be regarded as being in a transition phase between no motion and established motion of the solid particles. It is consequently very difficult to adapt Longinov's method to a range of sizes occurring at a particular point on the shore unless grain size is large relative to flow pressure.

A further difficulty arising from the method is that no information relating to turbulence of flows is included.

It has already been shown that the turbulent structure of the water column greatly influences the entrainment and transport of sediments. Thus, horizontal pressures along the bed supplemented by vertical velocity fluctuations may be expected to result in more intense sorting of sediments near the breaker than occurs further onshore where the flow lines have smaller vertical components.

It may therefore be concluded that the application of Longinov's method to flow pressure distributions in the swash zone has served on the one hand to add to present knowledge concerning the potential for sediment sorting in the swash zone. The analysis, together with that of flow asymmetry conditions has given a better understanding of the exchange processes involving both fluid and sediment grains up to and through the breakers to the nearshore bottom. Also, field confirmation of the theoretical sorting processes postulated by Eagleson, Glenne and Dracup (1963) has been obtained.¹⁴

On the other hand, the limitations of the method have been outlined. It is clear that for the swash zone of the study beaches at least, flow energies are at least one order of magnitude greater than in the area seaward of the breakers in Longinov's study area. Thus, while the analysis of proportional net pressures indicates the movement of coarse materials onshore, the method will not yield information on

the detailed aspects of subsequent sediment re-sorting, erosion and deposition in the swash zone. This is because at high flow energy levels where continuous disturbance of the bed occurs differentials in the flow rates of particles in the onshore and offshore directions determine the local bed level. Since the rate of sediment transfer by fluid flow depends upon the turbulent structure of the transporting medium it is now appropriate to examine these properties in greater detail.

TURBULENCE IN THE SWASH ZONE

In the previous discussion velocities have been referred to as either means or mean maxima occurring over an interval of time. The results presented therefore apply to time average states rather than to instantaneous flow conditions. The nature of turbulence has, however, been shown to be such that the general movement of fluid has superimposed secondary motions which are characterised by apparently random fluctuations (see equation 11).

While analysis of the magnitude and character of these secondary fluctuations indicates the state of turbulence (and thus yields further information concerning the erosion, transportation and deposition of sediments), it must be acknowledged that there are considerable practical difficulties involved in the measurement of rapid velocity fluctuations in water. Sundborg (1956, p. 149) notes that there are also other difficulties which occur in the interpretation of results since the data must be presented in statistical forms which mask some of the details of the actual physical processes involved in turbulent exchange.

An alternative method of examining fluid turbulence is provided by study of the water column structure in relation

to the geometric character of the flow channel. Amongst the appropriate parameters here are Reynolds Number and Froude Number, which, as has been demonstrated, control the type of flow regime.

From the previous analyses it can be seen that both of these aspects of turbulence are important in the swash zone. The fluctuations in velocity or pressure at a given location have been shown to exert strong controls over sediment motion on the one hand; while on the other, discharge and velocity profile patterns have indicated the existence of distinctly different water mass characteristics in different parts of the swash zone.

For these reasons both of the above complementary approaches to the analysis of turbulence have been employed in this investigation. The presentation and discussion of data relating to velocity fluctuations at discrete points in the swash and backwash will be followed by an examination of the turbulent structures of whole flow movements up and down the bed.

Velocity Fluctuations at a Point

Following Sundborg (1956, pp. 149-150), it appears that if the variable velocity vector at a point in the flow is represented by the three components, u , v , and w , parallel to the co-ordinates, x , y , and z , the appropriate relations

for the instantaneous flow velocity are:-

$$u = \bar{u} + u' ; \quad v = \bar{v} + v' ; \quad w = \bar{w} + w' \quad \dots\dots\dots 50.$$

where: \bar{u} , \bar{v} , and \bar{w} are the average values and u' , v' , and w' , are the superimposed, fluctuating components of the velocity. Similarly, for the varying pressure in a fluid:-

$$p = \bar{p} + p' \quad \dots\dots\dots 51.$$

Since \bar{u} , \bar{v} , \bar{w} , and \bar{p} , are defined as time averages, and \bar{u} (for example) is expressed as:-

$$\bar{u} = \frac{1}{T} \int_{t_0}^{t_0 + T} u(t).dt \quad \dots\dots\dots 52.$$

where $1/T$ represents the frequency of occurrence of the fluctuations, then the arithmetic averages of u' , v' , w' , and p' , sum to zero.

$$\text{i.e.: } \bar{u}' = \bar{v}' = \bar{w}' = \bar{p}' = 0.$$

Hence, the expressions $\sqrt{\bar{u}'^2}$, $\sqrt{\bar{v}'^2}$, and $\sqrt{\bar{w}'^2}$ represent the standard deviations (σ) of the fluctuating velocity components. The ratio $\sqrt{\bar{u}'^2} / \bar{u}$ is therefore a measure of the relative magnitude of the fluctuations in the x-direction.

While there have been many measurements of turbulent fluctuations in air flows (e.g. Chepil and Siddoway (1959) few measurements have been published for water owing to the

difficulties of measurement. Most data are confined to variations in the x-direction thus yielding no information concerning turbulence in the vertical plane.

Amongst the fluid flow studies is that by Kalinske (1943) which examined velocity fluctuations at a number of depths in the Mississippi River. The observed distributions of fluid flow velocity were shown to correspond to the normal error law so that statistical analyses similar to the above could be employed. Hence the standard deviations of the velocity distributions were used to describe the spread of velocity around the mean. The ratio, σ / \bar{V} , termed the relative intensity of turbulence, was adopted as the measure of turbulence level.

Sutton (1955) notes that turbulence in the air occurs at three basic scales of magnitude; large, intermediate and small. Large scale turbulence is defined as that manifested over an interval of one hour, the intermediate as that covering a period of one minute, and the small scale as that covering velocity fluctuations having a period of a fraction of a second.

The fluctuations examined in the swash zone velocity traces of this investigation are those pertaining to the maximum pressure of each flow. Thus, in terms of Sutton's classification the turbulence levels examined fall into the intermediate scale class. Though secondary inflections in

chart traces have been noted, the dynamometer is not a sufficiently sensitive instrument to justify detailed assessment of the magnitudes and characters of these eddies. Therefore, the following analysis will deal with intermediate scales of turbulence produced by variations between flows rather than with smaller scale fluctuations occurring within flows. However, it must be borne in mind that equally important short term (and probably longer term) aspects of turbulent fluctuations have not been treated.

Distributions of Velocity and Pressure in Swash and Backwash Flows

Fluctuations in velocity and pressure recorded with the dynamometer along the x-axis at different positions across the swash zone and occurring under different foreshore and wave conditions have been subjected to statistical analysis in order to assess the nature and levels of turbulence in the flows. This ensured that a suitable range of fluid drag velocity and surface roughness conditions was covered. Also, on one occasion estimates of turbulence were obtained at different heights above the bed in both the swash and backwash.

Since the velocity or pressure fluctuations in turbulent flow should be fully random their distribution about the mean should conform to the normal error law. Hence, cumulative frequency distributions of velocity or pressure plotted on arithmetic probability paper will yield a straight line if

they conform to the normal error function. For this reason several curves of velocity and pressure fluctuations are plotted in this fashion in Figures 38 and 39 respectively.

Because pressure varies as the square of velocity it follows that the frequencies of occurrence of both quantities cannot simultaneously fit the normal error curve. Chepil and Siddoway (1959, p. 415) note that at some distance above the surface in air the velocity distribution rather than that of pressure more nearly yields a straight line plot, and that very close to the bed neither pressure nor velocity may be expected to yield close fits.

In the case of the swash zone it is clear from Figures 38 and 39 that the frequency distributions of velocity are in better agreement with the normal curve than are those of pressure. This finding is consistent with that of Kalinske (1943) who demonstrated a similar situation for fluvial flows near the bed of the Mississippi River, but is contrary to the results obtained by Einstein and El-Samni (1949) for pressure distributions over rough surfaces.

It is interesting to note that the scales of turbulence exhibited by the frequency distributions of velocity are variable with respect to time rather than steady so that over a period of minutes there will be a cyclical rise and fall in the levels of maximum velocity associated with individual flows. Groups of strong flows (high waves) are

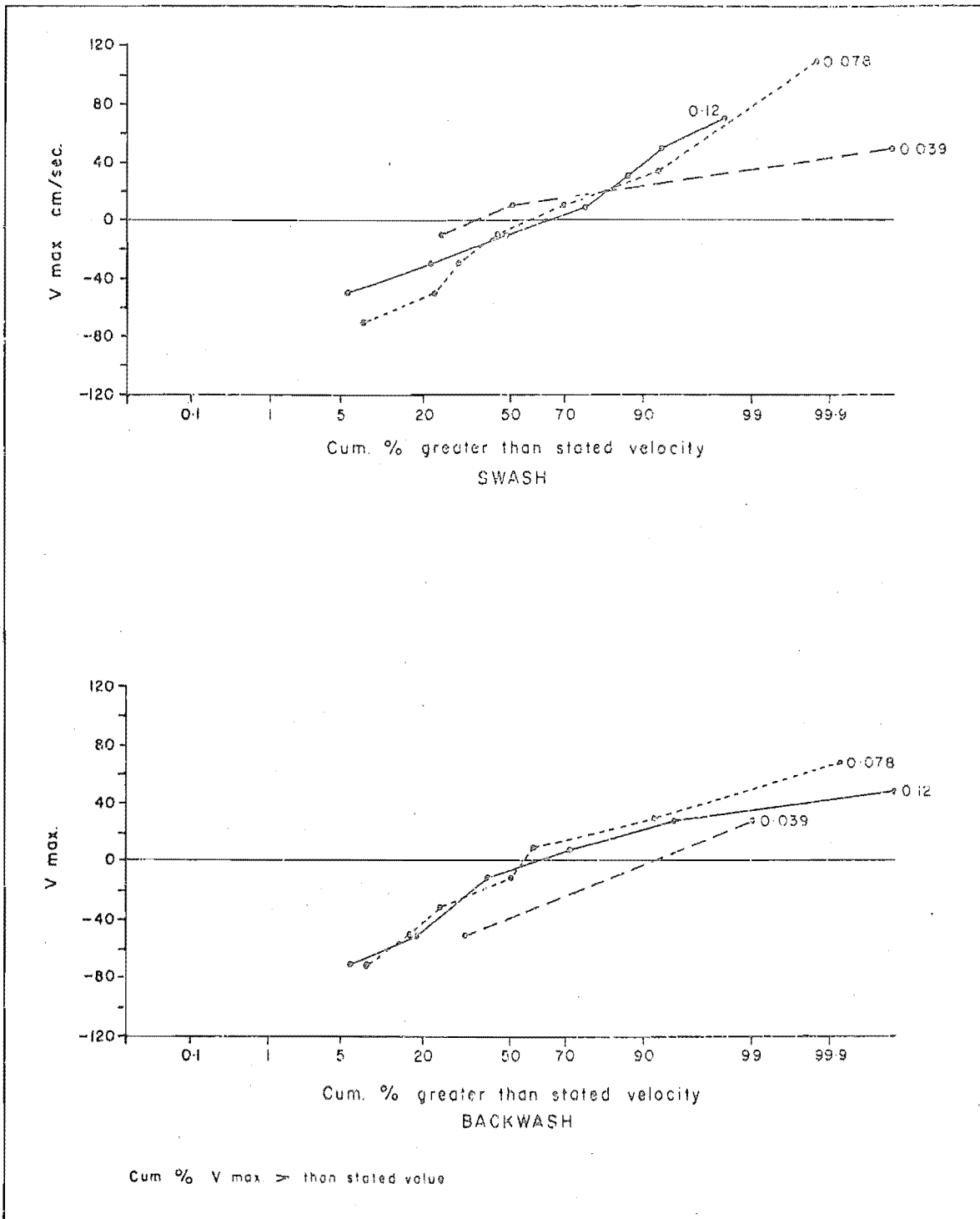


FIGURE 38. Cumulative probability distributions of swash and backwash velocity fluctuations.

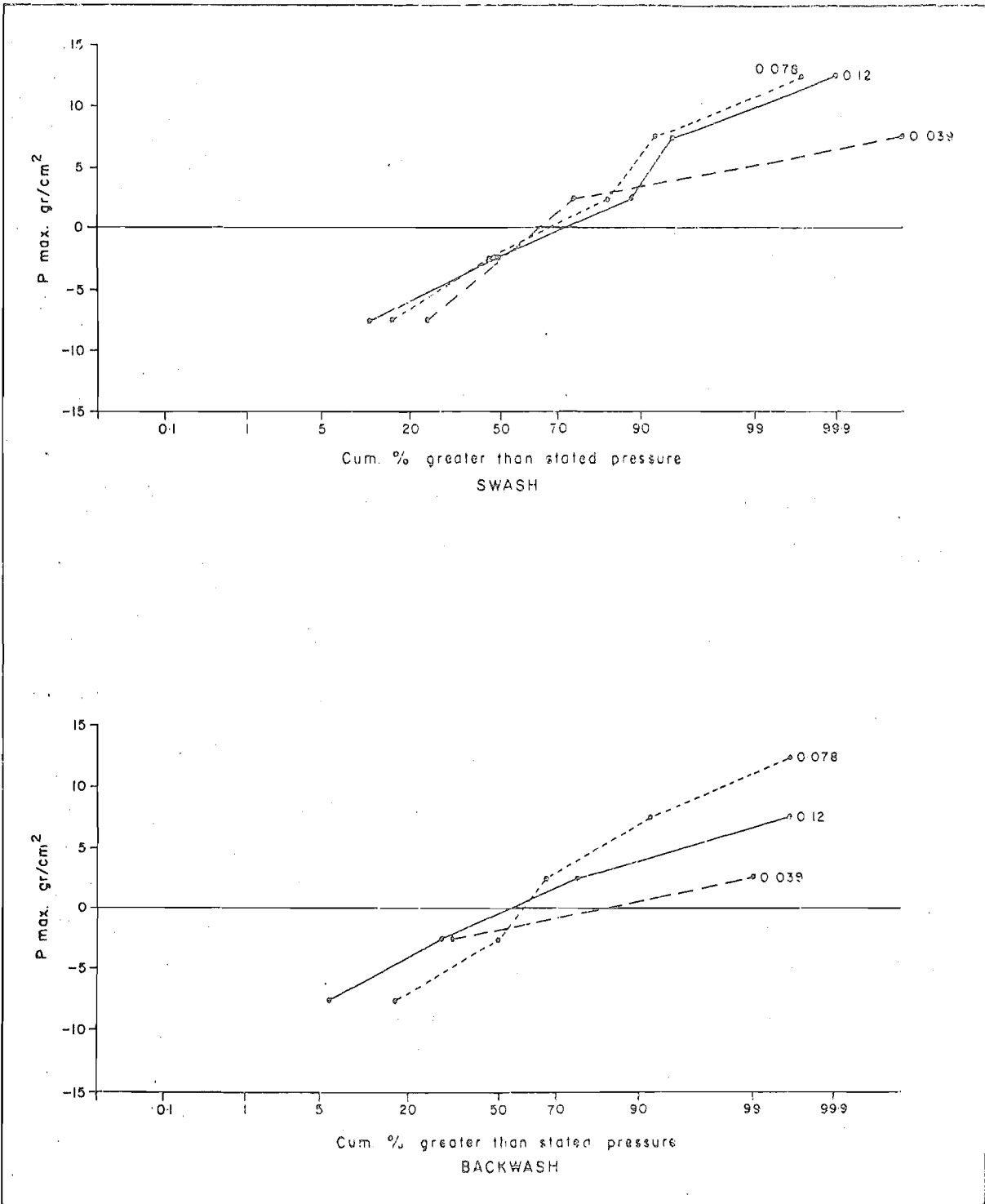


FIGURE 39. Cumulative probability distributions of swash and backwash pressure fluctuations.

followed by groups of weaker flows (lower waves), as can be seen from Figure 28. The curves of Figures 38 and 39 thus apply to variably turbulent flows in which the distributions of velocities and pressures may be seen to be skewed positively toward higher intensities.

Table 9 presents mean velocities, standard deviations and other statistics corresponding to a range of velocity distributions. From these and from Figure 38 it is apparent that the magnitudes of the fluctuations increase across the shore toward the breaker zone in both swash and backwash. Best agreement between the field curves and the normal error function occurs for the mid- and lower foreshore areas.

Also, there are striking differences between velocity fluctuations in the swash and in the backwash. The swash curves yield generally better approximations to the normal curve except for the areas near the landward limit of flow. By comparison, backwash flows, which are gravitational movements down the slope, exhibit more evenly extended ranges of velocity fluctuations. Thus, it is possible that flow turbulence is concentrated in the plane of measurement (parallel to the bed) in the case of the backwash whereas, in the swash, pronounced vertical components can be expected owing to the rolling imparted in wave breaking and to the resultant mixing occurring in the swash surge up the slope.

However, the generally good degree of fit obtained with

TABLE 9

Turbulence Levels of Velocity Fluctuations

| Flow | \bar{V}_{max} cm/sec. | σ cm/sec. | σ/\bar{V}_{Max} - | N - | $\sum t$ secs. | Frequ. N/t c.ps. | \bar{V}_{max}/N cm. | x/L_0 |
|------|----------------------------|---------------------|-----------------------------|--------|-------------------|------------------------|--------------------------|---------|
| sw | 156.0 | 39.0 | 0.25 | 4 | 14.3 | 0.28 | 557.14 | 0.039 |
| sw | 150.0 | 44.3 | 0.29 | 13 | 58.3 | 0.22 | 682.9 | 0.078 |
| sw | 161.0 | 28.0 | 0.17 | 18 | 57.0 | 0.32 | 502.2 | 0.12 |
| bw | 104.0 | 41.0 | 0.39 | 3 | 7.7 | 0.39 | 266.7 | 0.039 |
| bw | 137.0 | 38.0 | 0.28 | 11 | 46.7 | 0.24 | 570.9 | 0.078 |
| bw | 137.0 | 33.0 | 0.24 | 17 | 61.2 | 0.28 | 489.3 | 0.12 |
| sw | 148.0 | 44.0 | 0.29 | 6 | 22.5 | 0.27 | 548.1 | 0.039 |
| sw | 157.0 | 27.6 | 0.17 | 11 | 39.5 | 0.28 | 560.7 | 0.058 |
| sw | 151.0 | 40.0 | 0.26 | 12 | 40.3 | 0.30 | 504.7 | 0.078 |
| bw | 107.0 | 28.8 | 0.27 | 5 | 19.0 | 0.26 | 411.5 | 0.039 |
| bw | 126.0 | 53.0 | 0.42 | 10 | 48.0 | 0.21 | 598.6 | 0.058 |
| bw | 172.0 | 36.5 | 0.21 | 12 | 52.0 | 0.23 | 747.8 | 0.078 |
| sw | 119.0 | 41.0 | 0.34 | 25 | 71.9 | 0.35 | 340.8 | 0.068 |
| bw | 149.0 | 35.0 | 0.23 | 19 | 66.2 | 0.29 | 512.1 | 0.068 |
| bw | 190.0 | 29.0 | 0.15 | 5 | 26.5 | 0.19 | 1000.0 | 0.19 |
| sw | 141.0 | 14.6 | 0.10 | 5 | 18.1 | 0.28 | 504.9 | 0.19 |
| sw | 148.0 | 33.6 | 0.22 | 20 | 75.6 | 0.26 | 570.7 | 0.039 |
| bw | 93.0 | 41.0 | 0.44 | 14 | 38.4 | 0.35 | 255.7 | 0.039 |
| sw | 182.0 | 44.0 | 0.24 | 13 | 42.0 | 0.31 | 587.1 | 0.098 |
| sw | 162.0 | 51.6 | 0.32 | 14 | 46.9 | 0.29 | 558.6 | 0.098 |
| sw | 194.0 | 42.8 | 0.22 | 12 | 35.1 | 0.34 | 570.6 | 0.098 |
| bw | 112.0 | 52.7 | 0.47 | 10 | 44.3 | 0.23 | 486.9 | 0.098 |
| bw | 204.0 | 45.5 | 0.22 | 5 | 26.1 | 0.19 | 1073.7 | 0.098 |

the normal curve model for both swash and backwash suggests the validity of further statistical analysis of the recorded variations in flow velocity and pressure.

Relative Intensity of Turbulence

A. Distribution across the shore. Table 9 and Figure 40A indicate the range of values obtained for relative intensity of turbulence ($\sigma / \bar{v}_{\max.}$) at various points across the shore. Measurements were made parallel to the bed and the dynamometer plates were centered at 15 cm. above bed level. Kalinske (1943, p. 274) concluded from theoretical considerations that the relative intensity of turbulence depends on the Reynolds Number of the flow and on the relative roughness of the bed. Table 9 shows that the variance (σ) of the velocity distributions ranges widely for given mean velocity levels as well as for given locations on the shore.

Figure 40A indicates that, in general, the relative intensity of turbulence associated with the maximum velocity increases onshore toward the swash limit. This trend is paralleled at all positions across the shore by a rise in the level of turbulence with increasing breaker height.

Significantly, there is a close relationship between the onshore increase of the relative intensity of turbulence and the level of variability of swash length discussed previously. Thus, on the upper foreshore where velocities may be greater

FIGURE 40A. Relative intensity of
turbulence at different
points across the shore.

FIGURE 40B. Relative intensity of
turbulence at different
positions above the bed.

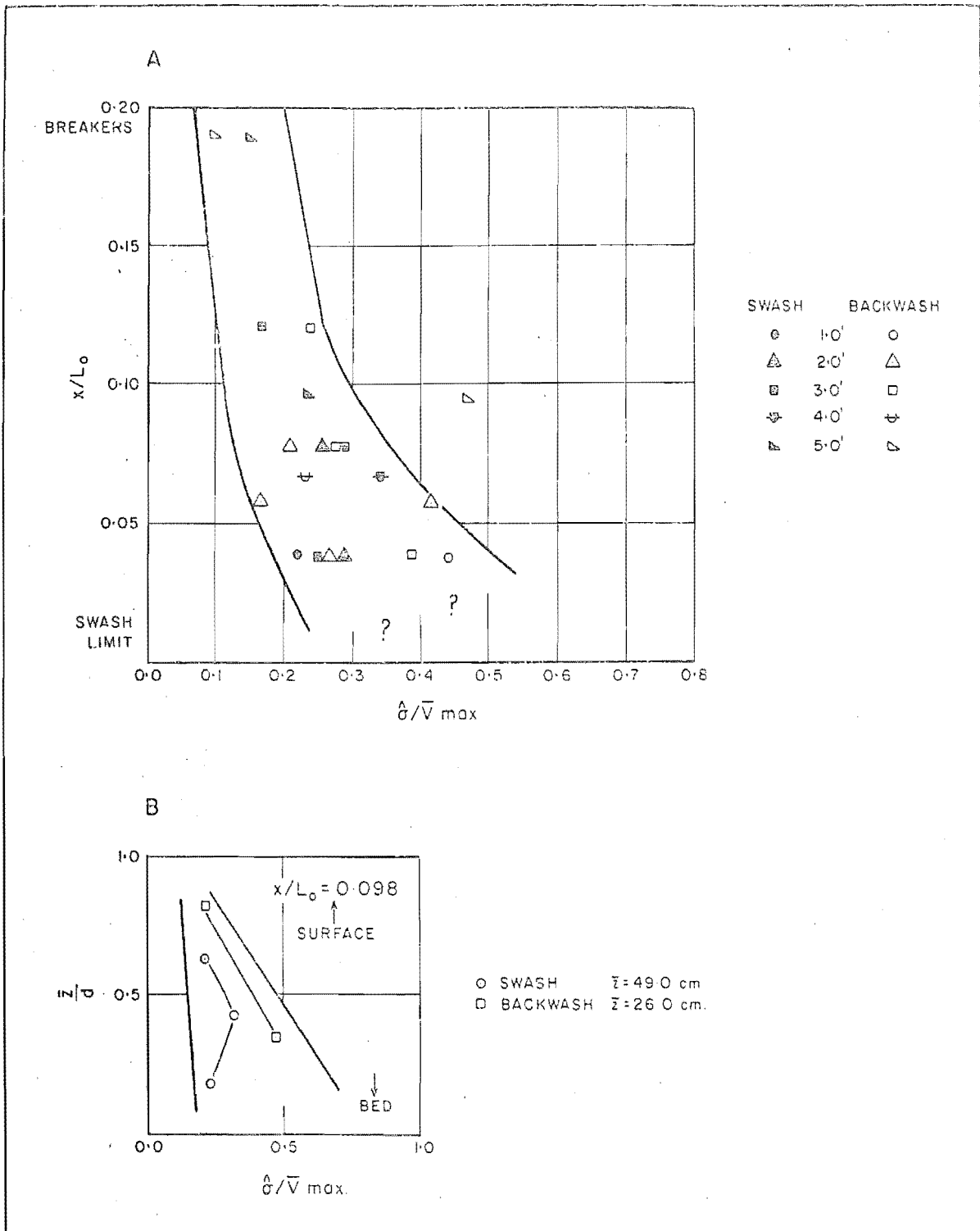


FIGURE 40. Relative intensities of turbulence.

than those occurring at lower levels, but where variation in strength between flows is high, the level of turbulence is high. Therefore, the upper swash zone is an area of locally high, intermediate scale turbulence as well as being an area of very rapid, net swash flow.

In the light of these findings it must now be concluded that the time-mean energy state of the upper portion of the swash zone at the study sites must be regarded as being high. This is contrary to previous studies in which this section of the swash zone is usually envisaged as a low energy area of flow decay. Indeed in terms of any one swash the latter has been shown to be a correct view, but if the time-mean state of flow appropriate to the time scale of the observed morphological effects is considered then the "overlapping" of a number of flows of variable length and strength results in a highly turbulent, high velocity flow regime located very near the upper limit of wave action on the beach face.

Lower on the foreshore where all flows reach a given observation point variability of velocity is lower, means are lower, variances are lower, and hence the relative intensities of turbulence are lower (see Table 9). A further factor contributing to a low value for turbulent intensity on the lower foreshore concerns the directions of water motion in this region. Thus, swash flow near the bed may be directed upward as well as onshore so that a smaller

component of velocity is detected by the dynamometer.

A further feature of interest is that the data shown in Figure 40A (which represent an areal spread across beaches), are roughly comparable to the spread obtained by Kalinske (1943) for a series of vertical sampling stations in the Mississippi River. Similarly, both Kalinske's data and those of this investigation suggest that maximum velocity fluctuations of the order of twice the mean velocity can readily be expected at points near the bed within turbulent flow (see Table 9 and Fig. 38).

From Table 9 it can be seen that the range of turbulent intensities in the swash (0.1 to 0.34) was lower than that in the backwash (0.15 to 0.47), but that the maximum values were derived for backwash flows. These findings indicate first that flow in both the swash and backwash is highly turbulent, and secondly, support the view that there are lower components of vertical motion in the backwash than in the swash.

B. Vertical Distribution of Turbulence. Though there are insufficient data to warrant general conclusions some indications of the vertical turbulent structure may be gained from Figure 40B. It should also be noted that the values again apply solely to turbulent fluctuations occurring in the x-direction. Measurements were made at three stations

above the bed in the swash and at two in the backwash. Mean swash depth during the observations was 49.0 cm. while for the backwash mean depth was 26.0 cm. The dynamometer was located at the mid-swash position ($x/L_0 = 0.098$).

It can be seen from the diagram that relative turbulence levels near the bed were again higher in the backwash than in the swash, with values declining upward from the bed in the backwash. By comparison, the maximum value for the swash occurred at a point approximately equal to half of the flow depth perhaps indicating the thickness of the water layer affected by the maximum turbulence. Above this level turbulent intensities declined toward the surface of the flow as in the backwash.

Turbulence Factor

The maximum impulses occurring in a flow were shown during the earlier discussion of sediment motion to be very important controls on the transportation of grains. However, the measure of turbulent intensity just examined fails to describe the actual magnitude or range of these impulses. Further, Chepil and Siddoway (1959, p. 412) note that no distinct absolute maximum pressure exists for a fully turbulent flow. To overcome the difficulty of estimating the value of this pressure the turbulence factor (equal to $\bar{P} + 3\sigma/\bar{P}$) was introduced. This measure indicates approx-

imately how much the maximum impulse forces of turbulent flow exceed those of uniform flow of equal mean velocity.

The measure is based upon the fact that if pressure fluctuations fit the normal error law then nearly all (99.73%) of the pressure range is contained within the interval $\bar{P} \pm 3\sigma$. Thus, for practical purposes 6σ may be regarded as a measure of the magnitude of pressure or velocity fluctuation.

Table 10 presents a representative range of recorded mean pressures and calculated turbulence factors including those values relating to the pressure distributions shown in Figure 39.

Turbulence factors for swash pressure can be seen to range from 1.29 to 1.89 with the maximum values occurring at the mid-shore stations. The values of the factor decline toward the swash limit and toward the breaker. This occurs largely because pressures become more uniform from flow to flow (i.e. low σ) on the upper foreshore though the velocities are uniformly high. Hence, flows on the upper foreshore have high relative intensities of turbulence but motion tends to be more uniform than elsewhere on the foreshore.

By comparison backwash turbulence factors are at a maximum low on the foreshore and range from 1.3 to 2.5. This result mirrors the distribution of relative intensity of

TABLE 10

Turbulent Variations in Flow Pressure

| Flow | $\bar{P}_{\max.}$ gr/cm ² | σ_{\max} gr/cm ² | 3σ gr/cm ² | TURB.Factor $\bar{P} + 3\sigma/\bar{P}$ | x/L_0 |
|-------|---|---------------------------------------|---------------------------------|--|---------|
| sw | 12.0 | 2.5 | 7.5 | 1.62 | 0.039 |
| sw | 13.5 | 2.0 | 6.0 | 1.44 | 0.058 |
| sw | 12.03 | 2.4 | 7.2 | 1.6 | 0.078 |
| bw | 6.5 | 1.5 | 4.5 | 1.7 | 0.039 |
| bw | 8.0 | 3.0 | 9.0 | 2.13 | 0.058 |
| bw | 15.5 | 2.1 | 6.3 | 1.4 | 0.078 |
| sw | 13.5 | 2.1 | 6.3 | 1.47 | 0.039 |
| sw | 12.0 | 2.5 | 7.5 | 1.63 | 0.078 |
| sw | 13.3 | 2.0 | 6.0 | 1.45 | 0.12 |
| bw | 6.0 | 2.4 | 7.2 | 2.2 | 0.039 |
| bw | 9.5 | 2.1 | 6.3 | 1.7 | 0.078 |
| bw | 9.5 | 2.05 | 6.15 | 1.65 | 0.12 |
| sw | 12.0 | 2.1 | 6.3 | 1.53 | 0.039 |
| bw | 5.5 | 2.1 | 6.3 | 2.15 | 0.039 |
| sw | 7.3 | 2.08 | 6.24 | 1.85 | 0.068 |
| bw | 12.0 | 2.1 | 6.3 | 1.53 | 0.068 |
| sw | 19.5 | 1.9 | 5.7 | 1.29 | 0.14 |
| bw | 10.0 | 1.0 | 3.0 | 1.3 | 0.14 |
| (1)sw | 17.0 | 2.5 | 7.5 | 1.44* | 0.098 |
| (2)sw | 14.2 | 3.0 | 9.0 | 1.63* | 0.098 |
| (3)sw | 19.5 | 2.9 | 8.7 | 1.45* | 0.098 |
| (1)bw | 7.0 | 3.5 | 10.5 | 2.5* | 0.098 |
| (2)bw | 20.5 | 2.6 | 7.8 | 1.38* | 0.098 |

* Vertical profile values. Values read from bed upwards.

turbulence so that the reasons for higher values of the two measures in the backwash are presumed to be the same.

The range of values derived for maximum impulses ($\bar{P} + 3\sigma$) is similar for both swash and backwash to that derived using Longinov's method but are generally a small amount lower than absolute pressures estimated directly from the dynamometer traces.

Turbulence factors for the vertical sample stations appear as the last five entries in Table 10. From these it can be seen that turbulence factors are highest at the bed in the backwash and at mid-flow depth for the swash, a situation which parallels the vertical distribution of the relative intensity of turbulence.

The Scale of Turbulence

A further characteristic of turbulence is the size of the eddies which Kalinske (1943) termed the scale of turbulence. This has been determined by measuring from records of velocity fluctuation the number of velocity cycles in a given time interval. Dividing the velocity, or the distance the fluid has travelled in that time interval, by the number of cycles in that interval gave a length factor which has taken as a relative measure of eddy size.

This parameter has been calculated for the flows discussed above in order to estimate the sizes of water

mass eddies associated with the maximum velocities. Frequencies in cycles per second and eddy dimensions in meters are listed in the seventh and eighth columns of Table 9.

Typically the swash has frequencies of occurrence of maximum velocity ranging from 0.22 to 0.35 c.p.s. The turbulent eddies associated with these flows thus have relative lengths ($\bar{V}_{\max.}/N$) of 3.41 to 6.83 meters (11.2 to 22.36 feet). These values are of interest because they permit an insight into the longitudinal structure of swash flows. Thus, it would appear that the maximum velocities relate to eddies dominating one tenth to one third of the swash length. Table 9 indicates that this eddy length compresses as the swash travels up the beach face. The surge form of the swash wave therefore appears to consist of a fast moving, highly turbulent "hump" located at the forward edge of the flow which is followed by fluid moving more slowly. It thus appears that the swash forms observed in the field are very similar to those described from flume studies by Rouse (1938). Since the maximum velocity is associated with the crest of a surge (see Figure 15), it may be concluded that for the study profiles at least, the crest length may occupy up to one third of the swash length over the mid and lower foreshore areas.

The backwash exhibits a much larger range of frequencies

of \bar{V}_{\max} . (0.19 to 0.39 c.p.s.), and consequently, a larger range of eddy size. Relative eddy lengths ranged from 2.66 to 10.74 meters (8.71 to 35.2 feet) suggesting once again uniform acceleration of the flow body.

Figure 41A shows that eddy length decreases onshore from the breakers in both swash and backwash. Hence, at successively higher positions on the shore the maximum velocity core is active for progressively shorter durations. Some tendency toward flow reformation following breaking is indicated by the fact that maximum swash eddy lengths occur slightly onshore of the break point.

As with the other measures of turbulence, the variation of eddy size with depth is not well known but Figure 41B demonstrates that the frequencies of maximum velocity are approximately constant with depth in the swash. Conversely, frequencies decrease markedly from the bed upward in the backwash. This result is partly due to the great range of backwash flow depth which results in fewer flows being recorded at some elevation above the bed than at positions immediately adjacent to it.

From the above it is clear that these eddies are macroturbulent phenomena occurring in the form of quasi-regular velocity pulsations. According to Mathes (1949) such fluctuations affect bottom velocities more than surface velocities and this would appear to be a valid interpretation

FIGURE 41A. Scale of turbulence
at different positions
across the shore.

FIGURE 41B. Sizes of turbulent
eddies at different
elevations above the
bed.

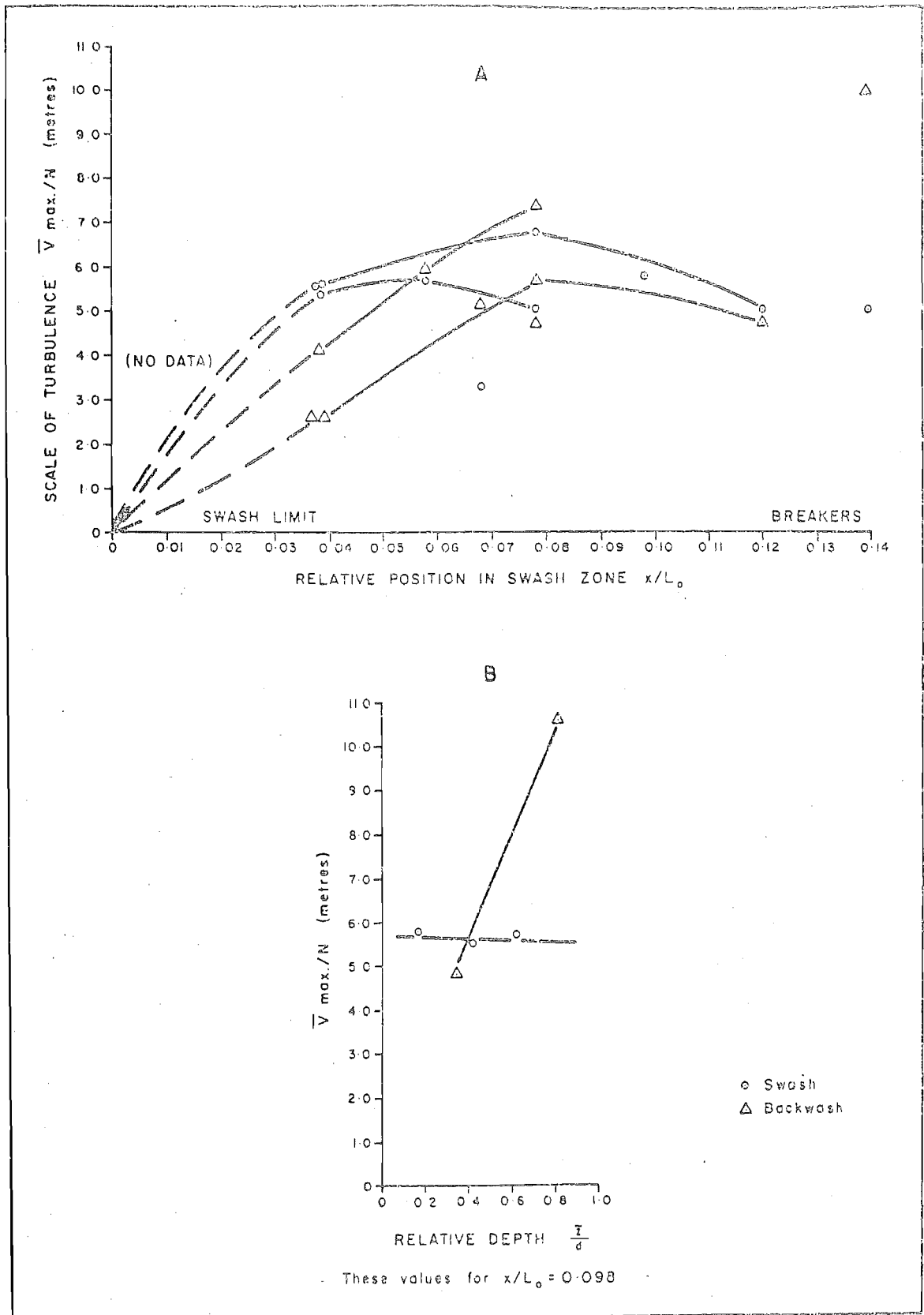


FIGURE 41. Turbulent eddy sizes in the swash and backwash.

of the swash zone flows just described. Sundborg (1956, p. 161) states "it is generally realised that eddies ordinarily originate near the bed (in fluvial flow), move along with the general flow, and undergo continual changes".

"The vortices when first formed may be more or less cylindrical or probably ring-shaped; however, because of the complex forces acting on such a vortex due to the mutual interaction of neighbouring vortices, it is quickly deformed into an extremely complex shape, so that its individuality is practically lost. As individual vortices move about, they may combine with others or break down into smaller ones" (Kalinske, 1943, p. 267).

To these bed-originated eddies, which may be expected to be the principal type occurring in the backwash, must be added rolling vortex motions with horizontal axes imparted to the swash by wave breaking.

Thus, both swash and backwash are comprised of a series of large scale eddies of complex form produced by breaking action and bed roughness. It is probable that these eddies obtain energy from the mean flow and that this is dissipated in turbulent friction and in viscous forces against the bed (Townsend, 1951 - in Sundborg, 1956, p. 161), as in other types of fluid flow. The energy of the eddies is thus transmitted through a whole scale range of eddy sizes to the sediment grains comprising the bed.

The above analysis of turbulence has concentrated on the largest of these eddy scales (that associated with maximum flow), and has demonstrated the zones of highest flow turbulence in the swash and backwash. Also, the regions of

longest duration of application of maximum turbulence have been demonstrated. It is therefore now possible to proceed to a consideration of the interactions between turbulent eddies in the fluid and the sediment grains which comprise the flow boundary.

Variations in Flow Regime

Bed Roughness. From the point of view of morphological changes occurring in the swash zone the relations between turbulent flow regime and bed grain size have been shown to be very important (see equation 14 and Table 3). Grain size conditions bed roughness and hence the nature of flow in the immediate vicinity of the sediment grains. Similarly, flow depth exerts an important control over the flow regime for a given mean current speed. Thus, in a shallow flow at high velocity turbulence is high at all points through the flow. As depth increases the flow becomes tranquil and a new rate of energy dissipation must be established. The latter may result in the formation of standing waves and/or hydraulic jumps which in turn may result in considerable alterations to bed morphology.

It was noted earlier that there is some critical friction velocity at which the bed alters from a hydraulically smooth state to a hydraulically rough one. Also, it was demonstrated that in terms of critical erosion velocities necessary for

sediment transport the limiting friction velocity corresponds to a grain size of 0.18 to 0.20 mm. For grain sizes larger than this the bed is effectively rough and for smaller sediment diameters it is smooth, though there is a diffuse region of transition in flow state.

In order to clarify swash zone sediment transportation in relation to the morphological activities of other types of flow several combinations of mean nominal diameter and mean maximum flow velocity have been plotted in Figure 42. The diagram was derived from Sundborg (1956, p. 177, Fig. 13) and the various types of flow - rough, transitional and smooth - are also indicated. For purposes of comparison the critical erosion velocities for aeolian erosion were included by Sundborg and the curves apply to uniform materials of constant density ($\rho_s = 2.65 \text{ gr/cm}^3$). Though field data have been plotted on a theoretically derived system it is thought that the procedure is justified in order to demonstrate some general points concerning the nature of the swash/backwash energy/sediment system. Also, the density of the virtually monomineralic greywacke beach deposits is very similar to that for quartz, for which the diagram has been drawn.

The grouping of points from the swash zone serves to emphasise the general dynamic character of the environment. In terms of a grain size-velocity co-ordinate system the sedimentation environment of this investigation may therefore

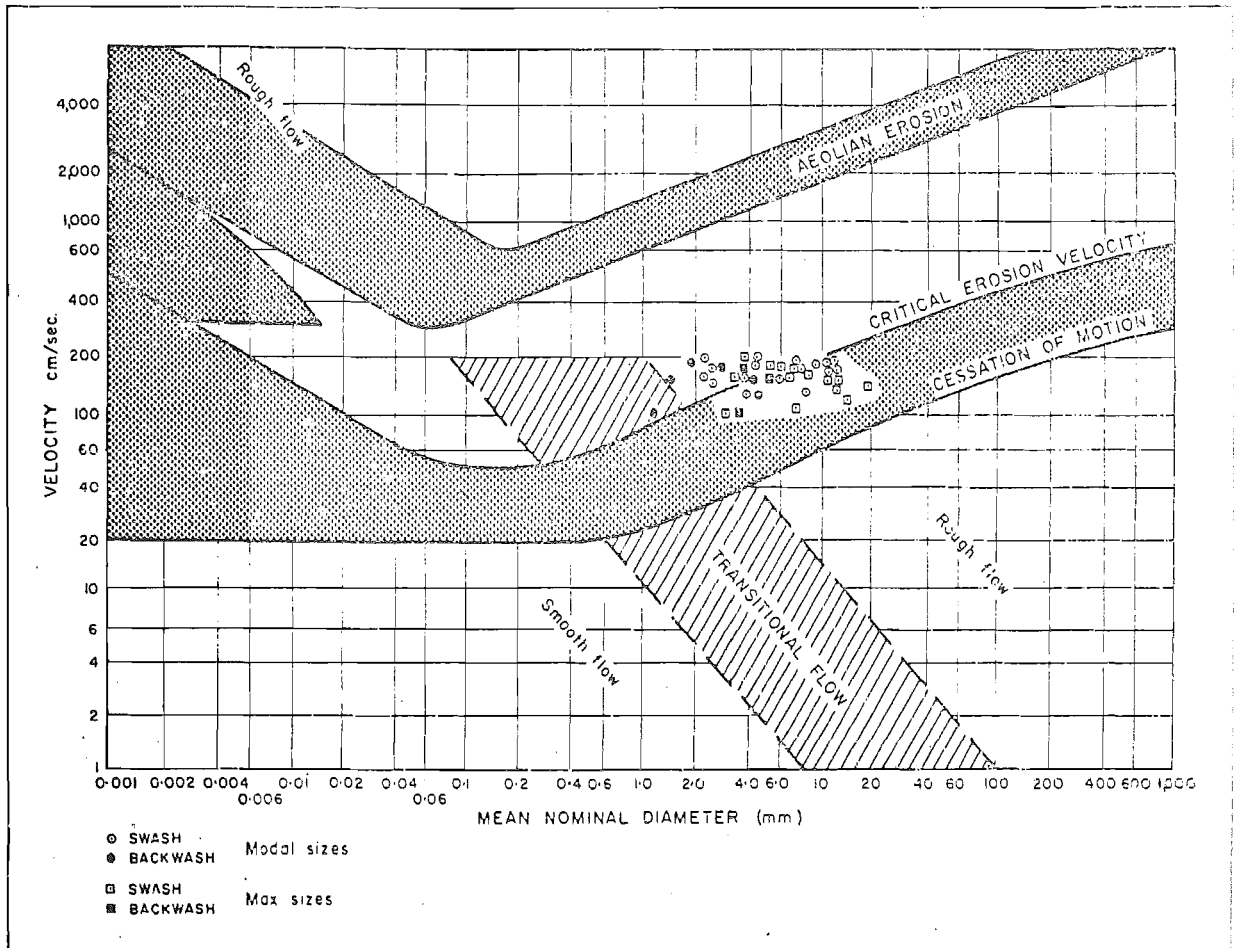


FIGURE 42. Particle sizes and flow speeds of swash zone sediments in relation to flow type. Curves are for uniform materials of density = 2.65 gr/cm³ (Sundborg, 1956, Fig. 13, p. 197).

be described as lying between approximately 100 and 250 cm/sec. on the velocity axis and between 1.0 and 50.0mm. on the grain size co-ordinate.

It can be seen from Figure 42 that this area of the flow/sediment system is characterised by transitional and rough flow in both the swash and the backwash. Though the limits are diffuse, and despite the fact that the mean nominal diameters plotted are derived from grain size distributions containing a wide range of sizes, it can be seen from the graph that many of the grains undergo intermittent motion. Thus, many of the data points lie in the broad transitional range between critical erosion velocity and cessation of motion.

This very generalised plot serves therefore to indicate something of the complexity of motion of sediment grains in the swash and backwash. While at some points in the flow the bed will be hydraulically rough and sediment motion will be clearly established, at others the flow will be transitional and thus the forces on sediment grains may be nearer threshold conditions of transportation or deposition.

Further, the diagram suggests a reason for the complexity of morphologically significant processes occurring on mixed sand-shingle beaches such as stations C and D of this investigation. As has been previously discussed the addition of fines to (for example), a pebble surface may result in

either an effective decrease in the critical erosion velocity for the pebbles, or in a decrease in bed roughness due to infilling between the pebbles, depending on the relative proportions of sand and pebbles in the mixture. Therefore, re-distribution of sand by swash/backwash action on a pebble foreshore can have complex effects on the intensities and locations of zones of erosion and deposition by either increasing or decreasing the susceptibility to grain transport at various points across the bed. Of course, identical effects may be produced by lateral sorting of sediments along the beach.

Thus, the general flow/sediment system of the study beach foreshores is a complex of interlocked, interacting variables amongst which chance relations between grain size composition and current speed can be expected to result in widely differing morphological effects. To some extent a similar complexity underlies other littoral transport systems which have been studied from the standpoint of the potential for sediment motion existing in given flows (for example Cornaglia's theory of sediment sorting on the offshore bed and the many formulations for longshore drift which are based on energy and momentum transfer along wave crests during refraction).

Standing Waves and Hydraulic Jumps. As has been shown previously there are at least two other aspects of turbulence relating to the swash zone which are important to consider.

These are first, the Reynold's number of the flow which indicates the effects of fluid viscosity, and, secondly, the Froude number which relates the effects of gravitational acceleration (or slope) and flow depth to the state of turbulence in the flow. The Froude number is of especial significance in the examination of the morphological effects of swash and backwash flows because it has already been demonstrated that the flows exhibit gravity wave surge characteristics.

The formation of standing waves and/or hydraulic jump waves was shown to occur when the Froude number passes from greater than unity to less than unity (i.e. flow state passes from shooting to tranquil). In the region $1 > F < 2$ standing waves were shown to occur while the hydraulic jump attains a maximum development at $F = 2.77$. The occurrence of these flow features (particularly of the hydraulic jump) in the swash zone may be taken as indications of zones of greatly enhanced erosion potential since they indicate areas of adjustment in the energy grade line of the flow. Thus, at the location of a jump wave some of the kinetic energy of the flow is released violently, the effects of this process appearing as alterations to the surface profiles of both the fluid surface and the level of the sedimentary bed. Gravity waves formed in this way may either move upstream scouring the bed down to a slope more consistent with energy grade requirements (sediment

transport occurring in the form of antidunes), or remain over the site of flow transition if the necessary readjustment of the flow energy level is small.

Grant (1948) drew attention to the possibility of scour resulting from the formation of hydraulic jump waves in the backwash and Kemp (1958; 1960) included a Froude number term in his dimensional analysis of swash flow conditions but the writer is not aware of any previous detailed study of the occurrence of hydraulic jumps and standing waves in the swash and backwash.

Both Reynold's numbers and Froude numbers for mean state swash and backwash flows have been combined in Figure 43. It is apparent from this generalised diagram that swash and backwash occur as both the shooting and tranquil types of flow regime. This results from the fact that both flow velocity and flow depth decline onshore of the breakers. Hence, water motion on the lower foreshore occurs as tranquil flow while on the upper foreshore where turbulence is high throughout the water column the flows occur in the shooting phase. Nowhere is laminar flow indicated for the recorded velocities so that areas of this type of flow are probably confined to the immediate neighbourhood of the swash limit. There are therefore clearly established zones of flow transition which occur in both the swash and backwash.

From the foregoing it can be seen that the formation of

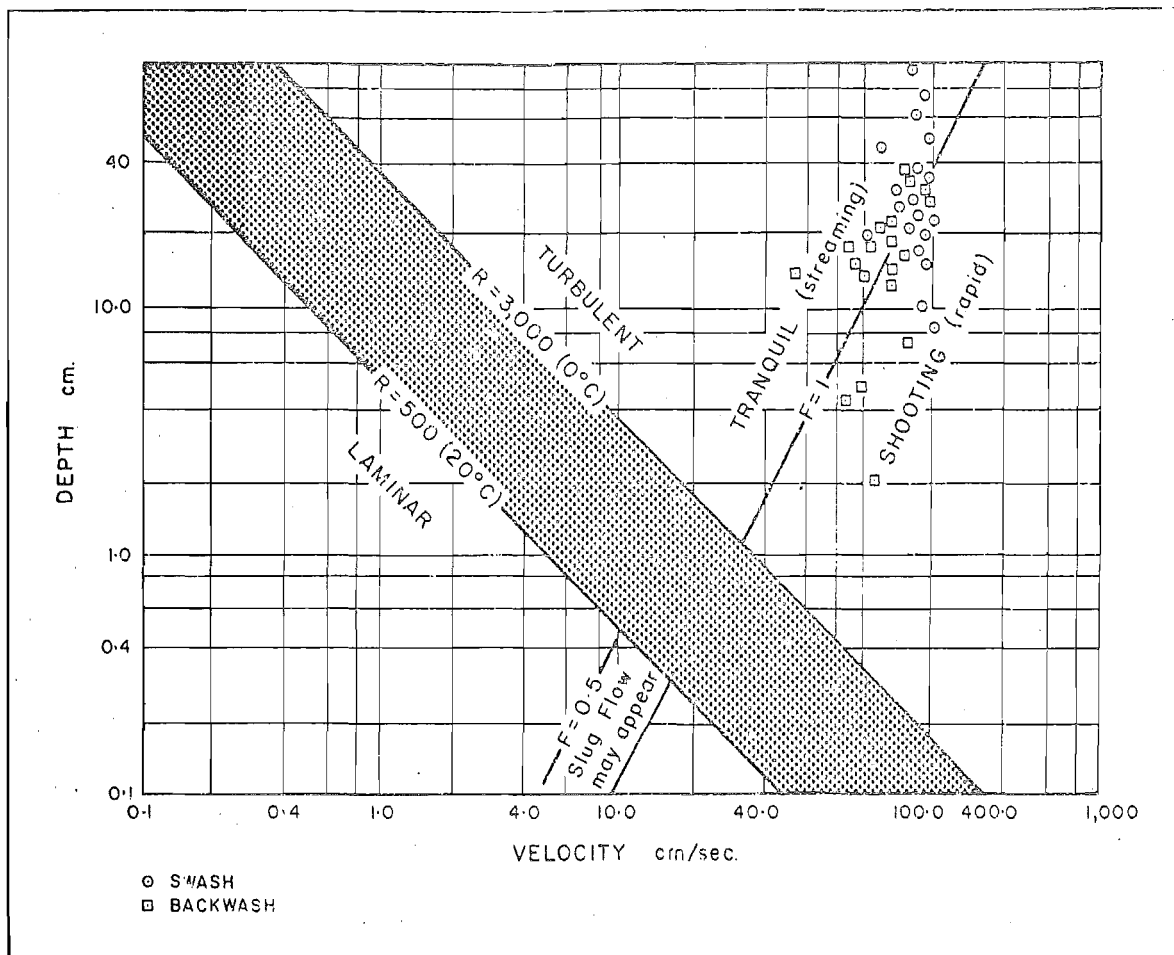


FIGURE 43. Flow regimes in the swash zone plotted as functions of flow depth and velocity.

hydraulic jumps and/or standing waves will ordinarily be confined to the backwash since in these flows Froude number decreases seaward as the water mass accelerates and gains depth down the beach face. Two examples will be presented in order to clarify the nature of these changes.

Figure 44A indicates the depth and velocity profiles for two different sets of backwash flow conditions. For both sets of observations breaker height averaged 5.0' and wave period was 10.0 seconds. However, the data were obtained at different stages of the tide, set 1 being recorded near the peak of the tide when swash is longest and fastest, while set 2 was recorded at mid-rising tide when water levels are rising and groundwater outflow is weak.

Case 1. From the diagram it can be seen that for the first situation water depth increased slowly for the first half of the backwash length and then increased rapidly toward the breaker from a point at the mid-shore position. Conversely, backwash water depth tended to increase in a uniform exponential fashion for the second situation. The locations of the beach water table and the relative strengths of outflow from it undoubtedly contributed to the very different depth profiles for the two flow conditions.

These depth and velocity profiles have been combined in Figure 44B using a flow regime co-ordinate system similar to that of Figure 43. From this plot it is clear that

FIGURE 44A. Two examples of backwash flow depth and velocity profiles for $H_b = 5.0'$; $T = 10.0$ secs.

FIGURE 44B. Progressive changes in the flow regimes of both swash and backwash for the two examples.

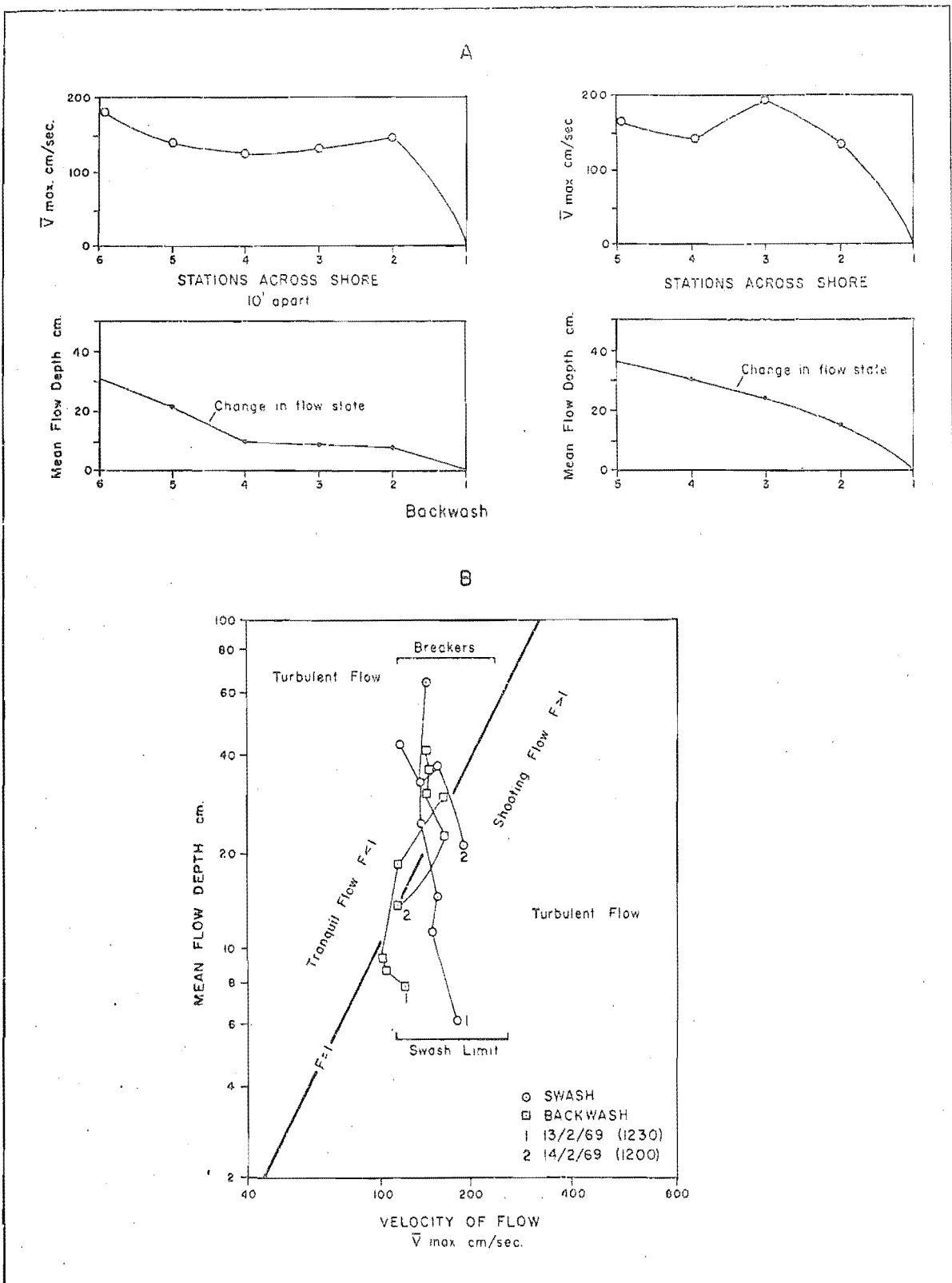


FIGURE 44. Changes in backwash flow regime across the shore.

considerable differences existed in flow regime between the two cases. In case 1 where the swash zone was wide the change in flow state in the backwash was not abrupt. Rather Froude number declined rapidly in the upper section of the backwash but remained near the transition value of unity for much of the flow distance. The maximum value of F for case 1 was 1.64 so that flow around external disturbances on the bed (such as large pebbles lying on the surface) would result in the formation of a standing wave system near the source of the disturbance which would lead to enhanced transport conditions both for the grain promoting the flow distortion and for those finer particles comprising the bed in the immediate vicinity. Thus, case 1 may be taken to indicate a transitional flow regime accompanied by the development of standing waves in the backwash. This increased sediment entrainment by the backwash over a considerable width of the foreshore and resulted in the recording of net bed scour at the upper stations.

Case 2. On the other hand, in case 2 the diagram shows that Froude number actually increased on the upper foreshore. The transition from shooting to tranquil flow then occurred very abruptly and there was no extensive zone of transitional flow regime. There was therefore, only a localised area of potential scour at the mid-shore position since the higher

mean velocities and mean flow depths resulted in dominantly tranquil flow. In such circumstances swash deposition may be expected to exceed backwash erosion so that increases in foreshore elevation may result.

A very important feature common to both the examples is that the flow transition (and therefore the development of gravity wave phenomena), occurs most frequently at the mid-shore position rather than near the base of the breaker as was suggested by Grant (1948).

Since hydraulic jumps and standing waves may form at points of rapid flow deceleration there will be a tendency for their formation where opposing flows are out of phase. For high phase conditions it has already been shown that the backwash attains high flow energy levels and that the water mass tends to override the oncoming swash. Under such circumstances rapid changes in Froude number and flow state would be accompanied by intensive bed scour in the zone of adjustment.

Effects of Varying Breaker Heights on Backwash Scour. Examination of the variations in backwash Froude number across the shore for a range of breaker heights supports the above suggestion (see Figure 45). Though the curves were derived from all four of the study profiles there is clearly an increased probability of occurrence of gravity wave phenomena with increasing breaker height. Hence, for low phase, low breaker

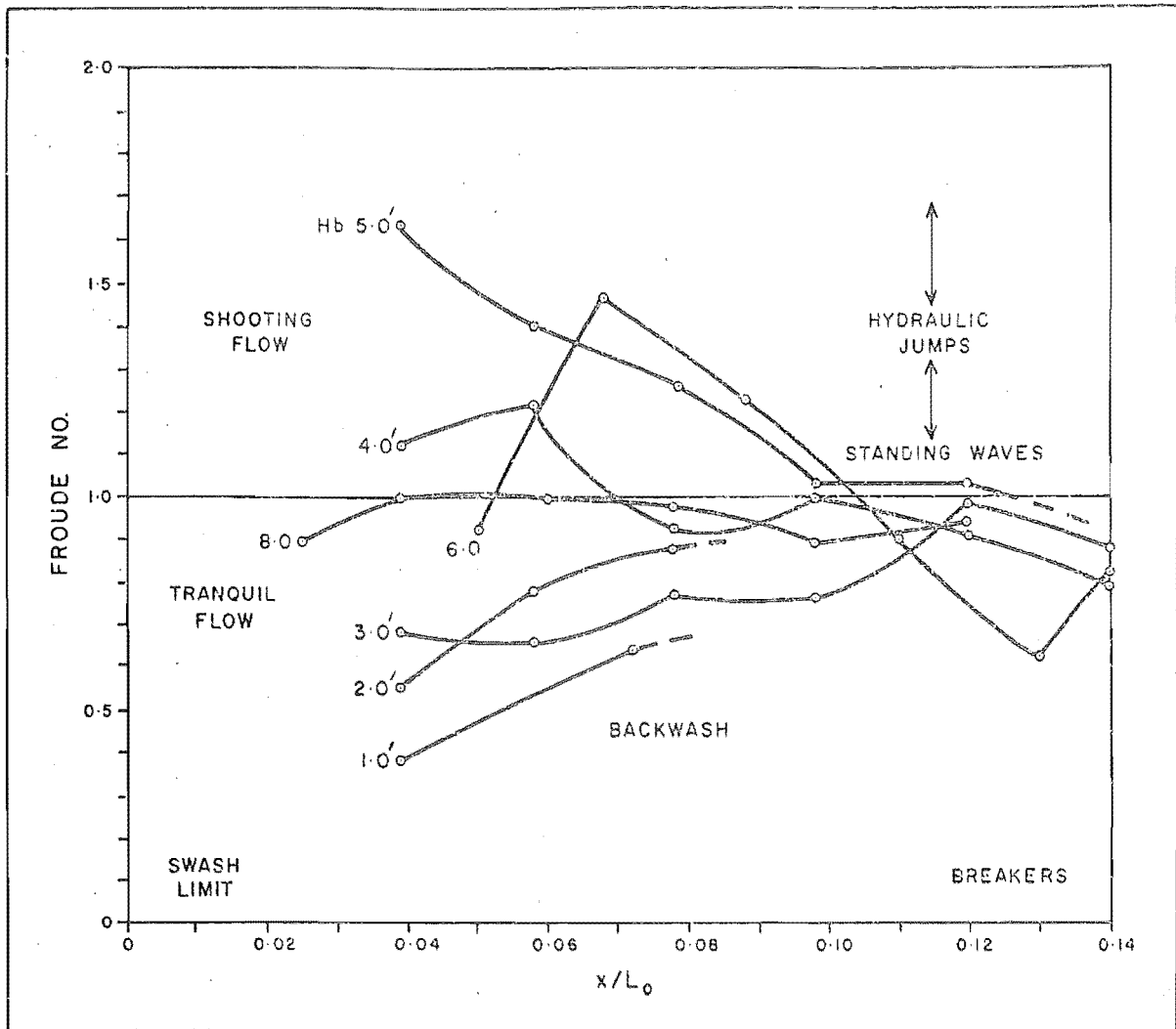


FIGURE 45. Backwash Froude number profiles for varying breaker heights.

height conditions the backwash flow occurs dominantly in the tranquil state. Significantly, for breaker heights in excess of three feet standing waves form in the lower region of the backwash near the breaker. With subsequent increases in breaker height the zone of scour widens landward until for the largest breakers and highest phase conditions the scour zone developed in the backwash extends over more than half of the width of the swash zone.

It is therefore clear that the frequently observed dominance of backwash flow at high phase conditions is due to the action of at least two major processes; first, increased flow velocity leading to the entrainment of coarser and larger quantities of sediment grains, and, secondly, to the intensive scouring action developed locally in association with continual readjustments of the energy grade line in the backwash.

FLOW TURBULENCE, FLOW ENERGY APPLICATION
AND FORESHORE EROSION

While the analysis of flow energies, asymmetries and levels of turbulence has demonstrated many morphologically significant characteristics of swash zone flows the manner in which these influence foreshore erosion and deposition has not been directly considered. It is therefore appropriate at this point to integrate the above aspects of flow into a more unified expression of the manner in which swash and backwash flows interact to produce changes in foreshore elevation.

For the purposes of this discussion three types of foreshore change will be considered; first, erosion occurring over the whole length of the profile; secondly, deposition across the total profile length; and thirdly, a combination profile containing sectors of both erosion and deposition. The first and second conditions are regarded as extremes marking the end-points of a continuous spectrum of possible foreshore changes while the third (which can take many forms), is regarded as being an intermediate form of profile modification. A similar framework was adopted by Strahler (1964) who classified a combination of this type consisting of an upper and lower area of deposition separated by a zone of scour as the equilibrium bed configuration appropriate to tidal cycle changes in the swash zone. Both end-member changes and

combination forms were repeatedly observed during this investigation.

The problem to be examined at this point involves the assessment of the way in which the flow processes described result in these readily observable foreshore response patterns. In particular two aspects must be investigated:-

1. How do the flow forces interact to cause erosion under some circumstances, combination profiles under others, and deposition under still others?
2. Since bed elevation changes of all types occur in response to different levels of input flow energy, what conditions mark the change from one pattern to the next?

The resolution of these questions will be attempted by drawing together the process information of this and previous studies into an integrated model of foreshore morphological changes.

Discussion of Flow Processes

It will be recalled that an original aim of this investigation was to examine the swash and the backwash as independent but closely related flow events. While this approach has demonstrated many points of similarity between the two flow types, the existence of very important differences as well as the occurrence of distinctly different flow regimes

at different positions across the shore has been indicated.

Both swash and backwash are comprised of turbulent eddies of varying scales which result from bed friction and from the processes of wave breaking. The fluid sediment system is complex for both swash and backwash and is characterised by transitional and rough flow. Though absolute pressures and velocities are highest near the breaker in both, the magnitudes of turbulent fluctuations are greatest for the swash near the landward limit of wave action. This is closely linked with the degree of variability in breaker height and hence of swash length.

Also, the upper part of the swash zone is an area of net swash flow under a wide range of breaker conditions. This zone may be characterised by higher mean state velocities than points lower on the foreshore. Further, the development of turbulent fluctuations in the vertical plane appears to be more extensive in the swash than in the backwash.

For stations lower on the foreshore the analysis of water budgets and of distributions of proportional net pressures indicated that energy levels, and hence sediment transporting power, appeared to be more equal. As breaker height and swash phase number rise there is a corresponding rise in the level of backwash intensity since the level of water storage in the beach deposit remains at an approximately constant proportion of swash discharge. The frequency of interference

between swash and backwash increases and macro-turbulent structures are developed in the backwash. Further, there is a parallel rise in the degree of asymmetry of flows which is, in turn, reflected in growing intensities and scales of flow turbulence at all points on the bed.

In previous studies (Lewis, 1931; Strahler, 1964) the erosive activity of the backwash has been explained in terms of increased volume and velocity at high phase conditions. This investigation has shown however, that an important additional process relates to the incidence of standing wave and/or hydraulic jump phenomena under such conditions. These contribute greatly to the erosive potential of the backwash and the width of the zone affected by them increases with increasing breaker height, phase difference and frequency of interference between flows.

Therefore, there are important differences in the type of flow regime occurring in both the swash and backwash at given stations on the foreshore. Thus, equality of flow velocities and durations in the onshore and offshore directions at a given station does not indicate equal transport potential in each direction if the depths of flow are appreciably different. Swash flow at such a station may be in the tranquil phase while backwash occurs as shooting flow. In such a situation the distributions of sediment in the water columns of each flow may be expected to be significantly

different. Clearly, flow depth (and thus Froude number) are measures which must be considered in addition to the more usual inequalities in net water volume and velocity distribution in order to more fully understand the processes of erosion and deposition occurring in the swash zone.

As was previously discussed, the analytic methods of assessing sediment transport from velocity potentials recorded at particular stations on the foreshore are valid for only a small range of conditions. Thus, for the study sites where energy levels are at all times high, and the maximum grain diameter is small in relation to the prevailing maximum velocities of swash and backwash, sediments are transported at high rates. However, the rate of transport of grains depends upon the efficiency with which power is transmitted to the bed by the flow and, in turn, this efficiency level is partially determined by the turbulent structure of the water column. Figure 45 demonstrates wide variations in structure across the shore for both swash and backwash so that the rate of transport of grains may be expected to vary accordingly.

For these reasons only low correlations can be demonstrated between flow pressures and observed changes in foreshore grain size characteristics if methods such as the proportional net pressure approach of Longinov are employed for the swash zone. Similarly, Figure 46 indicates that there are only low correspondences between mean flow energy

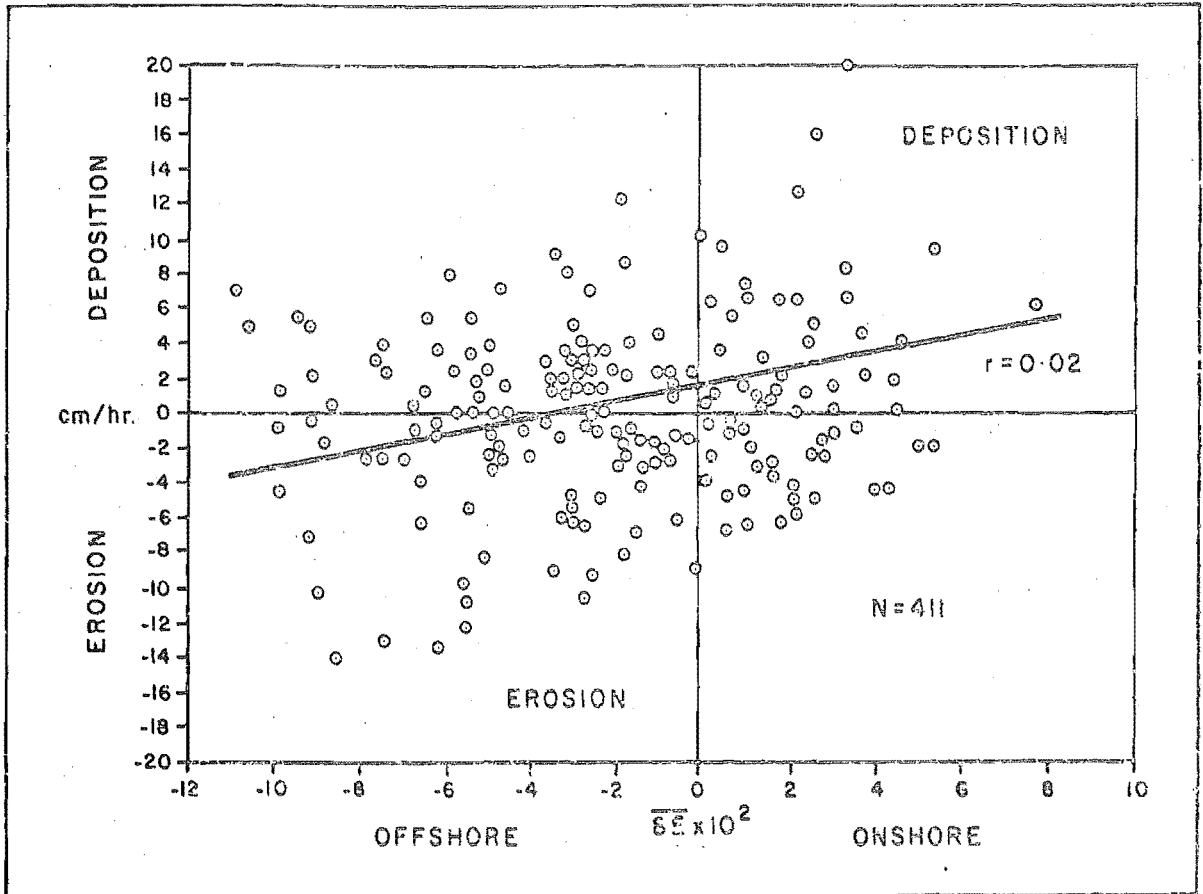


FIGURE 46. Changes in foreshore elevation as a function of net mean relative energy level.

and changes in foreshore elevation irrespective of the location of the observation point on the foreshore. Thus, net deposition was recorded in areas of net offshore energy flux and erosion was recorded for stations located in zones of net onshore energy balance. At least two factors are thought to account for this situation; first, there is undoubtedly some degree of lag involved in that the flow energy measured above the bed at one point will affect the bed at some other point further upstream since the flow is neither steady nor uniform; and secondly, but more importantly, the data spread reflects differences in the turbulent structures associated with the onshore and offshore flows that cannot be assessed by a direct measurement of the energy contained within them.

Relations Between Flow Volumes, Flow Regimes, and Elevation Change

All of the above variations in flow characteristics have been presented diagrammatically in Figure 47 in terms of their observed effects on the three types of profile modification outlined. Patterns of foreshore erosion and deposition were measured for 21 field experiments conducted at the study sites and the following discussion seeks to organise these into characteristic groups according to the types and intensities of processes giving rise to them.

Net Deposition. It is suggested that the swash/backwash conditions most likely to result in net deposition over the whole profile are those shown in Figure 47A. Here the level of percolation in to the beach is such that up to one third of the swash volume may be effectively stored in the beach deposit. Net discharges thus tend to favour the swash and the backwash is correspondingly weak. Since this situation occurs at low phase levels there is little or no interference between flows (see Plate 6) so that each swash moves up a "dry" foreshore and deposits more sediment than can be removed by the backwash. Because there is no interference the long crest of the swash surge is deformed only by the frictional effects of the slope so that the maximum velocity core of the flow is active for maximum durations.

Flow in both the swash and the backwash is dominantly in the tranquil phase and no zone of scour is developed. Since pressures and velocities are relatively low in both the onshore and offshore directions sediment size distributions resulting from these conditions are likely to be of the truncated form where the finer sizes are disturbed but coarser materials are at rest. Some deposition of coarser grains intermittently moved occurs at the swash limit. Circulation through the breaker is not extensively developed at low phase conditions.

Erosion and Deposition. As phase level rises and becomes

FIGURE 47A. Relations between foreshore change and flow processes for surge and low phase flow.

FIGURE 47B. Flow-foreshore relations for transition phase conditions. Note the similarity of the bed profile to Strahler's (1964) "equilibrium", configuration.

FIGURE 47C. Flow-foreshore relations for high-phase flow states, i.e. storms, short period steep waves, and/or strong onshore wind conditions.

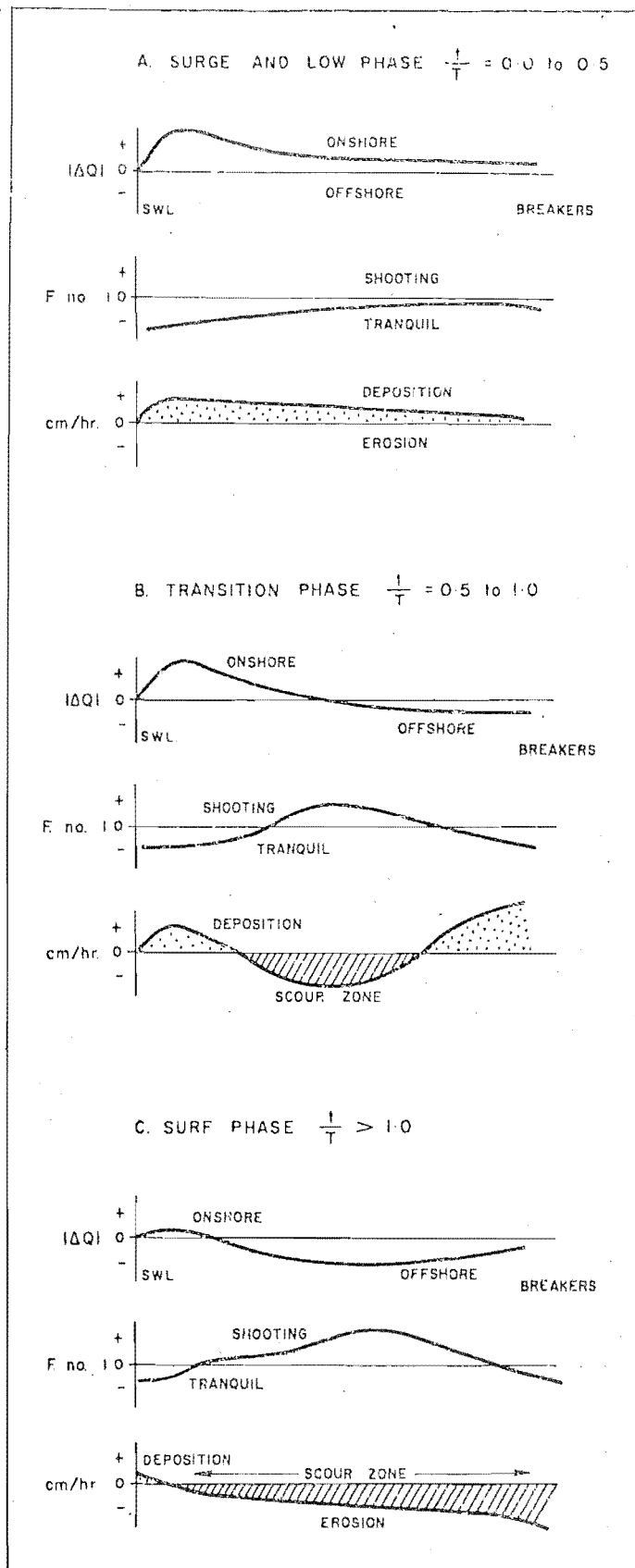


FIGURE 47. Interactions between flow processes and bed morphology.

transitional in character, the flow regime becomes correspondingly transitional in nature (see Fig. 47B). Absolute pressures and velocities increase in both the swash and backwash, as do the various asymmetry coefficients of the flow. Turbulence and hence the capacity for sediment transport increase and the relative proportion of the swash volume stored in the beach deposit by infiltration declines (see Plate 7).

There are also wider variations in breaker height, swash length and swash velocity so that interference between flows is more frequent. It is suggested that at this stage ($t/T = 0.5$ to 1.0), a scour zone is developed at approximately the mid-shore position of the backwash.

Since there is also no large scale circulation through the breaker at this stage deposition of backwash transported sediments will occur at the base of the breaker. This latter condition has been frequently observed at transition phase levels where grains similar in size to those at all other points in the active swash zone have been deposited in lenses up to 20cm. thick at the base of the breaker over periods of one to three hours.

Because net swash flow still prevails near the landward limit of the swash zone the resulting profile consists of two areas of net deposition separated by a scour zone of small width.



PLATE 6. Low phase swash flow at station D. Note the small depth of flow.



PLATE 7. Transition phase conditions at station A. There is some interference between flows and standing waves are extensively developed on the backwash flow surface.

This is the form of Strahler's (1964) suggested equilibrium profile so that the present study confirms this finding as well as specifying the range of flow conditions applicable to its occurrence. However, in this study the scour zone is regarded specifically as being the result of macro-turbulent gravity wave action at the site of a transition in flow regime rather than as the result of generally increased offshore transport capacity in the backwash. Therefore the occurrence of a small scour zone in association with transitional phase and flow conditions is seen here as an incipient condition which achieves wider areal expression and greater magnitudes of intensity at higher phase conditions.

Further, it must be noted that the erosional/depositional combination shown in Figure 47B was not the only complex form observed during the field experiments. Consequently, the transitional class of foreshore modification can be subdivided into two other common patterns of morphological response; a combination of lower foreshore erosion and an upper region of deposition; and, the reverse sequence.

The former condition will be developed if phase level is transitional but the levels of variability of breaker height, swash length and swash velocity are low. Thus, conditions identical to those described above obtain but the scour zone is located at the lower portion of the backwash near the breaker. Net swash deposition occurs as before on the upper

section of the profile.

The reverse situation typified by an upper zone of erosion and a lower section of deposition appears to be confined to steeper initial slopes and/or breaker conditions characterised by a wide range of heights. Hence, swash length is variable and groups of flows pass in and out of phase over a period of minutes so that an area of scour is located higher on the profile and swash action is weakened by interference from backwash flows. Breakers frequently land on the decelerating backwash sheet rather than on the exposed sediment bed. Mean grain size for these transition stage events may coarsen in the zone of scour but will be more variable elsewhere depending upon the ratio of a given size fraction in the bed to the amount of that fraction being added from the flow.

Erosion of the Profile. For the highest phase conditions asymmetries of flow, pressures and intensities of turbulence are at maximum levels. Net discharge favours the backwash (see Figure 47C), and the rate of outflow from the groundwater table is high. As was previously demonstrated this outflow may result in considerable "fluidisation" of the bed and thus enhance sediment entrainment by the backwash. It was also shown that backwash flow overrides the swash and at times attains considerable velocities in the offshore direction

before the completion of swash flow at positions higher on the profile.

Circulation of sediment and fluid through the breaker to the nearshore bottom is continuous so that sediment entrained by the backwash may be lost from the beach face. Breaker height is variable and frequently individual breakers discharge onto the landward moving swash sheet of the previous wave (see Plate 8).

The scour zone is very wide and standing waves and/or hydraulic jumps may form at a number of positions. Swash flow is greatly decelerated and the flow in it appears to consist of a large number of very turbulent eddies capped with foam (see Plate 8). However, as noted by King (1959, p. 280) the action of storm waves is not entirely destructive. At infrequent intervals large swashes coincide with "windows" in the prevailing phase conditions and deliver large amounts of coarse materials to positions high on the foreshore. The final results of high phase events on sediment size distributions will be of the bimodal type with one mode corresponding to the equilibrium motion diameter and another to the incipient motion diameter if (as has been demonstrated), a sufficiently wide range of sizes is present on the foreshore.

The above synthesis of the principal morphological effects of the observed variations in flow characteristics is thought to provide a unified theory of swash/backwash erosive action. As well as providing a clearer understanding of the forces



PLATE 8. High phase flow at station A. Swash is short, slow and highly turbulent. Subsequent breaker is landing before previous swash has reached maximum excursion.

leading to the development of particular profile types, this approach clarifies the sequence of changes resulting from an increase in the overall energy level of the swash zone system as phase level rises with increasing breaker height and/or period.

Additionally the above discussion provides a method of unifying the relations between previous work concerned with flow conditions in the swash zone on the one hand (Kemp, 1958; 1960; Dolan and Ferm, 1966), and on the other, with the explanation of patterns of observed morphological alterations (Palmer, 1834; Cornish, 1898; Lewis, 1931; Strahler, 1964; and Dolan and Ferm, 1967).

In terms of the four study sites of this investigation it may be stated that surge and low transition phase conditions typify the steeper profiles of stations A and B. Higher transition phase conditions are more common at stations C and D where the slopes are lower, grain size is more variable and the swash zone is wider. Of course all four stations are affected in a similar fashion by very high phase conditions resulting from the incidence of either north-easterly or southerly storms.

It will next be demonstrated that the analyses of sediment transport rates and the transport rates of individual size fractions support the general model presented above. Since all of the above processes have been shown

by previous work to vary with the stage of the tide it will then be appropriate to consider the cyclic variations in each type of beach change pattern occurring during the tidal ebb and flow of mean water level.

BED SEDIMENTS

The analysis and explanation of the types of particle size distributions occurring in natural sedimentation environments is a complex field of research and one which has long occupied many investigators. This is because characteristic of particle size distributions identified in the active environments of the present may be applicable to the study of past sedimentation events, the net results of which are evident in the stratigraphic record. Thus, the study of particle properties can yield information concerning velocity, distance, direction and agent of transport as well as on the environments of transport and deposition.

However, the study of aggregates of natural sediment grains is complicated by the fact that individual grains owe some aspects of their form and size to mineralogic composition, others to diagenetic history, some to primary erosive processes, some to weathering both physical and chemical, and yet others to alterations in grain morphometry occurring in process of active transport or deposition. It is therefore extremely difficult to separate influences due primarily to "source area effects" (Folk, 1965), from those produced in a given environment of sedimentation.

More particularly, on beaches where the degree of sediment sorting is high relative to other environments, the problem is even more complex, since grain transport is not always unidirectional, as shown by Kidson and Carr (1959; 1961) and Jolliffe (1964). Kuenen (1964) drew attention to the important distinction between rolling distance and migration distance of bed-load transported particles on beaches. He suggested that the net migration of pebbles was probably less than 0.1% of the distance particles were rolled to and fro on the shore.

While such works as Folk (1962), Mason and Folk (1958), Friedman (1961; 1967), Tanner (1958; 1964; 1966) and many others have demonstrated many of the distinctive characteristics of sand-size distributions derived from dune, beach and river environments comparatively little work has been concerned with mixed coarse/fine and coarse sediments. Further, progress in the study of sediments from the beach environment requires more knowledge concerning the forces governing the selection and winnowing of aggregates of grains by littoral zone flows.

Therefore the purposes of this and the following sections of this report are to first examine characteristics of the sediment size distributions occurring in the swash zone of the study beaches; and secondly, to interpret these properties in the light of detailed data on the flow processes acting at the times of sampling.

Mean Size and Sorting of Swash Zone Sediments

Because of the variable flow regimes and high energy nature of the sediment/fluid flow system of the study beaches the sorting processes acting on particles are complex. For this reason other particle properties such as shape, roundness and imbrication of the grains (Bluck, 1967) as well as mean size, sorting and skewness would appear to be significant. McLean and Kirk (1969, p. 139) note that sorting is likely to be an especially important property of sediment distributions on a mixed sand/shingle beach where average grain diameter can disguise a wide spread of sizes in the sampled material. Sorting has also emerged as a useful parameter in the distinction between environments of sedimentation. Folk (1965, p. 4) for example, compares the "bean spreading" action of waves on sediments to the dumping action of river and other types of flow.

Hence, in recent years much attention has been paid to the significance of the degree of sorting of beach sediments. As a result a general correspondence between grain size and sorting has been noted by numerous investigators (e.g. Inman, 1949; Griffiths, 1951; Folk and Ward, 1957) but this relationship has been interpreted in two different ways. As has been previously discussed Inman (1949) examined sorting in the light of fluid mechanics and concluded that degree of

bottom roughness, settling velocity, and threshold velocity were the primary factors. This view (that sorting can be attributed to hydraulic forces acting in the beach environment), is also implicit in the work of Tanner (1958; 1964; 1966) in that sediment sorting is held to be the result of a "statistical filtering process" acting on sediment grains.

Conversely, Folk and Ward (1957) postulated a "source area effect" to account for the sinusoidal relationship they encountered for size/sorting data. They argued that two population "end members" in the sand and gravel sizes accounted for two strong minima of best sorting whilst poorer sorting in the intermediate sizes resulted from mixing of the two main population constituents present. Blatt (1958 - in Folk, 1962) confirmed this sinusoidal trend in sands and gravels from New Jersey beaches, the modes of best sorting occurring at 1 to 3 ϕ and at -3 ϕ units. Thus, in contrast to Inman, Folk (1962, pp. 237-8) has suggested that the first order control on sorting is mean size and that hydraulic factors such as swash/backwash flow exert only a second order effect.

Further light is shed on this problem by the work of Dahlberg and Griffiths (1967) who performed multivariate analysis on a number of textural characteristics of low rank greywackes. One aim of this study was to assess the relative contributions of source area effects and of hydraulic variables. Measurements were made from thin sections and the

data was subjected to statistical evaluation through the use of linear correlation and factor analytic techniques. Of a total of seven factors derived in this manner three having components relating to source area effect and two to hydraulic processes were found to influence the degree and direction of grain orientation. In contrast to this properties such as grain size and sorting loaded strongly on factors relating to hydraulic variables rather than to source area effects. The authors suggested that an overall dominance of hydraulic variables was indicated by the analysis and concluded that this was a reasonable interpretation of the textural characteristics of offshore sediments which had probably been through at least two cycles of particle morphogenesis.

For modern mixed sand/shingle beach sediments however, a more complex situation is indicated by the work of McLean and Kirk (1969). This study attempted to define characteristic patterns of size, sorting and foreshore slope for three mixed sand/shingle beaches along the east coast, South Island, New Zealand. Data were derived from more than 110 miles of beach including the study sites of the present investigation.

Data pertaining to the size/sorting and size/slope relations were subjected to polynomial regression (a curve fitting procedure), rather than to linear regression. In this way curves of up to order six were computed and the one which was statistically most significant was obtained for

each relationship.

This procedure yielded an order three curve of Folk's (1962) general sinusoidal form for the size/sorting relationship, the zones of best sorting being located at 0.0 to 1.0 ϕ (medium sand), and at -3.0 to -4.0 ϕ (pebbles). However, a major difference between the observed data and Folk's trend was that the area between the "end members" was typified by a wide range of sorting coefficients, rather than by a general decline in values. The authors concluded that this is "the region where hydraulic effects on the grain size distributions are most pronounced" (McLean and Kirk, 1969, p. 148). Since size and sorting exert strong controls over foreshore gradient (through permeability), it was subsequently demonstrated that the size/sorting curve was reflected in a curvilinear relationship between size and slope. The latter result differs markedly from the more usual linear relations presented for size and slope data.

Therefore, for the mixed sand/shingle beaches of this investigation it may be concluded that a source area effect characterises the sediments to the extent that size appears to be a primary control of sorting. However, the action of hydraulic forces is most apparent in sediments which consist of mixtures of the "pure" medium sand and pebble "end member" populations. Because it has been demonstrated that hydraulic processes on mixed sand/shingle beaches are most

intense in the swash zone, it will be apparent that it is this environment in which the intensity and variety of the mixing processes will be greatest.

Thus, the understanding of sorting processes occurring in the swash zone will be greatly aided by comparisons of changes in bed sediment size distributions with rates of flow of different size fractions in the swash and backwash.

Statistical Aspects of Grain Size Distributions

While Krumbein (1938) demonstrated the value of adopting a lognormal (ϕ scale) model for the description of size frequency distributions Tanner (1958; 1964) notes that many distributions of sedimentologic data are non-Gaussian in form. Thus, sediment size distributions commonly plot as zig-zag rather than as straight lines on probability paper. Further, Middleton (1962) in a discussion of methods used in the definition of naturally occurring probability distributions notes that no rational model has ever been proposed for the log-normality of sediments. "It is certain, nevertheless, that the log-normal model will continue to be used in sediment studies as an ideal model with which observed distributions may be compared (e.g. by the use of logarithmic moment measures)" (Middleton, 1962, p. 755)

According to Tanner (1958) this is because the Gaussian, or so-called normal distribution allows ease of statistical

manipulation in comparison with other forms of frequency distribution. How then are departures from the ideal curve to be regarded? Tanner (1958) demonstrates that it is necessary to decide what non-normal plots signify in terms of the physical processes giving rise to the sediment and to find parameters appropriate to the description of such non-normal distributions.

Tanner (1964) demonstrated that it was necessary to examine detailed plots of frequency distributions in order to resolve the above problems and suggested that a useful way of interpreting non-normal or "zig-zag" curves is to regard them as being comprised of mixtures of a number of normally distributed component elements having different means and/or standard deviations (sorting coefficients). Such a procedure is argued to permit analysis of regions of relative sufficiency and deficiency of grain sizes in natural sediment distributions. This is the method adopted in this investigation since it lends itself to comparisons between transported sediments trapped in the water column and bed sediment distributions.

In physical terms sorting is the process whereby particles of different sizes, shapes and specific gravities attempt to reach equilibrium with a given hydrodynamic environment. Pertinent to this, it has already been shown that the mechanics of sediment transport are conducive to a distinct

preference for transport of grains of 0.18 to 0.2 mm. diameter as opposed to particles of all other sizes (Inman, 1949). Further, Eagleson, Glenne and Dracup (1963) proposed two types of curve modification from model studies of sediment sorting by waves, which were dependent on the relations between incipient motion diameter and equilibrium motion diameter. As has been discussed previously, a single truncation of the size distribution resulted if D_i was less than D_e ; and a bimodal curve was produced if the reverse situation obtained.

Tanner (1966) observed inflexions of the former type in natural beach sand size distributions derived from low energy shores. He termed the truncated region a "surf break", which for the data presented, was located at approximately 1.5ϕ . Additionally it was suggested that the break would pass into the gravel sizes at higher flow energy levels. Kirk (1967, p. 80) analysed foreshore sediments from the high energy mixed sand/shingle beaches of the Canterbury Bight and concluded that swell sorting of the finer fractions resulted in marked "surf breaks" in the pebble fraction at approximately -1.5 to -3.0ϕ .

In terms of the present investigation something of the complexity of the processes forming such sediment distributions has already been indicated. Thus, in a high energy environment such as the swash zone considerable potential for the

formation of both unimodal, truncated distributions and bimodal distributions exists since different size fractions may move in contrary directions simultaneously. Furthermore, simple truncation has been shown to characterise only a limited range of grain size/current strength situations. Hence, simultaneous mixing and winnowing of wide ranges of sizes must be expected.

Characteristic Grain Size Frequency Distributions

Because of these factors all of the bed frequency distributions shown in Figure 48 exhibit marked zig-zag characteristics. Both bimodal and unimodal distributions having marked truncations are apparent. Two features of the grain size frequency distributions shown in the diagram must be noted at the outset. First, there is the source area effect discussed previously and secondly, there are effects related to swash and backwash action.

Curve A for example, consists of well sorted pebbles with a prominent fine tail of granules probably derived by deposition of fines in the interstices between pebbles. For curves B, C, and D, mixing of component distributions having different means and standard deviations is indicated. Thus, curve D can be regarded as a mixture of a coarse sand component and one containing a relative sufficiency of

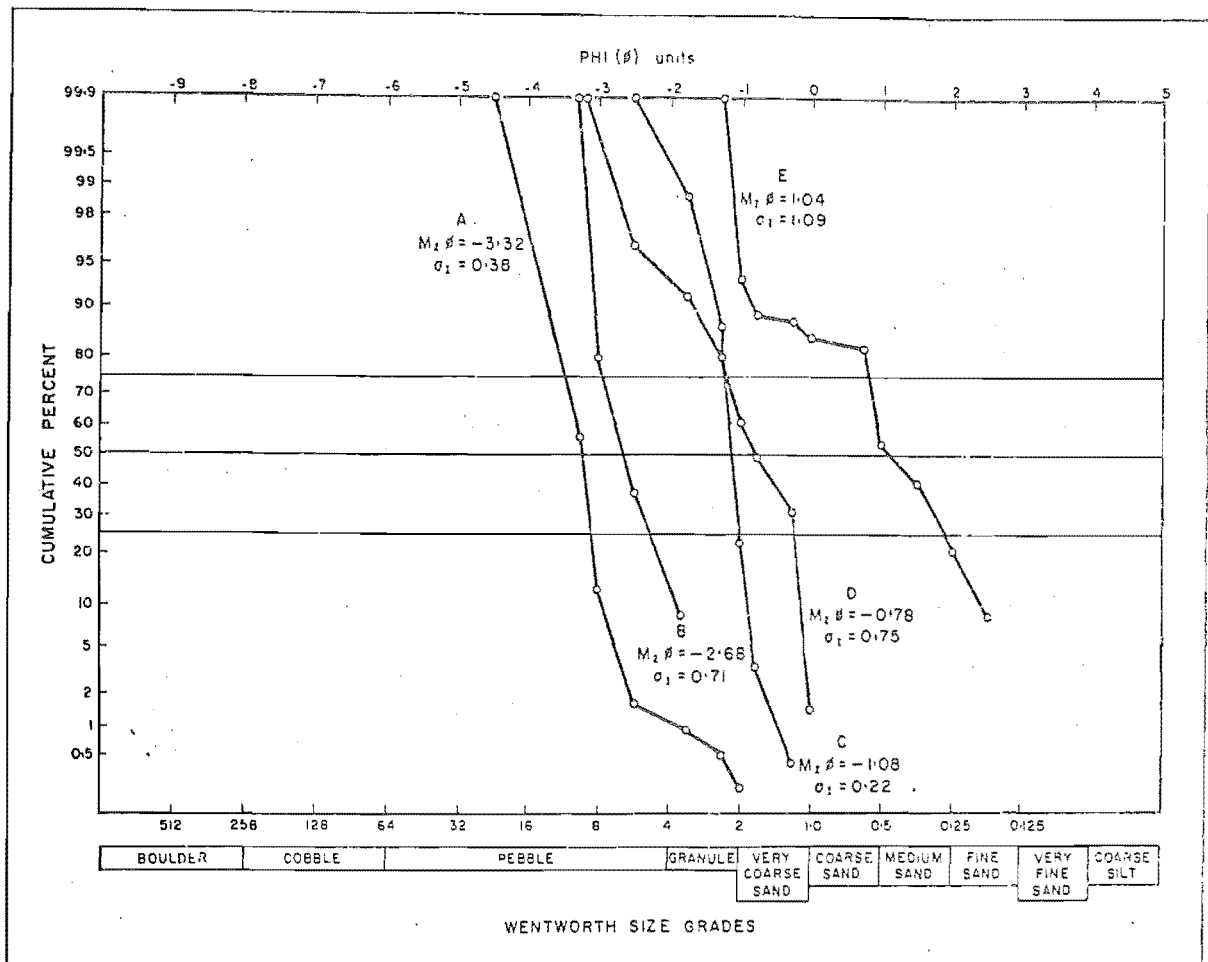


FIGURE 48. Representative bed sediment size-frequency distributions.

pebbles and granules. Curve E, containing the finest range of sizes, is markedly bimodal and consequently exhibits very poor sorting. The distribution can be seen to be rich in very coarse sand and granules and in fine sand, but is deficient in the medium to coarse sand fractions. Consistent with the high energy nature of the swash zone environment is the fact that best sorting is displayed by the coarser sediments. This is because coarse materials are more critically selected by the flow than finer sediments which are fully mobile as suspended load in all directions across and along the shore.

A further feature tending to favour this interpretation is that the curves which exhibit the greatest degrees of mixing and truncation occur in the region 0.5 to -3.0 ϕ . Tanner (1964) observed a similar situation and suggested that this critical size range occupies an intermediate position between "gravel bed load" and "sand bed load". It will next be demonstrated that curves of the above types are associated with distinctly different areas of the swash zone sedimentation system.

Size Frequency Distributions at Different Points Across The Shore

As was indicated during the initial discussion of the four representative profiles mean grain size and sorting vary widely across the shore. For steep, coarse profiles such as stations A and B mean grain size increases toward the breaker and sorting decreases. However, for flatter, mixed sand and shingle profiles such as stations C and D reverse trends have been observed, as have situations in which there was little variation in mean grain size across the foreshore. These trends in grain size properties will now be shown to conceal a wide range of variation in size and composition.

Figure 49 presents frequency distributions of size for a number of positions on the shore at station C. Initial and final curves are presented for the falling limb of a tidal cycle. Breaker height averaged 4.0 feet and the wave period was 10.0 seconds. Mean phase level averaged 0.71 and there was little variation in swash length. The pattern of morphological change over the six hour period was of the transitional type (see Fig. 47B), and consisted of upper and lower areas of deposition separated by a central zone of scour.

From Figure 49 it can be seen that little change in mean grain size or sorting resulted from these transitional flow

FIGURE 49. Initial (solid line) and final (dotted line) bed sediment size distributions from Station C.
Hb = 4.0'; T = 10.0 secs.;
mean swash length = 75';
 $t/T = 0.71$.
Samples were taken on a falling tide. i.e. initial set at high water and final set at next low.

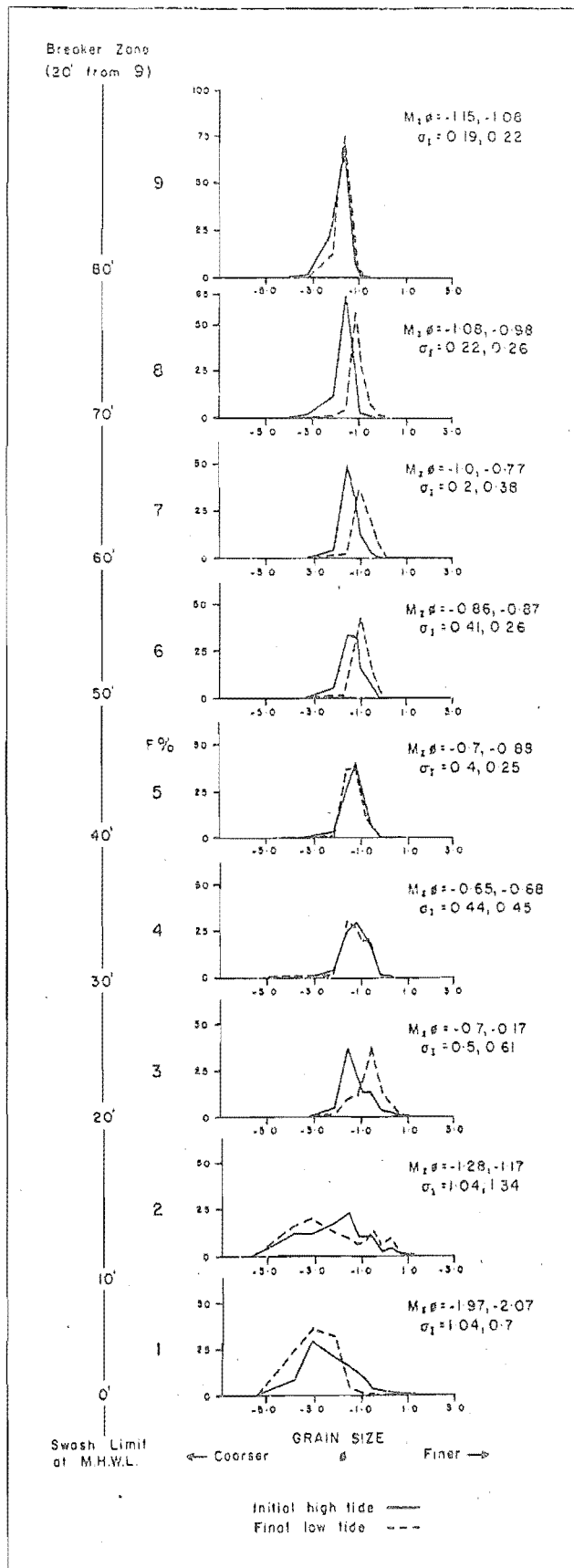


FIGURE 49. Size-frequency distributions from different points across the shore.

conditions apart from in the upper depositional section of the profile. In the latter region the spread of sizes is much larger than at other points on the shore and the resulting frequency distributions may be bimodal or even polymodal. It is this upper zone which undergoes probably the greatest degree of sediment mixing by deposition.

In the central section of the foreshore where scour occurred, the distributions were more regular in form and exhibit truncations in the coarse size fractions. Mixing and winnowing of grains by both swash and backwash is more intensive in this region than at points higher on the shore.

For the lower foreshore, where deposition was recorded, the size frequency curves are also regular in form and, consistent with higher flow energy levels, the mean grain size is coarser. Also, the coarse tails of the distributions are more pronounced. Larger particles eroded from positions higher on the profile were probably deposited in this area, the break in the sediment curves thus reflecting mixing of sizes by deposition as well as truncation due to the entrainment of smaller grains by the flow.

While little alteration is apparent in mean grain size for the near- equilibrium conditions shown in Figure 49, large alterations to sediment size distributions can result from higher phase, erosive flow conditions as is shown in Figure 50. The data are derived from station D, a mixed sand and shingle

profile, for a breaker height of 3.0 feet and a period of 10.0 seconds. Mean phase ratio was 0.8, only slightly higher than that for the previous example, but variations in breaker height and swash length were much greater. Again the initial and final curves relate to half of a tidal cycle (six hours) but in this case to the rising rather than to the falling limb. Net erosion of up to 10.0 cm. was recorded across the whole profile for the six hour period with some initial deposition near the swash limit during the first two hours.

As with the previous example, it can be seen from the diagram that the distributions of grain size were most variable for the upper section of the swash zone, a number of bimodal distributions persisting throughout the tidal rise.

For stations lower on the foreshore an interesting feature was the development of bimodal frequency distributions during process of bed erosion, the modes being located in the sand and pebble sizes.

For the lower foreshore, near the breaker, sorting improved over the half-tidal cycle save for immediately beneath the breaker, the size range of sediments decreasing and the modes becoming more pronounced. For this situation, which is considerably more complex than that shown in Figure 49, the movements of sediments giving rise to the final distributions are more difficult to understand.

FIGURE 50. Initial (solid line) and final (dotted line) bed sediment distributions at Station D. $H_b = 3.0'$; $T = 10.0$ secs.; mean swash length = $90'$; $t/T = 0.8$. This set of samples taken on a rising tide. i.e. A low water and at the next high water level.

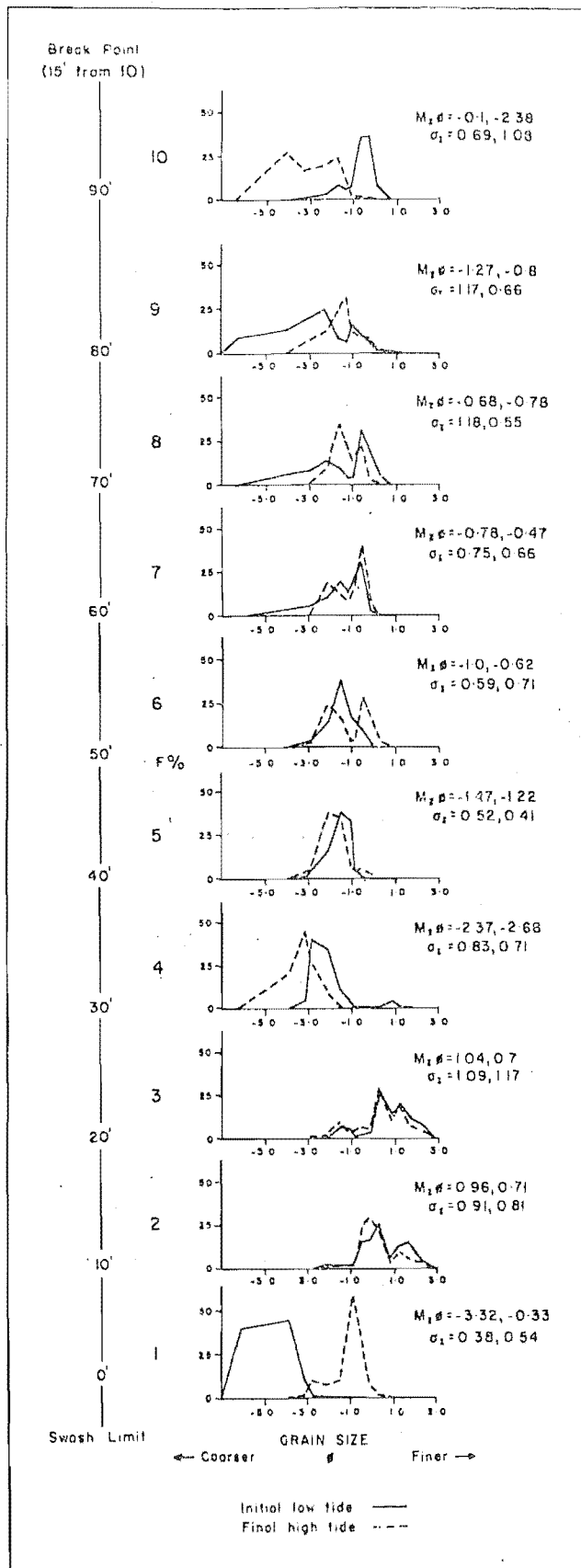


FIGURE 50. Bed sediment size-frequency distributions.

It is clear, however, that considerable mixing and truncation must have occurred. Moreover, the association of profile erosion with frequency curves of a bimodal nature suggests a sorting mechanism similar to that proposed by Eagleson, Glenne and Dracup (1963) for high phase conditions (i.e. $D_i > D_e$).

Certainly, several processes of mixing, truncation and selection of grain size fractions appear to occur in the swash and backwash. In order to clarify the nature of these processes the rates of transport of bed materials in the swash and backwash will first be compared to the levels of erosion and deposition measured at the bed. Sorting processes will then be analysed by considering the net rates and net directions of transport of the different size fractions comprising the flow sediment load at different positions on the shore.

MODE AND RATE OF TRANSPORT OF BED

SEDIMENTS

As has been demonstrated, a stream of water must attain a certain minimum velocity before particles lying on the bed may be moved. Depending upon the speed of flow the sediment motion may be of one of three types, each being associated with different sediment discharge rates and forms of bed disturbance (Menard, 1950). At low speeds the particles will roll or creep along the bed at low rates but at high speeds they will be transported at the velocity of the current in a suspended state and at high rates. For intermediate speeds particles may saltate or move in leaps owing to eddies in the flow and to abrupt changes in velocity (Zenkovich, 1967, p. 94).

Clearly, the mode of transport and the manner of deposition (which is partly controlled by the size and shape of grains), have very important effects on the sorting patterns of bed sediments, so that determination of the mode of grain motion is a necessary prerequisite to understanding sorting processes in the swash zone.

Further, since fluid flow in the swash and backwash is neither steady nor uniform, the rate of discharge of sediments will be variable across the shore. This situation makes

for difficulties in the application of theories of sediment transport such as those reviewed previously because most of the relevant expressions rest on the assumption of an equilibrium concentration of sediment in the flow (i.e. there is no density stratification, and the concentration profile is logarithmic in form). Since these criteria cannot be met in the case of the swash zone where considerable asymmetry of flow and wide variations in flow structure and bed shear have been demonstrated, a less satisfactory approach must be adopted. Hence, the form of the concentration profile and the mode of transportation have been estimated from materials trapped at a number of elevations above the bed. Also, sorting processes will be examined by comparison of estimates of sediment discharge in the onshore and offshore directions with current speed and other flow properties, as well as with patterns of observed bed disturbance.

Vertical Distributions of Transported Sediment

While few observations of the vertical distributions of velocity were obtained, a number of sediment concentration profiles were obtained using the traps previously described. It is important to remember that the seven nozzles of the sampler are each 3.5 cm. in diameter (9.62 cm^2 in face area), and are spaced at 10.0 cm. vertical intervals. The lowest trap is centered 3.5 cm. from the bed and the sampler was

operated for periods of two to five minutes facing onshore and offshore. A total of 131 samples (81 from the swash and 55 from the backwash) were obtained in this manner for a wide range of flow conditions, positions on the shore and elevations above the bed.

Data for size of the trapped particles are expressed in terms of nominal diameters (i.e. the diameter of a sphere having the same volume as the measured grain). This was done in order to eliminate shape effects and to enable comparisons with laboratory investigations of sediment transport.

In relation to the sorting effects on bed sediment distributions described above, it is interesting at this point to examine the range of sizes trapped above the bed in the swash and backwash. An example is presented in Figure 51. The data relate to three stations under transition conditions for which bed sediment curves have been presented (see Fig. 49). The two landward stations of Figure 51 were located in the scour zone while the third set of samples was obtained near the breaker in the zone of accretion.

Both amounts and dispersions of sediment through the flows can be seen to increase toward the breaker, reflecting increasing water depth, velocities and flow durations. Significantly, transport in the backwash was confined to levels near the bed while grains were dispersed to greater

FIGURE 51. Distribution curves of transported sediments at three stations across the shore. The vertical interval between samples at a given station was 7.0 cm. Stations letter from the bed upward and stations numbered seaward from near the swash limit (station 4). $H_b = 4.0'$; $T = 10.0$ secs.; mean swash length = 75'; $t/T = 0.71$. Sediments were trapped during bed sampling shown in Figure 49. Maximum flow depth at $x/L_o = 0.14$ was 60.0 cm.

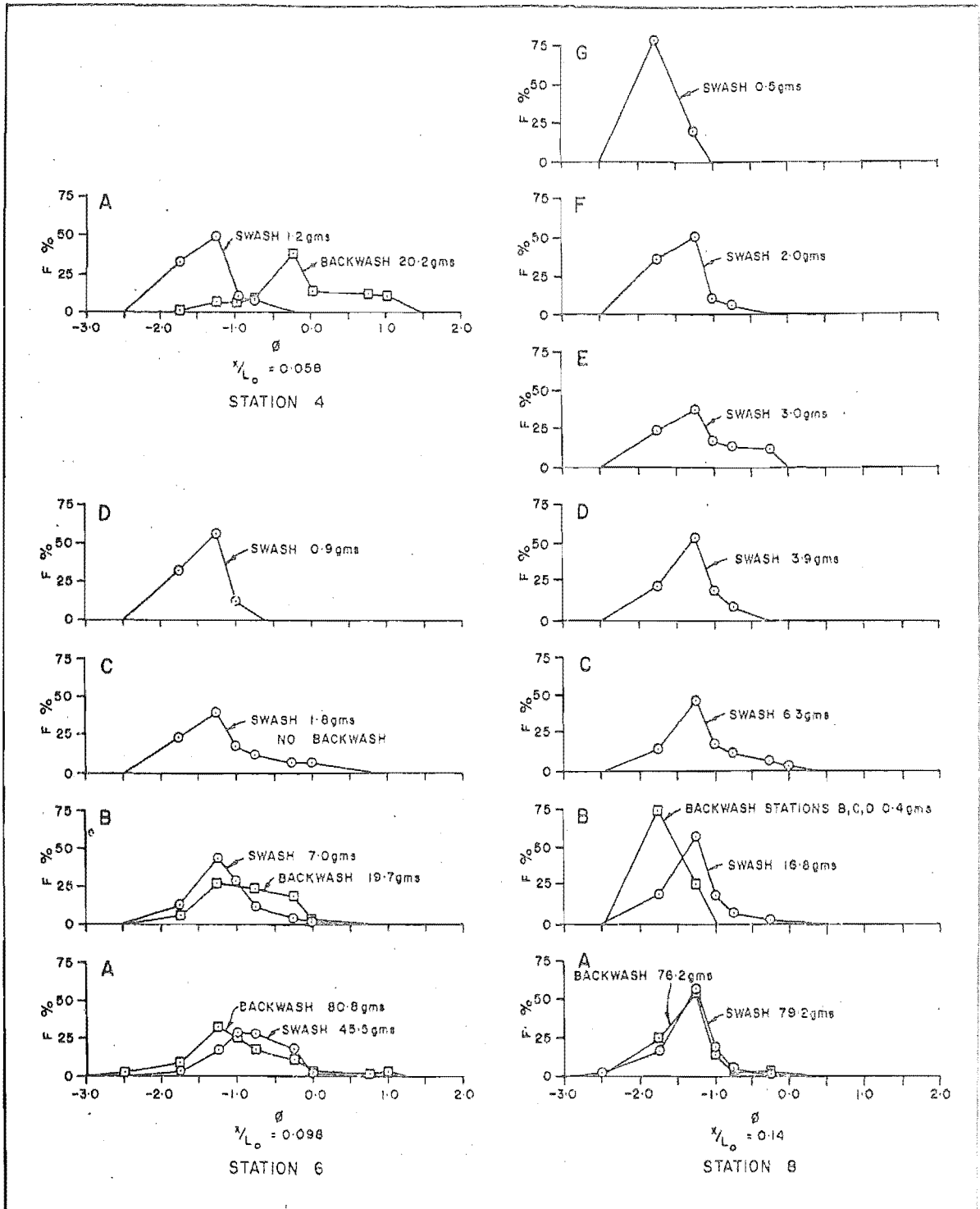


FIGURE 51. Size-frequency distributions of suspended sediments.

elevations in the swash. Of equal importance is the fact that both swash and backwash carry wide ranges of sizes. For both types of flow characteristic ranges of sizes are transported and distinct modes in the distributions are supplemented by well developed "tails" of coarser and finer materials. Further, it can be seen from the diagram that the amounts of sediment trapped decrease with elevation above the bed but that the size distributions of the upper materials generally reflect those nearer the bed. An important exception to this is that particles trapped at the upper levels of the swash have pronounced fine tails.

Near the bed for the stations in the scour zone the backwash removed almost double the amount of coarse materials transported by the swash while for the lower foreshore station almost equal amounts and size ranges were transported in the onshore and offshore directions. However, the diagram yields no information concerning the transport rates of individual size fractions.

Further characteristics of the vertical distribution of transported sediments can be demonstrated from an analysis of the concentration gradients in the swash and backwash. Figure 52A presents cumulative frequency distributions of materials trapped at different elevations above the bed. Depth is expressed in a relative fashion as the ratio of the depth of a given trap to the total depth of flow (z/d). From

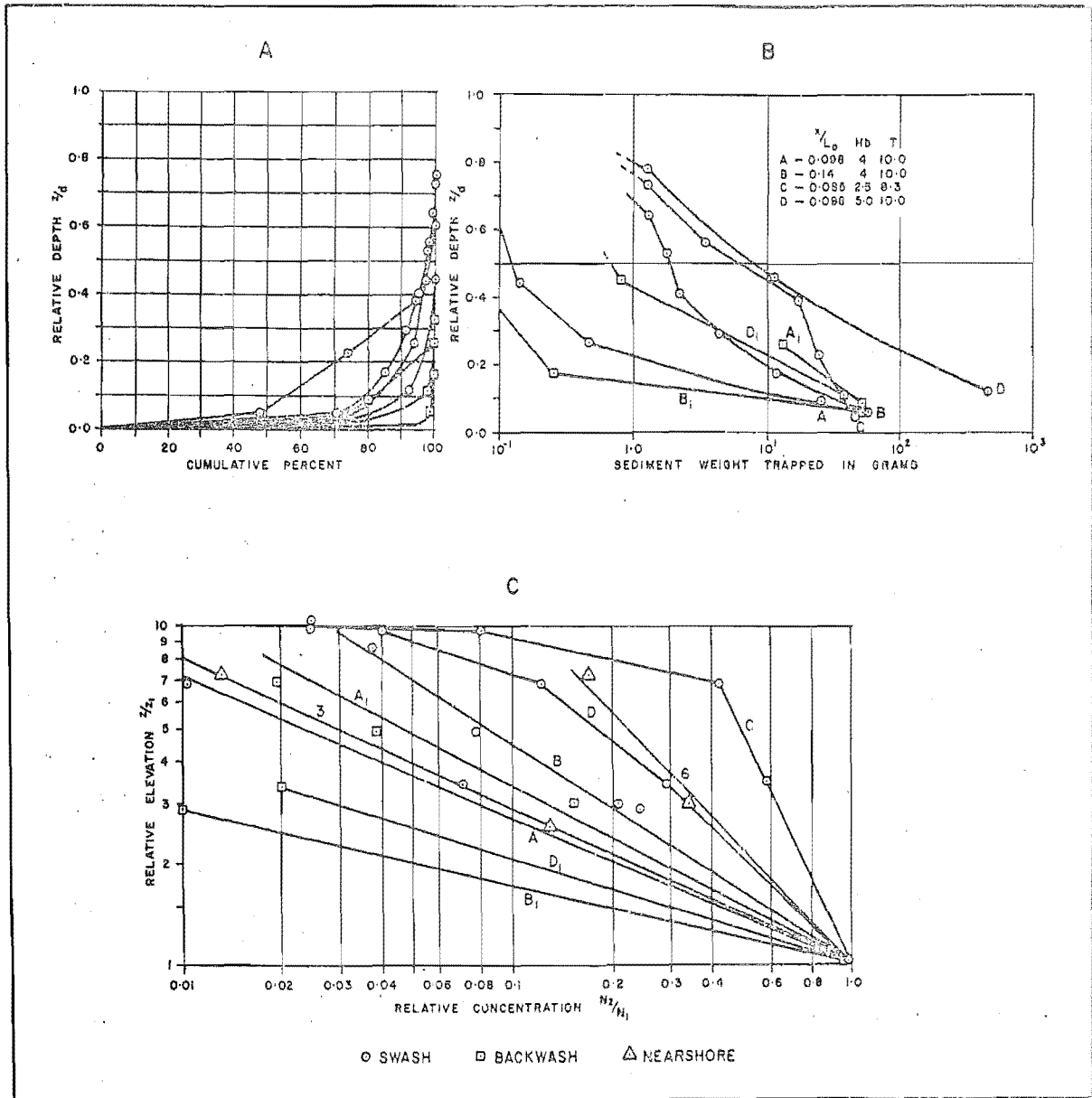


FIGURE 52. Vertical concentration gradients of transported sediments.

A. Cumulative percentages of load trapped at given levels.

B. Weights trapped at given levels.

C. Relative concentration profiles for swash and backwash.

Nearshore data from Inman (1949b - In Shepard, 1963, p.131).

this diagram it may be seen that 55 to 90% of all sediment in motion was trapped in the lower one tenth of the water column, this condition being especially pronounced in the backwash. Hence, only 2 to 5% of the trapped sediment in the backwash was derived from higher than $z/d = 0.1$. By comparison with Figure 52B which indicates the weights of material trapped at the various elevations, it can be seen that the amount of material in transport at a given level increases with increasing phase level as well as with proximity to the breaker. This trend is reflected in a similar rise in backwash concentration levels. It is also clear from Figure 52B that considerable variations in the forms of the vertical distributions occur.

In order to clarify the latter observation Figure 52C was prepared. Here the relative height above the bed (z/z_1) is expressed in terms of the reference level ($z_1 = 3.5$ cm.), rather than in terms of the relative water depth (z/d). Also, relative concentrations of suspended materials (N/N_1) have been computed in order to compare the widely different levels of transport indicated in Figure 52B.

As was demonstrated previously, the form of the concentration profile under conditions of uniform flow is logarithmic (see equations 30-35). Accordingly Figure 52C has been plotted on logarithmic axes. Of equal significance is the fact that by definition relative sediment concentration

values must range from unity at the bed (where the number of grains is theoretically infinite), to zero at some elevation in the flow.

Included in Figure 52C for comparison are two curves of relative sediment concentration derived from the nearshore zone of a sand beach (Inman, 1949B - in Shepard, 1963, Fig. 61, p. 131). The materials in this case were thus set in motion by the orbital velocities of unbroken waves and Inman notes that this type of flow is an exceedingly complex periodic variable depending upon wave height, water depth, distance from the plunge point of the waves, and roughness of the bottom. Despite the complexity of the flow it is interesting that the relationships of suspended sediment concentration to relative depth were logarithmic in form. However, it is clear from the diagram that the two curves differ markedly in form and slope. Inman suggests that this is due to the development of higher levels of suspension under the action of shorter period waves (curve 6). The curve is thus steeper and there is an increase in the concentration of material at the upper elevations of the water column. Conversely, during longer period waves (curve 3) the gradient is less steep indicating a relative decrease at the upper levels.

The greatest amount of material was thought to be placed in suspension during the maximum orbital velocities accompanying the wave crests and troughs. With long period

waves a large proportion of the suspended material settles to the bottom during the intervals between crest and trough. During short period waves the frequency of maximum velocity is greater and relatively more material is maintained in suspension.

For the asymmetric flows of the swash zone Figure 52C demonstrates a comparatively wide range of concentration gradients. In the case of the backwash it can be seen that the profiles are logarithmic in form at all times and for all positions on the shore. While gradients increase for both the swash and backwash with increasing phase level a more complex situation is apparent for the swash.

While on the one hand, gradients similar in form and steepness to those of Inman were obtained, on the other, a number are obviously non-logarithmic in form. Significantly, concentration gradients for the swash tend to be higher than for the backwash. At high phase conditions and for stations close to the breaker there are marked inflections in the curves. Thus, the lower portion of the water column of the swash at these locations appears to be characterised by high logarithmically distributed concentration gradients, while secondary, smaller gradients of suspended materials occur in the upper zones of the flow.

This trend is similar in form to that observed for the vertical distribution of velocity and would thus suggest the

existence of strong vertical components of motion in the swash. However, it is important to note that this effect is confined to the highest phase conditions and to stations near the breaker so that any vertically directed rolling motion imparted to the swash by breaking appears to be confined to the lower foreshore.

The finding that the concentration gradients of suspended sediments increase with increasing phase level complements Inman's results for the nearshore zone and supports the view that beach erosion is associated with extensive transport of materials as suspended load. Hence, increasing phase levels and variation in swash length are linked with the development of backwash scour and increases in the proportion of load in both the swash and backwash that is transported in a suspended state.

Mode of Sediment Transportation

While it has been shown that sediment is lifted to progressively greater heights in larger amounts with increasing flow energy and asymmetry it is not possible to demonstrate the actual magnitudes of transport by given modes from the above analysis. It was demonstrated during the review of suspended sediment transport that the accepted criterion of significant suspension is usually taken at a relative

concentration (S_z/S_a or z/z_1) of 25% i.e. the concentration at the next upper level is at least 25% of that at some reference level close to the bed if significant suspension is developed (Sundborg, 1956, p. 219).

By use of equation 35 and relevant data concerning flow depth, velocities, sampling levels and roughness length Figure 53 was calculated. The flow depth chosen was 50 cm. and the two reference levels as 6.0 cm (S_a) and 14.0 cm (S_z). The calculations refer to materials of density equal to 2.65 gr/cm³ and a water temperature of 16°C. ($\mu = 1.197 \times 10^{-2}$ poise - after Miyake and Koizumi, 1948). Settling velocities apply to spherical grains and were derived from Rubey (1933). The procedure used in computing the concentration curves was the same as that of Sundborg (1956, pp. 214-219) and was performed for velocity intervals of 25, 50, 100, 150, 200, and 250 cm/sec. These velocities are maxima and are thus comparable with those recorded by the dynamometer.

The roughness parameter (z_0) has been taken to be 0.2 cm. in accordance with Sundborg. This value corresponds to an equivalent grain diameter of 6 cm. so that the calculations are valid for the range of sediments covered in this investigation. The effects of slope have been ignored because critical erosion velocities for the slopes of the swash zone are 95-98% of those for planar slopes (see Sundborg, 1956, Fig. 18, p. 202). The value of the ratio z/d employed

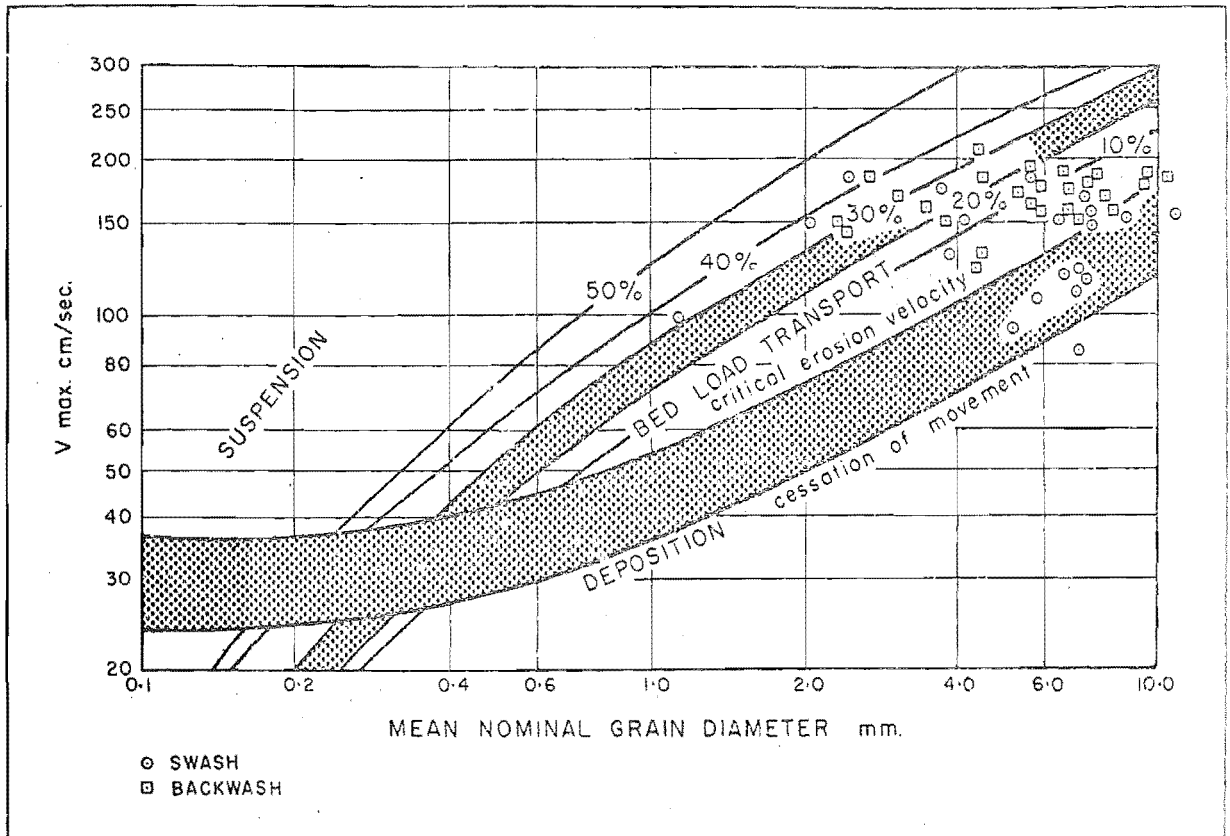


FIGURE 53. The relation between flow velocity, grain size and dominant state of sediment motion. Flow velocities are those in the lower one third of the water column and the sediments are assumed to be of uniform density = 2.65 gr/cm³.

(0.28) signifies that the calculations apply to the sediment concentration in the lower one third (16.0 cm.) of the flow. This is the zone spanned by the dynamometer plates and is therefore the area to which the observed velocities are applicable. It should therefore be noted that \bar{V}_{max} in Figure 53 does not apply to the surface as in Sundborg but rather to the zone occupied by the center of gravity of the transported sediment cloud. Finally, the concentration curves derived in the above manner were interpolated on the critical erosion velocity and settling velocity curves of Figure 53.

The transportation diagram resulting from the above procedures can be seen from the figure to have a narrower bed load transport region than the more generalised form shown in Figure 19 but the diagrams are directly comparable in all other respects.

A number of maximum velocity/ mean nominal diameter combinations have been plotted on Figure 53 for both swash and backwash flows. From the spread of values it can be seen that most transport occurs as bed load, but that significant suspension (S_z/S_a greater than 25 to 30%) is developed at times. Also, some of the sediments trapped were associated with current speeds indicating the onset of deposition. A further check on the calculations used in formulating the diagram is provided by the fact that the observed relative sediment concentrations near the bed are

in general agreement with the calculated contours for given current speeds and grain sizes.

Therefore, it may be concluded that the movement of sediment by swash and backwash occurs dominantly as bed-load but that significant suspension is developed for lower foreshore flows at high phase conditions. The competence curve of critical erosion velocity plotted on Figure 53 is a useful line of reference because the various forms of bottom phenomena do not occur until the bed-load is in motion (Menard, 1950). Thus, comparison of Figure 53 and Figure 20 will demonstrate that most bed-load transportation in the swash and backwash will occur predominantly as sheet flow. Ripples are not developed since the velocities are high and the bed is coarse. However, it will be shown that they can be developed by the shallow, relatively slow flows of the groundwater sheet.

Additionally it has already been demonstrated that conditions appropriate to the formation of standing waves and hydraulic jumps occur in backwash flows so that sediment transport in the form of antidunes moving contrary to the flow direction is also probable. Langbein (1942) noted an association between shooting flow and antidune transportation.

Near the swash limit where the flow is shooting and depths are small saltation of particles undergoing swash transport has frequently been observed (see Plate 9 and Frontispiece). At such times particles are in intermittent



PLATE 9. Saltation of large pebbles in shooting flow near the swash limit at station A. Note that the phenomenon is confined to the extremely turbulent leading edge of the flow.

contact with the bed and impact forces may be such that the particles are thrown clear of the water column. Plate 9 indicates that this transportation mode is associated with the leading edge of the swash wave and is not confined to the smaller grain sizes present.

The transportation of mixed sand and shingle deposits has already been shown to be complex so that considerable differences in mode of transport and form of bed disturbance may occur at different points on a profile consisting of mixed sizes. For example, Hooke (1968) concluded from an examination of the effects of adding granules to a sand bed undergoing active flume transport, that local variations in the concentration of coarse material may result in the formation of stable humps in the sand bed. These features, once formed, significantly influence subsequent sediment discharge over the reach in which they are located. Therefore, the addition of sand lenses to the upper parts of mixed sand and shingle profiles such as those of stations C and D may decrease the rate of bed alteration at these locations.

In summary it may be stated that sediment motion in the swash and backwash occurs in the sheet, antidune and saltation phases of bed load transportation. Suspended load transportation is minor and is confined to swash at lower foreshore stations. However, this mode of sediment transport assumes a more significant role at high phase conditions when swash

turbulence is high. At such times it has been shown that the time interval between swash and backwash is very short. Thus, sediments lifted and dispersed through the water column by the swash may be almost immediately transported seaward. Conversely, at lower phase levels sediments set in motion by either landward or seaward flow may settle to the bed in the interval between successive flows.

Rates of Sediment Transport Across the Profile

As has been demonstrated, a working hypothesis linking rate of transport of sediments across a bed to flow characteristics has resulted from the application of the principle of conservation of mass to the mechanics of the fluid/sediment system. Thus, a stream of water carrying sediment may be viewed as a transporting machine, and the immersed weight of grains as the load of this machine. It is then of interest to consider the power required to move this load (Inman and Frautschy, 1965).

Bagnold (1968, p. 48) adds that the essential problems facing studies of sediment transport are to understand the processes of transport and how the rate of transport is related to the flow of the transporting fluid. While there have been some evaluations of theory for natural fluvial channels (Colby and Hembree, 1955 - in Shepard, 1963, p. 141), and for laboratory flumes (Inman and Bowen, 1963), few measurements

have been made under natural wave environments for stations either landward or seaward of the breakers. Most beach studies relate rate of sediment transport to properties such as deepwater wave steepness (King, 1959; Iwagaki and Sawaragi, 1958), rather than to flow velocity, pressure or power.

The theory of sediment transport by fluids is thus derived largely by deductive reasoning from the concepts of general physics. According to Bagnold (1968) this has yielded a series of broad principles which are in need of further critical examination in both the laboratory and the field.

For the purposes of this investigation the consideration of transport rates has been confined to bed-load i.e. to sediment mass trapped per unit time at the reference level. This has been done in order to simplify the discussion and is justified on the grounds that half to nine tenths of the measured transport occurred at, or near this level. Thus, the transport rate data to be presented are point estimates derived from a series of positions across the shore. Since the most usual measure of transport rate across a unit area of bed is the immersed weight ($M \cdot \frac{\rho_s - \rho_f}{\rho_s} g$, where the density term relates to excess density of the sediment over the fluid; and g represents gravity), rather than the dry mass (M ; which was measured in the form $gr/cm^2/sec.$); the

transport data have been expressed in this form. The dynamic transport rate of bed-load (i_b) has the units M/T^3 and is expressed in this study as $gr/sec.^3$. Though this method of deriving bed-load transport rates is approximate it is thought to provide a valuable estimate of the relations between bed-load transport, bed disturbance and sorting processes for flows which vary widely in structure and for beds which exhibit equally wide ranges of sediment characteristics.

King (1959, pp. 125-127) examined rates of landward and seaward transport of swash zone sediments for a model beach of 1:12 slope. It was concluded that the magnitude and direction of net transport was a function of wave steepness. The steepest waves ($H_o/L_o > 0.04$) moved large volumes of sand seaward inside the breakpoint and offshore transport was apparent for all waves above a critical steepness of $H_o/L_o = 0.012$. Below this value sand was moved onshore at all depths. Differences in swash and backwash relative velocities (related to differences in wave steepness) were thought to account for the observed results.

However, more detailed laboratory studies by Iwagaki and Sawaragi (1958) resulted in a number of differing transport profiles which were dependent upon grain size, initial beach slope and wave steepness. For waves of steepness greater than $H_o/L_o = 0.03$ and coarse sands two peaks in the sediment transport profiles were found for both swash and

backwash, one being situated near the shoreline, and the other near the plunge point. Also, for profiles not at equilibrium the transport rates in the swash and backwash were unequal. Consequently, up to three zones of erosion, deposition and equilibrium transport were observed at varying positions on the shore. Hourly determinations of the pattern of net transport indicated progressive alterations in the distributions of transport rate with approach to equilibrium, coincidence between total swash and total backwash transport occurring at equilibrium.

An interesting feature of the experimental profiles was that the rate of transport decreased in the immediate vicinity of the breakers for all wave steepnesses (0.0093 to 0.0815). The authors concluded from this that "the initial point of remarkable sediment transport at natural beaches of several mm. grain size is near the breaking point" (Iwagaki and Sawaragi, 1958, p. 83). They termed this the "critical point of sediment transport" and suggested that it was associated with a critical water depth.

Figure 54 presents four profiles of dynamic transport rate of bed sediments for the swash zone of the present study. From these it is clear that wide variations in net transport rate and direction were observed. Sediment transport rates are high in both swash and backwash but a point of initial rapid transport near the breaker is not apparent.

FIGURE 54A. Transition conditions.
 $t/T = 0.96$, $H_b = 5.0'$,
 $T = 10.0$ secs., Station C.

B. Surf phase. Station C,
 $t/T = 1.37$, $H_b = 6.0'$,
 $T = 10.0$ secs. Note wide
scour zone.

C. Transition conditions.
 $t/T = 0.71$, $H_b = 4.0'$,
 $T = 10.0$ secs., Station C.
Scour zone here is narrow.

D. Surf phase conditions.
Station A, $t/T = 1.50$,
 $H_b = 2.5'$, $T = 8.5$ secs.
Short period waves gave
rise to a narrow swash
zone dominated by a
relatively wide zone of
scour.

Note: Sediment transport data
are those for lowest
(reference) level traps
in both swash and backwash.

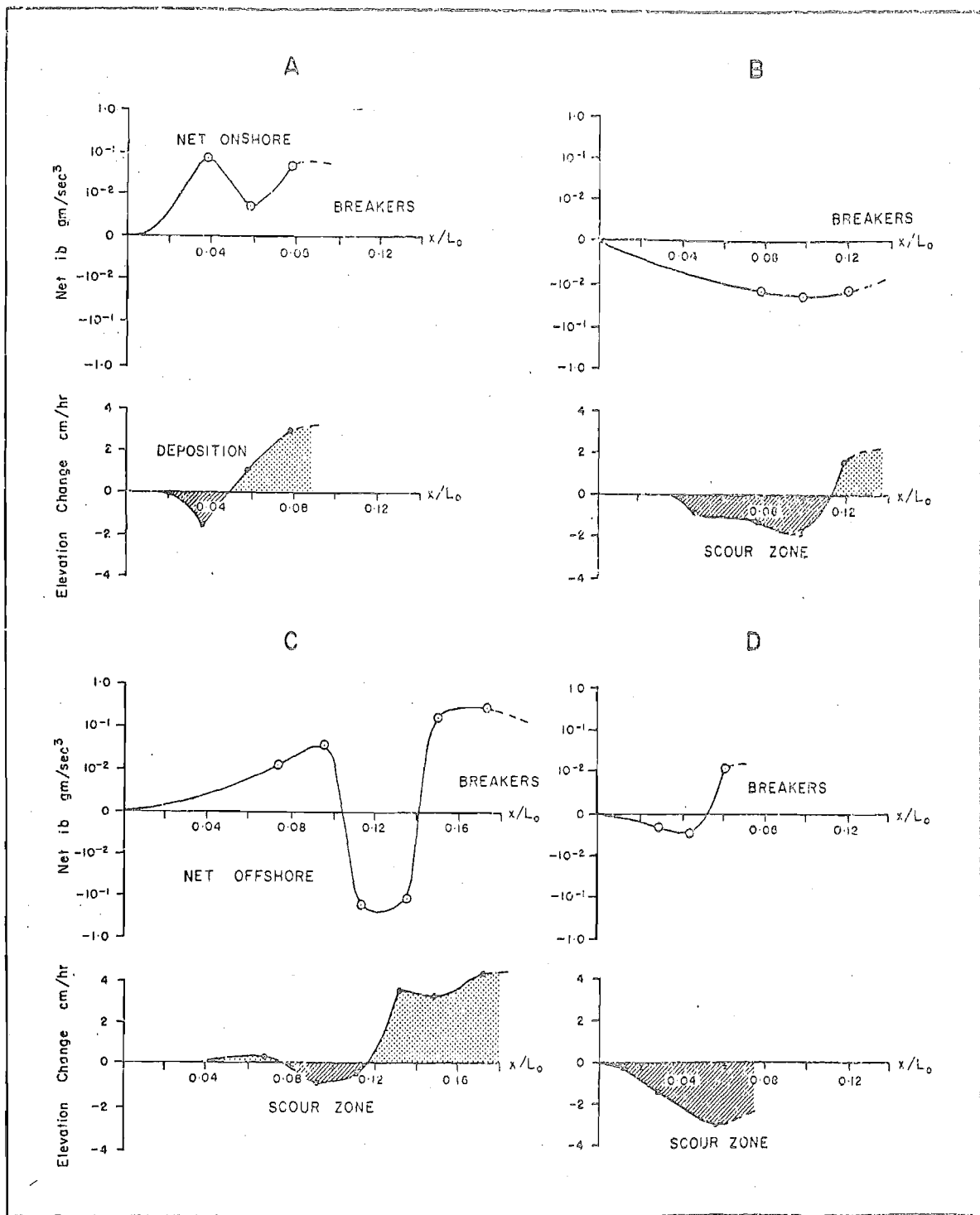


FIGURE 54. Four profiles of net dynamic sediment transport rate (ib) and foreshore elevation change.

The most significant feature of the diagram is, however, the general correspondence between the rates of bed-load transportation and the measured patterns of bed disturbance. Thus, for low phase transitional conditions sediment transport can be seen to be dominantly onshore, this situation being associated with bed deposition (see Curve A). For higher phase conditions transitional sediment transport and bed disturbance profiles were recorded. The scour zone for curves B, C, and D can be seen to be of variable width depending upon phase relations in the flow.

Though there is correspondence in form between the transport and bed profiles it is clear from the diagram that lags occurred. Hence, the points of inflection in the transport profiles do not coincide with points of alteration from bed erosion to bed deposition. This is because sediment transport measured at any given point in the flow may be expected to affect the bed at some other point further downstream rather than at the point of measurement. Of course, this effect applies to both swash and backwash. Another interesting feature of Figure 54 is that bed deposition was recorded a number of times near the breaker where net sediment flow was offshore. This suggests that the backwash load is not transported through the breaker under the flow conditions measured, and therefore it would appear that circulation of sediments through the breaker is not developed

until high phase conditions are developed as was suggested previously. However, despite the above anomalies Figure 55A shows that net bed load transport rate is strongly correlated with both sense and magnitude of bed elevation change.

Of great importance is the fact that the observed agreement between the bed profiles and rate of transport confirms the model of swash zone erosion and deposition proposed earlier in this report. Hence, it is now clear that low phase conditions with low velocities and levels of turbulence result in net onshore sediment transport as well as in foreshore accretion. Similarly, high phase conditions characterised by strong backwash action and high levels of turbulence result in offshore transport of sediment, the development of significant levels of suspension in the swash and in ultimate bed erosion over much of the profile. For transition conditions, a variety of erosional and depositional combinations may result, the location and intensity of the scour zone (which is universally associated with an area of net offshore transport in Figure 54), varying with swash phase level and the degree of variation in swash length.

Fluctuations in rate of sediment transport for natural foreshores of mixed sand/shingle beaches, at least for those of this investigation, are more similar to the laboratory findings of Iwagaki and Sewaragi (1958) than to those of

King (1959), but are different from both of these in that wave steepness has been shown to be of little direct relevance as a predictive parameter of beach erosion. Rather, phase level of swash flow and the level of inherent variability in this property for given wave trains arriving at the shore have been demonstrated to be more useful measures in describing observed foreshore changes. This is because these latter parameters, as opposed to steepness, are measured easily, and yield information which is directly referable to levels and magnitudes of flow turbulence, asymmetries of pressures, times and velocities of flow, rates of sediment transport in both swash and backwash; and, of course, to bed elevation changes.

Further, Figure 54 provides confirmation of the previous conclusion concerning the applicability of null-point considerations of sediment movement in high energy environments. Longinov's method of proportional net pressures for use in indicating potential sediment movements is thus greatly aided by an examination of the rates and directions in which sediments are actually transported.

Relations Between Transport Rate and Measured Flow Properties.

Figure 55B presents regression lines for the relations between mean maximum power developed at the dynamometer and measured dynamic bed-load transport rates for both swash and backwash. The importance of these

FIGURE 55A. The relation between dynamic rate of bed load transport ($\text{gm}/\text{sec.}^3$) and rate of bed elevation change.

FIGURE 55B. Relation between flow power expended at the dynamometer and dynamic rate of sediment transport.

FIGURE 55C. The relation between mean maximum current speed and weight of sediment trapped near the bed.

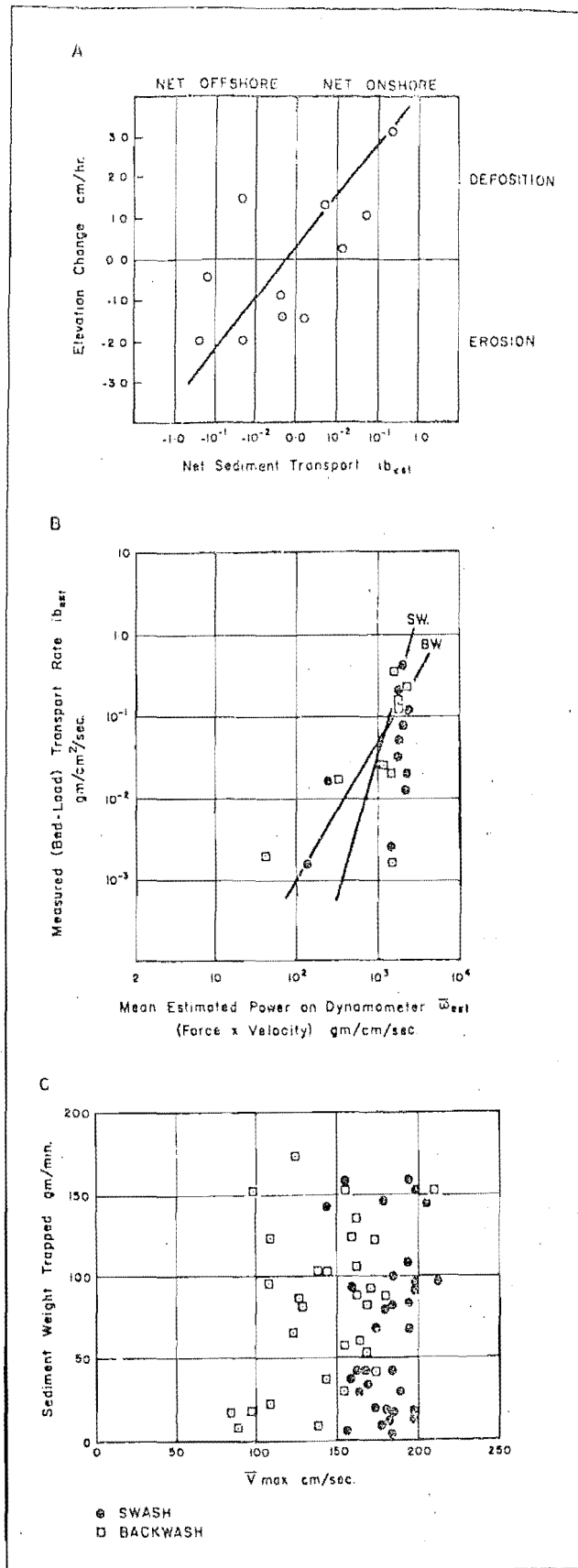


FIGURE 55.

relationships lies in the fact that if the fluid flow is regarded as a transporting machine then:

Rate of Transporting Work Done = Power Supply x Efficiency

$$\text{or: } i_b = K \omega$$

(see equation 38). Hence, i_b , the bed-load transport rate is proportional to ω , the power available from the kinetic energy of the flow. It was shown during the discussion of total transport in a stream that K may have values greater than one, and that its magnitude is usually several times larger than the sum of the efficiency coefficients for bed-load (e_b) and suspended-load (e_s) transport. This is because the value of K includes the effects of bed slope, angle of intergranular friction, and settling velocity as well as of the efficiencies of energy application (see equation 38).

Though the power value referred to in formulae is that for the flow, the values plotted in Figure 55B are those for the mean maximum power developed on the dynamometer plates by the flow. Clearly this quantity will be affected by fluid drag over the plates thus giving rise to an efficiency term in the same manner as for the application of flow power to the transported sediment grains.

However, it would appear that the use of power expended at the dynamometer (i.e. force x velocity) is a useful estimate of the relations between fluid flow and sediment transport rate. The values of K obtained from the slopes

of the lines are 3.33 for the swash and 1.54 for the backwash, the higher value for the swash being consistent with the more extensive development of vertical lift forces in this flow as opposed to the downslope velocity vectors of the backwash.

By comparison, Inman and Bowen (1963) obtained good relations between sand transport rate and wave flow power for model experiments simulating quasi-symmetrical wave action in the offshore zone. However, when the system of waves and superimposed drift currents was subjected to water motions which were both strong and asymmetric the basic assumptions of the energy theory were violated and the relation deteriorated. Under such conditions, it was argued, that the effects of wave drift velocity gave way to a dominance of phase-dependent phenomena. In the swash zone where the flow regimes have been shown to be markedly asymmetric, it is therefore doubtful if the energy theory described previously would be applicable. Because of this it is suggested that empirical, statistical estimates of power application such as that employed in this investigation may be of more value than direct estimates of flow power in practical studies of foreshore erosion and deposition.

Figure 55C presents the scatter of data resulting from the correlation of sediment transport rate (dry mass per unit time) and mean maximum flow velocity. In comparison with Figures 55A and B the degree of control exerted on sediment

transport by flow structure is abundantly clear. While current speed does not reflect variations in levels of turbulence except in a most general fashion, power expended at the dynamometer is strongly influenced by the scale of flow turbulence. As has been demonstrated, the scale of turbulence (size of eddies) is reflected in the duration of maximum velocity and therefore in the times for which the largest forces are operative. Further characteristics of sediment transport may be ascertained from consideration of the dynamic behaviour of grains moving in the fluid flows.

Particle Dynamics. The manner of transportation of grains is not only related to the laws of fluid flow but also depends upon the dynamic characteristics of the grains undergoing motion. It is therefore of interest to know whether viscous or inertial forces, or both condition the flow around the sediment particles.

The behaviour of grains can be described by Reynolds Number in much the same fashion as can the turbulent motion of fluids. Following the procedure of Harrison and Morales-Alamo (1964) Reynolds Numbers and drag coefficients of particles trapped in the water column of the swash and backwash have been computed. Thus:

$$Re = \frac{\rho_f D_n \cdot c}{\nu} \dots\dots\dots 53.$$

where: ρ_f is the fluid density; D_n is the nominal diameter

of the grain in cm.; c is the grain settling velocity in cm/sec.; and μ is the fluid viscosity (taken as 1.221×10^{-2} poise for $T = 15^{\circ}\text{C}$. and $\text{Cl}\% = 18.0$ from Miyake and Koizumi, 1948).

Settling velocities were derived from Rubey (1933) for mean nominal diameters rather than from settling tube data as in the case of Harrison and Morales-Alamo. Therefore Reynolds Numbers for particles of this investigation are approximate mean values only.

The quantity expressing the resistance of particles to flow is the drag coefficient (C_D) and this is determined in part by grain shape as well as by particle size. Values of the drag coefficient were abstracted for mean nominal diameters, mean Reynolds Numbers and mean effective settling sphericities ($\bar{\Psi}$) from Table 1 in Harrison and Morales-Alamo (1964, p. 26). Though the authors employ Corey Shape Factor to describe grain form effective settling sphericity was adopted as the shape coefficient for this investigation since Sneed and Folk (1958, pp. 120-122) demonstrate that this parameter has greater dynamic significance than other shape indices. Comparisons of the two measures revealed that $\bar{\Psi}$ values are larger than Corey Factors for a given grain (e.g. $\bar{\Psi} = 0.64$ and Corey S.F. = 0.51 for the same particle).

Values for Reynolds Number and drag coefficients are presented in Table 11. The data relate to grains undergoing

transport during the experiments presented as curves D, A, and B respectively in Figure 54. A range of transitional and high phase flow conditions has therefore been examined.

From the table it can be seen that Reynolds Number for the sediment grains ranged from 79.3 to 217.0 for the swash. The backwash is characterised by comparatively more uniform particle dynamics ($Re = 136.0 - 181.0$); the coefficients applying to a size range of particles 2.3 to 4.5 mm. in diameter.

Reynolds Number expresses the relative proportions of viscous (μ) to inertial forces ($Dn.c$) acting on the grains, and Harrison and Morales-Alamo (1964, p. 19) suggest that for Re greater than 1,000 inertial forces might be ignored. Also, in the range $Re = 3$ to 20 flow conditions near grains may be regarded as transitional between laminar and turbulent motion. Beyond $Re = 20$ separation around individual grains is well established and the flow is fully turbulent.

It is therefore clear from Table 11 that for the swash zone sediments of this investigation inertial forces predominate. Hence, the formation of turbulent wakes occurs at the downstream edge of grains and boundary layer separation is developed around bed particles. By comparison Harrison and Morales-Alamo (1964) obtained Reynolds Numbers in the range 3 to 15 for medium sands 0.25 to 0.30 mm. diameter on a sand beach foreshore. Clearly, for the latter environment flow near the bed was transitional in nature, except for the

breaker zone where Re was highest.

As can be seen from Table 11 values of the drag coefficient closely parallel Reynolds Number, which in turn, can be seen to reflect grain size. All of the drag coefficients are close to unity (1.07 to 1.45), thus reflecting the high Reynolds Numbers and the relatively small viscous effects on the grains. Drag resistance offered by the larger swash zone particles of this investigation is much lower than for the much finer sand grains studied by Harrison and Morales-Alamo. The effects of particle shape on sediment transport would thus appear to be relatively insignificant in relation to effects of size for the range of grain sizes presented in Table 11. On the other hand, for smaller grains shape effects appear to be of greater relative importance.

In accordance with Reynolds Number drag coefficients are lowest at the breaker and at the swash limit where grain size again increases. The central foreshore is thus the zone of highest drag values. Significantly, this is the location at which transitions in flow state take place and at which the scour zone forms in the backwash. Hence, it is clear that Reynolds Numbers and drag coefficients of the bed sediment grains reflect in a generalised fashion the variations in flow occurring across the shore. It will next be demonstrated that the zone of highest grain drag values and transitional flow is also the zone of maximum bed disturbance.

Depth of Disturbance

Figure 56 indicates the range of values obtained for erosion at different points on the shore. From the diagram it can be seen that degree of disturbance increases seaward of the swash limit to a point on the lower foreshore, beyond which values rapidly decline. Since the foreshore is continually disturbed regardless of surface erosion or deposition the data presented are only estimates of maximum disturbance. Deposition was recorded for the immediate vicinity of the breaker on many more occasions than erosion. Disturbance of the bed may occur at rates of up to 15cm./hour and is clearly at a maximum for the mid-shore area.

King (1951) examined depth of disturbance for natural sand beaches by use of columns of dyed sand of known lengths buried in the foreshore at low tide. Following the tidal cycle the columns were excavated so that the amount of truncation of the sand column could be measured. King concluded that the depth of disturbance in cm. was about equal to wave height at the break point in feet i.e. depth of disturbance was 3 - 4% of breaker height. Maximum disturbance occurred in the swash zone.

Also, it was noted that coarse sands were disturbed more deeply than fine sands. From this it was argued that, "the depth of disturbance would be greatest in shingle, where if

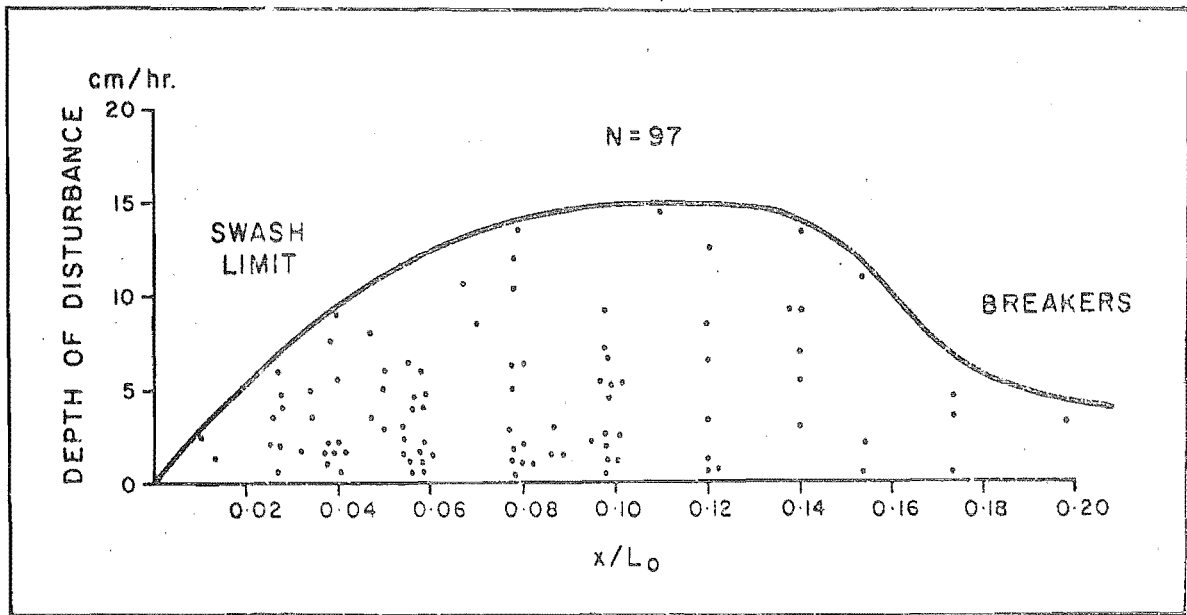


FIGURE 56. Rate of depth of bed disturbance in the swash zone.

only two or three layers of pebbles are moved the depth of disturbance would be greater than for a fine sand beach" (King, 1951, pp. 137-138).¹

Otvos (1965) observed tidal sedimentation cycles on sand beaches using the dyed sand-wedge method and concluded similarly that depth of disturbance varied with wave height and grain size.¹ However, Otvos reported a far wider range of disturbance values than King, measurements of erosion of up to 20 to 40% of breaker height being obtained.

Kirk (1967, pp. 84-86) carried out similar experiments for a gravel beach ($Mz\phi = -3.08$) in the Canterbury Bight for breaker heights of up to four feet in order to examine further King's suggestion concerning the erosion of gravels. Disturbance values here ranged from 1.9 to 10.2 cm.¹ over a tidal cycle with greatest values occurring on the mid foreshore. The range of disturbance values obtained lay between those obtained by King for fine sands and those of Otvos for medium and coarse sands. It was concluded that this result was due to the differing responses of pebbles and sand to wave energy. Further, Samad (1968) recorded disturbance values ranging from 1.0 to 18.0 cm.¹ on mixed sand shingle foreshores at Kaikoura. These very high values resulted from short period (8 seconds) high phase wave action and maximum disturbance occurred near the base of the breaker.

From Figure 56 it can be seen that a very wide range of estimates of disturbance was obtained for the present investigation. In the light of the foregoing discussion of swash processes it appears that depth of disturbance is closely related to phase conditions in the swash zone and therefore to the incidence and severity of backwash scour. The correspondence between breaker height and depth of disturbance noted by King and Otvos is thus thought to be due to the controlling effect of breaker height on swash length. Consequently, the differences in degree of disturbance between the two studies for given increments of breaker height would appear to be at least partially due to variations in swash length, phase level, and therefore in the location and severity of bed scour. While Figure 56 indicates a tendency for maximum disturbance to occur at the mid-shore position reference to Figure 54 will confirm that it may occur at any position on the profile. It is therefore indeed fortunate if the maximum disturbance coincides with the location of one of a series of dyed sand or painted stone columns buried in the foreshore of the swash zone.

It remains to describe the sediment sorting processes associated with the above dynamic transport profiles and to examine the variations in all of the processes that have been detailed with tidal rises and falls in mean water level at the shoreline.

SEDIMENT SORTING IN THE SWASH ZONE

Sorting For Size

While it has been shown that distinctive patterns of net sediment transport exist for different types of flow conditions in the swash and backwash, the ranges of sizes comprising the total weights trapped have not yet been examined. As has been demonstrated, a conventional approach to the dynamics of sediment sorting has been from the standpoint of the initial or incipient velocities required to promote grain motion (e.g. Inman, 1949; Eagleson, Glenne and Dracup, 1963; Miller and Zeigler, 1958; Longinov - in Zenkovich, 1967). For the swash zone of the study beaches, however, where bed stress is high and flow structure is variable, these conditions are rapidly and frequently exceeded for most, if not all of the grain sizes present. Therefore it was proposed that the rate of grain transport was the most appropriate measure for use in the description of bed elevation changes and the validity of this approach was subsequently demonstrated.

It will now be demonstrated that for high energy environments and given ranges of grain size that this is also potentially a most useful standpoint from which to

examine processes of sediment sorting.

As might be expected in a high energy flow environment, Figure 57 shows that there are only small variations in the mean sizes of sediments trapped at different elevations above the bed in both swash and backwash. It can be seen that for most cases mean size was slightly smaller for positions higher in the water column than for sample points nearer the bed, but the differences are not pronounced. However, in some swashes there is an evident sharp decrease in particle size near the surface of the flow.

From this and the fact that most of the measured transport occurred in the lower part of the water column it is concluded that size-sorting processes can be adequately described for present purposes at least, by analysis of the size composition and net transfer rates of sediments trapped near the bed, since modal sizes at higher elevations are not significantly different from those near the bed and because the proportional sediment weight contributions to unit bed sediment distributions from the upper parts of both swash and backwash flows are small.

Transport rates of component size fractions have been presented in Figures 58A and B for the four net sediment transport profiles shown in Figure 54. It should be noted at the outset that the sorting processes evident from these diagrams are considerably more complex than those indicated

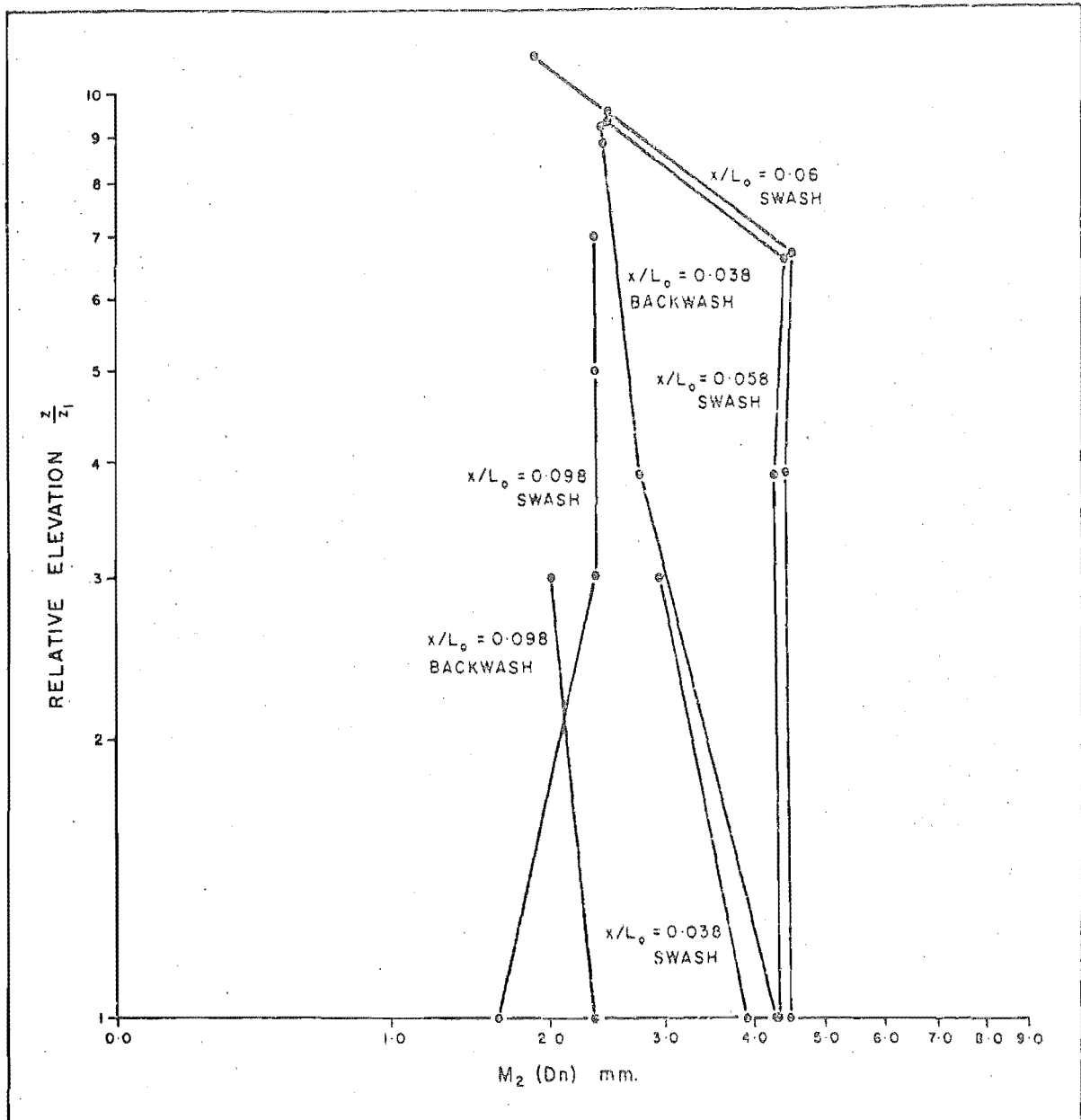


FIGURE 57. Vertical distributions of mean nominal diameter in the swash and backwash.

by the Longinov proportional net pressure diagrams corresponding to these four sets of swash/backwash conditions (see Fig. 37).

Thus, even though velocities in the swash and backwash may be approximately equal, transport rates of given size fractions in each direction may differ by up to two orders of magnitude owing to differences in turbulence and flow depth. Hence, for the first case of Figure 58A net transport of all size fractions is onshore, but it can be seen that conditions favouring deposition of coarser grains (8.0 - 11.3 mm.) were best developed near the swash limit. Fine grains (less than 2.8 mm.) on the other hand, were actually removed in very small quantities from the swash limit and exhibited a slight preference for deposition at the mid-shore position. It can be seen that the intermediate size fractions, which comprised the bulk of the samples, were transported at relatively high rates at all positions on the shore.

For a more complex pattern of net transport and bed disturbance the second example of Figure 58A exhibits well established zones of net inflow and outflow of particles. However, it should be noted that erosion of one size fraction from a given station may be offset by deposition at that point of some other size fraction. Thus, the smallest grains present were eroded in small quantities from both the upper and lower foreshore areas and deposited at the mid-swash

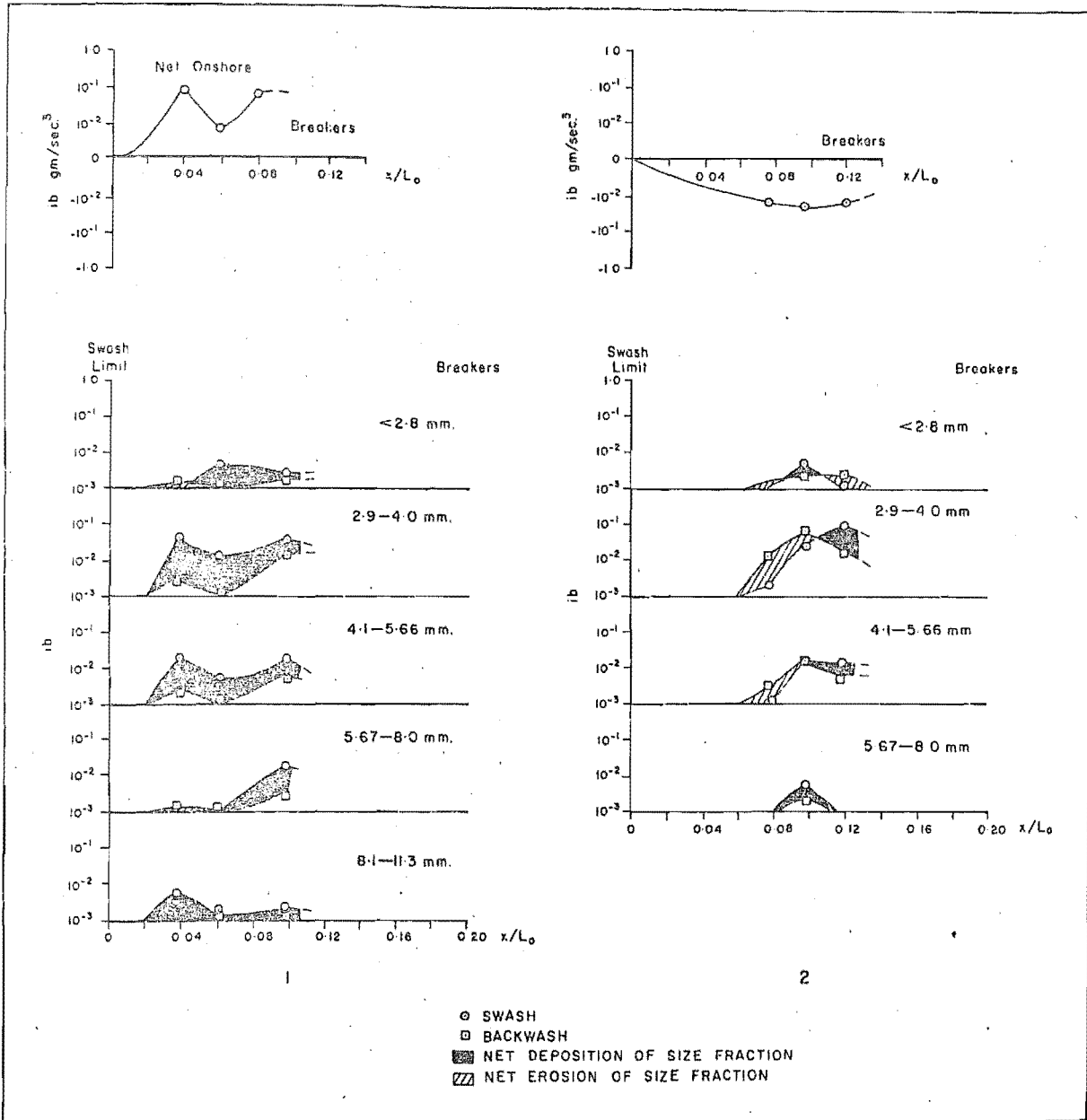


FIGURE 58A. Net sediment transport profiles and rates of net motion of individual size fractions comprising total load.

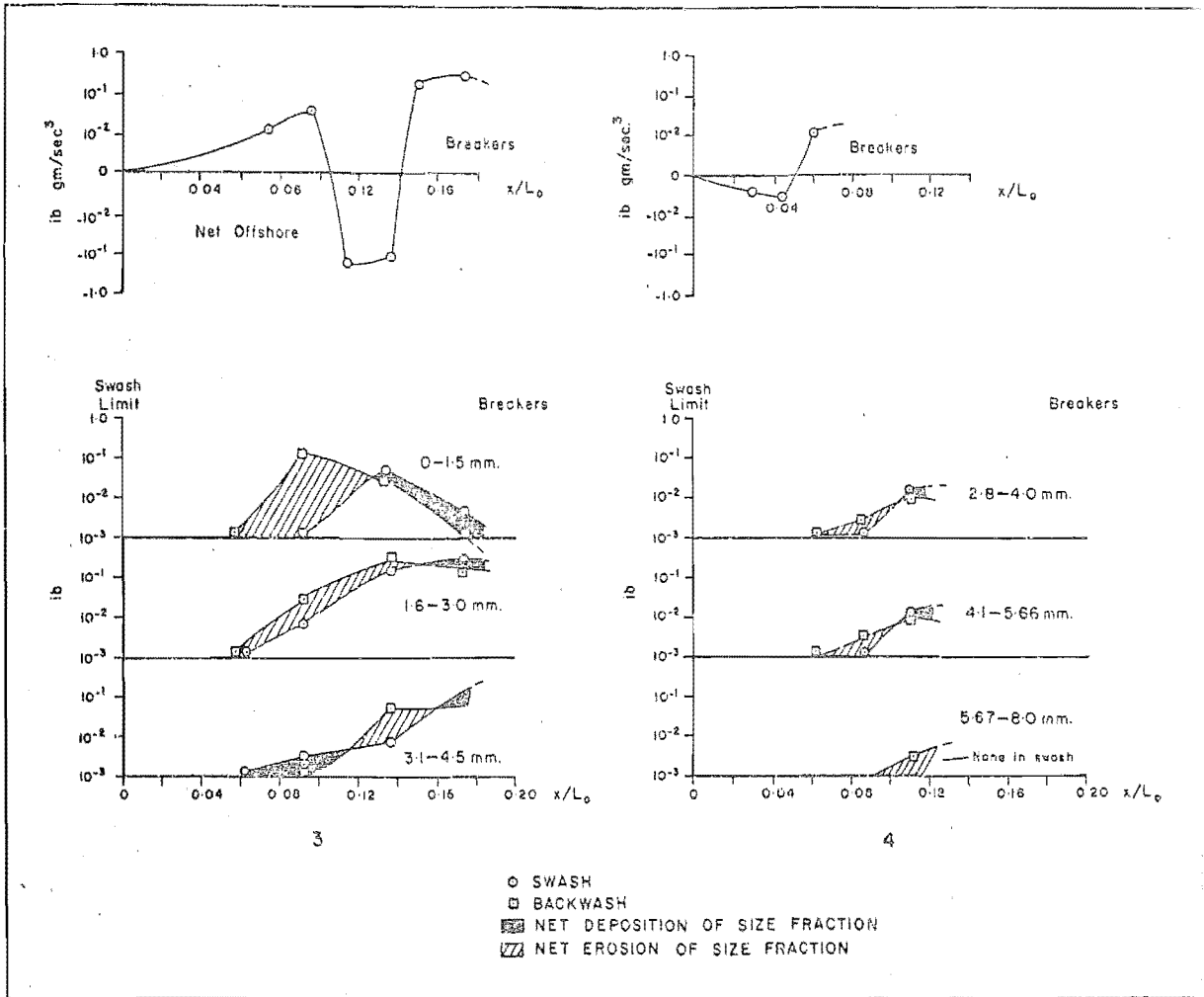


FIGURE 58B. Net transport rates of individual size fractions comprising total load.

position. In contrast to this, coarse grains (5.66 - 8.0 mm.) could only be transported in the central foreshore region by both swash and backwash, and only at slightly greater rates in the former than in the latter. Once again the mid-range fractions which comprised the bulk of the trapped sediments reflected the net sediment transport profile most closely.

The most important aspect of the smaller, subequal amounts of finer and coarser materials is thus the potential for alteration to the sorting coefficients and skewness values of the bed sediment distributions. Another feature of interest is that a small amount of deposition was recorded on the bed near the breakers (see Fig. 54B) and this appears to result from the deposition of coarser grains, as indicated in Figure 58A(2).

For a sediment transport profile combining elements of net onshore and net offshore motion, Figure 55B(3) indicates an even more complex situation. It may be seen from the diagram that net removal of fines (0 - 1.5 mm.) occurred from the upper foreshore, the backwash removing grains of this size approximately 100 times faster than they were contributed by the swash. Though some of this eroded material was deposited on the lower foreshore much would remain in continual motion. Also, the maximum rate of transport for fine particles occurred on the upper foreshore for the backwash, but on the lower foreshore for the swash.

It can be seen that for the mid-range fractions, transport rates were almost equal in the swash and backwash and that rates of transport in both flows increased almost linearly toward the breaker. In relation to the net sediment transport profile, and by contrast with the previous examples, the coarse size fraction (3.1 - 4.5 mm.) appears to yield best correspondence. Thus, coarse materials were eroded from the central foreshore area and deposited at the extremities of the profile near the base of the breaker and toward the swash limit. An important point here is that the deposition of coarse materials at the swash limit more than offset the high net rate of removal of fines from this area, thereby resulting in net deposition and an increase in mean grain size in this area (see Fig. 49). It can also be seen by comparison of these two diagrams that there was little change in mean grain size on either the central or lower foreshore areas, since at the former location erosion of all fractions occurred while at the latter deposition of all size fractions accrued at nearly equal rates.

Figure 58B(4) indicates a comparatively simple situation in which the transfer of all component size fractions reflected the form of the net transport profile, with the exception of the coarsest grains (5.66 - 8.0 mm.). These grains were in net offshore motion on the lower foreshore only and may have been deposited in the zone immediately landward of the breakers.

From these examples it is clear that characteristic size/sorting patterns result from varying transport conditions acting upon given ranges of grain sizes. Hence, increases in mean grain size toward the breaker may result from the deposition of successively finer particles with increasing distance from the breaker (low phase conditions); or from the erosion of progressively coarser grains with increasing proximity to the breaker (high phase conditions). It will shortly be shown that characteristic types of grain size frequency curves are associated with each of these conditions. Transitional flow conditions, by contrast, may result in little alteration to either mean grain size or sorting coefficients since the rates of transport into and out of a given section of the bed may be approximately equal. Thus, trends in grain size determined by previous flow events may be preserved wholly or in part, or grain size and sorting values may become quasi-uniform over much of the swash zone.

It has been further demonstrated, that even within a net transport regime directed wholly onshore or offshore significant variations in the rates of motion of the component size fractions occur. Because of this it is possible to record either net removal or net gain of some fractions at a particular point even though the total net transport may be directed in the opposite direction.

Simultaneous movements of different sizes in different

directions typifies all of the examples of Figures 58A and B and it should be noted that this situation differs markedly from that indicated by the Longinov diagrams for some of these cases (see Fig. 37).

Further, the analysis of the net rate of transport of individual size fractions has illuminated some of the sorting processes responsible for the formation of bed sediment distribution curves such as those shown in Figures 49 and 50. The upper portion of the swash zone thus emerges as an area of net swash flow where a wide range of sizes may be deposited, but only a lesser range removed by the backwash. Simultaneous mixing (by the swash), and truncation (by the backwash) are therefore well developed in this area. Sand lenses, deposited by the swash on mixed sand and shingle profiles may persist for considerable durations since deposition exceeds the rate of backwash removal of fines. Alternatively, fines may be eroded rapidly by the backwash but deposition of coarser grades by the swash may more than offset the amounts of fine material removed. Thus, the upper swash zone of the study beaches is the area of widest range in grain size and consequently, the most variable in mean size and sorting coefficients.

Lower on the foreshore size tends to be less variable and sorting values higher. Here the final results of sets of flow events on the bed sediment distributions may involve a complex interplay of processes including simple mixing,

winnowing, truncation, selective transport of particular size ranges, and/or deposition of wide ranges of sizes. More detailed examination is required to establish the nature of these processes and the conditions under which they occur.

Effects of Transport Rates on Bed Distributions. Enrichment and/or removal of individual grain size fractions by the flow has been estimated in Figure 59 by plotting the percent contribution (added or removed) to unit bed sediment distributions at the point of measurements. The procedure thus involved expressing the net dynamic transport rates of individual size fractions as percentages of the size ranges occurring in a unit bed sediment distribution. If the fraction was undergoing net onshore transport at the point of observation then the corresponding proportion of that size has been added to the amount of the same size occurring on the bed. Net offshore transport of fractions has consequently been treated as a loss to the bed at any point and this accounts for the negative percentages apparent in Figures 59E and F; i.e. Negative proportions indicate that the flow was removing more of a given fraction than was present on the bed at that point.

This serves to underline a shortcoming of the technique in that the flow of sediments past any given point does not necessarily influence the bed at that station, as has been

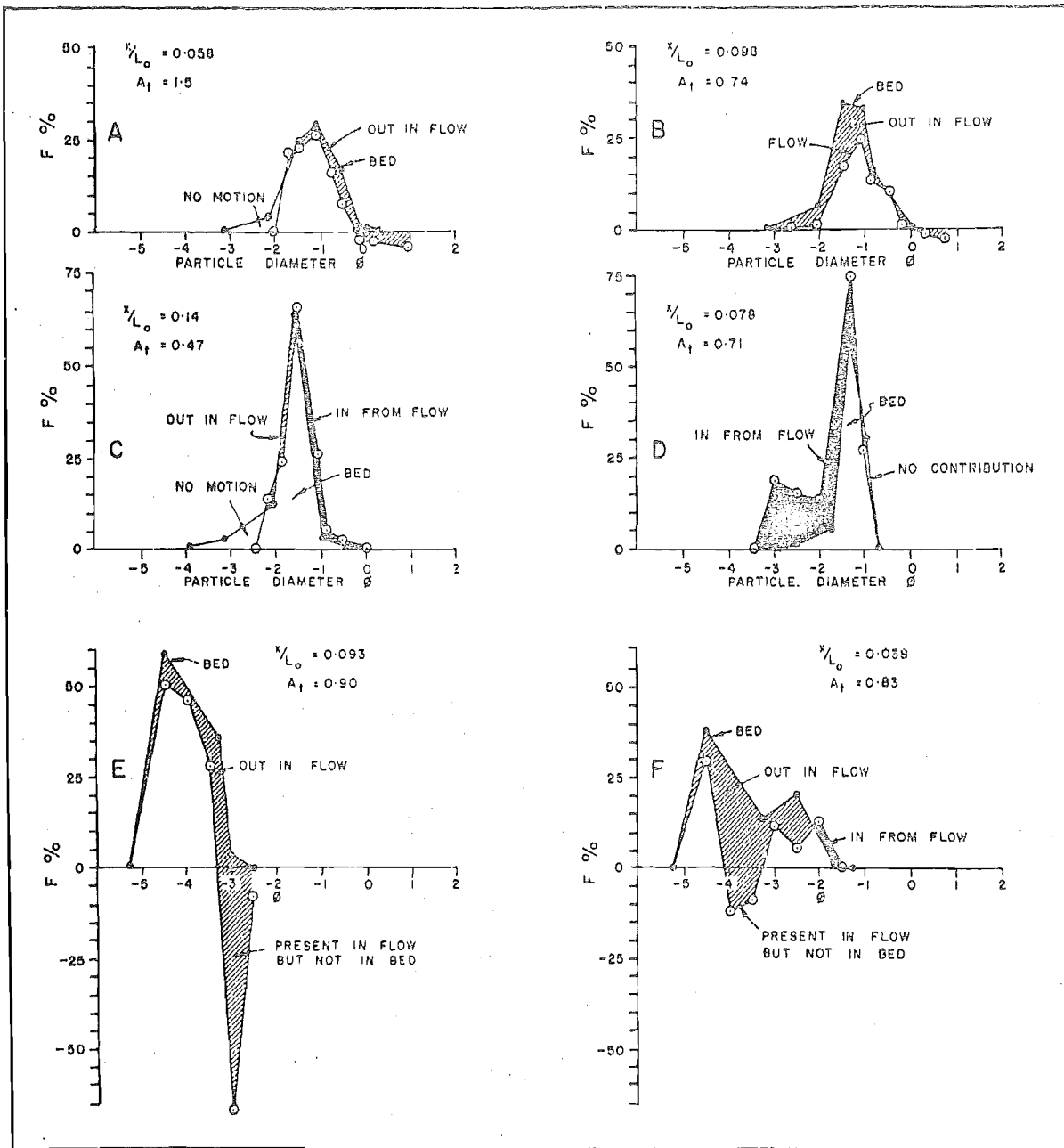


FIGURE 59. Comparative effects of differential transport rates of component size fractions on local bed sediment distributions. A_t = coefficient of asymmetry of flow times. At values of the coefficient greater than unity the backwash is dominant.

demonstrated, but rather it is released at some other point downstream in both swash and backwash. Therefore, while it cannot be argued that the "final" curves combining transported sediments and bed distributions represent the ultimate form of the bed sediment distributions, it is argued that the method allows further insights into the processes controlling sediment sorting in the swash zone. In addition to this, "final" distributions of the types shown in Figure 59 have been sampled under known field flow conditions in the swash zone of the study beaches, so that it would seem reasonable to assume that similar processes have given rise to them (compare Fig. 59 with the curves of Figs. 49 and 59).

Figure 59 indicates six examples of sorting action affecting the bed sediment distributions. These in turn can be grouped into three classes depending upon the principal type of modification apparent. Thus, truncation of distributions forms the first class (Figs. 59A and C); transport of whole distributions a second (Figs. 59B and E); and the development of bimodal distributions a final group (Figs. 59D and F).

However, within each of the three major groups other effects are evident. It can be seen for example, that varying degrees of mixing can be associated with any of the major effects save for situations in which whole distributions are eroded (e.g. truncation and mixing as in Fig. 59C;

bimodality and mixing as in Figs. 59D and F). The diagram therefore serves to clarify the roles of differential rates of transport of individual size fractions. It is clear that within any of the three classes of modification the "end" result on the bed sediment distributions may involve alteration to any of the descriptive measures of mean size, sorting or skewness, or to all.

In Figure 59A for example, fines were eroded probably leaving a coarse-skewed distribution with little altered values of mean size and sorting. This process is even more pronounced in Figure 59C where truncation and mixing occurred in very small amounts. In the case of Figure 59A flow times favoured the swash ($A_t = 1.5$) so that material removed was probably deposited higher up the profile. Conversely, backwash flow of a transitional nature dominated the second example and the effects on the bed were comparatively minor. It should be noted that these two examples conform to the low energy sorting effect postulated by Eagleson, Glenne and Dracup (1963) and to the "surf break" model of Tanner (1966). In agreement with the latter author's suggestion, the break can be seen to be located in the pebble sizes at -2.0 to -3.0 ϕ units.

For situations in which transport of whole bed size ranges was evident (though the individual fractions moved at differential rates), the effects of sorting are less easy to

predict. However, both Figures 59B and E indicate little alteration in mean size but corresponding increases in degree of sorting. This can be seen to result from removal of either the coarse tail (Fig. 59B) or of the finer components (Fig. 59E). This type of grain size modification, which was not considered by either Tanner or Eagleson, Glenne and Dracup, has been shown to be extremely frequent on the study beaches where flow energy is high relative to the mean and maximum grain sizes present. Both of the curves shown relate to flow conditions dominated by the backwash and therefore conform to either transitional swash conditions (the samples being obtained from the scour zone in this case); or to high phase flow conditions.

The final type of effect observed, the development of bimodality in bed sediment frequency curves, is the most complex and has been the object of previous study. However, here there is a conflict in the interpretation of sediment distribution curves between Folk (1962) who attributes bimodal curves to a "source area" production of distinct modes and subsequent mixing of these; and Eagleson, Glenne and Dracup (1963) who attribute such curves to hydraulic action on the null point indicator sizes of the incipient motion and equilibrium motion diameters. Tanner (1966) on the other hand, implies the formation of bimodal distributions by selection of particular size ranges in the gravel fraction

under high energy conditions.

While it is not possible to resolve this problem from the present analysis where hydraulic action on sediments only has been considered, it is clear from Figures 59D and F that at least two processes deriving from hydraulic action alone can result in the production of bimodal sediment distributions in the swash zone. However, it should be remembered that the applicability of the source area concept of Folk to the sediments of the study beaches has already been demonstrated so that the processes evident in Figure 59 must be regarded as dynamic recombinations of particle size ranges which are probably supplied to the study beaches in unequal quantities.

First, Figure 59F indicates a bimodal distribution resulting from transport of the whole range of available sizes but with particularly intense erosion occurring in the pebble fraction at -3.0 to -4.0ϕ units. There is some minor mixing of fines, but the dominant sorting process would give rise to two almost equal, strong modes in the pebble and sand fractions. It should be noted that the available range of grain sizes in this case is very wide for both the bed and the flow so that the curves may be taken to represent selection and erosion of a range of sizes central to the distribution. This example therefore, is in agreement with Tanner's (1966) suggestion concerning the formation of bimodal sediments and it is significant that such distributions are

associated with pronounced bed scour at transitional or high phase conditions.

By contrast, another type of bimodal distribution is shown in Figure 59D. Here the modes are again pronounced but they involve widely differing proportions of material. Hence, a strong sand/granule mode dominates a lesser, secondary mode occurring in the pebble sizes. It is also clear that the secondary coarse mode is derived by deposition rather than by erosion as in the previous case.

This situation might be argued to be more akin to that proposed by Eagleson, Glenne and Dracup (1963) wherein D_i is much larger than D_e . The coarse mode thus represents the incipient motion diameter while the finer mode corresponds to the equilibrium motion diameter at that point in the swash zone. Conversely, the curve might be explained more simply as onshore transport of the main mode, present in relatively large quantities and actively undergoing transport; and deposition of a coarser mode some distance landward of the breaker by the swash. It is unlikely that the mode in the sand/granule fraction underwent equilibrium transport at the indicated flow state ($A_t = 0.71$) which was backwash dominated.

An important point arising from this is that distributions of a similar form may be produced near the base of the breaker where two modes in transit may be deposited at times when circulation of particles through the breaker is not possible.

Thus, an alternative explanation to the conventional "lag" explanation for coarse, bimodal sediments occurring near the breaker is that of deposition by decelerated backwash flow. It is possible that curves of the type shown in Figure 59F represent the winnowed "lag" type, while the "dump" type are more typified by unequal modal contributions of the kind shown in Figure 59D.

A further feature of importance is that bimodality produced by both mechanisms is more probable on mixed sand/shingle profiles exhibiting a wide range of sizes than on steep, pure shingle profiles where ranges of sizes are less. On the latter, the selective process may be reasoned to give rise to less well developed modal separation so that consequently, the dumping process by the swash at the upper parts of the foreshore would be a more probable cause of bimodality of bed sediments. It should also be noted that deposition at the upper part of the profile may result in polymodal as well as bimodal size-frequency distributions. In addition, one type of bimodal sediment distribution has not been discussed. A bimodal curve may also result from the addition of fines to a pre-existing unimodal, coarse size-frequency distribution.

Flow Phase State and Sediment Sorting. Since the distribution pattern of erosion and deposition in the swash zone depends upon the net transfer rates of bed materials and because the

former has been shown to be phase-dependent, it follows that both the locations at which characteristic sorting processes occur and the intensities of development of these processes will also be dependent upon the flow phase state.

For a shingle foreshore at low phase conditions simple truncation of the fine sizes low on the foreshore would occur and may be associated with positionally derived bimodality or polymodality higher up the shore. For increasing phase conditions, truncation would give way to transport of all sizes present with consequent decreases in skewness and increases in the degree of mixing of grains. Backwash scour may give rise to weakly bimodal distributions with accompanying increases in mean grain size. For the highest phase conditions very coarse sediments begin to move at high rates so that erosion of all size fractions occurs though there is a preference for offshore transport of the finer size grades.

On mixed sand and shingle profiles the processes are more complex. At low phase conditions mixing and truncation of distributions takes place on the lower foreshore. This gives rise to small alterations in mean size, but more significantly to fluctuations in sorting and skewness coefficients. On the upper foreshore polymodal or bimodal distributions may result from swash deposition or, alternatively, truncation of the fines by the backwash may occur depending upon the level of flow variability, ground-water storage levels, and stage of the tide.

At higher phase conditions suspension of fines becomes well developed in the zone near the breaker, as does backwash scour intensity higher on the shore so that an upper zone of depositional bimodality and a lower area of bimodal sediment distribution curves derived by selection of mid-range fractions may obtain. Alternatively, a lower zone of bimodal sediment curves produced by selection may be associated with an upper area of truncation, or whole range transport depending again upon flow variability and tidal stage. At extreme high phase conditions bimodality of sediments and erosion of all but the coarsest fractions on the lower foreshore would occur.

Sand lenses were observed to form at the swash limit under such conditions by Kirk (1967). It now appears that these originate as suspended load which is deposited by the swash at the landward limit of flow.

While the above sequence of changes in sediment size distributions is not exhaustive of the possibilities it is thought to closely reflect observed changes across and between flow types occurring on the study beaches; the more so, since the modifications to sediment size distributions resulting from differential rates and directions of transport agree very well with the observed sequence of morphological alterations occurring at different swash phase levels.

However, three further important features have yet to be examined. The first of these, the effects of particle

shape on sediment transport, is a much discussed problem which has received some study in the laboratory but which has been little studied from the point of view of operative processes on natural foreshores. Secondly, a number of workers have stressed the importance of both the relative elevation and intensity of outflow from the beach groundwater table as a modifying (possibly a controlling) influence in beach morphological alteration. Finally, some assessment of the variations in, and interactions between all of the above processes over the tidal cycle must be made.

Shape Sorting in the Swash Zone

It has been previously demonstrated that variations in particle shape will affect both the flow near the bed and the resistance to erosion because grain shape influences the drag coefficient and hence the critical tractive forces necessary to move a given particle. Similarly, motion of a grain settling from the flow will be affected by shape. For example, Sokolov (in Romanovskiy, 1966) found for coarse sand (0.3 to 4.0 mm.) that for grains of the same size class but different shapes, settling velocity could vary by a factor of more than two. Conversely, Sundborg (1956, p. 189) concluded that the influence of particle shape on critical erosion velocity is insignificant in comparison with the influences of grain size and density.

However, while particle shape appears to exert relatively minor influences on the fluid flow/sediment grain dynamic system it is well known that shapes are "sorted" into characteristic associations which give rise to distinctive depositional structures on many natural beaches. The interpretation of these features has been the object of much study since this provides a key to the interpretation of the genesis of paleo-sedimentary structures. Also, from the dynamic standpoint they are of importance since well developed imbrications of grains may strongly influence vectoral permeability through the deposit. Hence, vertical percolation velocities into the slope may be significantly different from those through the deposit in the plane of the gravity slope.

Kuenen (1964) has noted a preference for discoidal and flattened pebble shapes to occur in littoral environments and Sames (1966) argues that the main differences between morphometric associations of pebbles in rivers and on beaches lie in the lesser ranges of shapes and generally greater roundness of beach grains. Kirk (1967) demonstrated that shape sorting was only poorly developed both along and across the high energy, mixed sand and shingle beaches of the Canterbury Bight. In contrast to this well developed shape sorting zones giving rise to characteristic patterns of grain orientation and inclination (anisotropic apposition fabrics - Pettijohn, 1957) have been described by Krumbein

(1939), Cailleux (1945), Norrman (1964), Bluck (1967)

and others for pebble beach swash zones.

Norrman (1964, p. 109) notes that,

"on shingle beaches two types of orientation are found; one is dependent upon the way that the particles are transported, and the other on the reaction in the swash of the particles not transported. It is well known that, with regard to inclination, shingle on the middle and upper foreshore generally tends to be imbricated towards the land like an inverted roof slating. The material is predominantly affected by the uprush but not transported. . . . However, the reverse inclination with the axis inclined off the shore is found on the step as a result of the (backwash) and the (dominant) lifting action of the uprush".

Norrman also noted preferred orientations of pebbles in the horizontal plane which could be correlated with mode and direction of transport. Thus, grains rolled on the slope came to rest with their long axes perpendicular to the direction of motion while grains deposited from suspension had long axis orientations parallel to the flow line. Oblique orientations (with respect to the shoreline) resulted from the oblique swashes of incompletely refracted waves reaching the shore. Kirk (1967, pp. 72-75) observed similar orientation and inclination patterns of pebbles on the storm berms of mixed sand/shingle beaches in the Canterbury Bight but similar patterns were not observed in the active swash zone and shape sorting was not well developed.

Johannson (1965, p. 17) summarises the literature on grain fabric studies for fluvial and littoral environments

and suggests "that increasing velocity and turbulence cause diminishing stability, especially of flat particles High velocity, turbulent flow also causes decreased regularity of orientation", so that the patterns observed for the storm berms of the Canterbury Bight may reflect zones of low or declining flow energy relative to grain size and density. It will next be demonstrated that this situation is partially responsible for the lack of well defined shape sorting in the swash zone of the present study beaches.

Table 12 presents the distributions of shapes occurring in 15 samples from a total of 42 for which shape distributions have been analysed. These 42 samples are considered to be representative of the range of shapes and shape sorting occurring in the 131 suspended load samples for which mean nominal diameter and settling sphericities were computed.

From Table 12 it can be seen that blade shaped particles are by far the most frequent on the study beaches. There were very few spherical particles or elongated grains present in the distributions. This was also found to be the case with the greywacke-derived sediments of the Canterbury Bight which are comprised of over 95% bladed and disc-shaped grains and only 2.5% spheroidal grains (Kirk, 1967).

Form ratios listed for the samples confirm that the dominant shape is bladed. Positive values of the ratio indicate a prevalence of disc-shaped or platy particles;

TABLE 12

% Pebble Shapes in Samples From
Swash and Backwash

| Form Class | 1 | 2 | 3 | 4 | 5 | 6 | 7 | 8 | 9 | 10 | 11 | 12 | 13 | 14 | 15 |
|--------------------|-------|-------|-------|-------|-------|-------|--------|-------|----|----|----|----|----|----|----|
| Compact | 8 | - | 8 | 4 | 4 | - | - | 4 | 8 | 4 | - | - | 4 | - | 4 |
| Comp. -Platy | - | 4 | 24 | 8 | 30 | 4 | 12 | - | 8 | - | - | 4 | 8 | - | 8 |
| Comp. -Bladed | 20 | 20 | 8 | 12 | 12 | 12 | 8 | 32 | 16 | 32 | 16 | 24 | 32 | 4 | 32 |
| Comp. -Elongate | 12 | 16 | 4 | - | 20 | 4 | 8 | 4 | 20 | 20 | 8 | 8 | 8 | 28 | 16 |
| Platy | - | 4 | 16 | 8 | 20 | 24 | 28 | 16 | 16 | 8 | 8 | 8 | 8 | 12 | - |
| Bladed | 36 | 36 | 36 | 48 | 12 | 44 | 32 | 40 | 20 | 24 | 32 | 12 | 24 | 20 | 24 |
| Elongate | 12 | 12 | - | 16 | - | 8 | 4 | - | 12 | - | 24 | 8 | 16 | 28 | 12 |
| Very Platy | - | - | - | 4 | 4 | - | - | - | - | - | 4 | 1 | - | 4 | - |
| Very Bladed | 16 | - | - | - | - | - | 8 | 4 | - | 8 | - | - | - | 4 | - |
| Very Elongate | - | - | - | - | - | 4 | - | - | - | - | 4 | - | - | - | - |
| | | | | | | * | | * | | * | * | | * | | |
| FORM RATIOS | -0.19 | +0.29 | +0.04 | +0.27 | 0.0 | -0.42 | -0.17 | -0.3 | | | | | | | |
| | | -0.14 | -0.02 | +0.06 | +0.14 | -0.04 | +0.125 | -0.42 | | | | | | | |

* Backwash samples

negative values a dominance of rod-like or elongated pebbles. Values near zero reflect a dominance of bladed pebbles or subequal amounts of platy or elongate pebbles (Sneed and Folk, 1958, p. 141). Values of this ratio for Canterbury Bight sediments ranged from 0.8 to -0.4 (Kirk, 1967, pp. 69-70), as compared to 0.29 to -0.42 for the values shown in Table 12. It is therefore clear that even though the range of sizes is extensive the range of shapes occurring on the study beaches is not wide. This constitutes one reason for the lack of well developed shape sorting in the swash zone. That is, "selection" for grain shape is well established for greywacke sediments in that only a narrow range of shapes is contributed to the shore. Kirk (1967, pp. 78-81) could find no statistically significant difference in either grain shape or roundness between the fluvial and littoral environments in the Canterbury Bight, and Dickson (1969) found only weakly significant differences between these environments in the Kaikoura area.

From Table 13 it can be seen that there is also little variation in shape with size of particle. Mean effective settling sphericity ($\bar{\Psi}$) varies over only 0.1 sphericity units (10% of the available range), while shape sorting coefficients range over only 0.01 sphericity units for mean nominal diameters ranging from 2.67 to 13.49 mm. A more detailed analysis of shape variation with grain size was undertaken for individual

TABLE 13

Mean Settling Sphericity, Shape Sorting
and Mean Size of Swash Zone Samples

| Sample No. | $\bar{\Psi}$ Mean Eff. Sett. Sphericity | σ_{Ψ} Shape Sorting Co-eff. | $M_z D_n$ Mean Nominal Dia. MM. |
|------------|--|--|------------------------------------|
| 1 | 0.64 | 0.09 | 2.67 |
| 2 | 0.68 | 0.08 | 4.50 |
| 3 | 0.67 | 0.11 | 2.82 |
| 4 | 0.66 | 0.09 | 3.41 |
| 5 | 0.68 | 0.09 | 2.93 * |
| 6 | 0.64 | 0.08 | 3.68 |
| 7 | 0.61 | 0.08 | 4.44 |
| 8 | 0.65 | 0.1 | 4.05 * |
| 9 | 0.71 | 0.11 | 6.17 |
| 10 | 0.70 | 0.10 | 5.95 * |
| 11 | 0.67 | 0.09 | 6.52 * |
| 12 | 0.68 | 0.11 | 13.49 |
| 13 | 0.69 | 0.08 | 7.51 * |
| 14 | 0.67 | 0.09 | 6.8 |
| 15 | 0.71 | 0.09 | 5.76 * |

* Backwash Samples

size fractions by Kirk (1967, Table 11) and this demonstrated similarly low levels of variability in shape with size.

Because of this little range in mean shape ($\bar{\Psi}$) or form ratio could be detected for sediments trapped at different elevations above the bed; or for bed sediments trapped at different points across the shore. Thus, any shape selection effects occurring on the study beaches would be weakly developed because of the small range of available shapes and the lack of variation in either mean shape or in the various proportions of shapes comprising samples, with variation in mean grain size.

However, given any range of particle properties, selection for shape also depends upon fluid flow characteristics so that the potential for the sorting of different shapes into characteristic fabric patterns will be conditioned by the level of flow energy and turbulent structure.

In this regard it has already been shown for the swash zone of this investigation that particle drag coefficients indicate fully turbulent flow around the grains. Shape influences are therefore minimal in the selection of pebbles for transport so that for the larger grains shape sorting is not well developed. However, orientation of grains in transit, whether they are above the bed, or rolling and sliding on it, does occur.

It is therefore interesting to note that in a high energy environment such as that of the study beaches where sediments

are transported at high rates, it will be the smaller grains (in the sand and granule sizes) which have lower Reynolds Numbers and higher drag coefficients, that will receive the greatest potential for shape sorting. This is because the flow will be transitional between laminar and turbulent around such grains in the immediate vicinity of the bed, and for given sizes will become turbulent over the more irregularly shaped particles. Similarly, shape sorting of pebbles may occur in a small area of the swash zone near the landward limit of flow where current speeds and turbulence are lower.

Thus, just as critical size-sorting in the swash zone was shown to occur only for a narrow range of grain size/flow energy conditions, so shape sorting (even for a narrow range of available shapes), is controlled by the level of flow energy. Orientation and imbrication patterns become unstable at high velocity, macro-turbulent flow conditions for the same reason that the size/velocity relationship deteriorates with increasing energy; i.e. sediments of all sizes flow at high rates. The important consideration under these conditions has been shown to be the net rate at which a given quantity of any particular size range is added or removed from the bed.

From this it is now argued that zones of established shape sorting high on storm berms of mixed sand and shingle

beaches reflect zones of low and declining swash energy in which the fluid flow responds more critically to differences between particles of diverse shapes and sizes. Therefore, the development of pronounced shape sorting on a pebble beach may well prove to be an indicator of short term approximate balance between the available ranges of sizes and shapes and the flow energy applied to them in the swash zone of the study beaches. The analogy applied to shape sorting here is with the development of current ripples which appear on the bed at current speeds only slightly in excess of that required for grain motion, and which are destroyed as the current speed increases further. Clearly, this is a hypothesis in need of detailed examination across a wide range of particle shape and flow conditions.

Sorting of Sediments by the Groundwater Sheet

There are at least two important aspects of groundwater storage which affect the processes of erosion and deposition occurring on natural foreshores. The first of these, the position of the water table relative to still water level, has been demonstrated to profoundly influence backwash energy and sediment entrainment by both swash and backwash. This aspect has been studied by Grant (1948); Emery and Foster (1948); Duncan (1964); and more recently in a quantitative fashion by Harrison (1969) - in press.

The second aspect, entrainment and transport of sediments by escaping groundwater, is a more direct effect but is probably quantitatively less significant in terms of amounts of sediment transported. Nevertheless, important micro-morphological features result from the short periods of surface runoff following each backwash.

Fluidisation of the bed by outflow under the backwash and the attendant rapid recovery of backwash volume has already been discussed. It was demonstrated that a "dry" foreshore with a low water table is conducive to swash deposition while a high water table yielding a strong outflow of percolated water results in backwash erosion. Both Grant (1948) and Emery and Foster (1948) show that because of lags in the adjustment of water table level to tidal fluctuations in still water level these conditions alternate throughout the tide. Hence, swash deposition may occur in the flood tide period when the water table is low relative to still water level, and strong scour in the ebb tide period when the falling water table lags behind the descent of still water level on the shore by up to three hours.

The second process, sorting by the groundwater surface sheet, has been studied by Demarest (1947) and Evans (1951) from the standpoint of conditions favouring the development of rhomboidal ripple marks and rills. Also, Emery and Foster (1948) demonstrated from an analysis of outflow from

a sand beach water table that velocities were sufficient for the elutriation of fine silt particles and concluded that rill marks denoted erosion by effluent groundwater at low tide.

Clearly, the controlling influence on both of these factors for a given flow regime and stage of the tide is the permeability of the beach deposit which Krumbein and Monk (1942) have shown to vary as the square of grain diameter and as the inverse exponent of sorting. Hence, for a given mean grain size a well sorted deposit is more permeable than a poorly sorted one and escape velocities will be higher from the former than from the latter. Because of this Powers and Kinsman (1953) argue that for given flow energy conditions the permeability of the sediment is the most important factor determining the depth of the zone of bed disturbance ("traction zone").

As well as this, differences in directional permeability (because of grain lamination and imbrication) have already been noted. Landon (1932) highlighted the importance of this aspect by suggesting that permeability in the vertical direction and surface runoff are inversely related. Stratification of grains in the foreshore thus affects vertical percolation rates whereas neither the bulk porosity of the deposit nor the permeability in directions parallel to the bed are necessarily affected. In agreement with this are

the results of Bryson (1956) who measured the permeability of laminated sands in three mutually perpendicular directions; vertically into the deposit, parallel to the shore in the horizontal plane, and at right angles to the shore in the horizontal plane. Average results for nine sets of measurements demonstrated maximum permeability at right angles to the shore (75 Darcies); minimum permeability in the vertical plane (36 Darcies), and intermediate values parallel to the water line (61 Darcies).

The 42 estimates of effective field permeability obtained during this investigation were derived by the Fluoroscein dye injection technique discussed previously and therefore apply to flow through the beach deposit in the plane parallel to the bed. No systematic study of the effects of tidal rise and fall of the beach groundwater table was undertaken but certain general statements concerning this effect have already been made.

Table 14 shows mean permeability and percolation velocities for three of the stations of the study area. As stated previously these values relate to the upper portion of the swash zone (where up to one third of the swash volume may be stored because of vertical infiltration), and are means from a number of trials amongst which variation was high. For station B, for example, which is a steep, well sorted pebble profile, permeability values were highest and most

TABLE 14

Mean Field Permeabilities Determined by
By Fluorscein Dye Injection

| Station | M_z ϕ | Sorting $\sigma_{I\phi}$ | Mean Permeability DARCIES | Slope | Mem Perc. V. cm/sec. |
|---------|-----------------|-----------------------------|---------------------------------|--------|-------------------------|
| B | -3.1 | 0.23 | 1,017.7 | 11°50' | 5.9 |
| C | -1.32 | 0.35 | 472.7 | 7° | 2.2 |
| D | -0.57 | 0.98 | 292.5 | 4° | 0.75 |

N.B. One DARCY = 10^{-8} cm²/second.

uniform (974.4 to 1,041.5 Darcies). At station C where some sand is intermixed with the pebble fraction permeabilities are much lower, as are the rates at which flow through the beach deposit occurs (see Table 14). Additionally, permeabilities measured at three feet intervals along the shore near the swash limit are more variable (649.5 to 2,046.4 Darcies) than on "pure" deposits. This would suggest in turn that there may be significant areal variations in erodibility related to fluctuations in grain size composition in the upper swash zone of mixed sand/shingle foreshores.

At station D there are well developed sand lenses on the upper foreshore and sorting tends to be poorer than for the stations just discussed. Hence, permeabilities are lowest along the profile at the locations of these lenses. However, it is important to note that because the sand fraction is concentrated in a discrete zone of the shore, very wide variations in effective permeability can occur within a few feet both along and across the shore. In turn wide ranges of percolation velocity must be expected over short distances on such deposits.

Finally, it can be seen from Table 14 that the field permeabilities obtained during this investigation are considerably higher than those recorded by Bryson (1956) for sand foreshores so that the potential for sediment entrainment must be regarded as correspondingly greater.

Though it is possible to obtain reliable estimates of the downslope surface velocities in the effluent groundwater sheet, it is very difficult to assess the sediment transport capacity of these flows since the flow depth is so small that surface tension effects become important. It is therefore difficult to determine the degree of flow turbulence.

All of the flow velocities shown in Table 15 were obtained by timing the passage of dye patches over measured distances but in no case was the flow depth more than two centimeters. However, it is clear from the table that appreciable downslope velocities were attained by some of these flows. As a rough guide to transport potential several pebbles and granules rolled downslope by the groundwater sheet were collected and measured (intermediate axis) with calipers. The faster flows of Table 15 moved maximum diameters of 8.0 mm. while granules were freely transported by the slower flows.

Demarest (1947) observed the formation of rhomboidal ripple marks under similar conditions on sandy beaches (for slopes of 6 to 12° and for flow sheet speeds of approximately 60 cm/sec.). Plate 10 shows that similar features could be developed at the sites of sand lenses on the study beaches. In contrast to this, rills are developed on the more freely draining, coarser gravel deposits, as can be seen from Plate 11. Rills in such gravels may be up to 3 cm. deep and several cm. wide. Large pebbles were frequently observed to move

TABLE 15

Velocities Attained by Effluent
Groundwater Runoff

| <u>Slope</u> | <u>Velocity</u> <u>cm/sec.</u> |
|--------------|-----------------------------------|
| 4° | 50.6 |
| 4° | 15.2 |
| 4° | 23.37 |
| 4° | 7.6 |
| 5° | 13.36 |
| 4° | 30.5 |
| 10°30' | 30.5 |
| 4°30' | 30.5 |

N.B. Velocities determined by dye patch method.

down these channels by rolling and sliding. An important feature of rills evident in Plate 11 is that their channel axes may be directed obliquely across the shore and not down the line of greatest surface slope. Presumably, this is because the development of rill axes follows the line of greatest hydraulic slope (which is conditioned by the trend of permeability across the shore), rather than the line of maximum topographic slope; the two gradients not necessarily being directionally coincident.

As concerns sorting effects produced by these flows, it is probable that the role of the groundwater sheet is minor since its effects are intermittent, short lived and are superseded by each new swash. However, it is clear that intensive study of the role of the groundwater table may yield new insights into foreshore processes.

For example, sufficient evidence has been presented concerning lateral and shore-normal variations in effective permeability to warrant detailed assessment of this factor in relation to the little-known processes of beach cusp formation. Though waves break parallel to the shore and both swash and backwash follow the line of greatest topographic gradient, inherent areal variations in foreshore permeability (and hence erodibility) may result in considerable lateral motion of water within the beach deposit and on the surface in the groundwater sheet. Considerable relocation of the

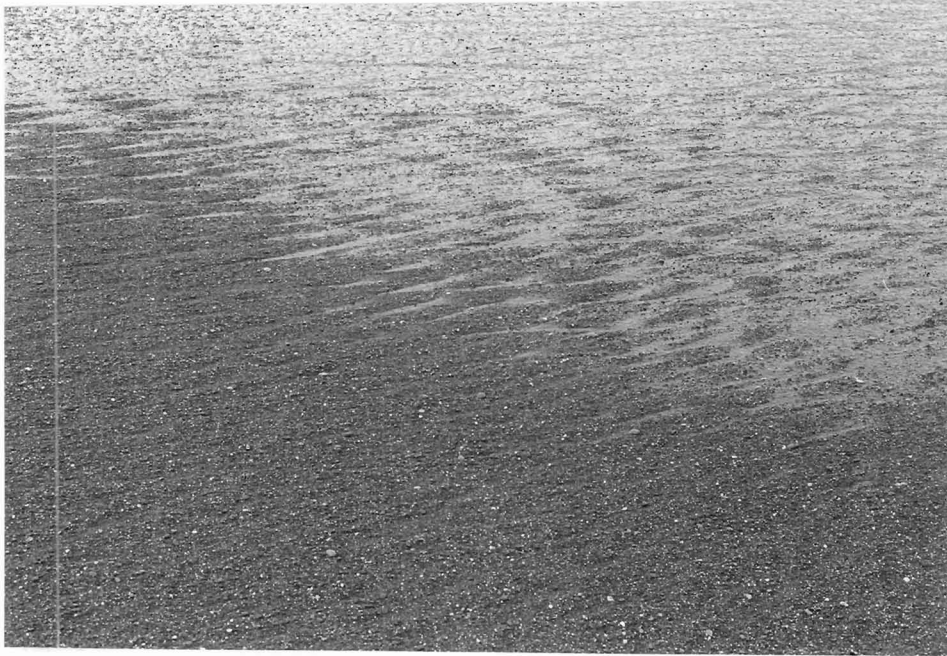


PLATE 10. Rhomboidal ripple marks at station C. Note that the water table is high and that the bed is comprised of mixed sand and pebbles.



PLATE 11. Well developed rills at station D. The water table is high but the grain size is much coarser. Note that the rill axes are aligned oblique to the shoreline.

finer fractions of the beach deposit may take place in this way.

Concerning the role of the tide-dependent rises and falls in the water table level and the effects of this on scour and deposition by the main flows it has been shown that considerable differences exist between pure pebble and mixed sand/shingle deposits. The lag effect created by groundwater storage will be more pronounced on the finer, less well sorted mixed deposits than on freely draining gravels.

The manner in which this process acts in concert throughout the tidal cycle with those previously detailed will next be described.

TIDAL VARIATIONS IN SWASH ZONE

PROCESSES

The principal effects of the tides on morphologically significant processes occurring in the swash zone have been shown to consist of rhythmic variations in flow energy at given points across the shore as the water level rises and falls. This fluctuation in energy results from varying flow depths and structures and from the water table effects previously discussed. Hence, given points on the bed may undergo periods of successive or alternating scour and deposition through the tidal cycle. Strahler (1964) has demonstrated that if equilibrium conditions prevail over the tidal interval then the foreshore will be restored to the original conditions of grain size composition, bed slope and bed elevation at the end of the cycle. The present study has established the conditions resulting in this "equilibrium" form in relation to other types of morphological response pattern encountered in the swash zone and has detailed the processes which give rise to all of these.

It is now proposed to conclude the analysis with an examination of the variations in flow energy for different positions across the shore at all stages of the tide.

Following this one example of the fluctuations in, and inter-relations between several flow parameters and bed response factors over a single tide will be presented. This will be for transitional flow conditions (quasi-equilibrium) on a shingle profile and effects occurring under other types of flow regime on other types of profile will be described in relation to this standard.

Variations in Flow Energy Through the Tide

Figure 60 presents a summary of all the data pertaining to mean swash energy, mean backwash energy, and mean relative energy that were gathered at different tidal stages during the course of this investigation. It is important to note that these data are derived from many positions in the swash zone, from different slopes and for different flow regimes, breaker heights and periods. Also, the study beaches are meso-tidal in that maximum spring range is 6.3 feet and neap range is only 5.4 feet. The tides occur at semi-diurnal frequencies.

Reference to the diagram will show that grand mean curves have been superimposed on the energy envelopes in order to indicate trends in energy level throughout the tide for three levels on the foreshore. These are first, the upper swash zone ($x/L_0 = 0.0$ to 0.04); secondly, the central foreshore ($x/L_0 = 0.08$ to 0.12); and finally, the lower foreshore near

FIGURE 60. Variations in mean energy envelope curves through the tidal cycle. Data are those for all breaker heights, periods and profile stations sampled. Grand mean curves are plotted for the upper foreshore ($x/L_0 = 0.0-0.04$); mid-shore ($x/L_0 = 0.08-0.12$) and lower foreshore ($x/L_0 = 0.16-0.20+$).

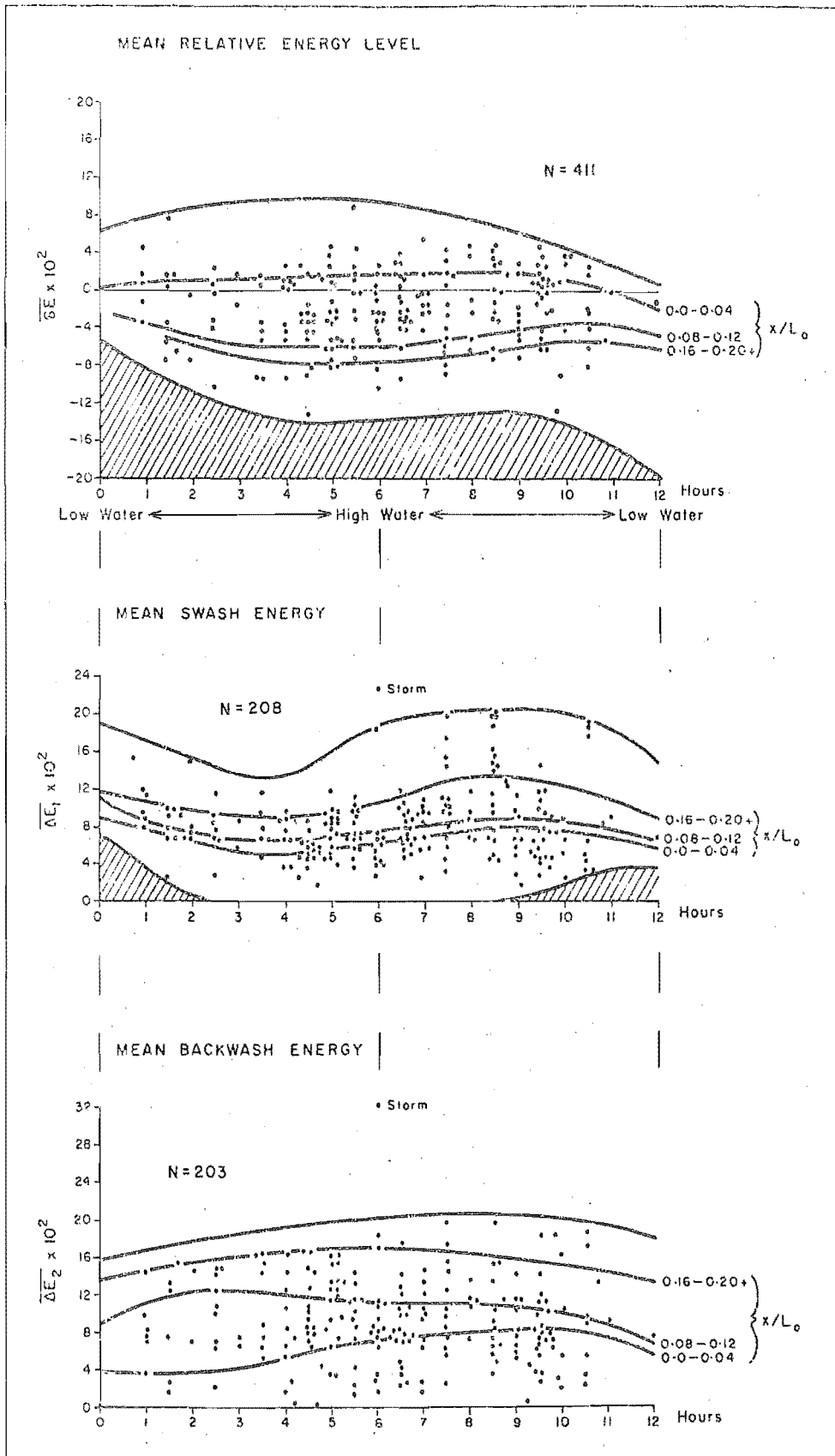


FIGURE 60. Tidal fluctuations in mean energy envelope curves.

the breaker ($x/L_0 = 0.16$ to $0.20+$).

From the curves for mean relative energy level it can be seen that the main effect of the tidal rise is to increase the offshore energy component for any given station and since it was earlier demonstrated that there is little tidal translation of the breaker zone on the study beaches it is evident that the effect derives from increased flow depths, volumes and turbulence toward the time of high water.

Further, it can be seen that net onshore energy prevails in the zone of swash seepage on the upper foreshore throughout the tidal cycle. For the central and lower foreshore zones net offshore energy is at a maximum in the period immediately preceding high water when the water table is still located low on the foreshore and contributes to the backwash at these positions.

Consequently, swash energy can be seen to be at a maximum for all stations in the period after high water when the water table is high and infiltration losses are relatively small. This is an important finding which has not been stressed by previous workers. While the importance of groundwater storage in relation to backwash energy was stressed by Grant (1948), Emery and Foster (1948) and Duncan (1964) none of these studies detected the action of a corresponding effect on the swash which exhibits a time lag effect comparable in importance with that noted for the backwash. Therefore, the

different morphological responses attributed to flow over "dry" and "wet" foreshores by Duncan (1964) must also be applied to swash action. It will later be shown that this can profoundly influence net transport rates of bed sediments at different stages of the tide. This finding adds a further aspect to the importance of the groundwater table in controlling foreshore morphological changes.

From Figure 60 it can be seen that water table effects on the swash appear at all positions across the shore but the magnitudes of the fluctuations decline with distance landward of the breakers. This is because the bed is permanently saturated at the lower stations.

Mean backwash energies, on the other hand, can be seen to exhibit more complex tidal fluctuations. Thus, the upper swash zone reflects the expected trend resulting from displacement of the water table so that maximum energy occurs some time after high water. However, for positions on the central foreshore it appears that backwash energy is at a maximum early in the tide when there is strong outflow from the effluent zone at this position. As the tide, and subsequently the level of the groundwater table, rises backwash energies remain high since the flow receives water discharged from the beach deposit at positions higher on the profile.

Low on the foreshore near the breaker the grand mean

curve of backwash energy is very low in amplitude and little time lag is noticeable. This is because stations in this area receive backwash flows containing large components of effluent water at all stages of the tide. However, there is some increase in quantity later in the tide so that backwash energy level for the mid-tide and early ebb tidal phases is slightly greater than at times of low water.

Finally it should be noted from the diagrams that the energy levels of storms far exceed the range of prevailing energy conditions encountered during tidal cycles occurring at lower phase swash conditions.

The Tidal Cycle of Changes in Morphological and Sediment Characteristics

As an example of the interrelations between water table effects, tidal characteristics and flow regime Figure 61 presents plots of several flow and bed response characteristics over one complete twelve hour tidal cycle. The experiment was conducted at station A, a steep shingle profile ($7^{\circ} 50'$) made up of a wide range of grain sizes (granules to cobbles). Breaker height for the experiment averaged 3.0 feet and there was little variation in height or form, most breakers occurring as plunges. Mean wave period was 8.5 seconds and phase difference ranged from 0.68 to 0.80 through the tide. Flow conditions were therefore transitional in nature. A stake was set in the foreshore at the mid swash position

($x/L_0 = 0.013$) at low tide and all subsequent measurements of bed elevation, grain size, bed-load transport rate, flow velocities and energies were made at this point. At high tide the observation point was located at $x/L_0 = 0.121$ and was therefore situated (in terms of flow dynamics) in the lower swash zone. By the succeeding low tide level the station was located at $x/L_0 = 0.05$ thus indicating some net increase in swash length over the full tidal period but this effect was not large.

The first important feature apparent from Figure 61 is that both swash and backwash velocities were maximised at high tide. It is interesting that backwash velocity (as compared with backwash energy) exhibits the greater fluctuation through the tide as a result of water table oscillations. However, time lags in the flow velocities did not occur for either swash or backwash. Another notable feature evident from the diagram is that the distributions of maximum velocities across the tide are reflected in the mean nominal diameters of the bed load for both swash and backwash. Thus, mean nominal diameters of transported sediments were greatest in both swash and backwash at high tide. Significantly in the light of the processes previously demonstrated it is clear that though maximum sizes and maximum velocities coincided in time, maximum velocities and rates at which the sediments were transported did not correspond. Also, for these transitional (near equilibrium) flow conditions it is

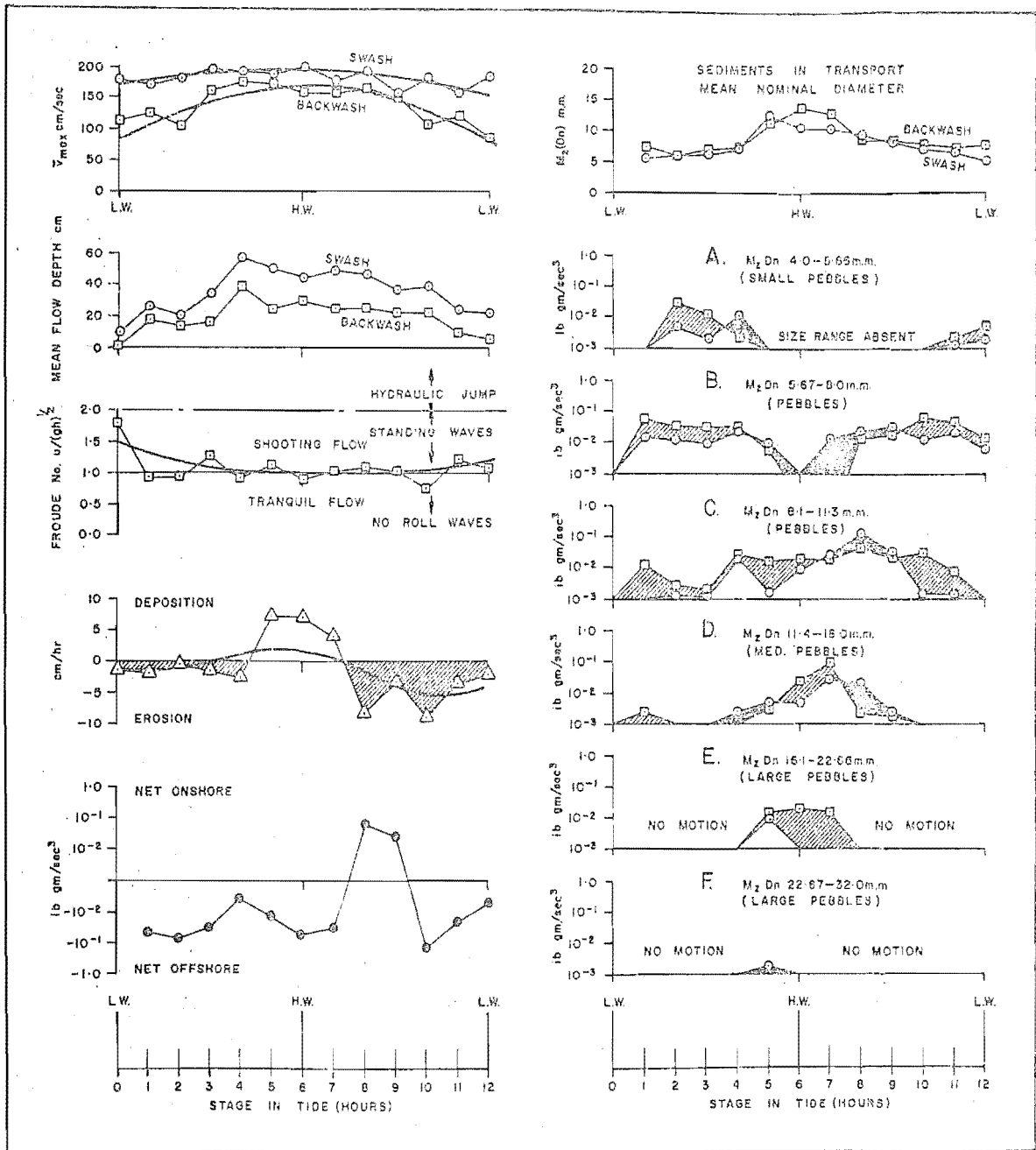


FIGURE 61. Characteristic tidal cycle of transition conditions on coarse gravel. $H_b = 3.0'$; $T = 10.0$ secs.; $t/T = 0.68$ to 0.80 .

significant that original conditions of mean grain size were restored in both swash and backwash by the end of the tidal cycle.

The tidal effects on flow depth are also clear from the diagram, swash depths being consistently greater than for the backwash. The groundwater storage effect on flow in both directions is apparent from the fact that depths increased uniformly before high water but lagged at high values for a substantial proportion of the ebb tide.

As discussed previously this feature is reflected closely in the tidal distribution of backwash Froude number at the observation point. The potential for scour by the formation of hydraulic jumps and/or standing waves was clearly highest during the early and late phases of the tidal cycle, flow at the observation point tending toward the tranquil state for the hours around high water. Note that the tidal distribution of erosion and deposition on the bed corresponds very closely to the pattern of flow turbulence.

The pattern of bed disturbance can be seen to be of the transitional type described by Strahler (1964) as the equilibrium form. Only slightly more material was removed over the tidal cycle than was supplied and the observation point moved through a cycle of erosion, deposition and subsequent further erosion. The succession of profile changes described by Strahler was therefore mirrored at one

point on the bed. However, it should be noted that the data apply to one point on the bed only and that other patterns may have been obtained higher and lower on the profile. Confirmation of the previous suggestion that the scour zone is not wide in extent at transitional flow levels is also provided by the diagram since the two scour phases are separated by a period of deposition.

Again confirming previous analysis is the evident correspondence between net transport rate of bed-load sediments and flow structure, the latter parameter here representing flow power, turbulence and asymmetry. There is however, a strong lag in the correspondence between the times of foreshore deposition and of maximum net onshore transport. This very interesting finding serves to provide confirmation of the "wet" and "dry" foreshore effects produced in the swash and backwash by tidal variation in the level of the beach water table. Thus, the period of maximum net onshore transport occurred after high water when the water table was high, the bed around the observation point was saturated and infiltration losses from the swash were lower. The swash therefore possessed increased transport capacity at this time and net onshore transport was established. Also, comparison with the bed elevation changes suggests that this period of onshore transport reflects the removal of sediment deposited at high water to a position higher up the profile near the swash limit.

Concerning the sediment sorting processes operative during these near equilibrium flow conditions it can be seen from the plots of the movements of individual size fractions that a wide range of sizes was transported in markedly different quantities and directions throughout the tidal cycle. Given sizes moved in different directions at different positions on the shore and in different directions for given positions at different times.

Thus, in accordance with the measured pattern of bed scour fines and mid-size fractions were eroded for the early flood and late ebb phases of the tidal cycle. An important feature of the rate of sorting plots in relation to tidal fluctuation in flow energy is the fact that fine grains disappeared from the bed-load for much of the central, higher energy stages of the tide. From the incidence of deposition at high water and from the reappearance of fines at a late stage in the tide it seems reasonable to conclude that the fine fractions were buried early in the tide and re-circulated after excavation in the falling tide. Conversely, increasingly coarse grains were entrained and transported by both swash and backwash for the high energy period around high water. In fact, it can be seen that the largest sizes present could only be moved at low rates by the swash for a short interval at high tide.

The sorting curves also reflect a time shift in the

deposition phase of fine and mid-range fractions. That is, fine grains were deposited before high water and were then buried; mid-range sizes were then deposited at high water, and coarser grains were deposited both before and after high water. The erosion of very coarse grains by the backwash occurred at maximum rates after high water when the groundwater table exerted maximum effects on backwash volume and energy.

In terms of selection, truncation and mixing processes operating on the bed grain size frequency distributions it can be seen by reading selected verticals through the diagram for the early tidal stages that initial sorting effects resulted in truncation of the fine and mid-fractions from the shore, leaving coarse skewed distributions. By mid-flood tide (hours 3-4) flow energies were sufficient for the development of selective bimodality. That is, fines were being deposited as were the coarser grains while the mid-fractions were selectively eroded. Note that this occurred during scour phase conditions.

By the time of high water, bimodality was still present but the mid-range fraction now subjected to selection included an even wider range of sizes than previously. Thus, sorting coefficients decreased and kurtosis of the distributions increased. It should also be noted that this sequence of grain size modifications for the rising tide begins with the low energy sorting process described by Eagleson, Glenne and

Dracup (1963) i.e. truncation where D_i is less than D_e and develops through selection of ever larger sizes to the bimodal condition in which according to the above authors D_e exceeds D_i .

At mid-ebb tide, when net bed-load transport was in the onshore direction, mean grain size of the sediments in motion decreased considerably and mixing of the fines and mid-range fractions with bed sediments is indicated. Fine skewness of bed distributions was therefore developed as buried fines were excavated by bed scour and entrained in the flow.

By the end of the tide (hour 12) mean size was almost fully restored to original levels and the truncation and erosion of the fine tails of bed sediment distributions again occurred. However, sorting at this end stage of the experiment was better than initial levels because a narrower range of the fine and mid-fractions was being removed. Four fractions were transported early in the tide as opposed to three in the later stages. Additional to these size-sorting effects it would be logical to expect the maximum development of shape-sorting under transitional conditions such as those just described but no study was made of this aspect during the experiment.

Thus, under these transitional, near-equilibrium flow conditions it has been shown how the initial conditions of elevation and grain size composition were recovered by the

end of the tide cycle, and the processes responsible for a 15.5 cm. fluctuation in bed level and a 9.0 mm. excursion in mean nominal diameter and the return to initial conditions have been presented and described. It is concluded that it is therefore useful to employ this sequence as a model of the complex relations among and between the many process and response variables operating at transitional flow conditions on mixed beach foreshores characterised by a wide range of available grain diameters. Against this other types of flow regime and profile morphologies may be measured and described.

Hence, for lower and higher phase flow regimes these tidally controlled effects on flow and sediment sorting processes are superimposed on all of the underlying processes already described. Thus, for low phase conditions characterised by minor flow asymmetries of velocities, pressures and times, and for which the flow is dominantly tranquil and the backwash weak; the profile builds and truncation of the fine tails of sediment distributions results. There is a minimum effluent effect on both the swash and backwash and bimodality or polymodality of sediment size distributions may result from preferential deposition near the swash limit. Net changes in mean size, sorting and skewness over the tidal cycle would be most apparent at high water but very small over the whole tide cycle.

For higher phase conditions asymmetries of flow times,

pressures and velocities are at a maximum. There is fully developed circulation through the breaker, flow times are dominated by the backwash and the swash tends to be under-ridden. Macro-turbulence in the backwash is fully developed and interference between masses of water moving on and offshore is frequent. The water table effect is at maximum development and the scour zone of hydraulic jumps and standing waves is very wide. Suspension of sediments of the finer size grades occurs in large quantities in both swash and backwash and fluidisation of bed sediments by groundwater outflow under the backwash may be pronounced. The profile erodes rapidly leaving bimodal sediment distributions, or where the range of sizes is less, uniformly removing whole size ranges seaward. Some sediment is thrown high on the profile to build storm berms and the steep seaward faces of these may present characteristic orientation and imbrication patterns of cobbles and pebbles.

On mixed sand/shingle profiles with poorer sorting and lower mean grain sizes these conditions yeild very high rates of erosion which are again maximised in the falling limb of the tide cycle. Whole range transport of all available sizes occurs and antidunes may develop in the backwash. Some sand may be deposited at the swash limit to form extensive lenses mantling the surface. Strong rill action will be developed particularly during the ebb tide when the outflow

from the groundwater table occurs at maximum rates.

Sediment moved offshore through the breakers as suspended load is lost sub-permanently to the beach face during these conditions.

CONCLUSIONS

The present study has centered around the building and application of instruments designed to sense a range of process and response variables thought to be significant indicators of morphological change and sediment transport in the swash zone. It must be stressed that all of the results apply to two dimensions, the vertical and the horizontal, both of which are oriented normal to the shore. Additionally, the results derived from the investigation apply only to mixed sand shingle beaches with steep nearshore beach toe slopes and where there is little tidal translation of the breaker zone. The results of this study cannot be extrapolated to sand beach foreshores where slopes are lower, the surf zone wider and more complex, where considerable tidal translation occurs, and where suspended load transport is extensively developed.

This study has yielded new insights into processes that have long been generally understood as well as demonstrated some new measures describing swash zone morphological change. Also, much knowledge concerning the interplay between factors under varying energy conditions has been gained.

To this extent the original aims of the investigation

have been more than fulfilled because the foregoing sections have developed what is thought to be the first coherent general theory and comprehensive account of swash zone processes which will explain the frequently observed wide variations in foreshore morphology and sediment characteristics. The spatial and temporal variations in the latter features which result from different wave conditions reaching the swash zone have also been described. It is thought that the study therefore opens many new problems appropriate to examination by geomorphologists and other specialists concerned with the littoral environments.

Perhaps somewhat less successfully, the study has linked the processes responsible for swash zone erosion and deposition with those of sediment sorting over a wide range of sizes for different flow regimes, positions on the shore and stages of the tide cycle. Certainly the characteristic processes giving rise to commonly encountered forms of bed sediment size frequency distributions have been determined. However, the specification of particular effects produced at discrete points on the bed under given flow regimes is difficult because the final result is universally conditioned in some measure by grain size components which are antecedent to the situation under study. Apart from cases where this element was known the sorting processes described in this investigation refer therefore to potential sorting effects

on unit distributions containing large ranges of sizes of approximately uniform density (2.65 gr/cm^3).

Another feature of the investigation is that it has yielded a large body of quantitative data on flow pressures, asymmetries, velocities, durations, turbulent exchange levels, flow depths, sediment transport rates and depths of disturbance etc.; from a range of natural beach foreshores. As well, many notions developed in laboratory experiments and in theoretical analyses have been subjected to varying degrees of assessment under field conditions. It is hoped that together with the data gathered, this will enable the extension of beach research through comparisons between field and laboratory results, between different types of natural beach and wave environments, and by enabling more rigorous testing of the present theory both in the field and in the dimensionalised models constructed in wave tanks.

Concerning swash zone processes one main conclusion emerges paramount above all others; Framing all of the processes outlined in this report is the overriding significance of phase relations in the flow. The importance of this factor, first isolated and defined by Kemp (1958), has recurred at all levels throughout the analyses of both process and response factors in the swash zone. Almost all of the flow events described and their morphological responses have been demonstrated to be phase-dependent.

Flow near and landward of the breaker is so asymmetric that phase relations between incoming and outgoing water masses control the initiation, location and intensity of bed scour, the levels of bed sediment entrainment, transport and deposition by swash and backwash; and the type of sorting pattern imprinted on any given distribution of bed sediment sizes.

The phase difference parameter thus has more dynamic significance on both real and model beaches where much of the flow energy is contained in second and higher order harmonics of the wave motion. As well there is no small significance to be attached to the fact that the quantities involved in phase ratio considerations are easily measured in the field.

Most importantly phase relations in the swash zone govern flow structure and type. The latter properties have been shown to be of greater significance than overall current speed since they reflect levels of asymmetry and turbulence in the water columns of the swash and backwash.

Swash waves on the four study profiles have been shown to be of the solitary wave (bore) form and crest length may be up to one third of the available swash zone width and decreases as the flow moves up the shore. The backwash takes the form of gravity wave motion and tends to accelerate uniformly down the foreshore toward the base of the breakers.

The importance of the wave lengths of these flows lies in the fact that longer waves are associated with greater durations of application of mean maximum velocity.

If time-mean velocity distributions across the shore are considered rather than instantaneous states an area of high velocity emerges in the upper section of the swash zone. Velocities at this point may be higher on average than lower on the shore for the swash and the area is one of net swash discharge. This occurs because of variations in swash length and speed, more variable conditions being recorded lower on the foreshore but only long, strong swashes reaching the upper levels. Mean swash energy is at a maximum on the mid and upper foreshore areas and there are indications of flow field reformation on the lower foreshore where rotatory motions imparted by breaking are converted to translatory swash movements.

An analysis of relations between the swash zone, breaker zone and nearshore bottom indicated that seaward return was not continuously developed except at high phase conditions. For lower phase conditions the drift profile is complex and sediment does not appear to be moved seaward through the breakers except in rip currents.

With increasing phase level there is an increase in the frequency of interference between flows and a rise in flow energy levels. Net mean relative energy levels become

negative (directed offshore) and there is a shift to flow at longer periods in the backwash. Swash flow is thus confined to shorter durations.

Analysis of the water budget of the swash zone indicated that percolation losses to the beach groundwater table may be up to one third of the swash volume at low phase conditions, the proportion declining to less than one eighth of swash discharge at high phase conditions. Significant bed fluidisation of sediments may result from the rapid return of this infiltrated water to the surface at times of high phase flow regime.

The role of the groundwater table in the modification of morphological processes occurring on the foreshore has been demonstrated to be very important since strong effects are exerted on both swash and backwash energy. This gives a strong tidal aspect to both types of flow. Permeability of the beach deposit is an important parameter because it governs both water table fluctuations and for given main flow states it controls bed erodibility. Effective field permeabilities for the mixed sand/shingle beaches under study were found to range from 200 to 2,000 Darcies. Significant areal variations in permeability and erodibility influence the pattern of morphological response to given flow conditions. Flow velocities in the groundwater surface sheet may achieve 50 cm/sec. or more and transported grains of up to at least 8mm. diameter.

Rilling and rhomboidal ripple marking were observed as results of this type of flow.

The main effect of the tidal rise and fall of water level is to produce higher flow depths, velocities and energies at time of high water. However, interaction with the beach water table results in displacement of these maxima and prolongs the periods of their action into the ebb tide phase. This occurs at all input wave phase levels and results in characteristic cycles of cut and fill, mean size variation, sorting patterns, and flow structure.

Absolute pressures on the profile have been shown to be greater for the swash zone than for the nearshore zone, maximum pressures of more than 30 gr/cm^2 being recorded in both swash and backwash. The swash zone of the study beaches is therefore classified as a high energy environment. Though onshore pressure deficits apply to all conditions as in the nearshore zone, increases in phase ratio result in increasingly asymmetric flow which leads to net offshore energy balances over much of the foreshore.

Analysis of the fluctuations associated with mean maximum velocities indicated that the relative intensity of turbulence increases landward of the breaker and with increasing phase level. This phenomenon is closely linked with variability of breaker height, swash length and frequency of interference between flows so that future studies should include measurement

of the level of variability in given wave trains. Though differences were found in turbulent structure between the swash and the backwash both were shown to be comprised of large scale eddies resulting from wave breaking and bed friction and occurring at frequencies of from 0.19 to 0.39 cycles per second. Smaller scale eddies were not measured owing to insufficient instrument accuracy.

The fluid flow/sediment grain system of the study beaches was demonstrated to be complex because it lay in a region of flow transition and was bounded roughly by current speeds of 100 to 250 cm/sec. and by grains sizes of 1.0 to 50.0 mm. diameter

The application of Longinov's method of proportional net pressures demonstrated a potential for size sorting at a level of more than 100 times that probable in the offshore zone. Thus, pressure intervals capable of moving all sizes up to cobbles and boulders were represented in the dynamometer records. It was concluded however, that the method was of little practical value in such a high energy environment because under such flow conditions it is applicable to only a narrow range of the ratio of flow energy to grain size (i.e. the larger sized particles). For smaller grains sediment transport was shown to occur at high rates depending on flow structure rather than current speed.

The importance of flow structure was also shown to extend to the mechanics of foreshore accretion and erosion. Thus,

the potential for bed scour is greatly increased by changes in flow structure in the backwash. This process attains appreciable areal expression and intensity at transition phase conditions and increases with further increases in flow energy. At high phase flow the zone of scour is wide and is dominated by the formation of hydraulic jump waves and standing waves. At low phase conditions the backwash is relatively weak, flow is predominantly tranquil, though fully turbulent and foreshore accretion results.

The dominant mode of sediment transport for much of the material on the study beaches has been shown to occur in the bed-load phase. From 55 to 95% of the moving load trapped was obtained from the lower one tenth of the water column. This is especially true of the backwash since greater vertical components of water motion in the swash disperse sediment to higher elevations than is the case for the backwash. Concentration profiles in both swash and backwash are logarithmic in form and sediment weights at given elevations increase with increasing flow energy. However, at high energies in the swash and for stations near the breaker marked departures from the logarithmic type of concentration gradient occur. It is therefore concluded that at high energy levels there is an increase in the level of sediment suspension in the upper layers of the swash, reflecting rolling motions imparted to the flow by the plunging action of the breakers. Also, there is well

developed seaward circulation through the breaker at such times so that these upper sediments may be transported seaward and lost to the foreshore. Mean grain sizes were demonstrated to decrease with distance above the bed in both swash and backwash.

Bed-load sediment movement on the foreshore occurs in the form of sheet flow, saltation near the swash limit where flow depth is small but energy level high, and as antidunes where standing waves or hydraulic jumps are developed in the backwash. Ripple formation was absent except for short durations between main flows when they were developed by the slower thinner groundwater sheet.

Rates of dynamic transport of bed sediments by both swash and backwash have been shown to be high and to increase with increasing flow turbulence and energy. A complex pattern of movements in which different sizes undergo transport in different directions and at varying concentrations has been demonstrated. Unequal sizes may move in contrary directions at the same time for a given position or reverse direction at other times.

Very good agreements between dynamic bed load transport rate and bed scour have been obtained though some lag is present in the bed elevation responses to variations in sediment flow. Also, good correlations were obtained for the relation between dynamic sediment transport and flow power expended on the

dynamometer plates. This is in direct contrast to the poor agreement demonstrated for the size/velocity relationship and highlights the significance of flow structure as a major control of swash zone processes on the study beaches.

Analysis of bed particle dynamics (Reynolds Number and drag coefficients) confirms that flow near the bed is highly turbulent for the pebble sizes and that flow energy levels near the bed are high. Relatively high grain drag coefficients for particles trapped at the mid-shore position in the backwash reflect the sometimes violent transitions in flow structure occurring at this point. As well, the dominantly low drag coefficients for pebbles, as opposed to sand grains, together with the limited range of available pebble shapes indicate that the potential for selection for grain shape is low on the study beaches save for areas of flow energy decline where water motion around individual grains is controlled by grain morphology. It is concluded that these conditions apply to pebbles on storm berms at long distances from the breakers, and to smaller grains on the study beaches. Paradoxically shape sorting is therefore better developed amongst the smaller grains than amongst pebbles and larger grains more usually regarded as intensively sorted for shape.

Depth of disturbance by swash and backwash flows was estimated from maximum scour depths and is at a maximum in the central foreshore zone where the backwash scour zone achieves

maximum intensity. Erosion rates of up to 15 cm/hour were recorded.

Characteristic processes of size sorting affecting bed sediment size-frequency distributions in the swash zone include simple truncation of a range of sizes, whole range transport of distributions (with individual fractions being transported at different rates and/or in different net directions), simple mixing by deposition of a range of sizes, bimodality as a result of active selection and erosion of a mid-size fraction and bimodality or polymodality of bed distributions resulting from deposition a wide range of sizes at varying rates. Distinctive alterations to mean size, sorting, skewness and kurtosis of bed size-frequency distributions result from these processes under different flow energy conditions. Similar fluctuations in grain size composition occur through the tidal cycle for any given set of flow phase relations.

SUMMARY OF PRINCIPAL RESULTS

1. A large body of quantitative data relating to a wide range of process and response factors has been obtained from natural mixed sand and shingle foreshores.
2. Since flow in the swash zone is markedly asymmetrical all of the major processes of morphological significance are dependent upon flow phase state i.e. The ratio of swash period to wave period. This is because phase level reflects flow type and structure.
3. Swash waves take the form of waves of translation the crest lengths of which may occupy up to one third of the available swash zone width.
4. Backwash waves are of the gravity type and the water mass tends to accelerate uniformly downslope.
5. The upper, landward section of the zone is swash dominated and, on time-average, is an area of relatively high velocity flow.
6. Mean flow velocities lower on the shore may be lower than those near the swash limit but energy levels are highest at the mid-shore position.
7. The water budget of the swash zone is such that up to one third of the input swash volume may be stored in the beach

deposit during low phase conditions. This proportion may decline to as low as one eighth of swash volume at high phase conditions.

8. Circulation of sediments seaward through the breaker is not well developed except during high phase events. For lower phase levels seaward circulation is intermittent and may occur dominantly in rip currents.
9. The time lag effect resulting from the storage of swash water in the beach deposit gives a strong tidal character to the distributions of flow energy. Both maximum swash and maximum backwash energies occur after high water when the water table is high and the foreshore is saturated.
10. Maximum pressures recorded in both the swash and the backwash were in excess of 30 gr/cm^2 . Pressures of this magnitude correspond to velocities sufficient to transport all sizes up to large cobbles. The swash zone of the study beaches may therefore be classified as a high energy environment.
11. Though an onshore pressure deficit was recorded for all experiments the asymmetry of flow is such that offshore energy balances were frequently recorded for the lower foreshore near the breaker.
12. The flow/sediment complex of the study beaches is characterised by high velocities (100 to 250 cm/sec.), and by a wide range of particle sizes (1.0 to 50.0 mm.).

13. Complexity of the sediment sorting processes stems from the facts that grains are transported at high rates and that considerable variations in turbulent structure occur in different parts of the flows.
14. Sediments are transported dominantly as bed load in both swash and backwash but significant amounts of material are moved as suspended load at high phase conditions.
15. During bed load transportation in the swash zone the potential for sorting of a wide range of sizes, as indicated by Longinov's method, may be as much as two orders of magnitude more intense than in the nearshore zone.
16. Characteristic sorting processes affecting the size distributions of sediments in the swash zone include mixing, truncation and whole range transport of component size fractions and the development of bimodal distributions by erosion of a central fraction or by deposition of a major secondary mode.
17. The erosive ability of the backwash is greatly enhanced by the development of standing waves and hydraulic jumps at the locations of alterations in backwash flow structure. These features are first developed at transitional phase levels and achieve maximum intensity and areal extent at high phase flow conditions.
18. For low phase flow conditions the flow in both swash and

backwash, though fully turbulent, occurs dominantly in the tranquil state.

The depth of foreshore disturbance is greatest for the central swash zone and decreases toward the swash limit. Maximum recorded disturbance was 15 cm/hour.

SUGGESTIONS FOR FURTHER RESEARCH

While this investigation has more than satisfied its original aims, it has been essentially exploratory and explanatory in nature so that a number of problems worthy of further research have emerged. It is suggested that these centre around two principal viewpoints which permeate much of contemporary coastal research.

The first of these is the need to develop a comprehensive working theory, essentially empirical in nature, which will satisfy the practical demands of the engineer concerned with designing structures to control and/or minimise shore face erosion. In connection with this the present theory is in need of further testing and of formulation into expressions which will more explicitly predict the relations between flow energy and morphological change.

Bagnold (1969, pers. comm.) has already suggested a way in which a, "whole mass transfer" approach to this problem might be made through the further employment of the dynamometer and depth recorder equipment. Additional to this it would be profitable to further pursue the usefulness of flow power expended at the dynamometer as a predictive parameter of sediment yield in the swash zone. Comparative wave tank

model tests of the energy/power/sediment yield relations formulated above for different, controlled flow phase conditions would be of great value.

The second aspect relates to the attempts of coastal geomorphologists to develop a comprehensive understanding of the processes of shoreline sculpture. Here effects at a number of time and areal scales must be considered so that the longer term results of the swash processes described in this study must be determined. Also, the present study has considered changes normal to the shore only so that an extension of the research to longshore variations in both process and response factors is required. An obvious single problem in this connection would be the study of areal variations in erodibility as controlled by foreshore permeability. This has relevance to the problem of understanding beach cusp formation and to other longshore variations in shore morphology and grain size composition.

In view of the significance of rate of transport, as opposed to the initiation of transport of grains of different sizes, for high energy beaches and the resultant effects on size-sorting and shape sorting much more field study might be undertaken for beaches which offer lower energy ranges and extremes, as well as for foreshores where ranges of available sizes and shapes are different. Such investigations may well provide information of great value in the interpretation of

paleo-imbrication structures and grain size textures.

Further, the present study has dealt with materials of approximately constant density, so that examination of mineral differentiation into areally separate zones and laminations has not been possible. The flow sensing instruments and appropriate sediment traps of the type employed in this investigation might be profitably applied to the study of processes of heavy mineral enrichment on beaches.

Similar studies to this might also be carried out on sand beaches where the proportion of sediment carried as suspended load is much higher and where there is wide tidal translation of the breaker zone.

Finally, much further field investigation of the swash zone/breaker system might be undertaken to assess more closely the significance of variability or "bandwidth" in incident wave trains because the present study has suggested that this property may exert a controlling influence on swash/backwash phase relations and therefore on the incidence and severity of bed scour. Certainly, for the oceanic swell environments of the East Coast, South Island, New Zealand, it would appear that it will be as necessary to record this factor as it traditionally has been to observe wave height, period and angle of approach to the shore. In addition general studies of sub-aerial beach changes which do not centre around the use of sophisticated instrumentation for measuring flow velocity and

energy should include measurements of swash length, swash duration, flow depths in both swash and backwash, and the level of variability in all of these properties. This follows from the fact that these fundamental measures have been demonstrated to be linked directly to such dynamic flow properties as level of turbulence, incidence of bed scour, level of suspension of sediments in the water column and asymmetry of pressure application to the bed. All of these phenomena are phase dependent and, happily, the basic measures detailed above are more easily measured in the field than more traditional quantities such as wave steepness near the shore and breaker type.

ACKNOWLEDGEMENTS

I wish to express my thanks to Dr. R.F. McLean, Department of Geography, University of Canterbury who supervised the project and who made available wave and profile data for the Kaikoura beaches. Dr. McLean also read and criticised the manuscript.

My thanks also go to Mr. Miles Reay of the Geography Department for his valuable assistance in the field; to Mr. L.D. Bowring of the Edward Percival Marine Laboratory, Kaikoura for his helpful advice and assistance with instrument maintenance in the field; and to Mr. J.S. Dickson who provided some of the grain size data for station A, Kaikoura.

The assistance and advice of Dr. A.J. Sutherland, Department of Civil Engineering, University of Canterbury with the calibration of the dynamometer is gratefully acknowledged. My thanks also go to Messrs. Scott and Sowerbutz of the Industrial Development Department, N.Z.D.S.I.R. Christchurch who constructed the dynamometer.

The financial assistance of the University Grants Committee and the Geography Department is gratefully acknowledged. I am obliged to Professor G. Knox, Zoology Department, University of Canterbury for permission to use the Edward Percival Marine Laboratory as a field base.

I would also like to thank my typist, Mrs. Judy Robertson, and Mrs. Claire McMichael and Mr. Graham Mitchell of the Cartographic Section, Department of Geography who drafted the diagrams.

In addition I wish to thank Mr. J.S. Burgess and my wife both of whom proof read the manuscript and offered many helpful suggestions.

REFERENCES

- Bagnold, R.A. 1940: "Beach Formation by Waves; Some
Model Experiments in a Wave Tank".
J. Inst. Civ. Engineers. 15: 27-52.
-
- 1942: The Physics of Blown Sand and
Desert Dunes. Methuen and Co.,
London, 265 pp.
-
- 1947: "Sand Movement by Waves; Some Small
Scale Experiments with Sand of very
Low Density". J. Inst. Civ.
Engineers. 27: 447.
-
- 1968: "Deposition in the Process of
Hydraulic Transport". Sedimentology.
10(1): 45-56.
- Bascom, W.N. 1951: "The Relationship Between Sand-Size
and Beach-Face Slope". Trans. Am.
Geophys. Union. 32(6): 866-74.
- Bluck, B.J. 1967: "Sedimentation of Beach Gravels:
Some Examples from South Wales".
J. Sedim. Petrol. 37(1): 128-56.
- Bowen, A.J.;
Inman, D.L.;
Simmons, V.P. 1968: "Wave 'Set Down' and 'Set UP'".
J. Geophys. Res. 73(8): 2569-78.

- Bretschneider, C.L. 1962: "Modification of Wave Spectra on the Continental Shelf and in the Surf Zone". Proc. 8th Conf. Coastal Eng. Ch.2: 17-33.
- Bryson, D.K. 1956: "The Measurement of Directional Permeability of Some Beach Sand". Univ. Sthrn. Calif. Unpubl. Report in Sedimentation: 13 pp.
- Cailleux, A. 1945: "Distinction des Galets Marins et Fluviatiles". Bull. Geol. Soc. France. 15(5): 375-404.
- Caldwell, J.M. 1956: "Wave Action and Sand Movement Near Anaheim Bay, California". U.S. Army B.E.B. Tech. Memo. No.68: 21 pp.
- Carstens, T. 1968: "Wave Forces on Boundaries and Submerged Bodies". Sarsia. 34: 37 - 60.
- Chepil, W.S.;
Siddoway, F.H. 1959: "Strain-Guage Anemometer for Analysing Various Characteristics of Wind Turbulence". Jour. Meteorology. 16(4): 411-18.
- Cornish, V. 1898: "On Sea Beaches and Sand Banks". Geog. Jour. 11 (6): 528-43.

- Dahlberg, E.C.; Griffiths, J.C. 1967: "Multivariate Analysis of a Sedimentary Rock for Evaluating Effects of Sedimentation Processes". Am. J. Sci. 265: 833-42.
- Davidsson, J. 1958: "Investigations of Sand Movements Using Radioactive Sand". Lund Studies in Geography. Ser. A. Physical Geography No. 12: 107-26.
- Davies, J.L. 1964: "A Morphogenetic Approach to World Shorelines". Zeits. fur Geomorphologie 8: 127-42.
- Defant, A. 1960: Physical Oceanography. Vols. 1 & 2. Pergamon Press, London. 729 and 598 pp.
- Demarest, D.F. 1947: "Rhomboid Ripple Marks and Their Relationship to Beach Slope". J. Sedim. Petrol. 17(1): 18-22.
- Dickson, J.S. 1969: "Aspects of Greywacke Beach Pebble Morphogenesis, Roundness, Sphericity and Form. The Hapuku River and North Bay Beach, Kaikoura". Unpubd. Masters Thesis, Dept. Geog. Univ. Canterbury, Christchurch, N.Z.

- Einstein, H.A.; 1949: "Hydrodynamic Forces on a Rough
El-Samni El Sayed Ah. Wall". Rev. Mod. Physics, 21:
520.
- Emery, K.O.; 1948: "Water Tables in Marine Beaches".
Foster, J.F. J. Marine Res. 7: 644-53.
- Emery, K.O.; 1951: "Swash and Swash Mark". Trans.
Gale, J.R. Am. Geophys. Union 32: 31-36.
- Evans, O.F. 1939: "Sorting and Transportation of
Material in the Swash and Backwash".
J. Sedim. Petrol. 9(1): 28-31.
- _____ 1949: "Ripple Marks as an Aid in
Determining Depositional Environment
and Rock Sequence". J. Sedim.
Petrol. 19(2): 82-86.
- _____ 1951: "Rhomboidal Markings Produced by
Swash and Backwash". Jour. Geol.
59(5): 508-9.
- Folk, R.L. 1962: "Sorting in Some Carbonate Beaches
of Mexico". Trans. N.Y. Acad. Sci.
Ser.2 25(2): 222-44.
- _____ 1965: Petrology of Sedimentary Rocks.
Manual. Hemphills, Austin, Texas.
154 pp. 2nd Ed.

- Granthem, K.R. 1953: "Wave Run-up on Sloping Structures".
Trans. Am. Geophys. Union 34(5);
720-24.
- Griffiths, J.C. 1951: "Size Versus Sorting in Some
Caribbean Sediments". Jour. Geol.
59: 211-43.
- Hamada, T. 1951: "Breakers and Beach Erosion".
Transp. Tech. Resch. Inst. Tokyo
December, 1951.
- Harrison, W.; 1964: "Dynamic Properties of Immersed
Morales-Alamo, R. Sand at Virginia Beach, Virginia".
U.S. Army C.E.R.C. Tech. Memo. No.9:
52 pp.
- Harrison, W.; 1965: "Predictor Equations for Beach
Pore, N.A.; Processes and Responses". J. Geophys.
Tuck, D.R. Res. 70(24): 6103-109.
- Harrison, W.; 1968: "A Time Series from the Beach
Rayfield, E.W.; Environment".
Boon, J.D.; ESSA Res. Lab. Tech. Memo. AOL-1:
Reynolds, G.; 85 pp.
Grant, J.B.
Tyler, D.

- Hayami, S. 1958: "Types of Breakers, Wave Steepness and Beach Slope". Coastal Eng. in Japan. 1: 21-34.
- _____;
Ishihara, T.;
Iwagaki, Y. 1953: "Some Studies on Beach Erosions". Disaster Prevention Resch. Inst. Bull. No. 5: 1-29. Kyoto.
- Healy, J.J. 1953: "Wave Damping Effect on Beaches". Proc. Minn. Inst. Hydr. Convn.: 213
- Hjulstrom, F. 1935: "Studies of the Morphological Activity of Rivers as Illustrated by the River Fyris". Bull. Geol. Inst. Univ. Uppsala. 25: 221-528.
- _____ 1939: "Transportation of Detritus by Moving Water". Recent Marine Sediments: 5-31. Ed. Trask.
- Hooke, R.L. 1968: "Laboratory Study of the Influence of Granules on Flow over a Sand Bed". Bull. Geol. Soc. Amer. 79(4): 495-500.
- Ingle, J.C. 1966: The Movements of Beach Sand. Elsevier Publishing Co. New York. 221 pp.

- Inman, D.L. 1949: "Sorting of Sediments in the Light of Fluid Mechanics". J. Sedim. Petrol. 19(2): 51-70.
- _____ 1963: "Ocean Waves and Associated Currents". Submarine Geology. Ch. 3. Harper and Row. 541 pp. Ed. F.P. Shepard, 2nd Ed.
- _____ ;
Bagnold, R.A. 1966: "Beach and Nearshore Processes: Part Two. Littoral Processes". The Sea. Ideas and Observations on Progress in the Study of the Seas. Vol. 3. Ch.21: 529-49. Interscience New York. 963pp. Ed. Hill. 2nd Ed.
- _____ ;
Bowen, A.J. 1963: "Flume Experiments on Sand Transport by Waves and Currents". Proc. 8th Conf. Coastal Eng.: 137-50.
- _____ ;
Frautschy, D. 1965: "Littoral Processes and the Development of Shorelines". Santa Barbara Speciality Conf. on Coastal Eng. Procs.: 511-536.
- Ippen, A.T. 1966:(Ed.) Estuary and Coastline Hydrodynamics. McGraw-Hill, New York. 744 pp.

- Ippen, A.T.;
Eagleson, P.S. 1955: "A Study of Sediment Sorting by
Waves Shoaling on a Plane Beach".
U.S. Army B.E.B. Tech. Memo. No. 63
- Iversen, H.W. 1952: "Laboratory Study of Breakers".
U.S. Nat. Bur. Stand. Circ. No. 521:
9-32.
- _____ 1952: "Waves and Breakers in Shoaling
Water". Proc. 3rd Conf. Coastal
Eng.: 1-12.
- Iwagaki, Y.;
Sawaragi, T. 1958: "Experimental Study on the
Equilibrium Slopes of Beaches and
Sand Movement by Breaker". Coastal
Eng. in Japan, 1: 75-82.
- Iwagaki, Y.;
Noda, H. 1963: "Laboratory Study of Scale Effect
in Two Dimensional Beach Processes".
Proc. 8th Conf. Coastal Eng.:
194-210.
- Johansson, C.E. 1965: Structural Studies of Sedimentary
Deposits. Lund Studies in Geography.
Ser.A. Physical Geography. No. 32.:
3-61.
- Johnson, J.W. 1949: "Scale Effects in Hydraulic Models
Involving Wave Motion". Trans.
Am. Geophys. Union, 30(4): 517-25.

- Jolliffe, J.P. 1964: "An Experiment Designed to Compare the Relative Rates of Movement of Different Sizes of Beach Pebbles". Proc. Geol. Assn. 75(1): 67-86.
- Kalinske, A.A. 1943: "Turbulence and the Transport of Sand and Silt by Wind". Annals N.Y. Acad. Sci. XLIV, Art. 1: 41-54.
- Kemp, P.H. 1958: The Effect of Groynes on Beach Formation and Erosion. Unpubl. Ph.D. Thesis, Univ. London. 2 Vols.
- _____ 1960: "The Relationship Between Wave Action and Beach Profile Characteristics". Proc. 7th Conf. Coastal Eng. 1. Ch.14: 262-77.
- _____ 1963: "A Field Study of Wave Action on Natural Beaches". Int. Assn. for Hydraulic Res. Proc. 10th Conf. 1: 131-38.
- Kidson, C.; Carr, A.P.; Smith, D.B. 1958: "Further Experiments Using Radioactive Methods to Detect the Movement of Shingle over the Sea Bed and Alongshore". Geog. Jour. 124(2): 210-18.

- Kidson, C.;
Carr, A.P.;
Smith, D.B.
-
- 1959: "The Movement of Shingle over the
Sea Bed Close Inshore". Geog.
Jour. 125(3-4): 380-89.
- 1961: "Beach Drift Experiments at
Bridgewater Bay, Somerset".
Proc. Bristol Nature Soc. 30:
163-180.
- King, C.A.M.
-
- 1951: "Depth of Disturbance of Sand on
Sea Beaches by Waves". J. Sedim.
Petrol. 21: 131-40.
- 1953: "The Relationships Between Wave
Incidence, Wind Direction and Beach
Changes at Marsden Bay, County
Durham". Trans. Inst. Brit. Geog.
19: 13-23.
-
- 1959: Beaches and Coasts.
Edward Arnold and Co. London. 403 pp.
- Kinsman, B.
- 1965: Wind Waves: Their Generation and
Propagation on the Ocean Surface.
Prentice-Hall Inc. New York. 676 pp.
- Kirk, R.M.
- 1966: "Depth of Disturbance by Waves on a
Shingle Beach over Single Tidal
Cycles". Unpubd. Mss. Geog. Dept.
Univ. Canty. Christchurch, N.Z.

- Kirk, R.M. 1967: Beach Morphology and Sediments of the Canterbury Bight. M.A. Thesis Unpubd. Geog. Dept. Univ. Canty. Christchurch, N.Z.: 173 pp.
- Koontz, W.A.;
Inman, D.L. 1967: "A Multipurpose Data Acquisition System for Instrumentation of the Nearshore Environment". U.S. Army C.E.R.C. Tech. Memo. No. 21: 38 pp.
- Krumbein, W.C. 1938: "Size-Frequency Distribution of Sediments on the Normal Phi Curve". J. Sedim. Petrol. 8: 84-90.
- _____ 1939: "Preferred Orientation of Pebbles in Sedimentary Deposits". Jour. Geol. 47: 673-706.
- _____ 1942: "Settling Velocity and Flume Behaviour of Non-Spherical Particles". Trans. Am. Geophys. Union.: 621-33.
- _____ 1947: "Shore Processes and Beach Characteristics". U.S. Army. B.E.B. Tech. Memo. No. 3.
- _____ 1953: "Statistical Problems of Sample Size and Spacing on Lake Michigan Beaches". Proc. 4th Conf. Coastal Eng. Pt. 2. Ch. 9: 147-62.

- Krumbein, W.C. 1959: "The 'Sorting Out' of Geological Variables as Illustrated by Regression Analysis of Factors Controlling Beach Firmness". J. Sedim. Petrol. 29(4): 575-87.
-
- 1963: "A Geological Process-Response Model for the Analysis of Beach Phenomena". U.S. Army Bull. B.E.B. 17: 1-16.
- Krumbein, W.C.; Pettijohn, F.J. 1938: Manual of Sedimentary Petrography. Appleton, Century, Crofts Inc. New York. 549 pp.
- Krumbein, W.C.; Monk, G.D. 1942: "Permeability as a Function of the Size Parameters of Unconsolidated Sand". Am. Inst. Mining and Metallurg. Engrs. Tech. Publ. No. 1492. Petroleum Technol.: 1-11.
- Krumbein, W.C.; Slack, A. 1956: "Relative Efficiency of Beach Sampling Methods". U.S. Army B.E.B. Tech. Memo. No. 90.
- Kuenen, Ph. H. 1964: "Experimental Abrasion 6: Surf Action". Sedimentology 3(1): 29-43.
- Landon, R.E. 1932: "Mutual Relations of Porosity, Vectoral Permeability and Resistance to Erosion". Jour. Geol. 40(2): 177-80.

- Langbein, W.B. 1942: "Hydraulic Criteria for Sand Waves". Trans. Am. Geophys. Union 23: 615-18.
- Le Mehaute, B. 1962: "On Non-Saturated Breakers and the Wave Runup". Proc. 8th Conf. Coastal Eng. Ch.6: 77-92.
- Lewis, W.V. 1931: "The Effect of Wave Incidence on the Configuration of a Shingle Beach". Geog. Jour. 78: 129-48.
- Manohar, M. 1955: "Mechanics of Bottom Sediment Movement due to Wave Action". U.S. Army. B.E.B. Tech. Memo. No.75
- Mason, M.A. 1952: "Some Observations of Breaking Waves". U.S. Nat. Bur. Stand. Circ. No. 521.: 215-220.
- Mason, C.C.;
Folk, R.L. 1958: "Differentiation of Dune, Beach and Aeolian Flat Environments by Size Analysis". J. Sedim. Petrol. 28: 211-26.
- Mathes, G.H. 1949: "Solids in Streamflow". Trans. Am. Geophys. Union. 30: 421-26.

- McLean, R.F.;
Kirk, R.M. 1969: "Relationships Between Grain-Size, Size-Sorting, and Foreshore Slope on Mixed Sand-Shingle Beaches". N.Z. J. Geol. Geophys. 12(1): 138-56.
- Menard, H.W. 1950: "Sediment Movement in Relation to Current Velocity". J. Sedim. Petrol. 20(3): 148-61.
- Middleton, G.V. 1962: "On Sorting, Sorting Coefficients, and the Log-Normality of the Grain-Size Distribution of Sandstones: A Discussion". Jour. Geol. 70(6): 754-56.
- Miller, R.L.;
Byrne, R.J. 1966: "The Angle of Repose for a Single Grain on a Fixed Rough Bed". Sedimentology 6: 303-14.
- Miller, R.L.;
Zeigler, J.M. 1958: "A Model Relating Dynamics and Sediment Pattern in Equilibrium in the Region of Shoaling Waves, Breaker Zone and Foreshore". Jour. Geol. 66(4): 417-41.
- _____ 1964: "A Study of Sediment Distribution in the Zone of Shoaling Waves over Complicated Bottom Topography". In Papers in Marine Geology: Shepard Commemorative Vol.: 133-53. McMillan. New York. Ed. R.L. Miller.

- Miyake, Y.;
Koizumi, M. 1948: "The Measurement of the Viscosity
Coefficient of Sea Water".
J. Marine Res. 7: 63-66.
- Munk, W.H. 1947: "A Critical Wind-Speed for Air-Sea
Boundary Processes". J. Marine
Res. 6(3): 203-18.
- _____ 1949: "The Solitary Wave Theory and its
Application to Surf Problems".
Annals N.Y. Acad. Sci. 51. Art 3.:
376-424.
- Muraki, Y. 1966: "Field Observations of Wave Pressure,
Wave Runup and Oscillation of
Breakwater". Proc. 10th Conf.
Coastal Eng. 1. Ch. 20: 302-321.
- Nevin, C. 1946: "Competency of Moving Water to
Transport Detritus". Bull. Geol.
Soc. Amer. 57: 651-74.
- Norrman, J.O. 1964: "Lake Vattern - Investigations of
Shore and Bottom Morphology".
Geografiska Annaler 46(1-2): 238 pp.
- 1969: New Zealand Tide Tables; 1969.
New Zealand Government Printer,
Wellington.

- Otvos, E.G. 1965: "Sedimentation-Erosion Cycles of Single Tidal Periods on Long Is. Sound Beaches". J. Sedim. Petrol. 35(3): 604-609.
- Palmer, H.R. 1834: "Observations on the Motions of Shingle Beaches". Roy. Soc. London, Philos. Trans. 124: 567-76.
- Pettijohn, F.J. 1957: Sedimentary Rocks. Harper and Bros. New York. 2nd Ed. 718 pp.
- Powers, M.C.;
Kinsman, B. 1953: "Shell Accumulations in Underwater Sediments and their Relation to Thickness of the Traction Zone". J. Sedim. Petrol. 23(4): 229-34.
- Putnam, J.A. 1949: "Loss of Wave Energy Due to Percolation in a Permeable Sea Bottom". Trans. Am. Geophys. Union. 30(3): 349-56.
- Putnam, J.A.;
Johnson, J.W. 1949: "The Dissipation of Wave Energy by Bottom Friction". Trans. Am. Geophys. Union. 30(1): 67-74.
- Putnam, J.A.;
Munk, W.H.;
Traylor, M.A. 1949: "The Prediction of Longshore Currents". Trans. Am. Geophys. Union. 30(3): 337-45.

- Rector, R.L. 1954: "Laboratory Study of Equilibrium Profiles of Beaches". U.S. Army B.E.B. Tech. Memo. No. 41.
- Romanovskiy, V.V. 1966: "A Study of the Fall Velocity of Coarse Sediment". Soviet Hydrology 1966 (1): - Selected Papers: 47-62. American Geophysical Union.
- Rouse, H. 1938: Fluid Mechanics for Hydraulic Engineers. McGraw-Hill, New York. 422 pp.
- Rubey, W.W. 1933: "Settling Velocities of Gravel, Sand and Silt Particles". Amer. J. Sci. 25(148): 325-38.
- _____ 1938: "The Force Required to Move Particles in a Stream Bed". U.S. Geol. Survey Prof. Paper. 189-E: 121-140.
- Samad 1968: "An Investigation into the Depth of Sand Disturbance over a Tidal Cycle". Unpubl. Mss. Geog. Dept. Univ. Canty. Christchurch, N.Z.: 12pp.
- Sames, C.W. 1966: "Morphometric Data of Some Recent Pebble Associations and their Application to Ancient Deposits". J. Sedim. Petrol. 36(1): 126-42.

- Savage, R.P. 1959: "Laboratory Data on Wave Run-up on Roughened and Permeable Slopes". U.S. Army B.E.B. Tech. Memo. No. 109.
- Saville, T. 1962: "An Approximation on the Wave Run-up Frequency Distribution". Proc. 8th Conf. Coastal Eng. Ch.4: 48-59.
- Schiffman, A. 1965: A Study of the Swash-Surf Energy System. M.S. Thesis Unpubd. Univ. Sthrn. Calif. Geol. Dept. 51 pp.
- Schwartz, M.L. 1968: "The Scale of Shore Erosion". Jour. Geol. 76(5): 508-17.
- Scott, T. 1954: "Sand Movement by Waves". U.S. Army Tech. Memo. No. 48: 37 pp.
- Shepard, F.P. 1963: Submarine Geology. Harper and Row. New York. 2nd Ed. 557 pp.
- Shepard, F.P.; Inman, D.L. 1950: "Near-Shore Circulation Related to Bottom Topography and Wave Refraction". Trans. Am. Geophys. Union 31(2): 196-212.
- Shields, A. 1936: "Anwendung der Aehnlichkeitsmechanik und der Turbulenzforschung auf die Geschiebebewegung". ("Application

- Sutton, O.G. 1955: Atmospheric Turbulence, John Wiley and Sons New York. 2nd Ed. 111 pp.
- Svendson, S. 1950: "Munch-Petersen's Littoral Drift Formula". Bull. B.E.B. 4(4): 1-31.
- Sverdrup, H.U.; Munk, W.H. 1946: "Theoretical and Empirical Relations in Forecasting Breakers and Surf". Trans. Am. Geophys. Union. 27(6):
- Tanner, W.F. 1958: "The Zig-Zag Nature of Type 1 and Type 4 Curves". J. Sedim. Petrol. 28(3): 372-75.
- _____ 1960: "Florida Coastal Classification". Trans. Gulf Coast Assn. Geol. Socs. 10: 259-66.
- _____ 1964: "Modification of Sediment Size Distributions". J. Sedim. Petrol. 34(1): 156-64.
- _____ 1966: "The Surf 'Break': Key to Paleogeography". Sedimentology. 7(3): 203-10.
- Thompson, W.O. 1937: "Original Structures of Beaches, Bars and Dunes". Bull. Geol. Soc. Amer. 48(6): 723-51.

- Van Dorn, W.G. 1966: "Theoretical and Experimental Study of Wave Enhancement and Runup on Uniformly Sloping, Impermeable Structures". Final Report Contract Nonr 2216(16). Univ. Calif. Scripps Inst. Oceanogr. Off. Nav. Res. Wash. D.C. 101 pp.
- Wadell, H. 1934: "Shape Determinations of Large Sedimental Rock Fragments". Pan Am. Geology. 61: 187-220
- Waters, C.H. 1939: Equilibrium Slopes of Sea Beaches. Unpubd. M.S. Thesis Dept. Engineering, Univ. Calif.
- Watts, G.M. 1954: "Laboratory Study of the Effect of Varying Wave Periods on Beach Profiles". U.S. Army B.E.B. Tech. Memo. No. 53.
- Wells, D.R. 1967: "Beach Equilibrium and Second Order Wave Theory". J. Geophys. Res. 72(2): 497-504.
- White, C.M. 1940: "The Equilibrium of Grains on the Bed of A Stream". Proc. Roy. Soc. London Ser. A. 174: 322-38.

- Wiegel, R.L. 1965: Oceanographical Engineering.
Prentice-Hall. New Jersey. 2nd ed.
532 pp.
- Yasso, W.E. 1965: "Fluorescent Tracer Particle
Determination of the Size-Velocity
Relation for Foreshore Sediment
Transport, Sandy Hook, New Jersey."
J. Sedim. Petrol. 35: 989-93.
- Yi-Yuan, Yu. 1952: "Breaking of Waves by an Opposing
Current". Trans. Am. Geophys.
Union. 33(1): 39.
- Zeigler, J.M.;
Hayes, H.R.;
Tuttle, S.D. 1959: "Beach Changes on Outer Cape Cod,
Massachusetts." Jour. Geol.
67(3): 318-35.
- Zenkovich, V.P. 1967: Processes of Coastal Development.
Oliver and Boyd. London.
Ed. J.A. Steers. 738 pp.

GLOSSARY OF TERMS

- BACKWASH: Seaward return of water from the swash limit under the influence of gravitational acceleration.
- BEACH FACE: Sloping seaward side of berm extending from storm berm crest to the step at the base of the breaker.
- BED-LOAD: Type of grain transport in which the grain weight is borne intermittently by the bed. Grains move by rolling, sliding, or saltating on or very near the bed. Concentration of grains in upper part of water column does not normally exceed 25% of that at reference level near the bed.
- BERM, SWASH: Low ridge or step on foreshore formed by deposition of material by wave action near the ordinary high water swash level.
- BERM CREST: The highest uprush (swash) point on the depositional beach face.
- BERM, STORM: Berm at highest uprush point on the backshore. Related to the swashes of storm waves.

- BREAKER, COLLAPSING: Type of breaker occurring on steep slopes and is intermediate between plunges and surges. Breaking occurs over the lower half of the wave and only a small air pocket is enclosed.
- BREAKER, PLUNGING: One in which the crest of the wave falls into the trough enclosing a pocket of air.
- BREAKER, SPILLING: One which breaks over a considerable distance. The wave does not lose its identity, but gradually decreases in height until it becomes swash on the beach. Usually delivers a longer swash than a plunging breaker, cet. par.
- BREAKER, SURGING: Confined to steep foreshore slopes and low wave steepnesses. Absence of a well defined plunge-point and there is a bore-like motion up the foreshore.
- EQUILIBRIUM BEACH: That configuration that the water would eventually impart to the beach deposit, in plan, profile and texture, if allowed to carry its work to completion. This would be a "steady state", or dynamic balance between energy and materials such that any

change would occur about a long term mean configuration, rather than to net erosion or net accretion.

- FORESHORE: That part of the shore, lying between the swash berm crest (or the upper limit of swell swash at high tide) and the step at the base of the breaker, that is subjected to swash/backwash action as the tide rises and falls.
- FORESHORE SLOPE: The angle between the horizontal and the foreshore surface. Measured at the reference point. Angle becomes larger for larger grains and conditions of net deposition.
- NEARSHORE BOTTOM: A zone extending from mean low water to an arbitrary depth of 30 feet below mean sea level.
- OFFSHORE BOTTOM: A comparatively large zone of variable width extending from the nearshore zone to the seaward edge of the continental shelf.
- REFERENCE POINT: That part of the foreshore which is traversed by swash at mid-tide (Bascom, 1951).

- SORTING:** The uniformity or dispersion of grain sizes. Results from the adjustment of individual grains to an equilibrium with local hydrodynamic environment.
- SPHERICITY:** The shape of a sediment particle expressed quantitatively as how nearly equal three mutually perpendicular axes through the grain are.
- SURF ZONE:** The zone of breaking waves and turbulent water between the breakpoint and the effective seaward limit of the backwash.
- SUSPENDED-LOAD:** Type of transport in which the grain weight is borne by the flow. Flow velocity is greater than the settling velocity of the grain. The concentration of grains at upper elevations in the water column is usually in excess of 25% of that at some reference level closer to the bed.
- SWASH:** The translation or rush of water up on to the beach face following the breaking of a wave. Takes the form of a Solitary wave of translation if there is no interference with outgoing backwashes. If swashes and backwashes are out of phase then motion is very irregular in form and highly asymmetrical.

SWASH-BACKWASH ZONE: That part of the shore subjected to the action of swash and backwash as the tide rises and falls. Coincides basically with the foreshore, though may extend to the whole of the sub-aerial profile under storm conditions.

LIST OF SYMBOLS

The following symbols are those most commonly employed throughout the report. It will be seen that in a few cases there are conflicts in usage which are due to application of the same symbols to different phenomena in different branches of the research field. No attempt has been made to standardise these since they are in common usage. In each case the particular meaning has been clearly stated at the point of usage in the text.

| <u>Symbol</u> | | <u>Units</u> |
|---------------------|---------------------------------------|--|
| A | Asymmetry of flow. | Dimensionless |
| A _p | Asymmetry of Mean Flow Pressure. | Dimensionless. |
| A _{p max.} | Asymmetry of Maximum Flow Pressure. | Dimensionless |
| A _{pt} | Asymmetry of impulse pressure. | Dimensionless |
| A _t | Asymmetry of Flow Durations. | Dimensionless |
| A _p | Absolute Maximum Flow Pressure. | gr.cm. ⁻² |
| A _z | Eddy Viscosity. | gr.cm.sec. ⁻¹ |
| C | Wave Phase Velocity in Shallow Water. | Ft.sec. ⁻¹ or: cm.sec. ⁻¹ |
| C _D | Drag Coefficient. | Dimensionless |
| D | Mean Grain Diameter. | mm. |

| <u>Symbol</u> | | <u>Units</u> |
|-------------------------|--|-------------------------------------|
| D_e | Equilibrium Motion Diameter. That sized particle which saltates around a mean position under given flow energy conditions. | mm. |
| D_i | Incipient Motion Diameter. The smallest particle which can undergo net motion in one direction in a given swash zone energy regime. | mm. |
| D_N | Mean Nominal Diameter. Mean diameter of spheres having same volumes as measured grains. | mm. |
| E | Flow Energy. (Force per unit Time) | $\text{gr.cm.}^2 \text{ sec.}^{-1}$ |
| $\overline{\Delta E}_1$ | Mean Maximum Energy of the Swash. Estimated in this investigation as:- | $\text{cm.}^2 \text{ sec.}^{-1}$ |
| $\overline{\Delta E}_2$ | Mean Maximum Energy of the Backwash. | $\text{cm.}^2 \text{ sec.}^{-1}$ |
| $\overline{\delta E}$ | Mean Net Energy Level. $\left(\overline{\delta E} = \frac{\overline{\Delta E}_1 - \overline{\Delta E}_2}{\overline{\Delta E}_1} \right)$ | $\text{cm.}^2 \text{ sec.}^{-1}$ |
| F | Force. | gr.cm.^{-2} |
| F | Froude Number. $U/(g.h)^{\frac{1}{2}}$ | Dimensionless |
| H_b | Breaker Height. | Ft. |
| H_o | Deepwater Wave Height. | Ft. |
| H_R | Runup Height of Swash above still Water Level. | Ft. |

| <u>Symbol</u> | | <u>Units</u> |
|-----------------|--|-------------------------------------|
| I | Total Dynamic Transport Rate of Immersed Solids per unit of bed area. | gr. sec. ⁻³ |
| I _b | Dynamic Bed-Load Transport Rate. | gr. sec. ⁻³ |
| I _s | Dynamic Suspended-Load Transport Rate. | gr. sec. ⁻³ |
| I | Intermediate (B) axis of three mutually perpendicular axes through a sediment grain. | mm. |
| J | Dry mass Transport of Sediment Across a Unit bed area. | gr. cm. ² sec. |
| K | Constant | <hr/> |
| K _G | Kurtosis of Grain Size Frequency Distribution. | Dimensionless |
| L | Longest (A) grain axis. | mm. |
| L _o | Deepwater Wave Length. $L_o = 5.12 T^2$ | Ft. |
| M | Mass | gr. |
| Mz | Graphic Mean Sediment Diameter. | ∅ |
| Q | Discharge. | Ft. ³ sec. ⁻¹ |
| ΔQ ₁ | Incremental Discharge Past a Given Point in the Swash. | Ft. ³ sec. ⁻¹ |
| ΔQ ₂ | Backwash Discharge. | Ft. ³ sec. ⁻¹ |

| <u>Symbol</u> | | <u>Units</u> |
|-------------------|---|-------------------------------------|
| ΔQ_3 | Incremental Discharge from Groundwater Table per unit bed area. | Ft. ³ sec. ⁻¹ |
| Re | Reynolds Number. | Dimensionless. |
| S | Foreshore Slope. | degrees. |
| S | Shortest (C) grain axis. | mm. |
| S _a | Concentration of suspended sediment at a reference level, a, above the bed. | gr.cm. ⁻³ |
| S _z | Concentration of suspended material at any level, z, above the reference level. | gr.cm. ⁻³ |
| SK _G | Skewness of Grain Size-Frequency Distribution. | Dimensionless |
| T | Wave Period. | seconds |
| U | Current Velocity. | cm. sec. ⁻¹ |
| \bar{U} | Mean Current Velocity. | cm. sec. ⁻¹ |
| U' | Instantaneous Current Velocity. | cm. sec. ⁻¹ |
| U _b | Velocity of Transport of Grains in Bed-Load Motion. | cm. sec. ⁻¹ |
| U _s | Velocity of Transport of Grains in Suspended-Load Motion. | cm. sec. ⁻¹ |
| U _{max.} | Maximum Velocity in x Direction. | cm. sec. ⁻¹ |

| <u>Symbol</u> | | <u>Units</u> |
|--------------------|---|--------------------------------------|
| V | Velocity of Swash or Backwash. Means and Maxima denoted as for current speed. | cm. sec.^{-1} |
| $V_{\text{crit.}}$ | Flow Velocity just Sufficient to Initiate motion of sediment grains. | cm. sec.^{-1} |
| W | Velocity Measured in y Direction. | cm. sec.^{-1} |
| a | Reference level in Flow | cm. |
| c | Constant | <hr/> |
| c | Settling Velocity of Sediment Grains | cm. sec.^{-1} |
| d | Water Depth. | cm. |
| e | Exponent or Natural Base of Logarithms. = 2.7183 | |
| e_b | Efficiency Coefficient of Bed-Load Transport. | Dimensionless |
| e_s | Efficiency of Suspended-Load Transport. | Dimensionless |
| f | Function. | <hr/> |
| f_c | Critical Drag Force on Sediment Grain. | $\text{gr. cm.}^2 \text{ sec.}^{-1}$ |
| g | Acceleration Due to Force of Gravity. 980 Dynes. | cm. sec.^{-2} |
| k | Constant. | <hr/> |
| k_o | Von Karman's Constant. = 0.42 | <hr/> |
| l | Swash Length. | Ft. |

| <u>Symbol</u> | | <u>Units</u> |
|----------------|---|-------------------------------------|
| p | Packing Coefficient of Sediment Grains. | n.cm. ⁻³ |
| q | Breaker Discharge per Unit Crest Length. | Ft. ³ sec. ⁻¹ |
| t | Swash Period. | Seconds |
| u _* | Friction Velocity. | cm.sec. ⁻¹ |
| u | Component of Velocity in x Direction. | cm.sec. ⁻¹ |
| v | Component of Velocity in y Direction. | cm.sec. ⁻¹ |
| w | Component of Velocity in z Direction. | cm.sec. ⁻¹ |
| x | Distance Seaward from the Swash Limit Parallel to the bed to Given Point in Flow. | Ft. |
| y ₁ | Depth of Undisturbed Flow Preceding a Hydraulic Jump. | cm. |
| y ₂ | Depth of Disturbed Flow Following Passage of a Surge. | cm. |
| z | Distance Above Bed in Flow. Measured Positive Upward. | cm. |
| z ₀ | Reference Depth taken immediately above Sediment Grains and employed as Roughness Length Parameter. | cm. |
| β | Local Angle of Bed Inclination with Respect to the Horizontal. | degrees |
| σ_I | Inclusive Graphic Standard Deviation. Sorting Coefficient of Sediments. | ϕ |

| <u>Symbol</u> | | <u>Units</u> |
|------------------|---|--|
| ϕ | Phi. Grain Diameter expressed as \log_{-2} of particle Diameter in millimeters. | |
| Tan ϕ | Angle of Intergranular Sliding Friction. | |
| Ψ | Effective Settling Sphericity of grain in relation to settling velocity of sphere of same volume. | Dimensionless |
| Ω | Total Flow Power. | ergs.sec. ⁻¹ or: Ft.pdl.sec. ⁻¹ |
| $j\epsilon$ | Longinov Proportional Net Pressure. | Dimensionless |
| t/T | Flow Phase Ratio. | Dimensionless |
| x/L _o | Relative Position in the Swash Zone. | Dimensionless |
| ρ_f | Fluid Density. | gr.cm. ⁻³ |
| ρ_s | Sediment Density. | gr.cm. ⁻³ |